

**Identification of new *Pseudomonas aeruginosa* lectin LecA
inhibitors using biochemical- and NMR-methods**

Dissertation

zur Erlangung des Grades

des Doktors der Naturwissenschaften

der Naturwissenschaftlich-Technischen Fakultät

der Universität des Saarlandes

von

Ines Alexandra Bräutigam (geb. Joachim)

Saarbrücken

2023

Tag des Kolloquiums: 21. Juli 2023

Dekan: Prof. Dr. Ludger Santen

Berichterstatter: Prof. Dr. Alexander Titz

Prof. Dr. Rolf Hartmann

Vorsitz: Prof. Dr. Dominik Munz

Akad. Mitarbeiter: Dr. Josef Zapp

Die praktischen Tätigkeiten zur vorliegenden Arbeit wurden von Oktober 2012 bis Mai 2016 unter Anleitung von Herrn Prof. Dr. Alexander Titz zunächst an der Universität Konstanz und später an der Universität des Saarlandes sowie am Helmholtz-Institut für Pharmazeutische Forschung Saarland (HIPS) angefertigt.

„So eine Arbeit wird eigentlich nie fertig, man muss sie für fertig erklären, wenn man nach der Zeit und den Umständen das Möglichste getan hat.“

Johann Wolfgang von Goethe

DANKSAGUNG

Ich möchte mich hier an dieser Stelle herzlich bei allen beteiligten Personen bedanken, die diese Arbeit ermöglicht haben. Der erste und ein besonderer Dank gilt Prof. Dr. Alexander Titz für die Möglichkeit eine Promotion in seiner Arbeitsgruppe durchzuführen, sowie das Überlassen des interessanten Themas, der Betreuung mit vielen guten Diskussionen, Inputs und Ideen während der gesamten praktischen Zeit im Labor und darüber hinaus. Und natürlich einer großartigen Atmosphäre in seiner Gruppe, in der ich ein Mitglied sein durfte. Weiterhin bedanke ich mich bei der ganzen Arbeitsgruppe Titz für die gemeinsame Zeit, den Zusammenhalt und die guten Diskussionen sowie Hilfe und Unterstützung aller Art. Roman, Steffi, Dirk, Matthew und Ghamdan ohne euch wäre die Zeit nicht die gleiche gewesen.

Prof. Dr. Rolf Hartmann danke ich für die Begleitung der Promotion sowie die Übernahme des Zweitgutachtens. Ausserdem ihm und seiner ganzen Gruppe für die herzliche Aufnahme am HIPS in Saarbrücken nach unserem Umzug aus Konstanz, der Einweisung in das Labor und fortdauernde Unterstützung, Diskussionen und den Austausch.

Ein besonderer Dank gilt außerdem meinen Bürokollegen Martina, Kristina, Christine, Benny, Martin, Steffi, Roman und Ghamdan die alle zu einer guten, wenn auch nicht immer leisen Büroatmosphäre beigetragen haben.

Alex, Kathrin, Roman, Anne und Andrea danke ich für das Korrekturlesen von Teilen oder der ganzen Dissertation.

Prof. Dr. Rolf Müller danke ich für die Möglichkeit die NMR-Geräte zu verwenden sowie ihm und seiner Gruppe für Hilfe und Anleitung jeder Art. Besonders bedanke ich mich bei Dr. Alberto Plaza und Dr. Kirsten Harmrolfs für die Hilfe beim Aufsetzen der NMR-Sequenzen und der ständigen Bereitschaft zur Hilfe bei Problemen.

Anne Imberty sowie ihrer gesamten Gruppe danke ich für eine großartige Kooperation über die Jahre und viele fruchtbare Diskussionen. Dr. Christoph Rademacher danke ich für die Möglichkeit das ^{19}F Screening in seinem Labor durchzuführen sowie die andauernde, erfolgreiche Kooperation und all die guten Diskussionen. Besonders danke ich Dr. Jonas Aretz für die Hilfe bei der Durchführung der ^{19}F NMR-Experimente in Berlin.

Susanne Striegler danke ich für die gute Zusammenarbeit bei der Untersuchung der Galactonoamidines und Galactolactams.

Zu guter Letzt möchte ich auch meiner Familie und bei meinen Freunden für ihre unermüdliche Unterstützung danken. Ihr wart mir ein großer Rückhalt, auf den ich mich stets verlassen konnte.

Table of content

Summary	IX
Zusammenfassung	X
List of abbreviations	XI
1 Introduction	1
1.1 <i>Pseudomonas aeruginosa</i> and its ability of biofilm formation	1
1.2 Lectins are carbohydrate binding proteins	3
1.3 Analysis of protein-ligand interactions using biochemical and biophysical methods	7
1.4 Determination of ligand protein interactions by NMR methods	10
2 Aim of the thesis	15
3. Results and Discussion	17
3.1 Optimization of D-galactose based lectin LecA inhibitors	17
3.2 Non-carbohydrate glyco mimetic as ligand of the <i>P. aeruginosa</i> lectin LecA	30
3.3 ¹⁹ F NMR screening for the identification of ligands for <i>P. aeruginosa</i> lectin LecA	38
3.4 A lanthanide-based NMR approach for the determination of new LecA inhibitors	60
3.5 Carbohydrate binding site mapping using TROSY-NMR	83
4. Conclusion	93
4.1 Optimization of D-galactose based lectin LecA inhibitors	93
4.2 Non-carbohydrate glyco mimetic as ligand of the <i>P. aeruginosa</i> lectin LecA	94
4.3 ¹⁹ F NMR screening for the identification of ligands for <i>P. aeruginosa</i> lectin LecA	96
4.4 Determination of the carbohydrate binding site by mapping of TROSY-NMR	98
4.5 A lanthanide-based NMR approach for the determination of new LecA inhibitors	99
5. Experimental section	101
5.1. Protein expression	101
5.2. Experimental information on NMR measurements	102
5.3. Experimental information on biochemical methods	104
5.4. Experimental information on synthesis	106
6. References	139
Appendix	i
Curriculum vitae	i
List of scientific publications	ii

Summary

Summary

Biofilm formation of *Pseudomonas aeruginosa* is one of the major threats of its treatment. *P. aeruginosa* expresses lectins, which are carbohydrate-binding proteins: LecA, specifically binding to D-galactose. The development of galactose-based inhibitors with high affinity towards LecA represents a promising way towards novel therapeutics. Derivatives of phenyl β -D-galactosides were synthesized and tested on their binding potential to LecA. Within the set of 44 synthesized D-galactose based inhibitors m-methoxy phenyl β -D-galactoside was determined as the best LecA inhibitor with a binding affinity in the low micro molar range and can now be used for further derivatization. In contrast to synthesis virtual screening and NMR screening of a ^{19}F library was used to identify novel LecA inhibitors. The determined hits were verified using biochemical methods. To identify fragments binding in the vicinity of the carbohydrate binding pocket a screening approach based on the functional replacement of Ca^{2+} in the binding pocket is developed. As Ca^{2+} is replaced with paramagnetic lanthanide ions resulting effects like signal shifts (PCS) and enhanced relaxation (PRE) give insight on distance and angle of potential binders. The developed screening approach based on paramagnetic effects can be used to screening further fragment libraries to identify new binding fragments or ligands.

Zusammenfassung

Die Biofilmbildung von *Pseudomonas aeruginosa* ist eines der größten Probleme bei der Behandlung. *P. aeruginosa* exprimiert kohlenhydratbindende Proteine, genannt Lektine. LecA bindet spezifisch an D-Galaktose. Die Entwicklung von Hemmstoffen auf Galaktosebasis stellt einen vielversprechenden Weg zu neuen Therapeutika dar. Es wurden 44 D-Galaktosederivate synthetisiert und auf ihr Bindungspotenzial an LecA getestet. M-Methoxyphenyl- β -D-Galaktosid wurde als bester LecA-Inhibitor mit einer Bindungsaffinität im niedrigen mikromolaren Bereich ermittelt und kann für weitere Derivatisierung verwendet werden. Zusätzlich zur Synthese und Evaluierung wurde ein virtuelles Screening sowie ein NMR-Screening einer ^{19}F -Bibliothek eingesetzt, um neue LecA-Inhibitoren zu identifizieren. Die ermittelten Treffer wurden mittels biochemischer Methoden weiter untersucht. Um weiterhin Fragmente zu identifizieren, die in der Nähe der Kohlenhydratbindungstasche binden, wurde ein Screening-Ansatz entwickelt, der auf dem funktionellen Ersatz von Ca^{2+} in der Bindungstasche basiert. Durch den Ersatz von Ca^{2+} durch paramagnetische Lanthanidionen werden Effekte wie Signalverschiebungen (PCS) und verstärkte Relaxation (PRE) beobachtet, die Aufschluss über Abstand und Winkel potenzieller Bindungspartner geben. Der entwickelte Screeningansatz kann nun für die Untersuchung weiterer Bibliotheken verwendet werden.

List of abbreviations

A	
Asp	Asparagin acid
C	
Ca ²⁺	Calcium ion
CdrA	cyclic di-GMP regulated adhesion
CPMG	Carr-Purcell-Meiboom-Gill
CSA	Chemical shifts anisotropy
CSP	chemical shift perturbation
Cys	Cystein
c-diGMP	cyclic di-GMP
D	
DD	Dipole-dipole
DMF	Dimethlyformamide
DNA	desoxyribonucleic acid
Dy ³⁺	Dysprosium ion
D ₂ O	Deuterium dioxide
E	
EDTA	Ethylenediaminetetraacetic acid

List of abbreviations

ELISA	enzyme linked immuno-S-assay
ELLA	Enzyme-linked lectin assay
F	
FP	fluorescence polarization
FimH	type 1 fimbrial adhesion of <i>E.coli</i>
FlpD	flagellar cap protein
G	
GacA	Global antibiotic and cyanide control protein
GacS	sensor protein
Gal	Galaktose
GalNAc	<i>N</i> -Acetyl β -galactoamine
GalNH ₂	Galactoseamine
Gd ³⁺	Gadolinium ion
GHz	Giga Hertz
Glc	Glucose
Gln	Glutamin
Glu	Glutamic acid
H	
His	Histidine

List of abbreviations

Ho ³⁺	Holmium
HRP	Horse-radish peroxidase
I	
IC ₅₀	half minimal (50%) inhibitory concentration
IPTG	Isopropyl β-D-thiogalactoside
ITC	Isothermal titration calorimetry
K	
K _d	Binding constant
KNIME	Konstanz Information Miner (Data Software)
L	
Las	Quorum sensing system of <i>Pseudomonas</i>
LecA	lectin A (of <i>P. aeruginosa</i>)
LecB	lectin B (of <i>P. aeruginosa</i>)
LW	line width
M	
MACCS	Molecular ACCess System
me-α-gal	methyl α-D-galactoside
MeOH	Methanol
MES	2-(<i>N</i> -Morpholino)ethansulfone acide
MHz	Mega Hertz

List of abbreviations

mM	milli molar
MOE	Molekulare Operation Environment
MRSA	Methicillin resistant <i>Staphylococcus aureus</i>
μM	micro molar
N	
NaCl	sodium chloride
NEt ₃	Triethylamine
NMR	nuclear magnetic resonance
NOE	Nuclear Overhauser effects
O	
OH	Hydroxy group
P	
PAA	poly acryl amide
<i>P. aeruginosa/ PAO</i>	<i>Pseudomonas aeruginosa</i>
PAINS	pan assay interference compounds
PBS	Phosphate buffered saline
PCS	Pseudo contact shift
PDB	protein data base
Pel	Polysaccharide of <i>Pseudomonas</i>

List of abbreviations

p-NPG	p-nitrophenyl β -D-galactoside
PRE	Paramagnetic relaxation enhancement
Psl	Polysaccharide of <i>Pseudomonas</i>
Pqs	<i>Pseudomonas</i> quinolone signal
R	
Rhl	Las system transcriptional activator
RNA	ribonucleic acid
S	
SPR	surface plasmon resonance
T	
Tb ³⁺	Terbium ion
TBS	Tris-buffered saline
Thr	Threonin
TMA	trimethyl ammonium chloride (internal standard used in all NMR experiments)
Tm ³⁺	Thullium ion
Tris	Tris(hydroxymethyl)-aminomethane
TROSY	<u>T</u> ransverse <u>R</u> elaxation <u>O</u> ptimized <u>S</u> pectroscop <u>Y</u>
Trp	Tryptophan
TSA	Thermal Shift Assay
Tyr	Tyrosin

List of abbreviations

T1 ρ	spin-lattice relaxation (longitudinal, along z-axis) in a rotation frame
T2	spin-spin relaxation (transversal, along xy-plane)
T3SS	type-3-secretion system
W	
WHO	World health organization

1 Introduction

1.1 *Pseudomonas aeruginosa* and its ability of biofilm formation

Wherever we are a multiplicity of bacteria are surrounding us. Most of these bacteria are not harmful to healthy individuals. However, as hospitalized patients suffer from a reduced immune system, these bacteria can become extremely dangerous leading to a series of severe infections, starting from inflammation, ending up in sepsis and death. Recently, the WHO acknowledged the bacterium *Pseudomonas aeruginosa* as being one of the most infectious bacteria and classified them as priority pathogens with the criticality critical due to the pathogens' resistance to a huge number of available antibiotics.^[1] *P. aeruginosa* is a gram negative, rhode-shaped, opportunistic pathogen. It is one of the main causes of hospital-acquired infections, and a serious threat for patients facing an impaired immune system. The enhanced antibiotic resistance is caused by a multiplicity of aspects, like the level of porins and membrane permeability for antibacterial agents. Moreover, the potential to express large numbers of efflux pumps increases potential of the excretion of antibiotic molecules from the bacterial cell. Second, *P. aeruginosa*, like many other pathogens, can easily acquire specific antibiotic resistance genes that are β -lactamases and aminoglycoside-inactivating enzymes. And most important, chronic infections caused by *P. aeruginosa* are accompanied by biofilm formation.^[2]

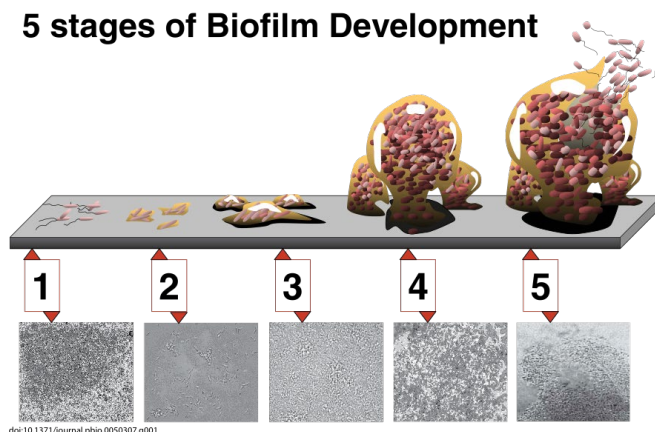


Figure 1 The five stages of *P. aeruginosa* biofilm formation are depicted in the cartoon. First, the reversible attachment of planktonic bacteria (1), followed by the irreversible attachment (2). Third, after reaching a final density (3), bacteria start to form a biofilm, which matures to a mushroom like structure (4). Finally, the mushroom shape disrupts, and planktonic bacteria are again released (5). The picture is taken from Don Monroe PlosOne. ^[3]

In general, bacteria can exist in either of two lifestyles: planktonic or sessile. Within the sessile stage, biofilm formation can occur. ^[4-6] A biofilm however is an endless life-cycle of a community of bacteria. This community surrounds itself with a matrix, consisting of polysaccharides, proteins, DNA and RNA. This matrix also prevents the single bacteria from antibiotic attack of the host immune system. ^[7-9] For *P. aeruginosa* the formation of the biofilm can be divided into five major phenotypic stages (Figure 1):^[3]

Introduction

The process of the biofilm formation starts with the reversible attachment of planktonic bacteria, followed by the irreversible attachment of bacterial colonies. Afterwards, these colonies grow to a threshold density, then starting to produce the bacterial biofilm, which grows up to mushroom shaped aggregates, until finally, parts of the biofilm are disrupted to colonize new surfaces and the process is started from the beginning. Within the biofilm, the single bacterium communicates using small chemical molecules. There are five signaling pathways known for *P. aeruginosa*: First the Rhl-system, using N-butanoyl-L-homoserine lactone (C4-HSL), second the Las system with its chemical messenger N-3-oxododecanoyl-L-homoserine lactone (3-oxo-C12-HSL) as well as the Pqs system owing the chemical messengers of the quinolone family.^[10-17] Other to them, a secondary messenger system using cyclic di-GMP (c-diGMP) can result in an increased expression of adhesins, exopolysaccharides like Pel, Psl or Alginate. While the Rhl, Las and Pqs are more important within a mature biofilm, c-diGMP is mostly involved in the switch from a planktonic to sessile lifestyle.^[10,18] In addition to that, a system based on RNA is present, using the two component system GacS and GacA which result in activation of the type-3-secretion system (T3SS).^[10,19] The biofilm protects the bacteria from attacks by either antibiotic, disinfectants, mechanical cleaning or the host immune defense system. Moreover, due to a decrease in nutrients within the biofilm, the bacteria on the bottom suffer from low oxygen content and low nutrients, changing them in so-called persister cells with an extremely reduced metabolism.^[20-22] These persister cells can be also protected by dead bacteria in the surrounding, and start to grow upon reaching growth favorable conditions.^[23,24] The combination of all the above mentioned factors contribute to the factor that often antibiotics are without long-lasting effects on bacteria in a biofilm. It was shown that antibiotic treatment of *P. aeruginosa* only leads to a short-lived improvement in patient situation, but no lasting improvement was observed with the use of different antibiotics.^[25] Attempts to combine antibiotic with efflux pump inhibitors like Mefloquine, epinephrine or theobromine have not significantly enhanced the potency of the antibiotic agents.^[26,27]

Bacterial adhesion is the initial step in colonization and biofilm formation; thus, the bacteria need a strong arsenal of adhesins. Although it was tried to describe bacterial adhesion with the parameter of the interaction of colloid particles with a surface, which could be accurate given the size similarity of both system, bacterial adhesion was found to be extremely complicated and thus it deviates from the adhesion models.^[28,29] *P. aeruginosa* expresses a number of different adhesins, starting with the flagellar cap protein FlpD, a mucin adhesin.^[30] 90 % of the bacterial adhesion is mediated by type-IV secretion system with the related pili.^[31,32] In addition, CdrA, a protein responsive to the biofilm promoting secondary messenger cyclic-di-GMP, is a *P. aeruginosa* adhesin.^[33,34] Above all, the two soluble lectins, LecA and LecB, are bacterial adhesins.^[35-38] Both of these C-type lectins are carbohydrate binding proteins. While LecB was already shown to be present on the outer membrane, LecA was shown to be an exotoxin.^[39-41] Both lectins were shown to be necessary in biofilm formation.^[38,42] As a result, a newborn child suffering from a *Pseudomonas* induced sepsis was treated successfully with a fucose and galactose solution, and later a small case study containing 11 patients inhaling a saturated galactose- and fucose solution showed a reduced bacterial load in the sputum.^[43,44]

1.2 Lectins are carbohydrate binding proteins

Bacterial adhesion, like many naturally occurring phenomena, is based on the interaction of a glycan surface with glycan binding proteins. Interaction of bacterial lectins with sugars, like exopolysaccharides or glycan surface of the host tissue or interaction of lectins with a host cell surface, and interaction of eukaryotic carbohydrate binding proteins like selectins are involved in cell-cell communication processes and processes of the innate immune system. [32,36–39] Carbohydrate binding proteins are called lectins. They do not have an enzymatic activity themselves, but they can induce biochemical reactions upon binding. [37,40] Lectins, the term derived from the Latin word „legere“ for reading, can influence a huge number of biochemical processes like cell-division, ribosomal protein synthesis and agglutination of cells, called hemagglutination for red blood particles. [41–45]

1.2.1 Biological relevance of *P. aeruginosa* lectins LecA and LecB

Cell-adhesion processes or host-pathogen contact are often enabled via carbohydrate-lectin interactions. [46] In contrast to other bacterial adhesins like flagella or pili, lectins are soluble proteins. [21,22,28,47–50] *P. aeruginosa* expressed two of this soluble lectins: LecA and LecB: Both were shown to be necessary for biofilm formation. [33,50,51] As lectins are adhesins, they need to be present on the surface.

Since the mechanism of secretion is still unknown, it is hypothesized, that lectins are secreted by lysis of victimized bacteria. [49] Little evidence of lectin secretion is present up to date, but it is well known, that both lectins are expressed under quorum sensing control. [52] Both tetrameric lectins are C-type lectins, meaning that they depend on the presence of at least one Ca^{2+} for functional ligand binding. [28,47,53]

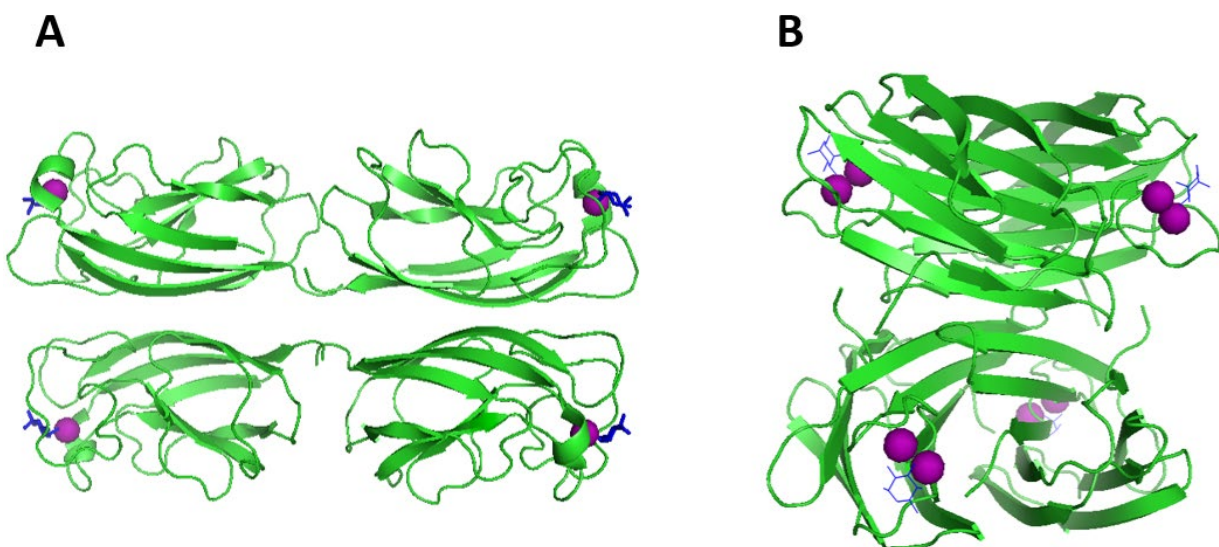


Figure 2: Crystal structure of LecA (A, pdb code 10KO) and LecB (B, pdb code 10XC) in complex Ca^{2+} (purple) with their carbohydrate ligands (blue). In case of LecA the carbohydrate ligand is p-NPG **19** and L-Fucose for LecB

Introduction

While LecB has two Ca^{2+} -ions in each binding pocket, LecA only bears one Ca^{2+} -ion. [27,30,31] LecB binds both, D-mannose and L-fucose whereas LecA exclusively binds to D-galactose and its derivatives. [54] Moreover, a study using a LecA over expression mutant PAO1-P47 showed enhanced biofilm formation, but the biofilm of the wild-type and the mutant were reduced substantially upon addition of the LecA ligand Isopropyl β -D-thio galactoside (IPTG). [33] However, an effect of the known LecB ligand p-nitro phenyl β -L-fucoside was not observed using the steel coupon assay reported by Diggle and co-workers. [29, 33, 55] In contrast, a study by Tielker and co-workers using on a static biofilm grown on glass slides reported on reduced biofilm of a PAO1-PAIT2 and PAO1-P27 mutant impaired in LecB formation. [29] In both cases, no general growth defect of the mutants was detected, as planktonic cultures showed the same growth rates as the wild type. [29,33]

1.2.2 Natural Lectin inhibitors

1.2.2.1 Inhibitors of the galactophilic lectin LecA

First in 1972, LecA, formerly named PA-IL, was identified from the heat stable fraction of a *P. aeruginosa* culture and was shown to be stable to temperatures up to 70°C and to enzymatic treatment. [26] Treatment of the bacterial hemagglutinin with ethylene diamine tetra acetic acid (EDTA) abolished the activity, and addition of Mn^{2+} , Mg^{2+} or Ca^{2+} reinstated it. [26,56] Numerous studies showed, the specific D-galactose binding of lectin LecA was depended on the presence of one Ca^{2+} ion in the binding pocket. [26,56,57]

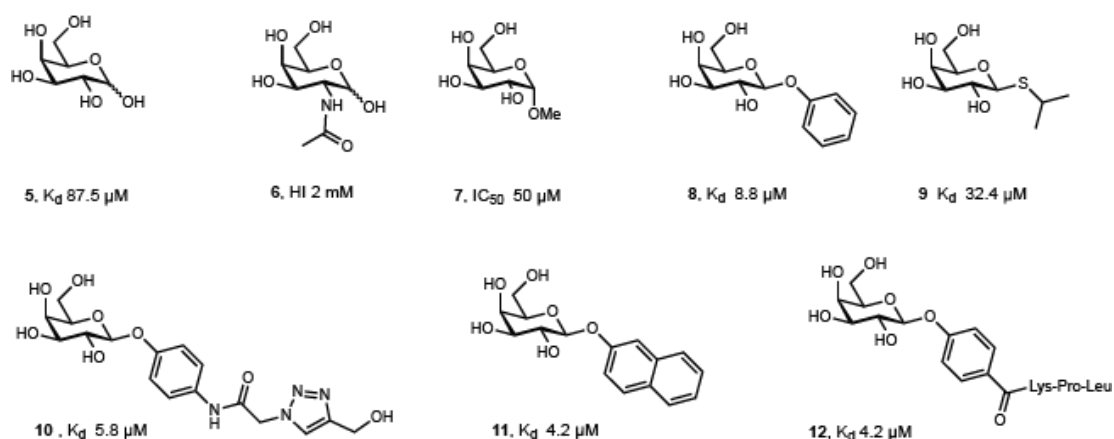


Figure 3 : Monovalent LecA inhibitors based on a galactose scaffold. The natural ligand D-galactose **5** was identified together with its galactosamine analog **6**, the ligands methyl α -galactoside **7**, phenyl β -D-galactoside **8** and the thio galactoside isopropyl β -D-thio galactoside (IPTG) **9** with improved affinity for D-galactose were identified in 1992. [58] Most recent advances in affinity improvement were made with the acetamido compound **10** developed by Vidal and co-workers, the naphthol derivative **11**, and the peptide substituted **12**. [59–61]

Within the past years, numerous D-galactose based ligands have been examined as potential LecA inhibitors. Starting from the natural ligand D-galactose **5** reported in 1992, with an affinity of 87.5 μM , methyl α -galactoside **7** was reported with an increased affinity. ^[58,62-63] Within the growing interest in LecA galactose interaction, a study showing the significance of the CH- π T-shape interaction between the His50 of LecA and the aromatic ring of the galactoside aglycon in ligands binding to lectin LecA from *P. aeruginosa* explained the enhanced affinity of aromatic β -galactosides. ^[60] Many studies in the past years have examined different aglycon to improve the binding affinity. It was demonstrated, that compared to the affinity of 8.8 μM of the unsubstituted phenyl ring in phenyl β -D-galactoside **8**, the substitution of the phenyl ring with an acetamido moiety in para position (**10**), or the addition of a tripeptide in the same position (**12**), the affinity was improved to 6 μM or 4 μM , respectively. ^[60,62] Moreover, the affinity of the naphthol D-galactoside **11** was determined with 4 μM . ^[60] Compared to the first monovalent specific galactose-based LecA inhibitors discovered by Gilboa-Garber in 1972, years later a natural ligand based on the globo-series glycosphingolipid was discovered as the first multivalent LecA inhibitor. ^[64] Globo glycosphingolipid is also known to be present on lung epithelial cells. ^[49,64] Previously it was shown that the natural disaccharide melbiose ($\alpha\text{Gal1-6Glc}$), and galabiose ($\alpha\text{Gal1-4Gal}$) can bind to LecA with micro molar affinities. ^[57,64] The affinities of the two identified binding globo-trisaccharides is 68 μM and 77 μM , respectively.

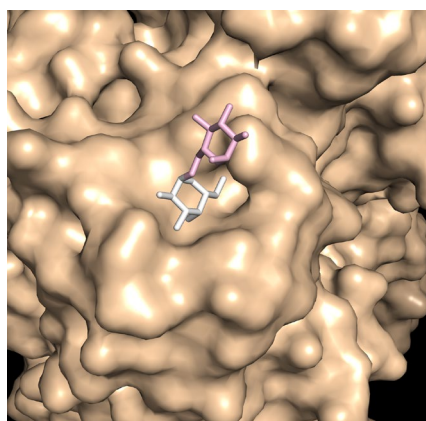


Figure 4. Surface representation of the sugar binding site of LecA in complex with Melbiose. Crystal structure of LecA in complex with Melbiose. (pdb code 4AL9) The galactose part of Melbiose is depicted in light grey and the glucose part is depicted in light red. The glucose does not make any contact with the amino acids of the carbohydrate binding pocket of LecA.

Looking at the crystal structure of the LecA in complex $\alpha\text{Gal1-3}\beta\text{Gal1-4Glc}$ trisaccharide the atomic basis of the specific binding of the second galactose residue is revealed. In the binding site, the non-reducing αGal is fixed within the binding site and participates in the coordination with the Ca^{2+} -ion. Although the hydrophobic contacts are rather limited since only the CH group at C_2 interacts with the side chain of Tyr61, the overall orientation of galactose is very similar to that observed in the complex between LecA and galactose alone. ^[56-57,64] Like nature uses multivalence to increase binding affinity, chemists have tried to enhance the binding affinities of galactose based inhibitors by multivalent display ^[65,66] However, showing affinities in the micro molar affinities both globo-trisaccharide are rather weak inhibitors, researches have been inspired enhancing the affinity to LecA by exploiting multivalent display. A dramatic increase in

Introduction

affinity was obtained using a poly-PA- α - or β -Gal ligand with binding constants of 4.12 μ M and 5.05 μ M, respectively. [67] The use of calixarene or fullerene scaffold increase the potential of a single galactose of up to 200-fold, leading to ligands with 176 nM and 44 nM. [68–72] Glyco nanoparticulates were also presented with an affinity of 50 nM and an increase in potency of 30-fold compared to the used single galactose monomer. [73] Exploration of the hydrophobic interactions, a peptide dendrimer linked with 4-carboxy phenyl β -galactoside was synthesized and tested with an affinity of 100 nM. [61,74] Due to their sugar moiety, D-galactose based LecA inhibitors have a good water solubility, which is an important feature for biomedical applications. [75] Moreover, due to the cluster effects of multivalent ligands, the affinity can be improved. On the downside, oral application in cystic fibrosis patients might be unfeasible with large ligands as the potential drug has to be administered as an aerosol. This is mainly because multivalent ligands are usually larger and have a higher molecular weight than monovalent ligands. Due to that, the oral bioavailability is decreased, as well as excretion rates and tissue permeability are decreased.

1.2.2.2 Inhibitors lectin LecB are based on D-mannose and L-fucose

Like LecA, LecB was isolated in 1977 from the heat stable fraction of a *P. aeruginosa* isolate. [28] Soon after the protein was identified as a mannose binding agglutinin, its ability to bind to L-fucose, L-galactose and D-fructose was determined. (Figure 5) [47, 55, 76–78]

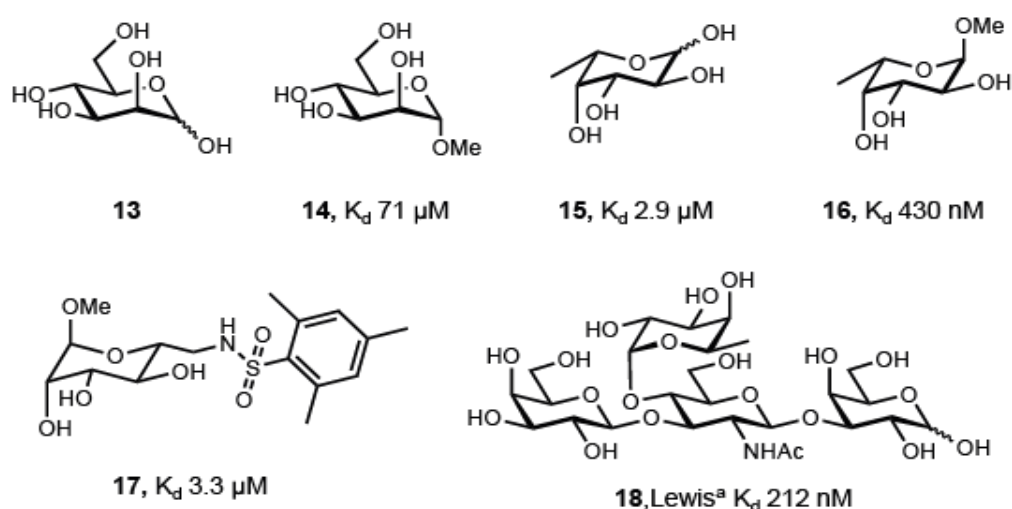


Figure 5: Ligands of the *P. aeruginosa* lectin LecB. The natural ligands D-mannose (13), and L-fucose (16). Enhanced affinities are obtained by introduction of a methyl moiety (15, 16). The synthetic mannose-based inhibitor 17 having an increased binding affinity. Lewis^a 18 is the most potent natural ligand.

1.2.1.3 Targeting of both lectins, *LecA* and *LecB*, simultaneously

Individual research on either of the two *P. aeruginosa* lectins in the past years have paved the way for the development of bivalent ligands. Since both lectins are suspected to be present on the bacterial surface and within the biofilm, a dual inhibitor could be an elegant way of targeting the bacterial virulence. Extensive studies on the individual contributions to *LecA* and *LecB* affinities make a rational ligand design of a combined ligand a promising approach. [78-85] Combined with the knowledge, that a mimic of Lewis^a has been tested with an IC₅₀ of 47 μM for *LecA* and 1 μM for *LecB*, this can be taken into account for a bivalent ligand. [49, 86-87]

1.3 Analysis of protein-ligand interactions using biochemical and biophysical methods

For the determination of potential ligands, testing systems are crucial. Within years of research, several methods emerged and have been improved. Every method offers advantages and disadvantages. For high through-put screening, fluorescence polarization (FP), a thermal shift assay (TS) and surface plasmon resonance (SPR) are most frequently used techniques. [6,59,88-91] In addition, enzyme linked lectin assay (ELLA) isothermal titration calorimetry (ITC) are also frequently used.

1.3.1. Isothermal titration calorimetry

Isothermal titration calorimetry (ITC) is a technique which measures the energy associated with the interactions of two molecules at constant temperature. It is a direct method for the determination of thermodynamic parameters associated with complex formation between two components, for example a protein and its ligand. [92,93] From one titration a complete thermodynamic profile, that includes all relevant data like enthalpy changes (ΔH), the association constant (K_a), which can be used to determine the binding affinity (K_d), and stoichiometry (n) can be derived. [63] Using this initially obtained data, changes in entropy (ΔS) and Gibbs free energy (ΔG) can be calculated and directly related to the mechanism of binding. [94,95] Up to date it is the most preferred method for measuring the thermodynamics of ligand binding. [96] In contrast to other techniques like SPR or FP measurement, ITC has no limitations like immobilization or the need of a fluorescent probe. [95] On the other side, the disadvantage of this method is the huge amount of material needed, and thus this method is not suitable for high-through put screening nonetheless it can be used to characterize binding behavior of selected ligands. [94] Up to date, isothermal titration calorimetry is becoming a major tool in drug discovery, mostly as a second screening technique to eliminate false positive screening hits. [94-96] Additionally, it is used to validate computational estimations of binding energetics, and can be used for hit selection and lead optimization. [97]

Introduction

1.3.2 Thermal shift assay (TSA)

Basically, the thermal shift assay measures the melting temperature of the target protein upon binding of the ligand using a fluorescent protein dye. ^[98-99] In the thermal shift assay (TSA), samples of a protein are mixed with a potential ligand and a fluorescent hydrophobic dye. Folded proteins will not bind to these types of dyes, but molten and denatured proteins as well as intermediates will bind them, resulting in a sharp increase in fluorescence. In case of a binding event of the ligand to the protein, the apparent melting temperature of the protein is shifted to a higher value. ^[98-100] This shift is caused by ligand induced stabilization of the protein due to energetic coupling and resulting changes in the midpoint for thermally induced melting curve. The shift can be observed by heating the sample in a fluorimeter with fluorescence read-out. In some cases, the binding of a ligand can also decrease the protein stability, causing it to denaturation with less temperature applied, depended on the protein structure. ^[101] This method has not only been applied in drug discovery, but also to optimize ligand and buffer conditions for crystallography. ^[100,102]

1.3.3 Fluorescence polarization assay (FP)

An assay based on fluorescence polarization (FP) is a versatile solution-based technique and have been widely used to study molecular interactions. Since Perrin first theoretical described the fluorescence polarization in 1926 it took almost 20 years to first use fluorescence polarization in studies on bovine serum albumin and ovalbumin conjugated with the fluorescent dansyl chloride. ^[103-105] From then on, the application has evolved to study of molecule-protein binding in high through put- and automated settings. ^[106-109] The principle of FP assays is based on the fact that the degree of polarization of a fluorophore, the so-called reporter ligand, is inversely related to its molecular rotation. FP is quantitatively calculated from the difference of the emission light intensity in parallel and perpendicular direction compared to the excitation light plane. Using these changes, the binding of a ligand is monitored by changes in the fluorescence polarization. As the free reporter ligand is bound to the protein, it tumbles slowly causing high fluorescence polarization, upon displacement from the protein, it is free in solution, rotates fast resulting in a low fluorescence polarization. ^[104,107,110-111] While the method has grown to more attention, multiple reviews on the FP method have been published covering the versatile possibilities of its applications in basic research and drug discovery. Despite the fact, that FP has become as a technique which allows miniaturization for high through put in many fields, the application in lectin-carbohydrate interactions has lagged. ^[88] One reason is the low affinity of this carbohydrate-lectin interactions resulting in the requirement for high protein concentrations has long delayed the development. From the first time, the method was used for plant lectins interactions, a high concentration of 200 μM plant lectin were needed, and an assay of the human E-selectin was done with 160 μM of selectin. ^[112-113] With growing advances in instrument sensitivity and ligand improvement FP assays are now used as a routine screening method for galectins and for the two pathogenic bacterial *E. coli* with its lectin FimH and for *P. aeruginosa* with its lectins LecA and LecB. ^[79, 81, 84, 85, 88, 110-111,114-115] In addition, it has already been used for the screening of new inhibitors

for *Burkholderia cenocepacia* BC-2LA. ^[116] Like every other biochemical method, FP has its pros and cons: The drawback of the FP assay is that it can suffer from auto fluorescence and fluorescence quenching by ligands. Effects like this can interfere with FP calculation. ^[117] Since this method is detecting the fraction bound of the tracer, saturation of the binding is needed and thus the total amount of protein being required is dependent on the binding affinity between protein and tracer. Consequently, high protein concentrations can be required. ^[108,112,117] In contrast, one of the many advances of the FP assay is that it is a simple, high speed method, that is relatively low in costs. In addition, the combined advances in the FP assay method make it applicable into new types of targets and for screening set ups. ^[117]

1.3.4 Surface plasmon resonance (SPR)

Since the first commercial surface plasmon resonance (SPR) instrument was available in 1991, this method has been widely used. ^[118,-119] It can be used to examine protein ligand interactions. In this method, one of the two binding partners is immobilized on a surface, typically a gold chip. Up to date, there are several immobilization methods known as formation of a self-assembled monolayer between sulphur and the gold surface or the covalent attachment to a carboxylated dextran membrane. ^[118] Polarized light from a laser source is directly applied on the gold surface of the chip and the generated plasmon reflection angle is measured. Changes in the reflection angle are observed upon binding of a ligand to the immobilized target protein. When the steady state is reached, thermodynamic data like K_{on} and K_{off} can be determined from SPR experiments, and so insight into binding behavior of ligands can be obtained. Besides the costly chips, the fact that the protein is immobilized and thus the function can be influenced is one of the great disadvantages. One advantage of the method is the fact, that the surface can be regenerated after an experiment and experiments can be started again. The lowest detectable concentration in SPR is a critical parameter and is set up dependent on numerous factors including the molecular weight of protein and ligand, optical properties of either of the two and as well as the binding affinity of the analyte molecule. ^[120-121] Moreover, the binding to a specific area of the protein cannot be assessed. But on the other hand, proteins with unknown function can be evaluated.

1.3.5 Enzyme linked lectin assay (ELLA)

Developed in 1984, the enzyme-linked lectin assay (ELLA) is derived from the earlier developed enzyme linked immuno-S-assay (ELISA). ^[122-123] In the lectin assay format, typically, a 96-well plate is coated with a sugar and after subsequent blocking, a biotin-labelled lectin is added. Binding to the surface is evaluated using a readout of the used label. Potential inhibitors are evaluated by their potential to compete with the immobilized sugar surface. ^[124] Based on this technique, the glycosylation of proteins and binding of lectins has been widely studied. ^[125-127] But since this method requires numerous handling steps, the reproducibility between different experiments is rather low. ^[128] On the pro side of the assay, the binding to a specific binding site can be evaluated if the carbohydrate preference is known. On the downside, it cannot be used to assay the interactions of lectins with unknown ligands and in high through put set-ups.

1.4 Determination of ligand protein interactions by nuclear magnetic resonance (NMR) methods

Nuclear magnetic resonance (NMR) measures the chemical shift of molecules in the magnetic field. In general, the method can have the ability to shed light on the structure of a molecule but also give information on molecule interaction on an atomic level.^[135] Since its commercial availability in the middle 1960s continuous instrumental improvements have dramatically increased the potential of NMR and is thus nowadays a powerful tool in drug discovery.^[129] Nowadays NMR has a great variety of potential applications e.g. the detection and characterization of a ligand binding to a protein or mapping and identifying the binding site in solution. In general, two different approaches can be used: protein-based NMR methods, in which signals and effects on the target protein are studied, or ligand-based approaches in which ligand effects are followed by NMR.

1.4.1 Ligand-based NMR methods

NMR methods using the ligand signals can be used. There are different ligand-based methods used up to date: Within the past years, a multiplicity of different ligand-based methods was established. The principle of nuclear Overhauser effects (NOEs) was already described in 1972; NOE experiments have then been used to determine the 3D structure of molecules due observing transferred NOEs.^[159-160] It can be distinguished between inter- and intramolecular NOEs, whereas intermolecular NOEs are used to examine ligand and receptor interactions, intramolecular NOE are the key to study ligand conformation in the protein bound state.^[161-162] Another technique, frequently used is the saturation-transfer NMR spectroscopy (STD-NMR). It is based on the fact, that for weak binding ligands, there is an exchange between free and bound state.^[163] For the STD NMR experiments, a spectrum with a selectively saturated protein (on-resonance), due to irradiating at a region of only protein resonances, is subtracted from the NMR spectra without irradiation. In the difference spectrum, only signals that have received saturation via spin diffusion from the protein will remain, all signals from non-binding ligands will disappear. Some information of the orientation of binding can be drawn from the fact, that only the signals of hydrogens that are in close contact of around 5 Å receive magnetization from the protein will have more intense signals.^[164-165] The difference between a STD and a normal NMR spectrum enables the possibility to screen compound libraries for binding to a target protein.^[159,166-167] Moreover, the binding of carbohydrate ligands to their target proteins has already been studied with the STD technique.^[141,159,167] Since the method depends on the exchange between free and bound state, the major drawback is the limited affinity range. Due to the high concentration needed for low affinity ligands and resulting solubility problems, low affinity ligands could be missed in screenings. On the other hand, very tight binding of ligands might have led to slow exchange and thus ligand signals in solution can also be missed.^[159,164-166] For very hydrophilic targets, the use of

saturation transfer through bulk water instead of the protein (waterLOGSY) can be used.^[168] The advantage of either of the methods is that no labelling is required since only the ligand signals are used, and unknown epitopes can be examined.^[129,148,168] Besides typical ligand based approaches like STD^[169], and waterLOGSY^[168], relaxation-edited approaches are nowadays widely used in drug discovery.^[150,155,170-171] Compared to the used protein targets, these small compounds have smaller relaxation rates R_1 and R_2 , but after a binding event, the small molecule share the NMR properties of the larger target. Thus, small molecules that show binding have a larger R_1 and R_2 .^[155] The transverse relaxation rate $R_2 = T_2^{-1}$ is directly depended on the overall molecular rotation correlation time.^[155,172] This is more evident in the $R_{1\rho} = T_{1\rho}^{-1}$ dispersion experiments, where magnetization along the spin-lock field in the rotating frame is followed.^[155,173] To measure transverse relaxation, Carr-Purcell-Meiboom-Gill (CPMG) or $T_{1\rho}$ experiments are used.^[155,157,170,172-174] This method has the advantage of the possibility to examine a mixture of ligands, and thus the potential application of it in high through put screening, but it does not give information on the binding site or ligand conformation.^[152]

In the time since its discovery, nuclear magnetic resonance (NMR) has become a powerful tool in medicinal chemistry as well as structural biology.^[137,143-147] Besides different developed methodologies ligand-based NMR approaches can have several advantages over protein-based approaches.^[139,144,148-151] Ligand-based approaches have the ability to detect binding up to ten-fold below the K_d value.^[152] One of the most promoted advantages of ligand-based methods is the applicability in the study of low affinity ligands.^[152-153] In fact, low-affinity ligands are perfectly suited for ligand-based NMR methods, as the exchange of low-affinity ligands is slow on the NMR time scale, and consequently the K_{off} is larger than the chemical shift difference between the free and the bound form, ending up with only one NMR signal.^[148,152] Even though ligand-based NMR methods look at ligand effects in solution, and the ligand-target complex is too short to be observed, the free ligand carries information obtained by binding to the macromolecule.^[146,148,152-156] Usually, ligands used for ligand-based methods have masses of smaller than 500 Da.^[155,157]

1.4.2. Protein-based NMR methods

In protein-based NMR methods effects on the protein are studied. Protein-based approaches are used to study structure, function, and dynamics of a target protein.^[130] To study proteins in NMR different approaches can be followed: First, the protein can be expressed using a ^{15}N tag and so 2D protein-based NMR techniques based on a hetero nuclear single quantum correlation, mostly using a ^1H - ^{15}N correlation can be applied.^[131] The chemically unique amide “NH”-groups give insight on the tertiary structure of the protein. Also, upon addition of a potential ligand to the ^{15}N labelled protein chemical shift perturbation (CSP) can be measured and like this, ligand specific binding can be monitored.^[132] CSP approaches have been extensively used in the binding site identification of small molecules, and CSP has gained even more attention after the introduction of the structure-activity relationship (SAR) by NMR technique in 1996.^[133]

Introduction

For the addition of SAR methodologies to the CSP approach data of a weakly binding compound with a known specific binding site are used for the optimization of the observed interaction. Using this optimization ligands binding to the adjacent site are identified, followed by the elucidation of the orientation and linking of the two weakly binding fragments to potentially obtain a more potent ligand. Since its first description in literature, SAR by NMR has been used successfully in the development of different potent inhibitors. [134–136, 302] Other protein-based methods using uniformly ^{15}N labelled protein are Transverse Relaxation Optimized Spectroscopy (TROSY), $^1\text{H}^{15}\text{N}$ Heteronuclear single quantum correlation (HSQC). HSQC was first used by Geoffrey Bodenhausen and D.J Ruben in 1980 and is measuring a 2D spectrum with one axis for the proton (^1H) and the other for the heteronucleus (for protein usually ^{15}N or ^{13}C). The spectrum then contains a peak for each proton attached to a heteronucleus. [135] The method can be combined with other NMR experiments like NOESY-HSQC (nuclear Overhauser enhancement spectroscopy) or TOCSY-HSQC (total correlation spectroscopy). In NOESY experiments magnetization is exchanged between all hydrogens using the NOE (Nuclear Overhauser effect) giving information on the structural arrangement of the nuclei. In contrast TOCSY is used to divide proton groups using spin-spin coupling of only ^1H nuclei.

TROSY is an NMR technique based on transverse relaxation mechanisms, which is used to determine the width and intensity of the acquired NMR signal with enhanced quality resolution. Pervushin and co-workers developed a sequence to obtain a signal transfer by a long delay for the magnetization transfer, allowing the seriously reduced magnetization due to a fast decay in T2 magnetization. [139] The additionally used WATERGATE-sequence was used to enhance the sensitivity of the measurements in non-deuterated solutions. [140] For lectins having molecular masses around 40 kDa, TROSY is a perfect approach. For larger proteins, the solvent exposed amides by TROSY (SEA-TROSY) experiment offers the advantages, that only exchangeable amino protons are detected. Sensitivity can be increased up to four-fold by applying cryo-probe technology. [141] It has been shown that the concentration of the ^{15}N -labeled protein can be reduced with a cryo-probe by a factor of four. The additional use of ^{13}C is not only more expensive, but also increases the complexity of the spectra and is consequently not widely used in the ligand- or binding site identification. Only ^{13}C proteins with selectively labeled methyl groups of valine, leucine and isoleucine have been used in ligand screening. [142] The above mentioned techniques are most frequently used in the identification of the binding site, or ligands binding to a target protein.

1.4.2.1 The use of spin labels in NMR techniques

In addition to both above mentioned approaches, spin labels can be used in protein-based methods. Spin labels are organic molecules or ions which possess an unpaired electron causing paramagnetic effects. In general spin labels can be attached covalently to the probe or non-covalent. In a variation of relaxation-edited approaches, the spin labels are attached to the protein side chains as a tool to identify interacting compounds (SLAPSTIC) method developed by Jahnke and co-workers. [175-176] In this approach, a spin label is covalently attached to the target protein, for example at the side chain lysine or cysteine, and binding

of a potential ligand in the vicinity of the spin label is detected.^[175] Paramagnetism of the introduced radical spin label, e.g. TEMPO, is caused by the unpaired electron. Compared to Nuclear Overhauser effects (NOE) which range up to 5 Å it has a long effective radius of 20 Å.^[177-179] In addition, the spin label can be introduced to a first site ligand, to detect a ligand binding at a potential second binding site.^[176] Besides the use of covalently attached spin labels, the use of paramagnetic ions is explored in NMR experiments.^[180-188] While paramagnetic ions are used commonly in structural biology, and protein-based NMR methods^[189-193] its applicability in ligand-based methods has developed slowly.^[187,193-194] But paramagnetic NMR probes bring several advantages like the possibility to observe pseudo contact shifts (PCS), paramagnetic relaxation enhancement (PRE) and residual dipolar couplings (RDC).^[187,190,193,195-196] In addition lanthanide ions have long-range paramagnetic effects ranging up to 40 Å.^[187,197-199] Lanthanides show different magnitudes of the associated anisotropy when placed in the same environment, resulting in different magnitudes of the observed paramagnetic effects.^[187,206-209] Compared to diamagnetic lanthanide ions, like La³⁺, Y³⁺, Lu³⁺ and Sc³⁺, the ions Er³⁺ and Yb³⁺ are mildly paramagnetic, and Dy³⁺, Tb³⁺ Ho³⁺ and Tm³⁺ are highly paramagnetic.^[206] Gd³⁺ has a special position within the lanthanides, as it only causes PRE but no PCS, and is very widely used in MRI contrast agents.^[187,208.] As lanthanides do not play a known role in biology, using lanthanides in NMR methods ensures bio-orthogonality. For the use in NMR techniques the natural metal ion, like Ca²⁺, Mg²⁺ or Mn³⁺ are replaced with lanthanide ions.^[187] With the emerging need to speed up the drug development processes, the use of paramagnetic metal ions has become more.^[194] Besides the ability to combine high through put screening with quantitative information, NMR offers the possibility to detect weak binders and secondary binding sites.^[170,194, 221-222] So far, the substitution of natural metal ligands, like Zn²⁺, Mg²⁺ or Ca²⁺, with paramagnetic metal ions has only been rarely used. But functional replacement of the natural metal ligand zinc in the matrix metallo proteinases with paramagnetic cobalt was one of first literature known examples for the use of lanthanides in NMR screening.^[194,227-232] It was shown, that more information are obtained from simple proton spectra in presence of paramagnetic ions, compared to diamagnetic ions because of an inhomogeneous signal decrease in presence of paramagnetic cobalt.^[194] Furthermore, the use of paramagnetic cobalt enhanced the sensitivity of up to 10 fold.^[194] While the natural metal ligand in metal binding proteins can be easily substituted with non-covalent binding proteins without a metal binding site have to be tagged, making them the less suitable targets.^[214-215,217,221]

Introduction

1.4.2.2 Angle- and distance determination using paramagnetic lanthanide ions

Paramagnetic ions cause two different effects: Paramagnetic relaxation enhancement (PRE) Pseudo contact shifts (PCS).

In general, the changes in chemical shift of an observed nucleus under influence of a paramagnetic centre are called pseudo contact shifts. They are mediated through space interactions and are dependent on the paramagnetic distance and the angles to the paramagnetic center.

Paramagnetic relaxation enhancement (PRE) describes the phenomenon of an enhanced drop in signal intensity of signals in the proximity of a paramagnetic probe. Since PRE effects are solely dependent on the distance to the paramagnetic center, the distance between the paramagnetic center and the nuclear active spin can be determined from increased relaxation rates.

The nuclear spin senses the unique magnetic moment of neighboring spins, electronic or nuclear ones. And under the experimental conditions, transversal relaxation time T_2 corresponds in approximation to T_1 in the rotating frame, i.e., $T_{1\rho}$. As this effect is strongly distance dependent, it decreases with the inverse sixth power of the proton electron distance r . This paramagnetic relaxation enhancement can be used to gaining information on the geometrical alignment of the binding ligand. Organic radicals like TEMPO bear one unpaired electron and therefore the electron spin S is $1/2$, resulting in measurable effects of the NO radical on proton relaxation up to 15 \AA . In contrast, paramagnetic transition metals have a higher number of unpaired electrons, resulting in a higher S number and therefore a higher resulting magnetic moment. These paramagnetic metals have consequently a stronger relaxation enhancing influence on remote protons. Making them the better choice for signals with a bigger distance to the paramagnetic centre, like in second site screening. In literature, paramagnetic relaxation enhancement of lanthanides is reported for a distance to the paramagnetic centre of up to 40 \AA . ^[198,226]

2 Aim of the thesis

Just as the work presented in this thesis, the aim can be divided in three parts: The first aim was the determination of a SAR on the anomeric position of D-galactose, starting from the known LecA inhibitor phenyl β -galactoside. With this SAR a LecA selective lead structure should be determined with an optimized C1 moiety. Compared to one of the first determined ligands, the unsubstituted D-galactose, substitution on the anomeric center has increased the affinity of substituted ligands by 8-fold. Moreover, each hydroxyl group of D-galactose is involved in the binding to LecA within a complex network of hydrogen interactions. Thus, the stereochemistry of D-galactose is important, and derivatives first are focused on the anomeric position (Figure 10).

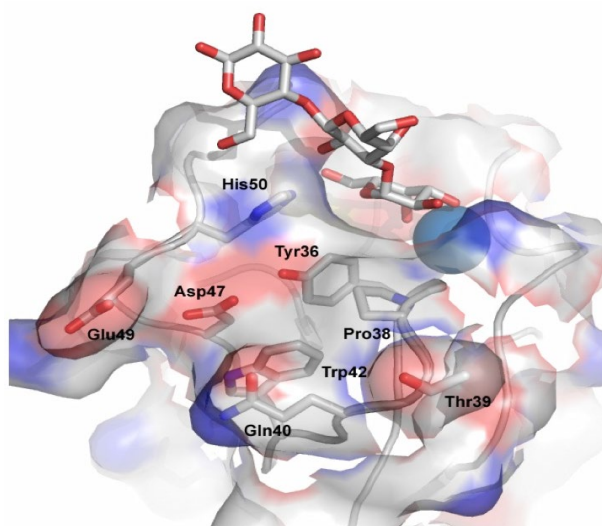


Figure 6: Crystal structure of the LecA binding pocket in complex with the known LecA ligand the globo trisaccharide. The amino acids of the binding pocket are shown (His50, Tyr36, Asp47, Glu49, Asp47, Pro38, Trp42, Gln40, Thr39). PDB ode: 2VJX

Since it was shown that the introduction of a phenyl ring has increased the affinity, the question on further optimization of this chemical structure arises. Hence, a SAR study on the substitution pattern of the phenyl ring will be presented in this thesis. To complete the SAR study, N-Acetyl galactosamine and its derivatives will be studied to investigate their binding on LecA. Moreover, an extended SAR on lactams will be included, to study the potential binding.

The second aim was the development of non-carbohydrate-based inhibitors for the lectin LecA. To achieve this, two different starting points are planned to be evaluated. The first starting point is a virtual screening conducted by Anne Imberty and co-workers. For this approach, the best hits from the virtual screening will be selected and tested in biochemical assays systems, FP, and TSA. The identified hits will then be further evaluated using NMR techniques. In contrast, the second approach is the the usage of a ^{19}F based ligand screening developed by Christoph Rademacher and co-workers. In this approach, a library of 300 fluorinated

Aim of the thesis

compounds will be screened using NMR screening and the determined hits are characterized using more elaborated NMR techniques and biochemical assays. Both above mentioned screening approaches aim at the identification of novel LecA inhibitors binding in the D-galactose binding site but have no sugar moiety.

The third part, the development of a ligand-based NMR method using paramagnetic lanthanide ions, will focus on the development of an NMR method to determine potential second site binders. LecA is a C-type lectin with one Ca^{2+} in the binding pocket which can be exploited in this set up by replacing the calcium with a trivalent lanthanide ion, making this a label free screening approach (Figure 7). For the NMR screening, the biophysical properties of the lanthanide ions will be used, as they cause paramagnetic relaxation enhancement and pseudo-contact shifts on protons with a distance of up to 40 Å to the paramagnetic center. Measuring those effects distance and angle to the effected protons can be calculated.

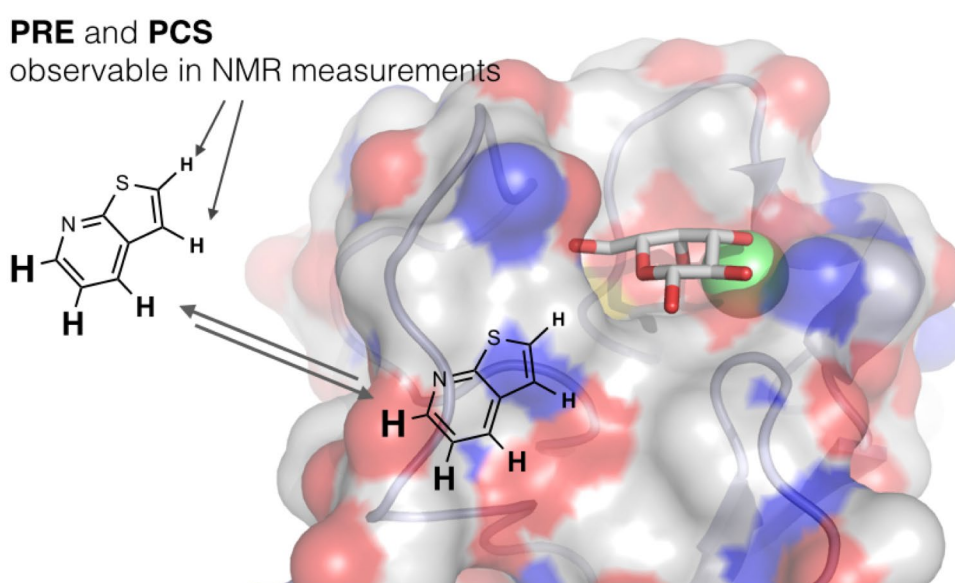


Figure 7: Schematic representation of the NMR screening approach using NMR paramagnetic lanthanides in ligand screening. Paramagnetic Ln^{3+} ion (green) is bound to LecA instead of its natural ligand Ca^{2+} . Upon binding of the ligand, its protons receive magnetization that is visible in the spectra by different relaxation ratios of the proton. The graphical representation of the screening principle is based on the crystal structure of LecA in complex with D-galactose (PDB code 1OKO).

For the NMR screening approach, the binding of the lanthanides to the protein is crucial. It will be assayed using an ELLA approach, because the functional replacement of the natural ligand Ca^{2+} is a key parameter for the screening. If functional replacement of the Ca^{2+} in the binding pocket is shown, evaluation of the method using known LecA ligand will be done. If a second site ligand is identified, it could then be combined with the known LecA inhibitor D-galactose to obtain a potentially more potent LecA ligand.

3. Results and Discussion

3.1 Optimization of D-galactose based lectin LecA inhibitors

In 1972, Garber and co-worker identified the specific binding of lectin LecA from *Pseudomonas aeruginosa* to D-galactosides. [48] Thereafter, glyco-chemists working on inhibiting LecA focused on the design of synthetic galactose analogues. [255–257] A key step for rational ligand design was solving the crystal structure of LecA, in addition classifying LecA as a C-type lectin with one Ca^{2+} in each binding pocket. [56,258]

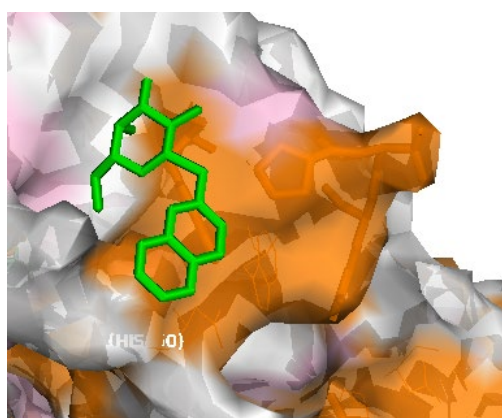


Figure 8: Crystal structure of LecA in complex with its D-galactose based ligand p-naphthol β -D-thio galactoside (green sticks). The pink surface represents hydrophobic areas, whereas the orange shows the aromatic surfaces. (PDB code 4A6S)

Within the multitude of the synthesized galactosides, hydrophobic β -galactosides are the most potent monovalent LecA inhibitors. [60,63] In addition to O-galactosides, thio-galactosides were described as potential LecA ligands. [259] However, a C-galactoside linked aglycon results in a decreased affinity to LecA of $37 \mu\text{M}$ for compound **23**. [260] Since it was shown that hydrophobic substituents in β -position increase the binding affinity of the galactose derivatives due to beneficial π -stacking interactions of the aromatic ring structure and the His50 of LecA. [60] Due to geometry reasons of α -substituted galactosides, the ring renders an altered configuration and thus hydrophobic α -galactosides have a much lower binding affinity to LecA. [58,60] Between O- and S-galactosides a slight decrease in binding affinity was observed for S-galactosides. [58,61,88] Compared to the unsubstituted phenyl ring, different substituents were shown to have influences on the binding affinity. While an electron withdrawing substituent like a nitro group in para position or flour substituents in various positions decrease the binding affinity, addition of a methyl group increases the affinity (**19**, **21**). Addition of a bulky acetamido-acetyl group **10** increased the binding affinity two-fold to $5.8 \mu\text{M}$. [59] Supplementing the phenyl ring with an acetyl linked tripeptide containing lysin, proline and leucine **24** also resulted in a two-fold

Results and Discussion

increased affinity compared to the unsubstituted phenyl **8**.^[58,60] Also for thio galactoside, recent work evaluating different thio-linked aglycons revealed differences in binding affinity between altering aromatic ring substituents.^[38, 61, 63, 85, 87- 90, 93, 260-268,]

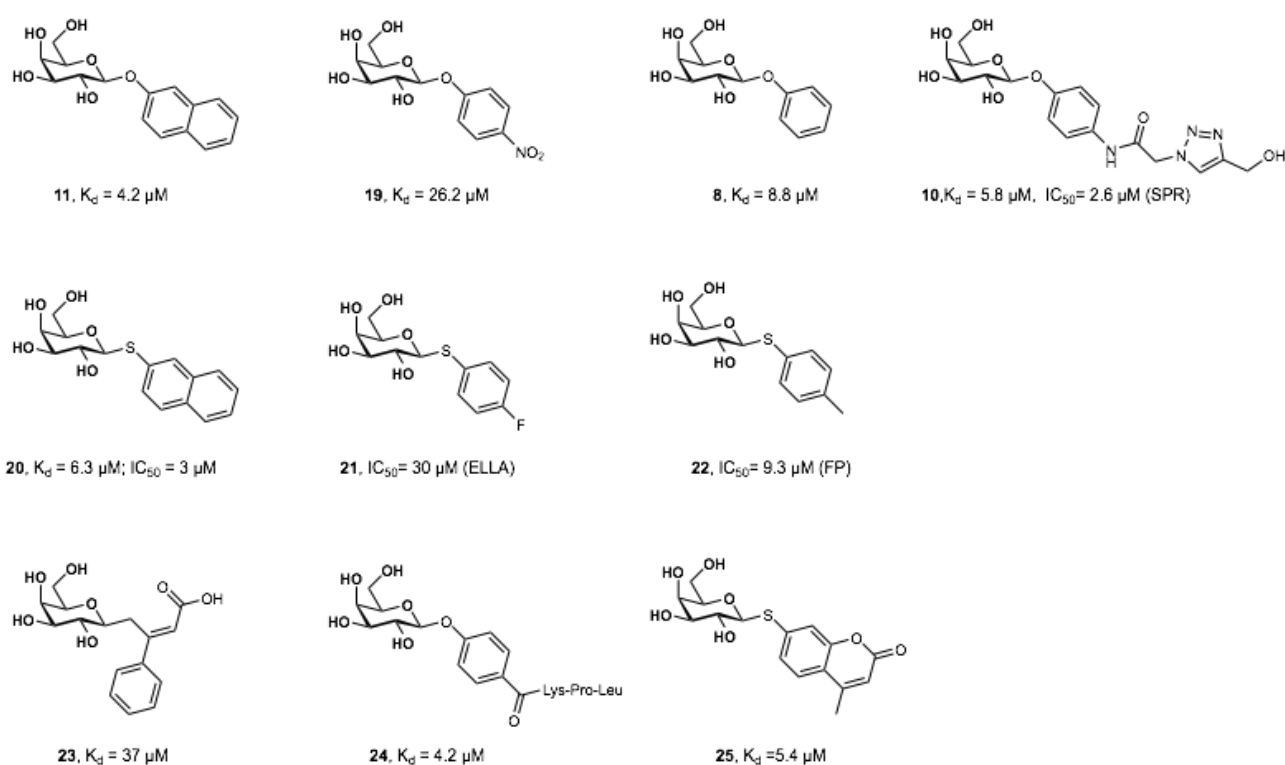


Figure 9: The published monovalent LecA ligands based on D-galactose have affinities in the range between 30 μM and the currently best known inhibitors **10** and **20** of about 3 μM . **11**, **25**, **24**^[60], **19**, **8**^[58], **10**^[59], **22**^[93], **20**, **21**, **22**^[259], **23**^[61]

As none of the evaluated ligands so far have binding affinities in the very low μM to nM range, attempts to enhance the binding affinity by exploring multivalent effects have been pursued by the groups of Vidal and Peters.^[70, 262, 261] In contrast, recently published results point to affinities of multivalent ligands in the lower μM range.^[59, 60] Compared to multivalent ligands, monovalent carbohydrate ligands have the advantages of a better oral applicability and lower molecular weight, making them more suitable candidates for future medicinal applications.^[85]

3.1.1 Enhancement of binding affinity by C1 modifications of D-galactosides

The question, how different substituents on the aromatic phenyl ring influence the binding affinity of the D-galactosides was assessed by synthesis and evaluation of a set of 44 different inhibitors based on the core structure **26**. Different positions of the substituents were tested because alterations in the electronic of the phenyl ring or steric demand of the ligand can influence the binding affinity (Figure 10).^[61, 88, 262]

To examine the above-mentioned question a set of totally 44 different D-galactose based derivatives were synthesized. Phenyl β -galactoside is a known LecA ligand, and to examine the electronic and steric effects of the different substituents 24 different ortho- meta- and para derivatives were synthesized (Figure 12). As the amide linked triazole derivate **10** was reported as a potent LecA ligand^[59], 12 amide- and 8 sulfonamide linked ligands were included into the study (Figure 10). Compared to the amide linkage, the sulfonamide linkage mimics in its geometry more the C-C linkage, and thus both are interesting for SAR studies on the LecA binding preferences. It was previously reported that there is a slight preference of S-galactosides compared to O-galactosides.^[35, 58, 61, 87, 89-90 263-268] And consequently, a small set of four thio galactosides were included in the study (Figure 12).

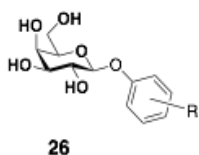


Figure 10: The general structure of the synthesized galactose derivatives with different substituents on the phenyl ring. The ortho, meta and para position of the phenyl ring have different effect on the electronic effects of the ring, as well as the result in different steric demands. Thus, ortho- meta- and para substituted derivatives have been planned.

The starting point of all synthesized galactose derivatives was the penta acetyl protected galactose. This was obtained via acetylation of the unprotected D-galactose to selectively obtain the β -penta acetylated D-galactose after recrystallization. All C₁ derivatives were obtained using a glycosylation reaction in presence of the lewis acid BF₃OEt₂ (Figure 11). Using this lewis acid, β -selective glycosylation was obtained. Only after reaction times of more than two days, the formation of the β -anomer was observed. Since purification of the acetylated product is easier than of the unprotected sugar, all derivatives were purified also on this stage to obtain highly pure compounds prior to deprotection. Then, all final compounds were obtained by removal of the acetyl groups using Zemplen conditions, namely sodium methanolate in methanol (Figure 11).^[262]

Glycosylation reactions typically does not have quantitative yields, and thus for the synthesis of the galactose derivatives over all good to moderate yields were obtained (Figure 11B). Within the O-galactosides, the ortho-substituted derivatives were obtained with the lowest yields. This might be explained by the fact, that the substituent in ortho position sterically hinders the hydroxy group of the phenol during the glycosylation reaction. The meta- or para position might not hinder the hydroxy group and thus the latter two react faster. The limiting factor of the glycosylation reaction is the stereo selectivity, as the favored β -anomer is formed first as the kinetic product. The thermodynamic product, the α -anomer is formed with longer reactions times. In this case the α -anomer is the undesired product and thus the reaction must be stopped prior to its formation.

Results and Discussion

Moreover, the unprotected sugar is a rather polar compounds and thus difficult to purify on silica columns. This explains the fact, that usually derivatives with bulky, hydrophobic substituents like the naphthol derivatives *e.g.* **20**, **48** were obtained with better yields than the more polar compounds, *e.g.* **40** (Figure 12). After synthesis of the set of potential LecA inhibitors, the binding affinity for LecA can be tested using the fluorescence polarization assay. [262]

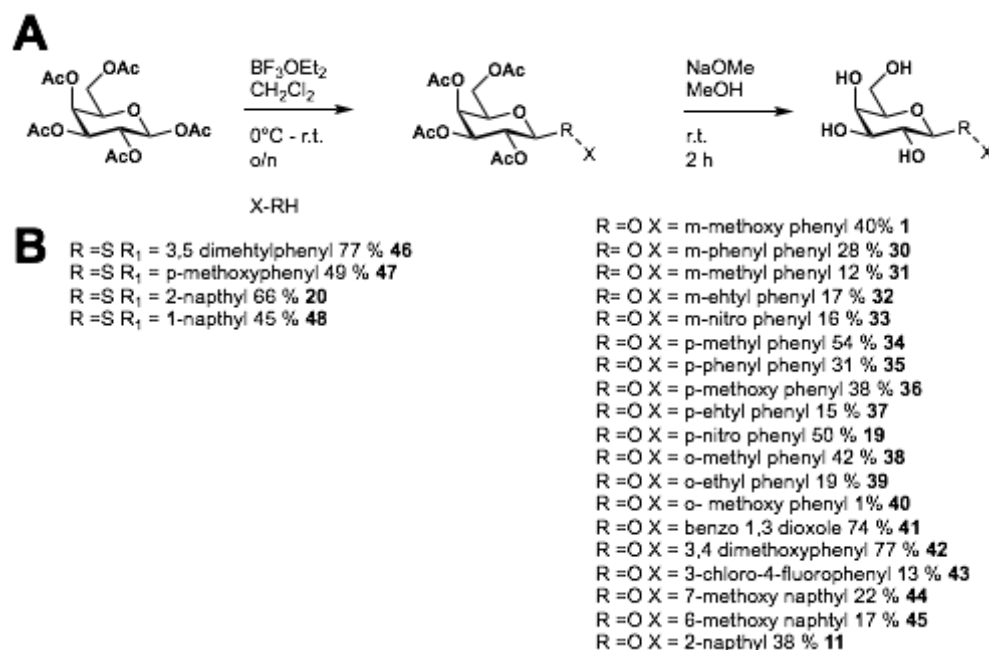


Figure 11: Glycosylation reaction for the synthesis of the C₁ O- and S-galactose derivatives. The glycosylation was done with the Lewis acid BF₃OEt₂ and the corresponding alcohol or thiole derivative. Compared to meta and para substituted phenyl derivatives, the ortho derivative showed decreased yields.

Within the 24 tested D-galactose based ligands, the 2-thio naphthol derivative **48** showed the worst IC₅₀ with 103 μM. In contrast, the 3-methoxy phenyl β-galactoside **1** was tested with an IC₅₀ value of 3 μM, and thus being the best ligand of the series. Within the series of ortho derivatives, the IC₅₀ value of the methyl substituted derivative **38** was in the same order of magnitude as the used standard phenyl β-galactoside **8**. The ethyl derivative **39**, the methoxy derivative **40**, and the nitro derivative **49** showed affinities of higher than 20 μM. This can be explained by the fact, that bulky substituents might have a negative influence on the affinity, as they might clash with the crystal structure of LecA.

A potential steric clash is more likely the explanation than the electronic effects as the nitro- and methoxy-derivatives have electronic withdrawing effects while the ethyl substituent has an electron donating +I effect. Within the series of meta substituted phenyl derivatives all synthesized ligands showed affinities lower than the unsubstituted standard phenyl **8**. Within the m-nitro substituted derivative **33** was the worst ligand with an IC₅₀ of 13.4 μM. For the para series, all derivatives, with exception of the nitro derivative **19**, showed lower IC₅₀ values than the standard phenyl β-galactoside **8**.

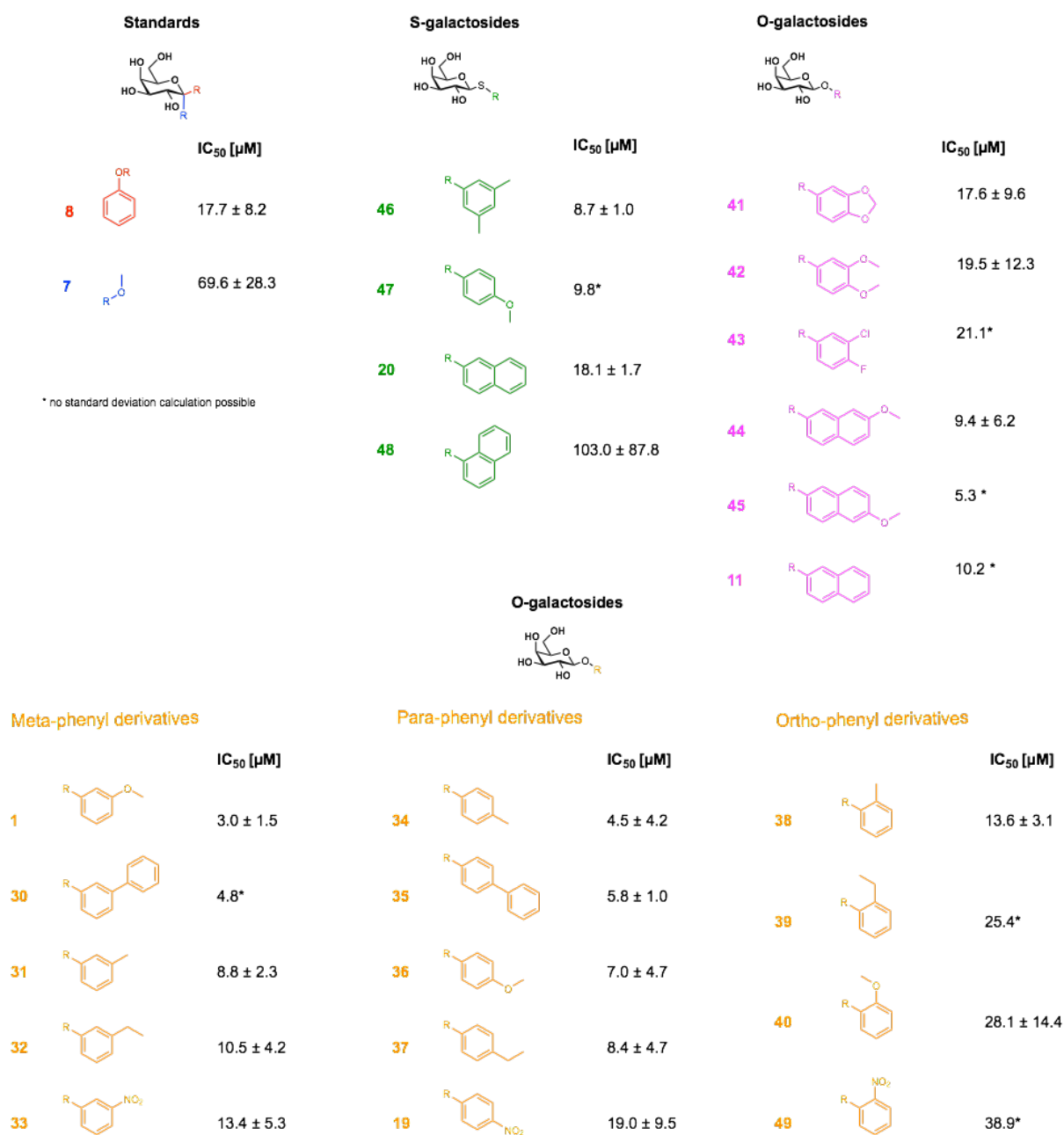


Figure 12: The evaluated D-galactose based inhibitors to obtain insight in the binding behavior of LecA. For the O-galactoside phenyl derivative, a SAR study on the different ring positions was done. In addition, bulkier, di-substituted ligands and naphthol derivatives with an O-linkage were tested. To compared S- and O-galactosides, a set of four thio-derivatives was tested as well.

Therefore, it can be concluded, that the nitro group in ortho meta- and para position is a less favorable ligand than the alkyl substituents methyl and ethyl, or the methoxy- or phenyl substituents. The comparison of S- and O-galactosides, it can be concluded that the binding affinity of p-methoxy phenyl O-**47** or S-galactoside **36** is with $7.0 \mu M$ - or $9.8 \mu M$ comparable. For this substituent, there was no difference between O- and S-galactosides. The published LecA ligand 2-naphthol β -D-thio galactoside (**20**) was tested with an IC_{50} of $18.1 \mu M$, while it was published with a K_d value of $6.3 \mu M$. Since the K_d determination was done with a direct

Results and Discussion

titration using ITC, the determination of the IC_{50} value was used by FP assay. This is an indirect method and explains the difference. Comparison between the two O- (**11**) and S-(**20**) galactoside, a slight preference for the O-galactoside was observed. In contrast, the affinity of the 1-naphthol β -D-thio galactoside (**48**) was with an IC_{50} value of 103 μ M significantly lower than the 2-naphthol derivative (**20**). Moreover, the substitution of the O-2-naphthol derivative (**11**) with a methoxy group in 6- (**45**) or 7- (**44**) position did not improve the affinity. Since the methyl- and methoxy substitution were favorable the di-substituted derivatives **42**, **41**, **43**, **46** have been analyzed. While the di-substituted methoxy derivative **42** showed an IC_{50} of 19.5 μ M, while the di-methyl substituted thio-derivative **46** showed an IC_{50} value of 8 μ M. From this it can be concluded that a substitution in 3, 5 position is more favorable than a 3, 4 substitutions.

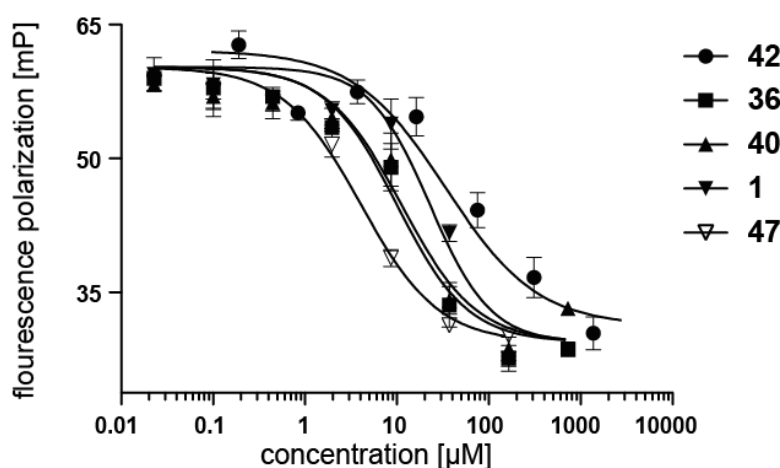
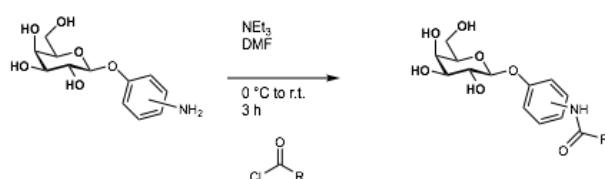


Figure 13: FP determination of the IC_{50} values of the ortho- (**40**), meta- (**1**) and para- (**36**) substituted phenyl β -D-galactoside, the p-methoxy-thiophenyl β -D-galactoside (**47**) and the di-methoxy phenyl- (**42**) derivative

To obtain more insight into the binding behavior of LecA a set of 12 amides- and 8-sulfonamides was synthesized to compete the SAR study. Both linkages are interesting for the SAR study the sulfonamide linkage mimics in its geometry more the C-C linkage. Compared to the previously described phenyl-based ligands, the amide- and sulfonamide ligands were synthesized using an amide formation with chloride (Figure 14). For this reaction, the deprotected amine derivative was dissolved in DMF, and after addition of NEt_3 as base and cooling to $0^\circ C$, the different chlorides were added. Because of the hydrophilic nature of the obtained product, purification of the reaction turned out to be difficult. Since reversed phase was not an option at the time of synthesis, only yields between 13 and 41 % of final product must be accepted.^[263] Also, enhancing the equivalents of chloride from 1.2 to 2 did not enhance the affinity significantly. To improve the yield of the reaction, DMF could be replaced with MeOH for the synthesis, obtaining a protecting effect of the surrounding MeOH molecules to prevent the OH groups of the sugar from reacting.

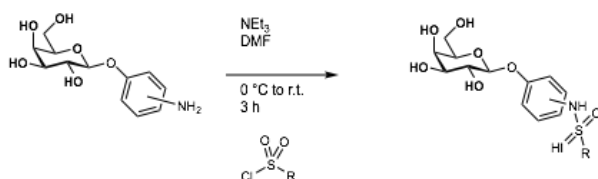
To obtain a full picture of the LecA binding preferences, amide as well as sulfonamide coupled ligands with para- and meta substitution was synthesized (Figure 14). Within the series of the amides, binding affinities between 5 and 20 μM have been determined. Again, the worst inhibitor of the series was the p-nitro derivative **64** with 19.9 μM . Compared to these results, the affinity of the synthesized sulfonamide derivatives was significantly lower (Figure 16). Within the series of the sulfonamides, the para substituted 4-fluorophenyl derivative **65** showed the best IC_{50} value of 10.5 μM , and the para naphthol derivative **67** with a binding affinity of 11 μM . The unsubstituted phenyl derivative **68** and the para nitro derivative **69** have a 10-fold higher binding affinity of around 100 μM . While both, the fluor group and the nitro group have a $-I$ -effect, but while fluor has a $+M$ effect the nitro has a $-M$ effect. This difference gives an indication, that electronic effects play a role in the ligand binding.

A. Amide Couplings



R = m-methylphenyl 35 %, **54**
 R = m-methoxyphenyl 29 %, **55**
 R = m-azido 64 %, **56**
 R = m-1-naphthyl 64 %, **57**
 R = p-thiophenyl 98 %, **58**
 R = p-methoxyphenyl 21 %, **59**
 R = p-azido 71 %, **50**
 R = p-phenyl 9 %, **60**
 R = p-4-Hydroxymethyl-1,2,3-triazol-1-yl 48 %, **61**
 R = p-1-naphthyl 81 %, **62**
 R = p-methylphenyl 24 %, **63**
 R = p-nitrophenyl 76 %, **64**

B. Sulfonamide Couplings



R = p-4-fluorophenyl 11 %, **65**
 R = p-2-naphthyl 23 %, **67**
 R = p-2,4,6, trimethyl phenyl 53 %, **66**
 R = p-phenyl 53 %, **68**
 R = p-4-nitrophenyl 13 %, **69**
 R = m-2,4,6 trimethyl phenyl 23 %, **70**
 R = m-4-nitrophenyl 46 %, **71**
 R = m-phenyl 44 %, **72**

Figure 14: Synthesis of the amide- and sulfonamide derivatives. The sulfonamides **66**, **68**, **69**, **70**, **71**, **72** were synthesized under supervision of Ines Joachim by Maike Lehner during her Bachelor thesis. Overall, both syntheses were carried out in DMF with addition of triethyl amine and addition of the chloride at 0°C. After stirring at room temperature, the final compounds were obtained. Yields are given for the shown synthesis steps.

Results and Discussion

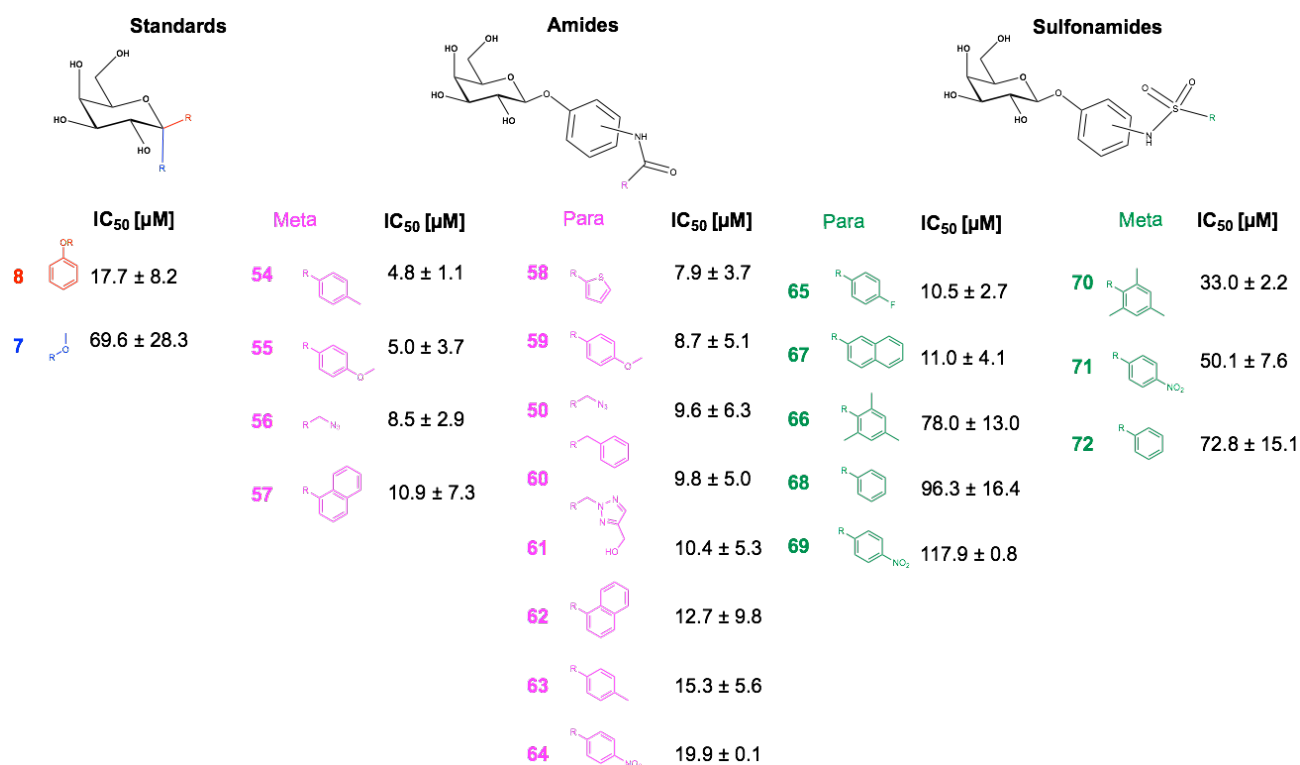


Figure 15: Binding affinity was determined using the FP assay. The determined IC₅₀ values for the amide- and sulfonamide structures showed decreased affinity compared to the C1 derivatives. **66, 68, 69, 70, 71, 72** were synthesized by Maïke Lehner in her Bachelor thesis.^[269] The amides (pink structures) showed better affinities compared to the sulfonamide structures.

Overall, it can be concluded, that both, the meta and the para position are more favorable compared to the ortho position. For the amide derivatives, this effect is even more pronounced, as the substituent is bigger and thus steric effects are more pronounced. Since the methoxy derivatives showed an enhanced affinity, the two disubstituted derivatives were synthesized and analyzed using the FP assay. In contrary to the expected, both derivatives showed a decreased affinity of only 17.6 µM or 19.5 µM, respectively. This result suggests that steric effects or electronic effects of the disubstituted derivatives are less favorable compared to mono substituted derivatives. In contrast, the disubstituted thio derivative with a meta-meta methyl substitution pattern did show an affinity in the same range as the mono substituted derivative. These results suggest as well that mono substitution is more favorable compared to disubstituted. Moreover, the analysis of the two synthesized naphthol derivatives suggest a steric clash of the ortho position since the 2-β-naphthol derivative is 10-times less potent than its 3-naphthol derivative.

From the synthesis of a set of 44 potential LecA ligands it can be concluded, that within the set of 24 phenyl β-galactosides it was observed that substitution in meta position of the ring is favored over para, this is true for substitutions on the phenyl ring and the amides. More significantly, meta and para are better than the ortho position. For the amides, no ortho linked amides were synthesized, because a close examination of the crystal

Results and Discussion

structure suggests a steric clash of ortho substituted ligands with the LecA surface. In comparison worse affinities have been determined for most of the amide- and sulfonamide derivatives. All in all, it can be assumed, that synthesis of C1 derivatives will not lead to a significant increase in the binding affinity compared to phenyl β -galactoside **8**.

Results and Discussion

3.1.2 Evaluation of galactosamine scaffold as potential LecA inhibitor

Within the first detected LecA inhibitors, besides several galactosides, *N*-Acetyl β -galactosamine was discovered to bind to LecA as well. [58] Consequently, the binding potential of galactosamine derivatives was evaluated. For this, galactosamine (GalNH₂) **75** and the substituted 4-Nitrophenyl-2-acetamido-2deoxy β -D-galactopyranoside (p-NP-GalNAc) **76** were tested using the FP assay. [88]

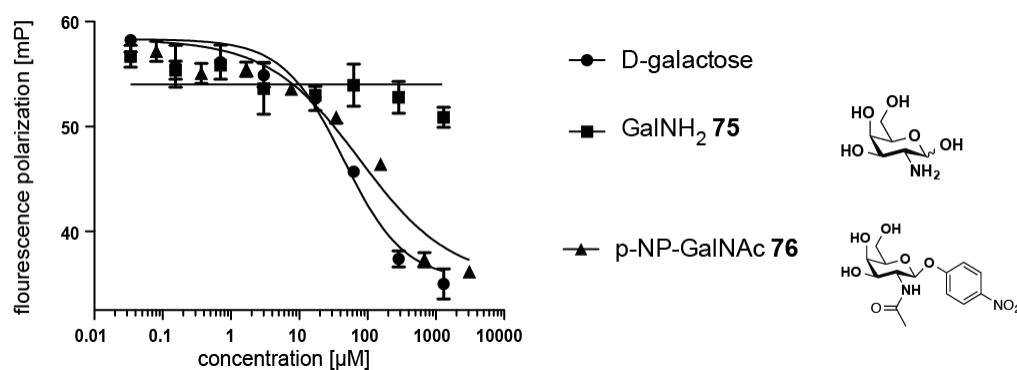


Figure 16: Determination of the binding affinity of galactosamine **75** and 4-Nitrophenyl-2-acetamido-2deoxy β -D-galactopyranoside (p-NP-GalNAc) **76**. Galactosamine **75** showed no binding, whereas p-NPG GalNAc **76** showed binding with a affinity of $136.3 \pm 49.1 \mu\text{M}$.

The unsubstituted galactosamine **75** did not bind to LecA in the tested concentrations, as well as the unsubstituted *N*-acetyl galactosamine. Only the tested 4-Nitrophenyl-2-acetamido-2deoxy β -D-galactopyranoside (p-NP-GalNAc) **76** showed an affinity of $136.3 \mu\text{M}$, which is in the same range as D-galactose. These results are in good agreement with previously reported results which showed a 50 % inhibition of galactosamine after equilibrium dialysis of $400 \mu\text{M}$ sugar derivative with $100 \mu\text{M}$ sugar. [58] Because of the worse affinity of **76** compared to phenyl β -galactoside **8** it can be concluded, that galactosamine is not a suitable starting point for new, more potent LecA inhibitors. Since the derivative **76** is already substituted with a *p*-nitro phenyl moiety in C1 and with an acetyl group at the amine position and has only a binding affinity of $136 \mu\text{M}$. From this one can conclude, that there is little room for improvement. One possibility to improve might substitution at the nitro moiety using different substituents.

3.1.3 Evaluation of Galactonoamidines or Galactolactams as potential LecA inhibitors

There are several LecA ligands known for LecA, but all of them are based on a D-galactose scaffold. [26, 38, 58, 90, 263] The group of Susanne Striegler developed galactonoamidines as binders for the β -galactosidase of *Aspergillus oryzae*. [87, 264] Since β -galactosidases are not only used in industrial processes of dairy products [89] and reporter gene assays [265] but also has a beneficial therapeutic effect in lysosomal disorders. [279] But most interesting, the galactonoamidines are also potent inhibitors of the *Streptococcus pneumoniae* -galactosidase BgaC. [267]

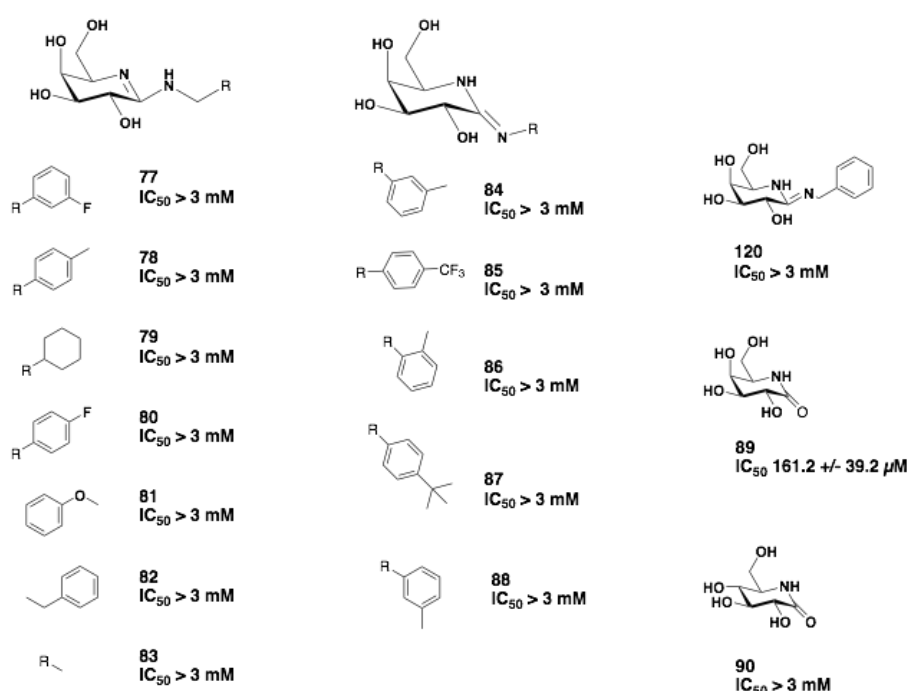


Figure 17: For all tested potential lactam inhibitors, only **89** showed binding to LecA using the FP assay. The ligands **77** to **87**, and **120**, **90** to **88** did not show binding up to 3 mM.

Results and Discussion

Moreover, the affinity of the galactonoamidines is based on the hydrophobic interaction with the methyl group as well as π -interactions of the aromatic ring. [87,264] Due to this reasons, the galactonoamidines might be an interesting potential ligand for the *Pseudomonas aeruginosa* lectin LecA. To test this hypothesis, the ligands provided by the group of Susanne Striegler **77** to **88** were tested in the fluorescence polarization assay (FP).

Within the 15 tested ligands, **77** to **88**, only the β -lactam **89** did show binding to LecA (Figure 17 and 18). The β -lactam **89** did show a binding affinity of 161.2 μ M, which is in the same range as D-galactose itself. In contrast, the glucose analog **90** showed no binding to LecA. This is in good agreement with the fact, that D-glucose itself does not bind to LecA. [58]

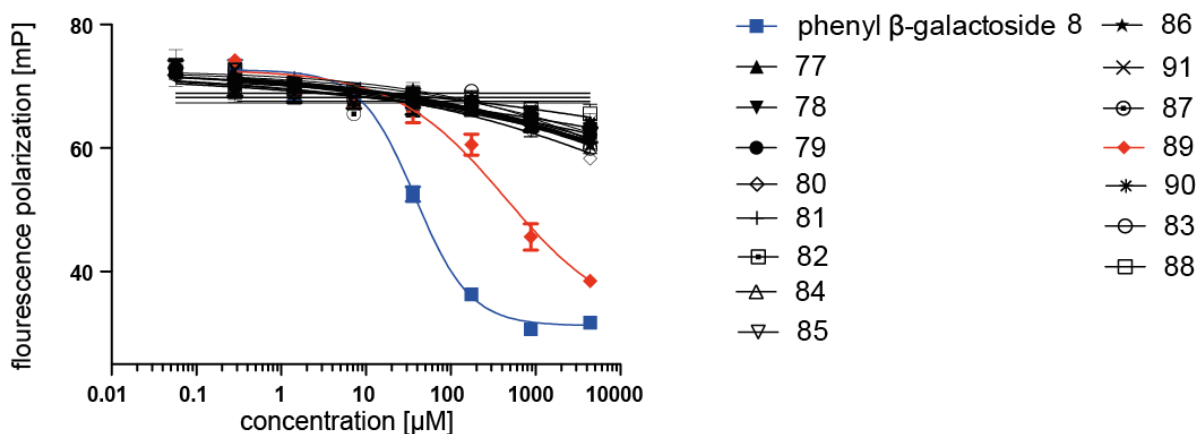


Figure 18: Representative FP assay titration for the tested galactonoamidine derivatives **77-82**, **84-87**, **88**, **83**, the lactam derivatives **89** and **90**, and phenyl β -galactoside as control. The blue line represents the control phenyl β -D-galactoside, the binding lactam compound **89** is shown in red and all nonbinding derivatives are shown in black.

It can be concluded that only the lactam structure based on galactose showed binding to LecA. All the presented amidines did not show binding, this might be explained by the differences in electronic differences between the nitro- or oxygen in C1 position. In contrast, the lactam structure based on glucose showed no binding, which can be explained by the different hydroxy orientation in the C4 position. Since hydroxy groups in position 3 and position 4 are involved in the binding to LecA, more specifically the coordination to the Ca^{2+} -ion. Moreover, there is a difference in the electronic effects between the amidine and lactam ring structure.

Within the amidines, the ring opposes and reverse anomeric effect, an effect that is termed after the preference of the positively charged nitrogen.^[268]

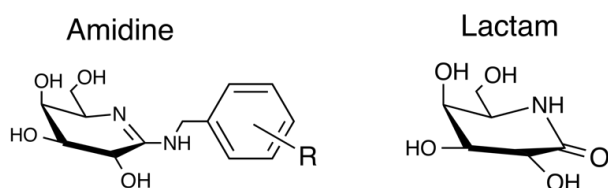


Figure 19 Geometric representation of the galactonoamidine derivatives. This structure varies from the D-galactose structure that binds to LecA.

In summary, new potential ligands can only be synthesized based on lactam structures but can not be based on amidine structures.

3.1.4 Conclusion on the SAR studies for D-galactose based LecA inhibitors

To conclude the SAR examination based on a D-galactose scaffold, m-methoxy phenyl substituted derivative (**1**) was tested as the most potent LecA ligand with an IC_{50} value of 3 μ M in the FP assay. Moreover, the -lactam galactoside (**90**) was shown to be very weak ligand with binding affinities in the mM range. In addition, the ortho position was determined to be the worst position for a substitution, while the meta and para position have been equally good. Compared to the published, best LecA ligands thio naphthol **20**, and the triazole published by Vidal **61**, no significant enhancement in affinity was observed. While *N*-Acetyl -D-galactosamine was reported as a LecA ligand, binding of -D-galactosamine **75** was not determined using the FP assay. The p-nitro phenyl *N*-Acetyl -D-galactosamine **76** showed an affinity of 162 μ M, showing the *N*-Acetyl -D-galactosamine is in need a LecA ligand. But as only the addition of a phenyl moiety at C1 position led to LecA ligand with a determinable IC_{50} value in the FP assay, the *N*-acetyl galactosamine scaffold is a less potent scaffold than D-galactose itself.

3.2 Non-carbohydrate glyco mimetic as ligand of the *P. aeruginosa* lectin LecA

In contrast to the previously describes approaches, which are all based on the natural LecA ligand D-galactose as a scaffold, non-carbohydrate inhibitors could be an alternative. As the known crystal structure of LecA was used as an inspiration for the synthesis of many compounds, they all are containing galactose scaffold to target the primary Ca^{2+} -dependent carbohydrate binding site. [62, 93, 257] The development of non-carbohydrate mimics could be an alternative strategy, opening a potentially large chemical space for novel inhibitors. But carbohydrate-protein interactions can be very complex because of different hydrogen bonds and hydrophobic contacts. For this reason, reported success stories of non-carbohydrate analogs have been limited. One of the very few success stories of a novel glyco mimetic was reported for the model lectin Concanavalin A. A set of glycol mimetic based on a shikimic acid scaffold have been shown to have good inhibitory activity against DC-SIGN, another C-type lectin. [270] Thus it can be concluded, that the presence of a Ca^{2+} -ion should therefore be no obstacle for a glyco mimetic strategy against LecA. To identify novel structures binding to a protein a virtual screening approach can be used. In this screening, a high number of ligands can be screened using a computational set up. Virtual screening could a powerful technique to identify potential ligands from a huge number of potential scaffolds.

For LecA a virtual screening approach was planned to determine new scaffolds, which are potentially binding to LecA in the carbohydrate binding site. This new scaffold will be identified by a virtual screening approach and tested on their ability to bind to LecA in a biochemical assay. For these biochemical assays binding to the first binding site of LecA, the galactose binding site is essential, as the biochemical assay is a competition assay using a reporter ligand with the known LecA ligand galactose. [93] Thus the virtual screening hits will be limited to those binding in the carbohydrate binding pocket.

3.2.1 Screening of the NCI database

The virtual screening was planned and executed by Anne Imberty and co-workers. In summary, the number of 1597 different molecules from the National Cancer Institute (NCI) diversity set IV were docked into the binding site of LecA and 60 were determined as potential hits. [303]

3.2.2 Biochemical evaluation of the determined hits

From the 60 determined binding hits 40 hits have been selected and tested in the previously published FP assay. [88] Using this assay it can be determined if a compound is binding to LecA in the carbohydrate binding pocket, as competition with a galactose derivative is used. In detail, the potential ligands are incubated with a LecA and reporter ligand, a D-galactose based ligand bearing a fluorophore. Various concentrations of the potential ligand are used. If the reporter ligand is tumbling free in solution the fluorescence polarization is low,

while the reporter ligand LecA complex causes a high fluorescence polarization. Thus, after an incubation time the fluorescence polarization of the solution is measured and plotted against the used ligand concentration to give insight to the binding of a potential ligand. This method is limited to ligands binding in the carbohydrate binding pocket, as completion with a D-galactose based ligand is used. Thus, only ligands binding in the carbohydrate binding pocket can be examined. Within all the tested compounds only two have been determined in the FP assay as potential hits, NSC27389 **92** and NSC73735 **93** (Figure 20).

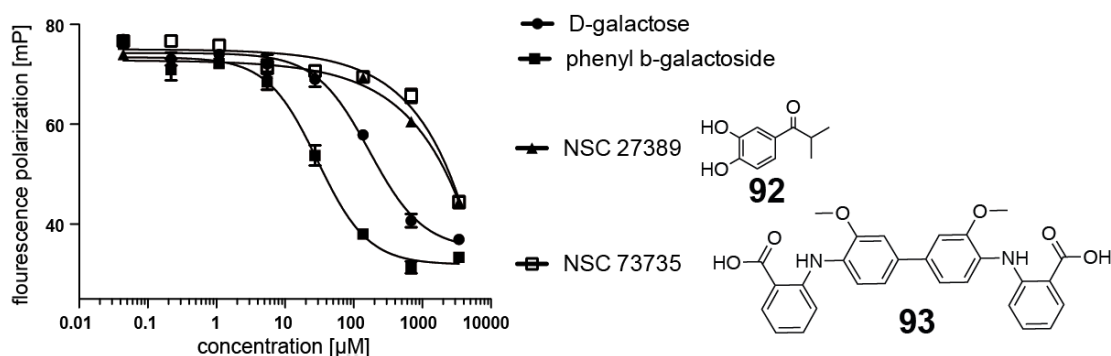
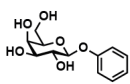
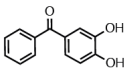
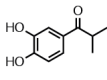
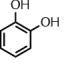
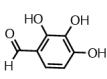
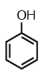
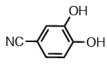
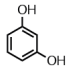
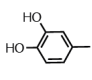
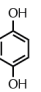


Figure 20: IC₅₀ determination using the FP assay using the conditions published before ^[88]. Both tested virtual screening derivatives influenced the determined fluorescence polarization. For both potential screening hits NSC27389 **92** and NSC73735 **93** no sigmoidal binding curves were obtained. The used ligand concentration was limited due to solubility of the ligands.

For both potential hits an influence on the fluorescence polarization was observed (Figure 20). Compared to the usual observed sigmoidal binding curve, *e.g.* for D-galactose, the binding curve of both virtual screening compounds differs in its shape. Both virtual screening compounds showed only in the highest concentration changes in the fluorescence polarization. From the determined IC₅₀ data, binding can neither be shown nor excluded. To decide on the potential binding of the compounds, a thermal shift assay was done, including the catechol derivatives **94** - **100**. Those derivatives were chosen as potential derivatives of NSC27389 **92**. For the thermal shift assay, LecA is incubated with fluorescent dye, which binds to the protein after denaturation. The LecA dye mixture is incubated in presence of different ligands. In theory, binding of the ligands should stabilize the protein and consequently increase the melting temperature. For the thermal shift assay temperature shifts of 0.4 °C are considered hits. ^[101] Since the theory of the thermal shift assay is based on the fact, that

Results and Discussion

binding of a ligand stabilizes the protein and thus enhances the melting temperature, usually only ligands with positive hits are considered.

	IC ₅₀ [μM]	Temp. Shift [°C]		IC ₅₀ [μM]	Temp. Shift [°C]
8 phenyl β-D-galactoside 	15.8 ± 8.3	1.67	97 3,4 Dihydroxy-benzophenone 	< 2700	0.46
92 NSC 27389 	< 3000	0.34	98 Catechol 	n.b.	-5.76
94 2,3,4 Trihydroxy-benzaldehyde 	n.b.	-3.25	99 Phenol 	n.b.	-3.25
95 3,4 Dihydroxy-benzonitrile 	n.b.	0.26	100 1,3 Dihydroxy-benzol 	n.b.	-0.10
96 1,2 Dihydroxy-4-methylbenzene 	n.b.	-9.58	101 1,4 Dihydroxy-benzol 	n.b.	0.26

n.b = no binding

Figure 21 Representation of the evaluated virtual screening hits using the FP assay and determination of the thermal shift (TS). For the thermal shift values, the difference between the melting temperature of LecA alone and the complex of LecA and the respective compound is shown.

From all the tested potential ligands the standard phenyl b-galactose **8** and 3,4-Dihydroxybenzophenone **97** were determined as hits in the thermal shift assay. The standard sugar ligand **8** was also determined as a LecA binder in the FP assay while for **97** no competitive binding was observed in the FP assay. But also, for **97** binding in the FP assay was suggested as changes in the fluorescence polarization were observed with ligand concentration of more than 2.7 mM. For NSC 27389 **92**, 3,4 Dihydroxybenzonitril **95**, and 1,4 Dihydroxybezol **101** positive thermal shifts were observed which are not considered significant since they are smaller than 0.4 °C. 2,3,4 Trihydroxybenzaldehyde **94**, 1,2 Dihydroxy 4-methylbenzene **96**, Catechol **98** and Phenol **99** big temperature shifts of more than 3 °C were observed. All those big shifts were negative, thus showing that binding of these ligands destabilizes the protein. In addition, negative hits can give a hint on a potential binding event, but then either due to unspecific interactions or with the tendency to destabilize the complex due to binding on hydrophobic regions. From the TS assay **97** was determined as potential hits (Figure 21). With a

thermal shift of 0.34 °C NSC27389 **92** was close to the threshold of 0.4 °C, thus remaining an inconclusive result on the potential binding of the screening hit. All ligands with a negative thermal shift were not considered hits since they showed no binding in the FP assay and probably of false positive hits from the TS due to unspecific hydrophobic interaction with the surface of LecA was too high.

The biochemical evaluation of the obtained screening hits failed to give a clear result on the binding of the potential hits. Since there has been a sign of binding for ligands NSC 27389 (**92**) and NSC 73735 (**93**) they have been examined in ITC experiments, but for both ligands no binding in direct titration experiments have been observed. Both potential hits were expected to have a binding affinity in the milli molar range, and because of the poor solubility of LecA and the ligands, determination of low affinity ligands with ITC is rather difficult. To enhance the probability of identifying low affinity ligands, a replacement titration was done with NSC 27389 (**92**). In this experiment, the target protein LecA is incubated with the potential ligand NSC 27389 (**92**) and titration with the known ligand p-NPG **8** is done. The binding constant of the low affinity ligand **92** can be calculated with respect of the determined titration data of LecA with known ligand alone. As well as the direct titration, the indirect titration failed to give a clear result on the binding to LecA, as well as no binding affinity could have reliably been determined from these experiments. One more method for the determination of binding of the ligands was the use of NMR to obtain more information. Compared to NMR spectrometry, the biochemical fluorescence polarization assay, as well as the thermal shift assay based on the read out of a fluorescent dye have several drawbacks, which can interfere with the obtained results. For both, the assay could have been disturbed by the colored screening hits or their potential of fluorescence enhancement or quenching. With these interferences it is impossible to determine a clear binding curve and it makes the discrimination between real binders and false positives very difficult. Moreover, for the catechol ligand oxidation was suspected that occurs during the incubation time and which caused the fluorescence of the ligand to disappear. Thus, it can be hypothesized, that catechol structures are not very suitable starting points for the determination of new, non-carbohydrate lectin LecA ligands. Since NMR is not influenced by fluorescence, this technique can be used to give a more reliable result on the binding in this specific case.

3.2.3 Determination of the binding affinity using a ligand-based NMR method

In case of small ligands with low binding affinities, one might face the problems with biochemical assays in hit evaluation. Since poor solubility, fluorescence issues or a massive consumption of expensive materials were experienced drawbacks in the verification of the obtained virtual screening hits, one potential hit NSC 27389 (**92**) was examined using a ligand-based NMR approach. This approach was just recently used to examine the binding of a whole library of potential, fragments binding with varying affinities to the heat-shock protein Hsp90. ^[271] Experiments based on ligands effect have the advantage that small amounts of protein are consumed, typically 1 to 10 µM of target protein (in 500 µL). ^[67] Moreover, the use of unlabeled target protein and ligands are a huge advantage. ^[67] Following this approach, affinities between 0.1 to 10 mM can be detected. Using a ligand-based NMR approach was a promising starting point as it is the only biophysical method which enables the detection of binding one order of magnitude beyond K_d ^[148] Thus making it an interesting and promising approach for poorly soluble and expensive ligands. Despite the fact, that NMR is the method with

Results and Discussion

the lowest absolute sensitivity compared to surface plasmon resonance (SPR) or fluorescence based (FP) methods, a variety of NMR techniques have been proposed to detect weak affinity binders.^[147] In general, the obtained proton spectra can be evaluated using the determination of the full width half maximum of the obtained signals, or the frequency of each observed peak. As reviewed in 2012 by E. Kovrigin, NMR line-shape analysis can provide information on ligand binding.^[179] While analyzing NMR line shape in complex transitions is difficult, but utilization for a proposed single binding event was shown to be a powerful tool.^[179] In contrast to the determination of the full width at half maximum, the frequency of the peaks can be used for determination of binding as well. The enhanced line broadening and the chemical shift changes are based on the changing environment due to the binding of a small molecule to the target protein, and thus the chemical environment changes. For the chemical shift determination, an approach to follow changes in the histidine residues of bovine ribonuclease was published already in 1974, and the implication of this method to determine the chemical rate and mechanism of a histidine titration with pH-dependent changes in line broadening was established by the group of Jonsson. Subsequent, the idea to measure proton shifts and use them to determine ligand binding was followed up by Roberts and co-workers in 1978 and transferred to observation of ligand effects. Despite the fact, that chemical shift mapping is used more frequently in protein-based NMR approaches, it can be applied to a ligand-based approach, if some aspects are carefully considered and reviewed:

To start the evaluation of such experiments, it must be examined which exchange conditions do apply for the examined system. In case of a diffusion driven association and dissociation, the exchange rate will be in the range from 10^7 to 10^8 $M^{-1} s^{-1}$ and this will be taken as a first rough estimation the equilibrium constant.^[180] In the event of a tight binder, the exchange will be slow on the NMR time scale. Thus, usually two different spectra are observed, one for the complex and one for the free specie if this occurs at the tested concentration. Usually, this binding applies for K_d values lower than 10^{-7} M. Entering values of around 10^{-3} M the binding will be weak and as a result the exchange will be fast on the NMR time scale. Then, the observed spectra are the average of resonance of the nuclei at the corresponding sites in the free and unbound state resulting in the observation of a single peak moving from the initial to a final position. The progressively shifting frequencies, for example after increasing the ligand concentration as one of the two binding partners, a binding curve is obtained by blotting the chemical shift against the used ligand concentration.^[179-180] Between the both extremes of a slow or fast exchange, intermediate exchange that does not fit to non-Lorentzian will render a clear determination of a binding constant difficult. For the theoretical determination of the binding, a one-to-one binding event is considered, in which ligand plus protein form a ligand-protein complex.^[180] Thus, both presented ways of evaluating the recorded proton spectra can provide insight in a binding event, the binding affinity and the mechanism.

Since the FP assay failed to give a clear result on the binding of the virtual screening compound NSC 27389 **92** the binding was examined using the described NMR approaches. For the NMR measurements, the target protein LecA was used with 100 μ M concentration containing an equimolar amount of $CaCl_2$ to ensure ligand

binding. NSC 27389 (**92**) was added in different concentrations between 100 μM and 5 mM and proton spectra and water suppressed proton spectra were recorded and evaluated. The DMSO concentration was adjusted to 5 % in every sample to prevent unspecific effects due to altering DMSO concentrations.

All four obtained signals, the isopropyl signal at 1.205 ppm (Figure 22, A), and the three aromatic signals at 7.058 ppm (Figure 22, B), 7.564 ppm (Figure 22, C) and 7.640 ppm (Figure 22, D) showed changes in frequency with increasing amounts of NSC 27389 (**92**). Since the DMSO concentration was kept constant in all samples, the changes in peak shifts are most likely caused by a binding event. If this binding event is within the carbohydrate-binding pocket cannot be determined from this experiment. The full width half maximum cannot be determined visually, thus the full width at half maximum of the determined peaks was measured and blotted. In case of binding, line broadening should be observed, as described by E. Kovirgin in 2012. ^[179]

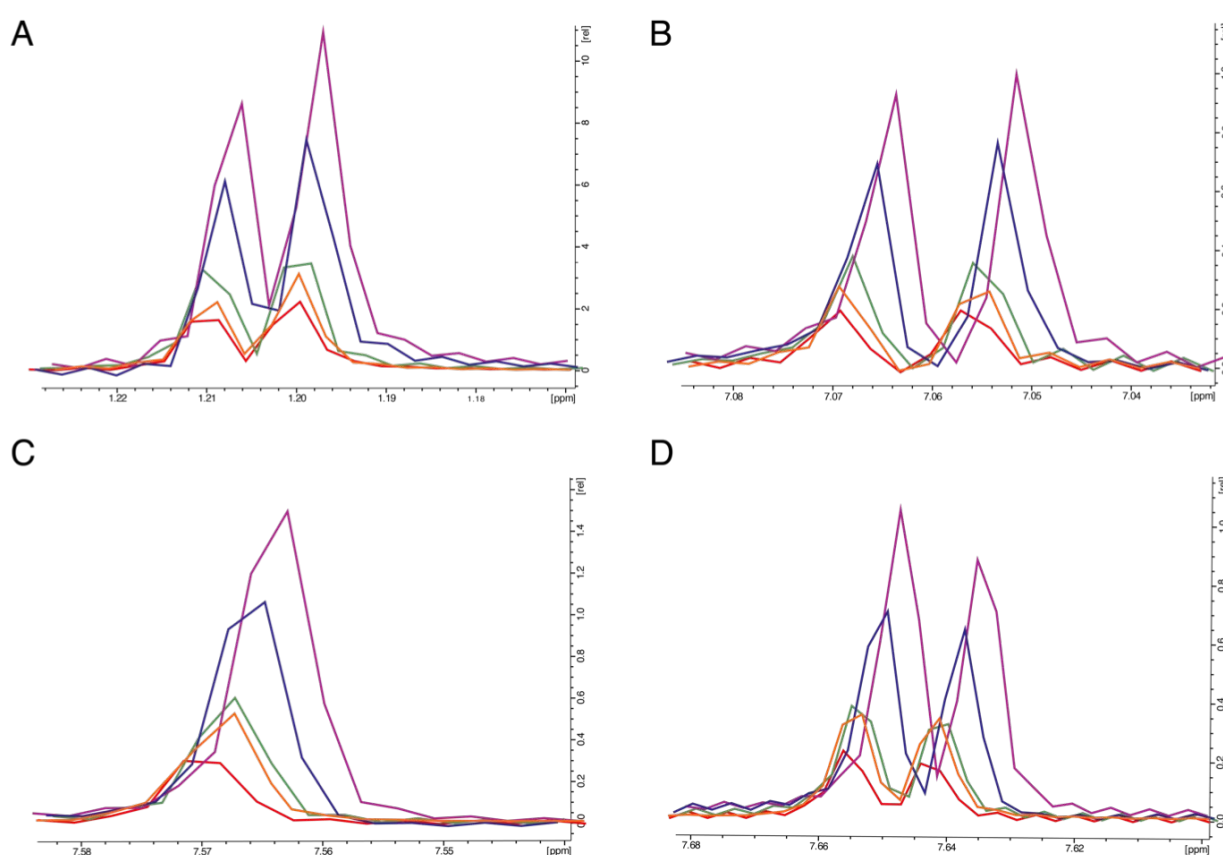


Figure 22: Shown are the determined peaks for NSC 27389 (**92**) in concentrations from ranging from 5 (purple), 3.5 (blue) 2.5 (green) 1 (orange) and 0.5 (red) mM. **A** the isopropyl-protons at 1.205 ppm **B** to **D** the aromatic protons. All spectra contain 100 μM of LecA with 100 μM CaCl_2 to ensure ligand binding and were referenced on the internal DMSO signal. All spectra contain a final DMSO amount of 5 % and were recorded with a number of 1000 scans a with water suppression.

The titration with 100 μM of NSC 27389 (**92**) had to be removed, as the signal to noise ratio was too poor for a valid determination of the full width half maximum or a clear peak.

Results and Discussion

On the one hand, the titration process can be followed by determination of the peak frequencies. This has been blotted in Figure 22. For all four signals, changes in the signal peaks have been determined with respect to the DMSO signal, which was used as an internal reference. But for all four signals, no sigmoidal could be determined using a free fit of the determined data. As summarized in Table 1, the free fit did not give valid curves for the signals at 1.21 ppm with a hill slope of 11.14 and at 7.66 ppm with a hill slope of 5.290. The two other aromatic signals at 7.57 ppm and 7.05 ppm did give hill slopes of 0.608 and 1.110. Thus, fixing the slope to 1 did not change much on the previously determined K_d values of 22.5 and 16.9 mM. Recalculating the curves with the fixed value, 27.4 and 16.1 mM were determined. In contrast, the free fit with the hill slope values strongly deviant from 1, the free K_d value of 2.7 mM for isopropyl and 4.4 mM for the aromatic signal at 7.66 ppm. Fixing the hill slope to 1, a K_d value of 1.4 mM was obtained for the isopropyl-proton signal, and 21.1 mM for the aromatic signal 7.66 ppm. The calculated fit curve for the isopropyl signal (Figure 23A) does not fit the determined values properly so the resulting K_d is unsure. Using all four determined K_d values, a value of 16.49 ± 9.60 mM was obtained. Without the isopropyl signal, a value of 22.53 ± 4.61 mM is obtained.

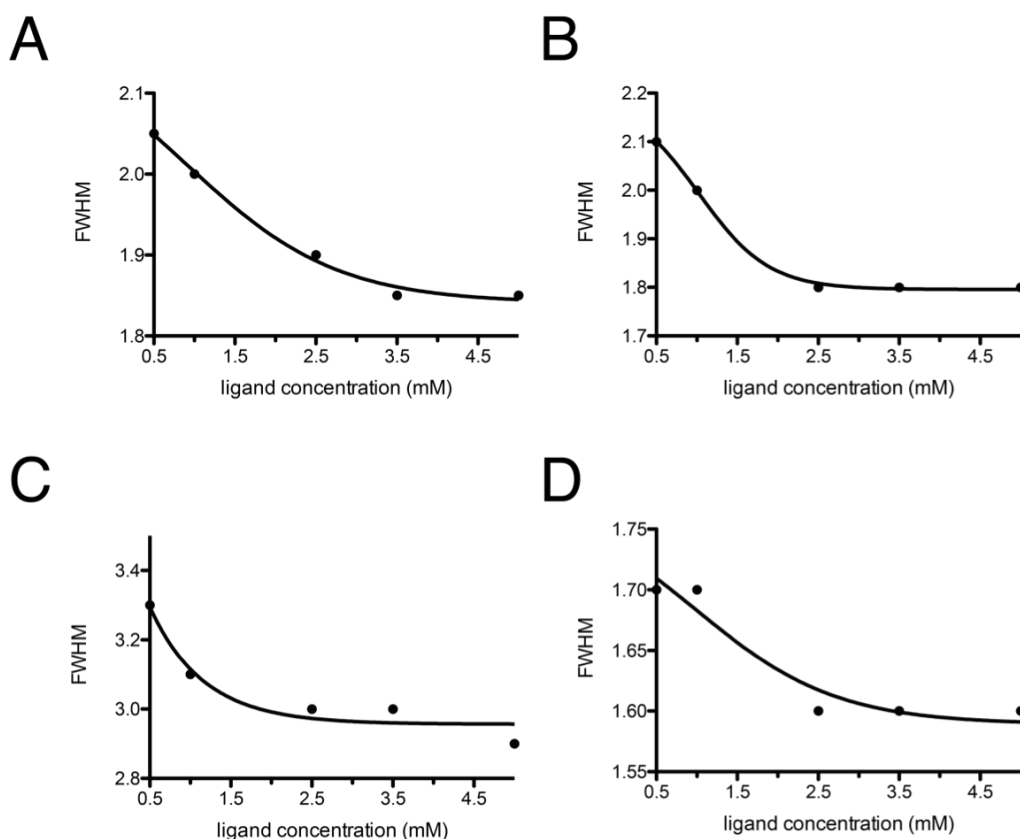


Figure 23: Titrations of NSC 27389 (**92**) with LecA (100 μ M) **A:** Isopropyl-H and the aromatic protons **B-D B:** the proton at 7.06 ppm, **C:** and the protons at 7.57 ppm and **D:** the protons at 7.66 ppm. Changes in the full width half maximum (FWHM) are determined for all four signals. Blotted is the ligand concentration against the measured full width half at maximum. Spectra were recorded with water suppression and 1000 of scans.

On the other hand, the full width at half maximum can be used to determine binding of a ligand to a target protein. Thus, the spectra were superimposed and referenced to the DMSO signal, and then the full width at

the half maximum was red out. For all four determined peaks, a rather small difference between the different full widths half maximum values were determined (Figure 23). In detail, the span of the experiment varied from 0.2 to 0.5. This can be explained in either of two ways, one being the poor binding affinity leading to only minor changes, or second being a hint of unspecific binding. Compared to published results for K_d values in the range of 10 mM, a span of 1 was observed for a similar experiment. But as this experiment was set up as a tool in fragment-based drug design, it was optimized to target long-lived states in NMR, increasing the intensity to a maximum compared to the recorded usual water suppressed proton spectra.^[271]

With the used NMR approach, a binding affinity of 8.1 ± 2.4 mM was determined. Looking at the determined Hill Slopes of the four fits, it is obvious that the quality of the curve with the signal at 7.06 ppm is poor, showing a Hill slope of 6.9 if not fixed giving a K_d value of 11 mM. Fixing this Hill Slope, and thus the slope of the curve, to 1, a K_d of 10.44 mM is obtained. Even though, the curve does now represent the determined values much better, it has only minor influences on the obtained K_d value. In contrast, not fixing the Hill Slope for the signal at 7.66 ppm, a Hill Slope of 16.9 not only was unreasonable, but also a K_d of 57 mM was obtained. Unspecific binding or the small span of the obtained values can explain this. If the Hill Slope is again fixed to 1, a reasonable curve representing the obtained data and a K_d of 9.8 mM are obtained.

3.2.4 Conclusion on the examined hits from the virtual screening approach

To conclude, one can say that there is a line broadening of the signal with decreasing amounts of ligand and that there is a shift in the peak signals with changing ligand concentrations. As a binding of a small molecule to a bigger target molecule, LecA in this case, does result in a signal broadening; this can be concluded to be a general hint for binding of NSC 27389 (**92**) to LecA. Moreover, the observed changes in peak signals can be taken as a sign for binding. For the first evaluation method, the blotting of the proton shifts, a K_d value of 16.5 ± 9.6 mM using all four peaks, and 22.5 ± 4.6 mM neglecting the isopropyl proton due to poor fit quality were obtained. In contrast, using the measurement of the full width at half maximum, a K_d of 8.1 ± 2.4 mM was calculated. Comparing both obtained values, the discrepancy of the two obtained values is obvious. Since both values are determined from the same spectra, this discrepancy can only be explained by either the obtained small changes in signal shifts or full width at half maximum due to weak binding or by the fact, that the binding is unspecific. For either of the evaluation methods, the determined K_d in the 10 mM range explained the observed problems in obtaining binding curves using the FP assay. Finally, one problem is the fact, that the binding per se is not clear. All calculations assume that the observed small effects are indeed due to specific binding. To verify this binding, the method should be applied to a known weak binding LecA ligand with a K_d in the same range, for example D-galactosamine.

The above mentioned results were used as a starting point for further experiments and were ultimately published in 2020.^[303]

3.3 Using a ^{19}F NMR screening for the identification of potential new carbohydrate binding site ligands for *P. aeruginosa* lectin LecA

While monovalent ligands based on fucose present nano molar binding affinities to LecB, galactose based LecA ligands show binding affinities in the lower μM range. [35, 87, 263-264] To enhance the binding affinity of known ligand growing approaches or derivatization can be used, the latter was successfully used to determine more potent LecB inhibitors. [87,264-266] In general two different starting points can be chosen: either starting from a known ligand, which could be D-galactose for LecA, or starting with a screening for the determination of binding structures which could also be without a sugar scaffold. It was shown by Rademacher and co-workers, that a fluorine-based NMR screening set up can be used to determine binding molecules for lectins without a sugar scaffold. [267] In this technique, a fragment library with members bearing a fluorine atom is screened in a two-step NMR approach using a ^{19}F screening and a CPMG sequence. [93, 267-268] The advantage of the fluorine NMR is not only the increased sensitivity, but also the reduced number of signals using ^{19}F NMR techniques enabling the combination of up to 36 compounds in one sample or so-called bins.

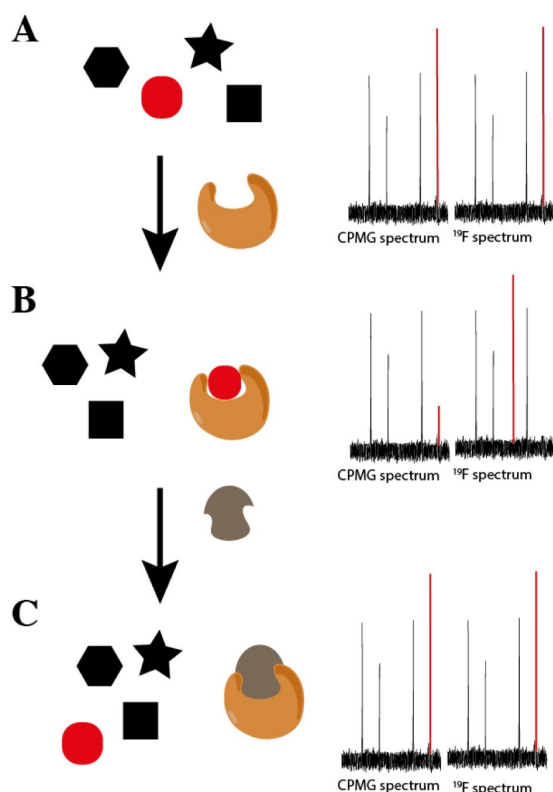


Figure 24: Schematic representation of the screening set up is shown starting the recording the compound libraries (bins) with ^{19}F and CPMG measurements (A), followed by recording the bins in presence of the target protein (B) identifying hits by a reduction in the signal intensity (CPMG) or signal shifts (^{19}F) shown for the red hit compound. To verify binding, the bins are recorded in presence of the target protein and a known inhibitor (grey, C), true hits are identified if the compound of A and C are the same.

For the NMR screening first, ^{19}F and CPMG spectra of the compound bins with a final concentration of $50\ \mu\text{M}$ per compound were recorded on a 600MHz NMR equipped with a cryo probe. Then as a second step the bins were measured in presence of $10\ \mu\text{M}$ of the target protein LecA (Schematically shown in Figure 29A). To reduce the obtained potential LecA binding hits to fragments binding in the carbohydrate binding pocket, spectra of the bins in presence of LecA ($10\ \mu\text{M}$) and $100\ \mu\text{M}$ of the known LecA carbohydrate ligand p-NPG are recorded (Schematically shown in Figure 24C).^[179] As the known ligand p-NPG has a K_d value of $26.2\ \mu\text{M}$, a concentration of $100\ \mu\text{M}$ was used to ensure competition even in case of strongly binding fragments.^[35, 90] NMR spectroscopy is a highly sensitive method so the reduction of the obtained binding fragments to those binding in the carbohydrate binding pocket was needed, because it reduces the number of hits and is an additional verification method to reduce false positive hits. Moreover, the FP assay for biochemical hit verification is based on competition with a D-galactose-based reporter ligand. Binding of potentials hits is identified as changes in the chemical shifts of ^{19}F NMR spectra. For evaluation the of potential hits in the ^{19}F spectra signal shifts were rated with 1 when a clear effect was observed or with 0.5 if effect was less clear. For the ^{19}F competition measurements with p-NPG signals were rated with 1 when the chemical shift changes back to the shift of the reference spectrum value after inhibitor addition.-Hits in the CPMG sequence are identified by a reduction of the signal intensity. For the CPMG experiments signals in presence of LecA were rated with 1 if a clear effect was observed which is a signal reduction of more than 50%. Signals were rated with 0.5 if an unsure effect was observed (signal reduction of more than 25%). For the CPMG experiments with p-NPG competition, signals were rated with 1 if a clear effect was observed (rise in signal intensity of more than 50%) and rated with 0.5 if unsure effect were observed (rise in signal intensity of more than 25%). The results of all analyzed compounds are summarized in Table1. All compound that scored at least a 1 in the ^{19}F or CPMG

Results and Discussion

measurement with LecA and at least a 0.5 in the competition measurement with p-NPG were considered as hits. In summary 192 different compounds combined in six bins were screened:

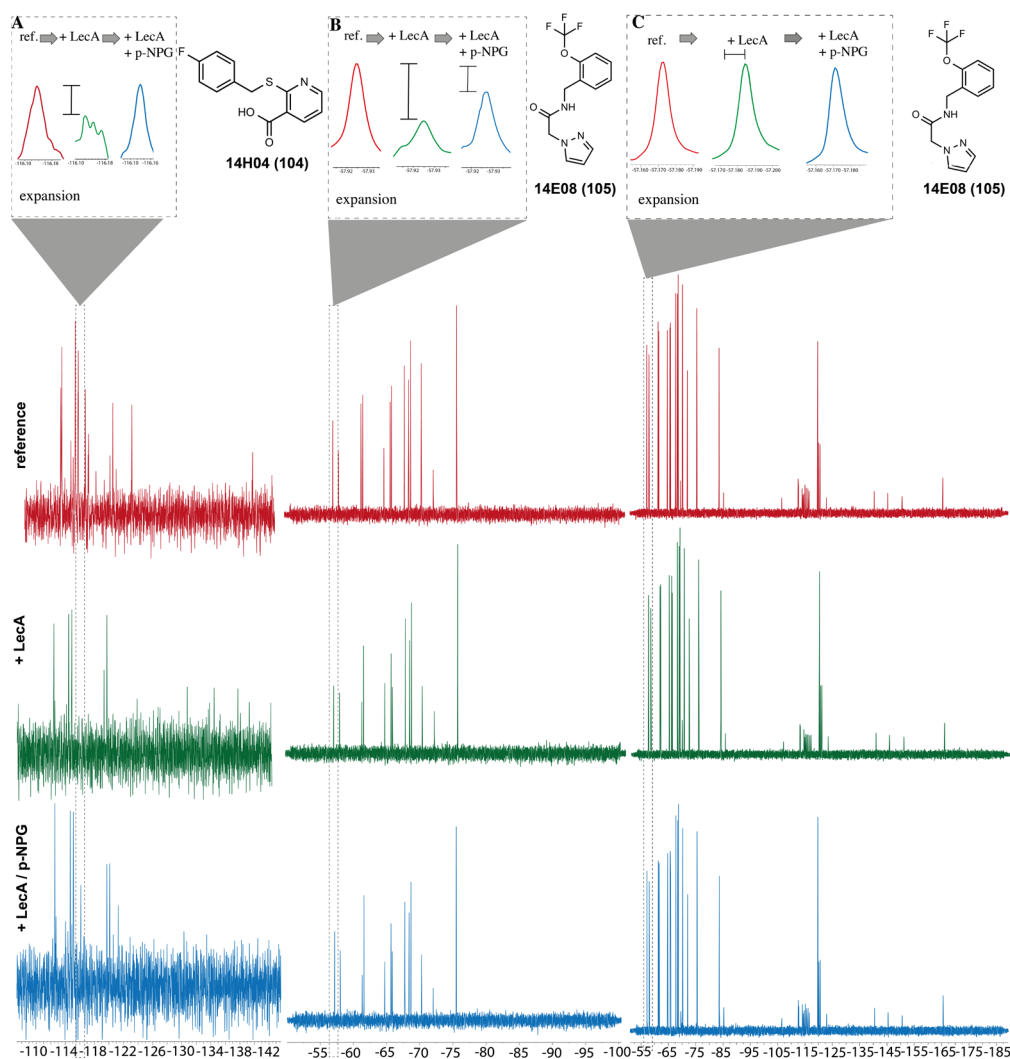


Figure 25: A shows the identification of the screening compound **14H04 (104)** with the CPMG measurement and **B** shows the identification of the screening compounds **14E08 (105)** with the CPMG measurement and **C** shows the ^{19}F measurement of compound **14E08 (105)**. The red spectra represent the measured compound libraries alone (50 μM , reference), the green spectra show the measurement of the library bin and LecA (10 μM , +LecA) and the blue spectra represent the NMR measurement containing the compound library bin, LecA and p-nitro phenyl β -D-galactoside (100 μM , +LecA/p-NPG). All chemical shifts are given in ppm. For **104** a clear signal reduction of 55 % was observed after the addition of LecA (A, red compared to green peak), and the signal was changed back to 73% of the initial intensity after the addition of p-NPG (B, blue peak). **105** showed an even stronger reduction in signal intensity after addition of LecA (B, red compared to green peak) than **104**, but the signal intensity was not completely restored after the addition of p-NPG (B, blue peak). The ^{19}F NMR measurement of **105** also revealed a signal shift (C, red compared to green shift) which was reverted after the addition of competitor p-NPG (C, green peak).

The first screened bin contained a total of 36 compounds and two hits were identified, namely **105** and **104** (Figure 25). For compound **104** only binding and competition effects were observed in CPMG measurements (Figure 25, A). After addition of LecA the signal of compound **104** was reduced by 55%, and a recovery of

40

the signal of 73% was observed after the addition of the carbohydrate binding site ligand p-NPG. However, no effects were observed for **104** in the ^{19}F measurement. In this bin a second potential LecA ligand was identified **105** (Figure 25 B, C). Compound **105** was identified as the second potential hit during the screening scoring in both, the ^{19}F measurements as well as the CPMG measurement (Figure 25, Table 1). For the CPMG measurement a value of 0.5 was scored with a signal reduction of 28% and a recovery of 39%, making this structure a potential weak hit. In the ^{19}F measurement a weaker shift was observed, leaving the compounds with a 0.5 score in the ^{19}F screening. The shifts were partially reversible after addition of p-NPG but no signal reduction was observed. Although compound **105** did only score a 0.5 in the individual measurement it is one of the rare cases that did show effects in both types of measurements and was therefore considered a potential hit.

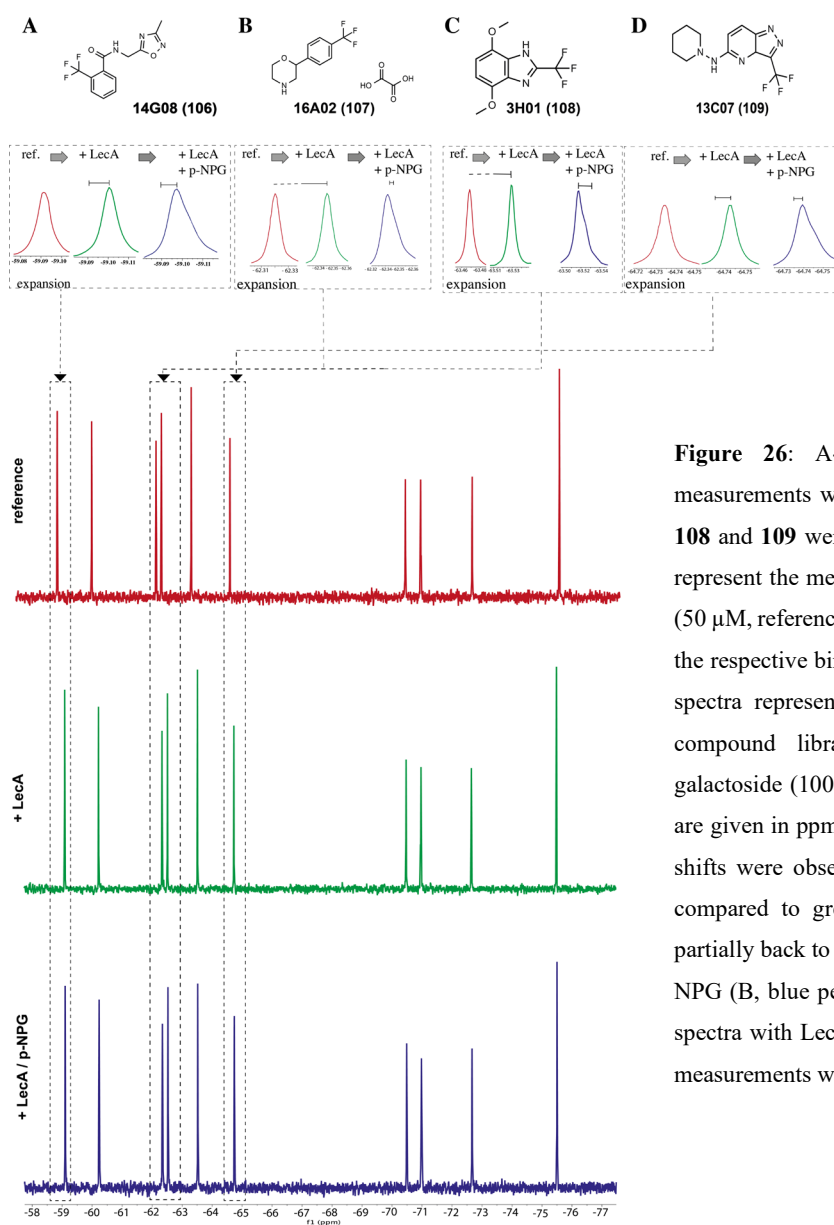


Figure 26: A-D. All spectra represent ^{19}F NMR measurements with the identified potential hits **106**, **107**, **108** and **109** were used as screening hits. The red spectra represent the measured bin of the compound library alone (50 μM , reference) the green spectra show the samples with the respective bin and LecA (10 μM , +LecA) and the blue spectra represent the sample containing the bin of the compound library, LecA and p-nitro phenyl β -D-galactoside (100 μM , +LecA/p-NPG). All chemical shifts are given in ppm. For all compounds **106-109** clear signal shifts were observed after the addition of LecA (A, red compared to green peak), and the signal was changed partially back to the initial intensity after the addition of p-NPG (B, blue peak). So, a score of 1 was assigned for all spectra with LecA and a score of 0.5 was assigned for all measurements with the competitor p-NPG.

Results and Discussion

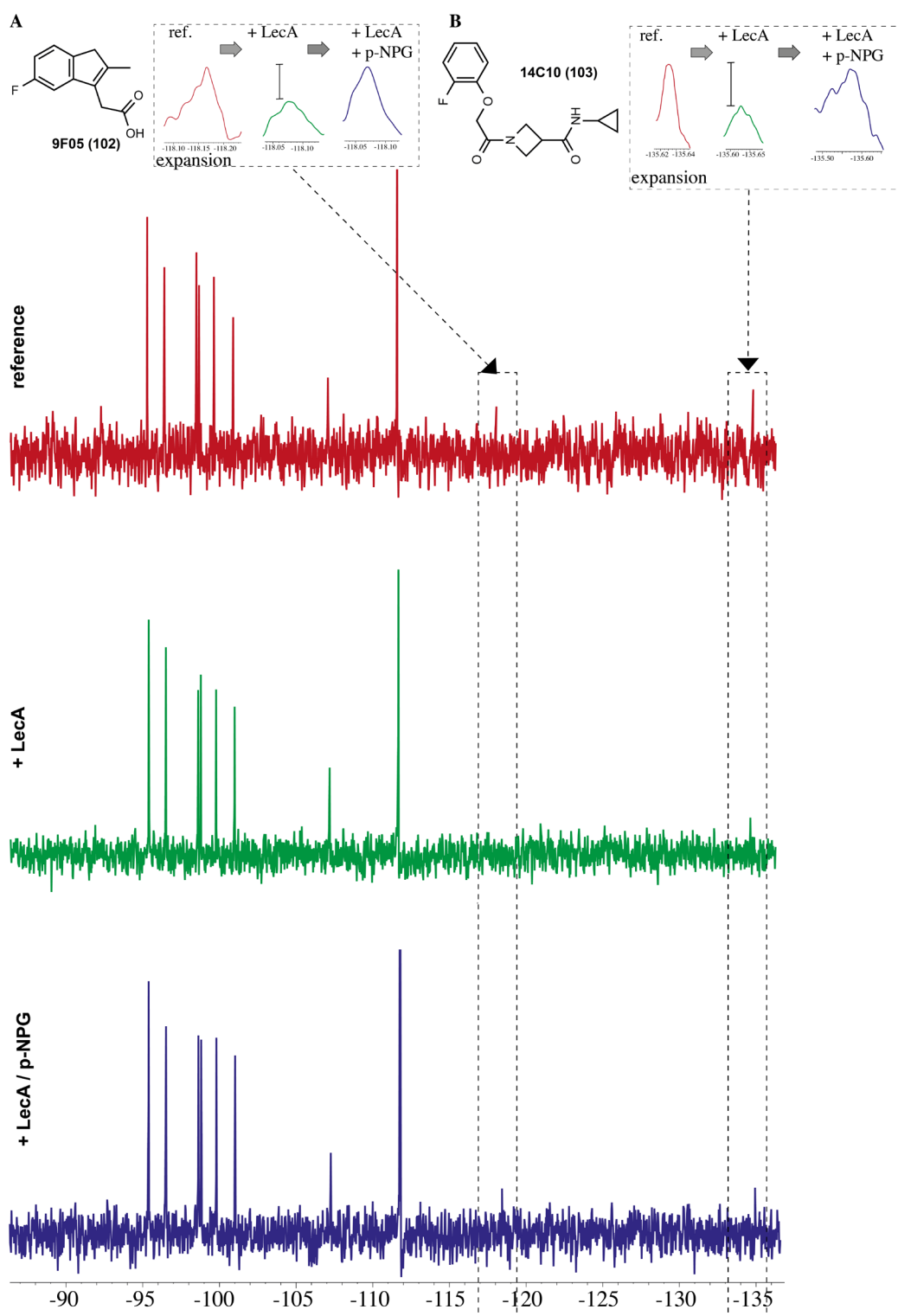


Figure 27: CPMG spectra of the two hits **102** and **103** of the second screened bin. The red spectra represent the measured bin of the compound libraries alone (50 μM , reference), the green spectra show the samples with the respective bin and LecA (10 μM , +LecA) and the blue spectra represent the sample containing the compound library, LecA and p-nitro phenyl β -D-galactoside (100 μM , +LecA/p-NPG). All chemical shifts are given in ppm. For all compounds **106-109** clear signal shifts were observed after the addition of LecA (A, red compared to green peak), and the signal was changed partially back to the initial intensity after the

addition of p-NPG (B, blue peak). So, a score of 1 was assigned for all spectra with LecA and a score of 0.5 was assigned for all measurements with the competitor p-NPG.

In the second screening bin containing 36 compounds of the total compound library in the ^{19}F NMR spectra four compounds were identified as potential hits namely **106-109**. All four hits scored a 1 in the ^{19}F measurement, which as described before means a clear signal shift (Figure 27). In the competition measurement all compounds only scored a 0.5, resulting in incomplete shifts back to the spectra of the reference bin alone. These results suggest that it is an uncertain hit. In addition to the four potential hits mentioned above two more potential hits were determined, but only in the CPMG measurement: **102** and **103** (Figure 27). All the four hits **106-109** determined from the ^{19}F measurement did not score a hit the CPMG measurement and **103** from the CPMG measurement only scored a 0.5 in the ^{19}F measurement with LecA but was not restored after the addition of p-NPG. For **103** a signal reduction of 51% was observed in the CPMG measurement which was restored up to 96% after the addition of p-NPG. **102** scored a 0.5 in the ^{19}F measurement with LecA but did not show competition in these measurement upon addition of p-NPG (Table 1, Figure 32). In the CPMG measurement **102** showed a signal reduction of 51% after addition of LecA and the signal was fully restored after addition of p-NPG.

In the third bin, that contained a total of 12 compounds, only one hit was identified **110**. This hit was identified only in the CPMG measurement where a signal reduction of 80% was observed after the addition of LecA, and the signal was restored by 91% after the addition of p-NPG (Figure 28, Table 1). In the ^{19}F spectra the compound **110** scored a 0.5 in the measurement with LecA but did not show competition in the measurement with p-NPG in the ^{19}F spectra (Table 1)

Results and Discussion

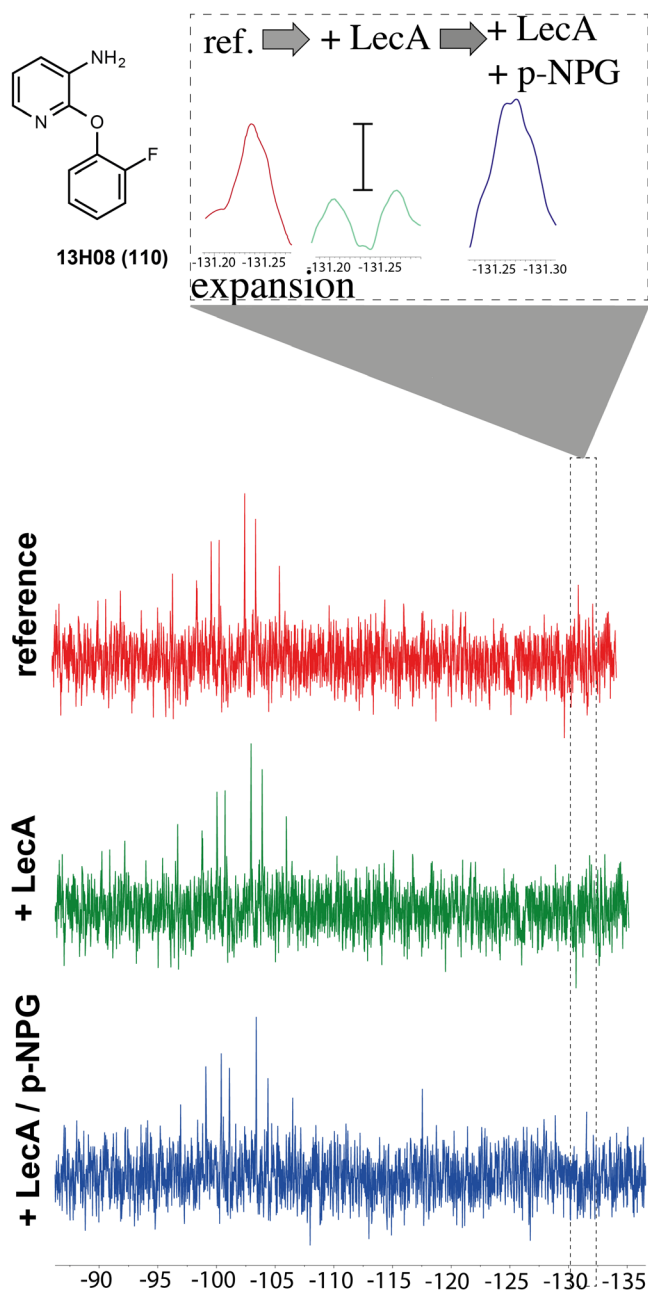


Figure 28: The determined hit from the CPMG measurement identifying **110** as a screening hit. The red spectra represent the measured compound libraries alone (50 μ M, reference), the green spectra show the samples with the respective bin and LecA (10 μ M, +LecA) and the blue spectra represent the sample containing the compound library, LecA and p-nitro phenyl β -D-galactoside (100 μ M, +LecA/p-NPG). All chemical shifts are given in ppm. For **110** clear signal reductions of 80 % was observed after the addition of LecA, resulting in a score of 1(A, red compared to green peak). The signal was restored by 91 % of the initial intensity after the addition of p-NPG, resulting again in a score of 1 (B, blue peak).

In the fourth bin containing 36 compounds six hits were identified as hits in the CPMG measurement: **111-116** (Figure 34, Table 1). All compounds **112**, **114**, **115**, **116** and **117** scored a 1 in the CPMG measurement

and the competition which means a signal reduction of more than 50 % and a recovery of at least the same after addition of the known LecA competitor p-NPG.

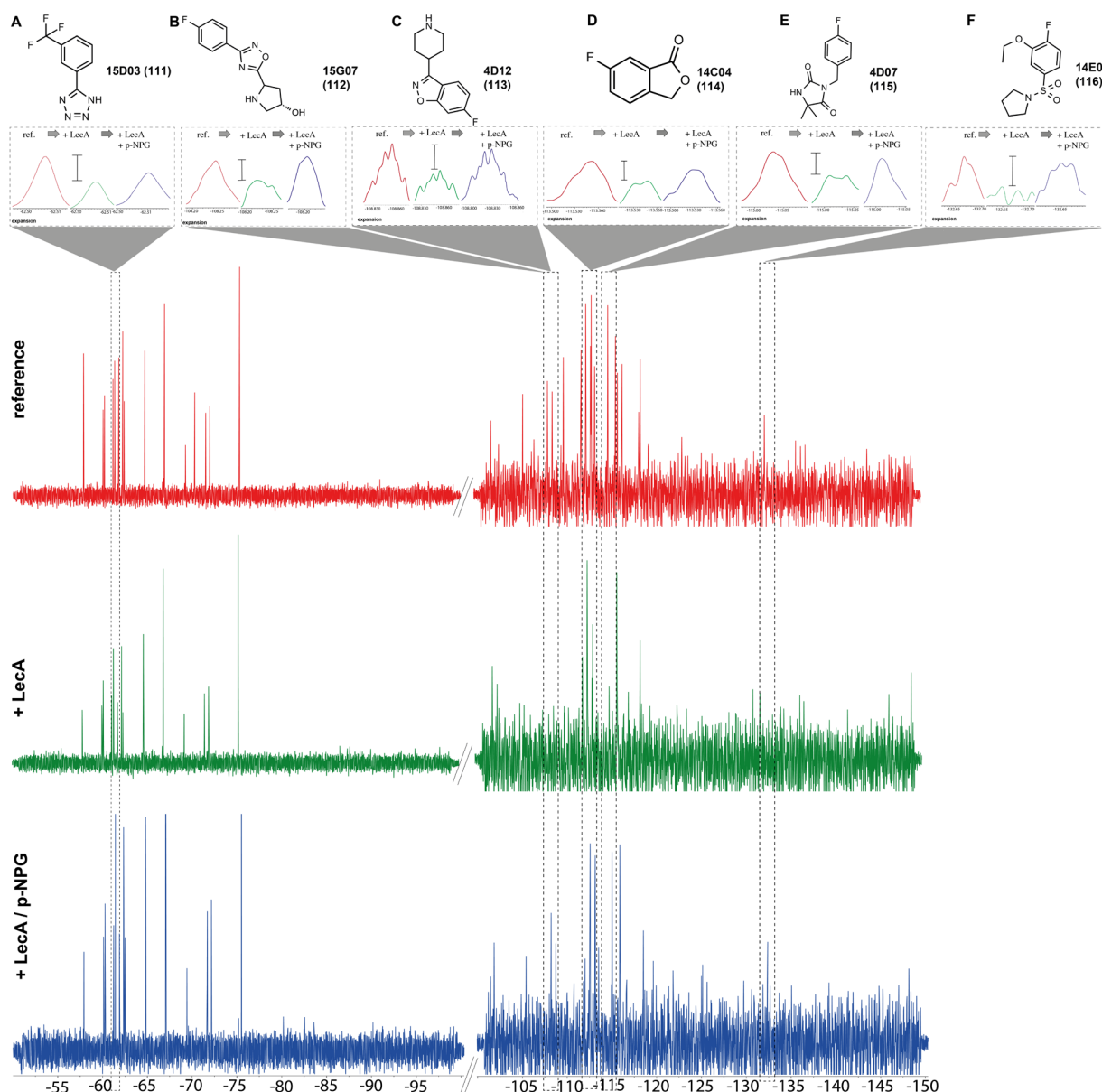


Figure 29: The determined hits of a bin containing 36 compounds. **111 (A)**, **112 (B)**, **113 (C)**, **114 (D)**, **115 (E)**, **116 (F)** were determined as hits from the CPMG measurement. The red spectra represents the measured compound libraries alone (50 μ M reference), the green spectra depict the samples with the respective bin and LecA (10 μ M, +LecA) and the blue spectra represent the sample containing the compound library, LecA and p-nitro phenyl β -D-galactoside (100 μ M, +LecA/p-NPG). All chemical shifts are given in ppm. In details, **111** showed a signal reduction of 53 % after addition of LecA scoring a 1 (A, red compared to green peak) and the signal was restored by 32 % after addition of p-NPG scoring a 0.5 (C, blue peak). For **112** a signal reduction of 61 % was observed, scoring a 1 (A, red compared to green peak). 100 % recovery was observed for the signal of **112** after addition of p-NPG, clearly scoring a 1 (C, blue peak). **113** showed a signal reduction of 48 % scoring a 0.5 in the CPMG measurement with LecA (A, red compared to green peak), but a score of 1 was reached upon addition of p-NPG as the signal was fully restored (C, blue peak). **114** showed a signal reduction of 67 % resulting in score of 1 (A, red compared to green peak), and the signal was restored by 61 % upon addition of p-NPG, resulting again in a score of 1 (C, blue peak). **115** showed a decrease in its signal by 61 % scoring a 1 in the CPMG measurement with LecA (A, red compared to green peak), and a clear score of 1 was reached upon addition of p-NPG as the signal was fully restored (C, blue peak). The last hit **116** showed the clearest results with a complete loss in signal in presence of LecA (A, red compared to green peak) and a full recovery of the signal upon addition of p-NPG (C, blue peak.), which means a score of 1 in both measurements.

Results and Discussion

In detail, **112** showed a signal reduction of 61% in the CPMG measurement and a full recovery of the signal after addition of p-NPG (Figure 29, B). For **114** the reduction a signal reduction of 67% was measured which was restored by 61% after addition of the carbohydrate competitor p-NPG (Figure 29, D). The signal of **115** was decreased by 61% after the addition of LecA and was fully restored after the addition of p-NPG (Figure 29, E). While **111** showed a reduction of its signal of 53% and the signal was restored by 32% after addition of p-NPG (Figure 29, A). This means that **111** is a weaker potential hit compared to the previously described **112** and **114**. It could also mean, that the affinity of **111** to LecA is less than for the other two, as **111** does not compete with p-NPG as efficiently. In contrast, **116** showed a complete loss of the signal after addition of LecA and a complete recovery after the addition of the galactose derivative (Figure 29 F, Table 1). The weakest hit of the CPMG measurement of the bin was **113**, which scored a 0.5 with a reduction of 48 % in the CPMG sequence and a 1 in the competition measurement with a recovery of 100 %. None of the hits mentioned above nor any additional hit were identified in the ^{19}F spectra. It is surprising that none of the hits did cause effects in the ^{19}F measurement because they did show clear results in the CPMG measurement. This might hint to the fact that the found compounds are weak binders. As both experiments were measured with the same probe, a sample error can be excluded as root cause of the observed result.

In summary, for this screening only compounds that scored at least a score of 1 in the ^{19}F or CPMG measurement with LecA were considered hits with the exemption of **113** which scored only a 0.5 in the CPMG spectra with a signal reduction of 48%. A reduction of 50% would result in a score of 1 and as 48% is very close and in addition the signal was fully recovered after the addition of the competitor, this compound was considered a hit even with scoring only a 0.5 in the screening with LecA. Table 1 is summarizing all screening results.

In summary using the described criteria, a total of 14 hits were identified using CPMG and ^{19}F measurements. Within these hits according to the above-mentioned criteria, **102** and **103** were determined the strongest hit. While compound **102** appeared as a distinct hit in the CPMG measurement with a signal reduction of 51 % and a full recovery of the signal after carbohydrate addition, no clear effect was observed in the ^{19}F measurement. Thus the total score of compound **102** was 2 out of 4 maximum possible. Compound **103** also was determined as a clear hit in the CPMG measurement with a signal reduction of 67 % and a recovery of the signal of 61 % after addition of the galactose derivative. **103** also scored a 2 in total. In the ^{19}F screening compound **114** showed and unsure effect with a signal reduction of over 50% but no chemical shift was observed. Usually signal reduction was observed in the CPMG measurements while in ^{19}F measurements mainly signal shifts have been observed. **115**, **110**, **114**, **116**, **104** and **112** were all clear hits in the CPMG measurement but did not show effects in the ^{19}F screening. This could be due to the enhanced sensitivity of the relaxation based CPMG method in contrast to the ^{19}F measurement.^[232] **108**, **106** and **107** all showed a clear effect in the ^{19}F measurement (rated with a 1) and for all three compounds the effect in the competition assay was not as pronounced (rated with a 0.5). A rate of 0.5 in the competition experiment does not necessarily mean that the determined hit has a worse quality it can also be a result of a strong binding of the ligand.

Results and Discussion

Remarkable however is the fact, that all these three hits did not show any effect in the CPMG measurement, which could potentially be a sign of unspecific binding. Compound **111** showed effects in the CPMG but not in the ^{19}F measurement. Only compound **105** showed effects in both, the ^{19}F and the CPMG measurement. **113** was the weakest determined hit with only a score of 0.5 in the CPMG measurement, but due to the fact that the threshold for a score of 1 is 50 % signal reduction and the compound showed 48 % signal reduction and a full recovery after addition of the inhibitor p-NPG the compound was also considered a hit. In total using the CPMG and ^{19}F NMR screening approach developed by Rademacher and co-workers six bins were screened with a sum of 192 compounds. In summary 67 compounds showed binding to LecA upon which 14 were competitive, thus a total of 15% of all determined LecA binding compounds could be specific LecA binding site ligands. For further evaluation of the determined potential LecA carbohydrate binding site ligands commercially available compounds were ordered for the biochemical evaluation in the competitive binding assay.

Results and Discussion

3.3.3 Biochemical evaluation of potential carbohydrate binding site ligand hits from the NMR screening using the fluorescence polarization assay as well as the thermal shift assay

One of the advantages of NMR based screening is the sensitivity of the method, but on the other hand, this makes it prone to false positive hits. [143, 228] Thus a method to is needed to verify binding of potential ligands determined in the NMR screening to LecA.

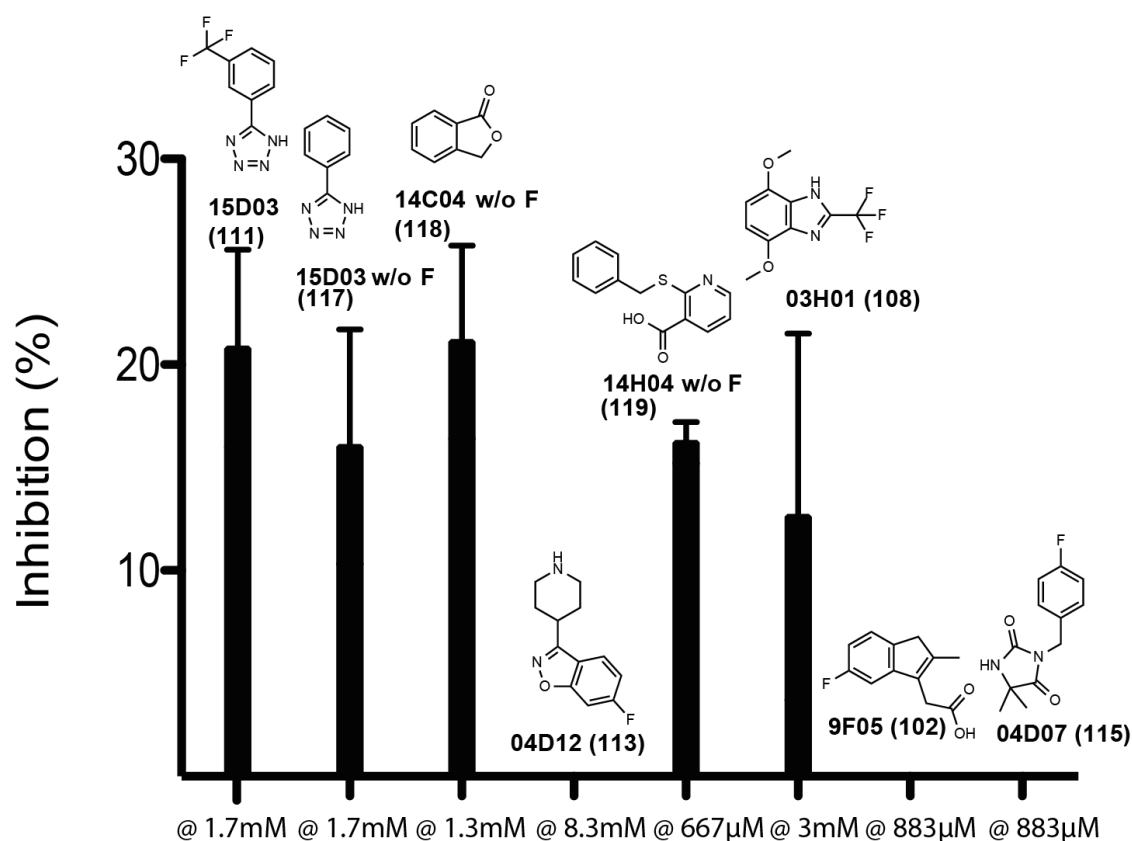


Figure 30: Evaluation of the eight derivatives tested in the FP assay. The inhibition at a maximum concentration is shown in the plot. Eight compounds were tested and five showed inhibition: **111** and its derivative without fluorine **117**, the derivative of **114** without fluorine **118** was tested as well as the fluorless derivative of **104**, **119** and compound **108**. LecA was used in 18 µM concentration, and the ligand was used in its individual highest possible concentration (see x-axis). None of the tested compounds showed a sigmoidal binding curve when used in increasing concentrations thus only the inhibition at the maximum concentration based on changes in the fluorescence polarization are plotted. The average and standard deviation are calculated from at least three independent experiments

The biochemical method for hit verification is potentially SPR, ELLA, TSA or FP. Since the screening included a competition with a known LecA carbohydrate binding site ligand only potential ligands binding in this pocket should have been identified. Thus, a method testing specifically for ligands binding in the

carbohydrate binding pocket would be of great benefit. Biochemical confirmation of the determined hits is crucial to distinguish between true binders and false positive hits. For the rapid evaluation of LecA inhibitors, the developed assay based on fluorescence polarization was used.^[270] In this assay, binding of a ligand is determined by competition of a fluorescently marked ligand. 15 compounds were used in the assay due to availability of the screening hits. The fluorine ions which were crucial for the NMR screening as it was based on a ^{19}F measurement. For the biochemical evaluation also three compounds (**111**, **114**, **104**) were in addition tested as derivative without fluorine. From the 15 screening hits only eight were selected due to availability of the needed amounts for the assay and due to cost limitations and tested in the FP assay. The clearest hit from the NMR screening, **102**, was included in the study.

In the FP assay only five compounds (**108**, **111**, **117**, **118**, **119**) out of the eight tested compounds showed effects. It was not possible to obtain sigmoidal binding curves for either of the tested ligands. This could potentially be a result or combination of poor binding affinities as well as a poor solubility of the ligands. One of the hits from the NMR screening was tested as fluorine- and fluorineless compound: **111** and the fluorine less derivative **117**. Both derivatives did show the same solubility as well as comparable inhibitory potential. **111** showed inhibition of $21 \pm 5 \%$ and **117** of $16 \pm 6 \%$. These results could be because the fluorine for this compound does not influence the binding affinity significantly. But the conclusion on less pronounced effects in the binding affinity cannot be made since no sigmoidal binding curve was obtained. The fluorineless derivative **118** was also tested in the assay and did show inhibition of $21 \pm 5 \%$. As this compound was tested but the original screening compound containing the fluorine **114** was not tested no conclusions on the role of the fluorine in these compounds can be made. Compared to **111** and **117**, **114** showed an inhibition of the same magnitude. In addition, **119**, which is the derivative without fluorine of **104** was tested and showed inhibition of $16 \pm 1 \%$ in the FP assay. The solubility of the compound was rather poor, resulting in final concentrations of only $667 \mu\text{M}$ in the assay. Also **108** determined as potential hit in the NMR experiment showed effects in the FP assay of $13 \pm 9 \%$, but the variance between the single measurements was high as the standard deviation of 69% clearly show. Also, with a final concentration of 3 mM and yet no sigmoidal binding curve, it can be concluded that the affinity of this ligand is poor. In Summary, **113**, **102** and **115** showed no inhibition in the FP assay while **111** and its derivative **117**, **118** and **119** showed inhibition of up to 21% at the highest tested concentration of each compound. For **108** only two of three experiments showed significant inhibition making its standard deviation with 69% unreliaibly high and so no conclusion based on these data alone is possible. NMR is a highly sensitive method compared to the fluorescence polarization assay. So, there are numerous reasons why a hit can be determined in the NMR screening but not in the FP assay. It can be possible limitations in the solubility of the compounds with respect to their binding affinity to LecA. In NMR measurements ligands with a low binding affinity can be determined while in the FP assay a ligand concentration of more than the binding affinity is needed. If a ligand is poorly soluble but has a low binding affinity it can not be determined in the FP assay. In addition, the fluorescence intensity of the reporter ligand can be influenced by the potential LecA ligands causing unwanted effects on the fluorescence. This was tested as the fluorescence of the ligands with the reporter ligand alone was tested and no significant effect on the fluorescence intensity was observed. Also, unwanted interactions with the dye or the carbohydrate of the reporter ligand could be the

Results and Discussion

reason for unclear effects in the FP assay. This can be excluded for the compounds presented in figure 35 as they were all tested against the carbohydrate reporter ligand alone and did not show any interactions. For further verification of the binding of the screening compounds a second biochemical evaluation using differential scanning fluorometry (DSF) based on the melting behavior of LecA was carried out.

The thermal shift assay is based on the principle that LecA and a fluorescent dye (sypro orange) are heated up and upon denaturation of the protein the dye can bind to the thereby presented hydrophobic regions of the protein. In theory, binding of a ligand enhances the complex stability and thus the determined melting temperature of the protein is higher. It is discussed, if decrease of the melting temperature can be counted as a binding event as well, but with an adverse energetic profile.^[304] However, due to experimental uncertainties, only a change in melting temperature of at least 0.4 °C is considered as significant. Sypro orange, which was used in this thermal shift assay, has an extinction maximum at 300 and 472 nm and emission maximum at 570 nm. In contrast to the fluorescence polarization assay, in which competition of the carbohydrate binding site is monitored, no conclusion on the binding site can be drawn from the thermal shift experiment as stabilization of the protein can occur upon every binding event regardless of the binding site. Both positive controls me- α -gal (**7**) as well as p-NPG (**8**) did show stabilization of LecA. me- α -gal (**7**) increased the melting temperature of LecA by 0.85 ± 0.20 °C and p-NPG (**8**) increased the melting temperature by 1.84 ± 0.04 °C. p-NPG (**8**) is a stronger LecA ligand with an K_D of 8.6 μ M than me- α -gal (**7**) with an IC_{50} of 50 μ M thus the determined stabilization is slightly enhanced. From all 8 tested screening ligands, **111** had the largest impact on the LecA melting temperature by increasing it up to 1.53 ± 0.07 °C. The derivative of **111** without the fluor atom **117** increased the LecA complex stability only by 0.57 ± 0.03 °C. This difference in melting temperature suggests that the fluorine has a positive influence on the binding capacities to LecA. Moreover, **119** also enhanced LecA stability by 0.97 ± 0.05 °C. **118**, **108**, **102**, **115** did not change the melting temperature of LecA. Only compound **113** decreased the LecA melting temperature about -1.19 ± 0.10 °C. LecA is in general a stable protein with a melting temperature of 83.6 °C and it cannot be reconstituted after melting. This was shown, as no binding, not even of the known ligands, was determined in a second round of thermal shift analysis (data not shown). To exclude false positive hits resulting of an interaction of the potential hits and the dye from the assay, sypro orange was tested with each compound alone, but none of the compounds showed interactions with the dye alone.

To summarize the results from the two above presented biochemical assays: **115**, **102** showed in both assays clearly no effect. **113** did not show effects in the FP assay but showed a negative influence on the stability of LecA resulting in a decreased melting temperature of the LecA/**113** complex. Thus, a conclusion on the binding to the carbohydrate binding site of LecA can not be drawn. The effects in the thermal shift assay could as well be due to binding of the ligand at another binding site of LecA. For **108** unsure effects were observed in the FP assay as binding was only observed in 2 out of 3 in dependent experiment and no change in the melting temperature on LecA was observed in the thermal shift assay. In conclusion, it remains questionable if compound **108** is a true LecA binder. As the FP assay never resulted in a sigmoidal binding curve and the

inhibition of fluorescence polarization not fully reproducible a specific binding of **108** to the carbohydrate binding pocket of LecA with an acceptable affinity is unlikely. **118** showed clear effects in the FP assay but did not have any effects on the melting temperature of LecA. This could be explained either of two ways: The compound could also bind to a second binding site close to the carbohydrate binding that does not contribute significantly to the stability of the protein. Since the reporter ligand in the FP assay is based on a β -phenyl-D-

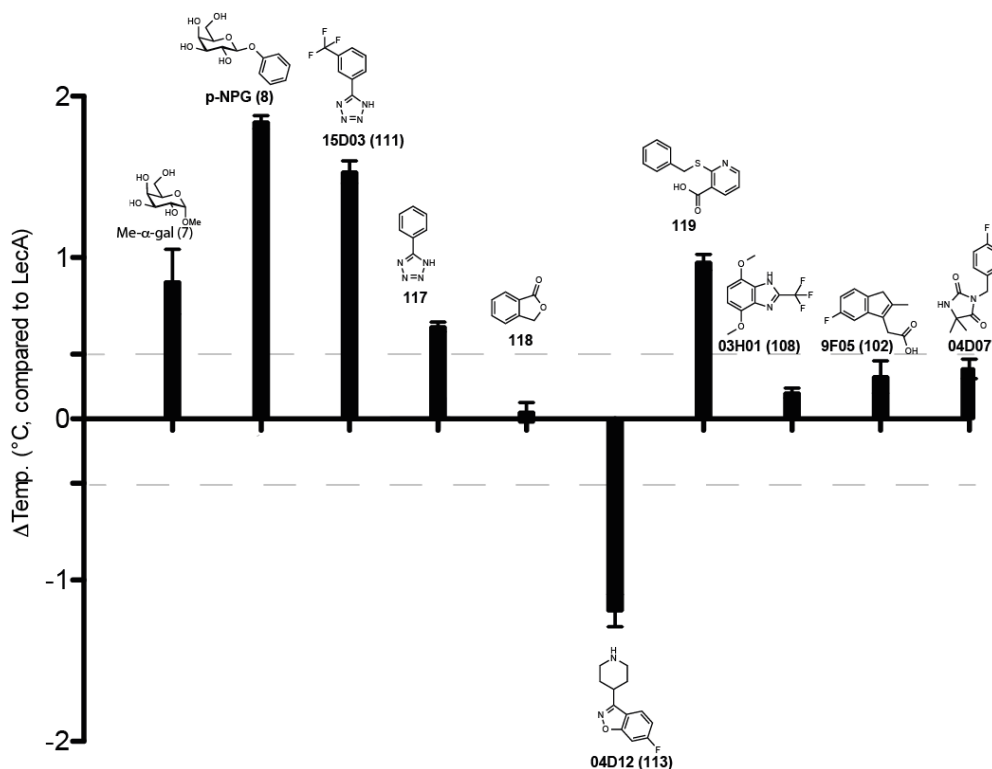


Figure 32: Thermal shift results of the screening ligands and known LecA ligands me- α -gal and p-NPG are shown. All ligands were used with 500 μ M concentration and shifts were calculated with respect to the melting temperature (T_m) of LecA of 83.6 ± 0.2 °C. LecA was used with 2 μ M concentration. The dashed line represents the threshold of 0.4 °C, beyond this shift, the effect was considered unspecific. **118**, **108**, **102**, **115** showed shifts of less than 0.4 °C. The known LecA ligands p-NPG showed the strongest shift with 1.84 ± 0.2 °C. Compound **111** determined from the NMR screening showed a comparable shift of 1.53 ± 0.07 °C. **117**, the derivative of **111** without a fluor atom showed a shift of 0.57 ± 0.03 °C. **119**, the derivative of **104** without fluor, showed a shift of 0.97 ± 0.05 °C. **113** destabilized LecA and caused a negative shift of -1.19 ± 0.10 °C.

galactose scaffold, it could be possible that **118** does not compete with the sugar moiety in the reporter ligand but the phenyl or part of the fluorescent dye. With this mechanism it could cause an effect on the fluorescence polarization in the FP assay. Another possibility is that the compound was a false positive hit in the FP assay. False positive hits in the FP assay can occur if the compound interaction with the reporter ligand or if it influences the fluorescence intensity. For compound **118** an interaction with the reporter ligand was excluded and the changes in fluorescence intensity was within the allowed range of 20%. However, since the fluorescence intensity was changed about nearly 20% the effect in the FP assay could be as well due to unspecific effects. Due to all the presented arguments this compound was considered a false positive hit and was not further investigated. In both assays the screening hits. **111**, as well as **117**, the derivative of **111** without

Results and Discussion

the fluor atom and **119** were determined as clear hits. For **111** both assays showed stronger effects for the fluorinated compound suggesting a beneficial contribution of the fluor to the binding affinity. Since binding in the thermal shift assay might be prone to false positive results due to unspecific interactions with the protein a concentration dependent measurement was performed for **111** and **119** to verify specific binding. In case of specific binding, it is expected that the melting temperature is influenced with an increasing magnitude when increasing the concentration.

The highest concentration possible in the experiment was determined by the fact, that the assay system only tolerates a final DMSO concentration of 5 %. As the compounds showed different solubility in DMSO, this fact determined the maximum possible ligand concentration used in the experiment. The results of the titration differ in its absolute values from the ones presented in figure 37 due to fact that these results are a single experiment with replicates and figure 37 is the average of at least three independent experiments. In each case, LecA was tested with the used DMSO concentration of the set up. For **111** an IC_{50} value of 1.7 mM was determined with a R^2 value of 0.9774 of the fit. Since this fit was only calculated with 4 different datapoint the p-value for the statistical significance was calculated. For **111** a p-value of 0.1256 was determined which considers the obtained data as not statistically significant. For compound **119** an IC_{50} of 540.1 μ M was calculated with a very good R^2 of 0.999 of the fit. In this case a p-value of 0.0316 for the determined fit data was calculated which are considered statistically significant making the obtained IC_{50} value a valid result.

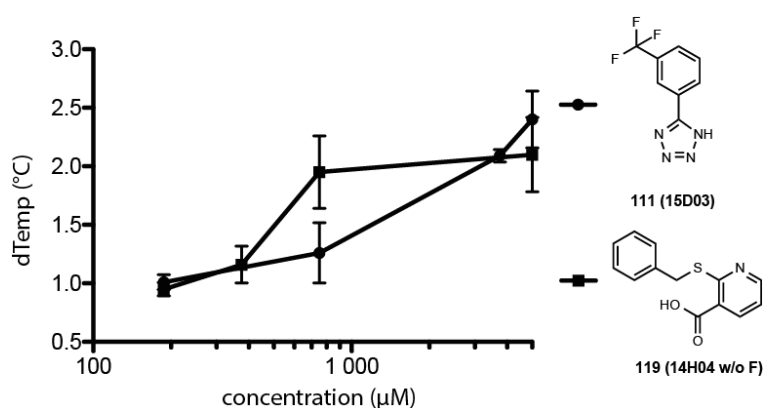


Figure 33: Concentration dependent changes in the melting temperature of LecA in presence of increasing concentrations of the two potential LecA carbohydrate binding site ligands **111** and **119** were monitored using the thermal shift assay. Both compounds did show changes to the melting temperature of LecA dependent on the concentration. For **111** an IC_{50} value of 1.7 mM was determined but as no saturation was reached the quality of the fit is rather poor. For compound **119** an IC_{50} of 540.1 μ M was calculated.

From the thermal shift assay with increasing concentrations of the derivatives **111** and **119** it can be hypothesized that there is no specific binding for **111** in the carbohydrate binding pocket. But the compound was identified in NMR screening using a LecA ligand as competitor. In addition, the melting temperature of

LecA was increasing with increasing ligand concentration it is likely that there is binding to LecA, but not in the carbohydrate binding pocket, but very close to the binding pocket. It is likely that the binding is close to the carbohydrate binding pocket as **111** showed effects in the NMR screening with p-NPG as competitor as well as effects in the FP assay with a p-NPG based reporter ligand. So, it can be concluded that the competition in the NMR competition experiment as well as the observed effects in the FP assay are not due to competition with the sugar part of the molecule, but due to replacement of the phenyl moiety of p-NPG. In addition, specific effects observed in the thermal shift assay show binding to LecA, but DSF does not allow a conclusion on the binding site. For **119** all obtained data show that the compound is binding to LecA, as binding was observed in the FP assay and DSF. Also, concentration dependent changes were observed in DSF which is a clear sign of specific binding. With the titration of **119** in the thermal shift assay a binding affinity of around 500 μM was determined, but no sigmoidal binding curves were obtained in the FP assay so the binding affinity could not be verified. As the maximum concentration in the FP assay was 1.7 mM due to solubility issue and issues with changes in fluorescence intensity of more than 20% a binding affinity of around 500 μM can not specifically be determined. But since a inhibition of 16 % was determined at a concentration of 667 μM with a low standard deviation of 1 % in three independent experiments binding was shown. In summary **119** showed binding in the NMR experiments as well as the FP and DSF assay so binding to LecA was shown.

*3.3. Evaluation of carbohydrate binding site shifts in ^{15}N TROSY experiments for hit verification of **119***

Within the screening campaign, the potential LecA ligand **104** emerged from a ^{19}F based NMR screening. The original screening hit was ordered from Sigma Aldrich as derivative without fluor **119** due to price reasons and tested in the FP assay and with TS assay. Both biochemical evaluations gave strong hits for binding but since no binding affinity could be determined binding was not fully proofed. So, the potential hit was tested

Results and Discussion

using the binding site mapping approach with a TROSY experiment. As no assignment of the protein exists, all numbers do not reflect the amino acid numbers of the protein but are randomly assigned.

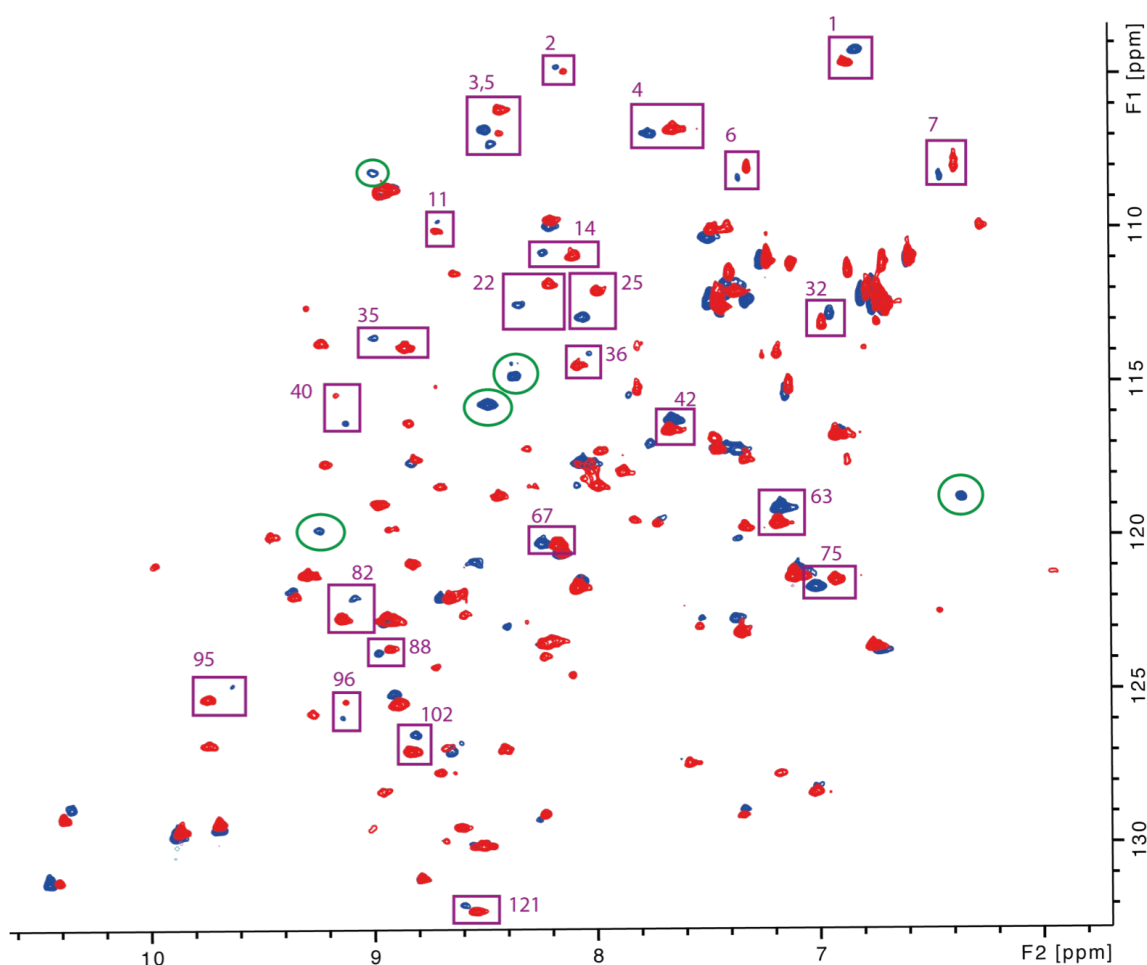


Figure 34: TROSY spectra of uniformly labeled ^{15}N LecA (291 μM) with 0.5 eq of **119** (145 μM) in presence of 1 eq of CaCl_2 (291 μM). LecA form with 0.1 % DMSO is depicted in red, the protein containing the potential ligand **119** in blue. All changes are marked with boxes and the respective peak numbers. The green circles represent newly emerging shifts or shifts that cannot be clearly assigned its peak in the protein spectra. 42 peaks were influenced by the addition of **119** to LecA, of which 31 match the shifts observed upon addition of the known LecA ligand me- α -gal and p-NPG. So, 74% of all shifts observed for **119** equal those of the know LecA carbohydrate binding ligands.

The examined compound **119** showed a total of 42 shifts upon which 31 are correspond to previously observed shifts for methyl α -galactoside and p-nitro phenyl β -galactoside. So, 74 % of the determined shifts for **119** are the same shifts in case of known LecA ligands and are thus within the carbohydrate binding pocket. From this measurement and comparison to known shifts of the carbohydrate binders me- α -gal and p-NPG it can be concluded that the determined non-carbohydrate inhibitor **119** is indeed binding within the carbohydrate binding pocket of LecA. In addition to the 31 known shifts 11 new shifts were observed in contrast to titration with the known sugar ligands. Three of them have been previously observed by titration with GdCl_3 . As it is assumed that lanthanide ions are binding instead of the natural ligand Ca^{2+} , which is in the carbohydrate

binding pocket, it can be assumed that the shift is close to the carbohydrate binding pocket. However, the huge number of shifts observed also leaves room for speculation on an additional binding site or other side effects caused by this compound.

Results and Discussion

3.3.5 Conclusion and Outlook on potential new ligands determined by the ^{19}F NMR high-throughput screening and biochemical evaluation

Table 1: Summary of the determined compounds from the screening of a sum of 192 compounds. Results of the screening using ^{19}F (hits marked aubergine) and CPMG (hits marked dark red) sequence. For the ^{19}F screening hits are rated with a 1 if clear effect that includes chemical shift are observed or a 0.5 if unsure effect that is a signal reduction of more than 40% without chemical shift. And for the ^{19}F competition test a 1 if chemical shift after inhibitor addition towards reference chemical shift or 0.5 if a rise in signal intensity of more than 20%. For the CPMG screening a 1 was scored if a clear effect that is a signal reduction of more than 50% or a 0.5 if an unsure effect that is a signal reduction of more than 25% is observed. For the CPMG sequence a 1 is scored if a clear effect that is a rise in signal intensity of more than 50% and a 0.5 if an unsure effect that is a rise in signal intensity of more than 25% is observed. The FP results are listed, and the hits marked in green and bold. The results from the TS assay are shown in orange and the significant this are marked bold, the shifts beyond the threshold of 0.40 °C are marked italic. In summary three compounds (or their flourineless analog) showed binding in a variety of different tests: **14C04**, **14H04**, **15D03**

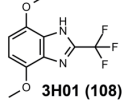
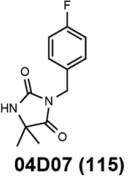
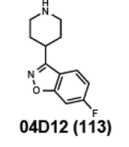
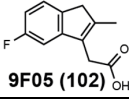
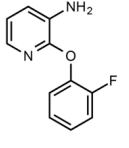
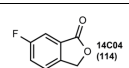
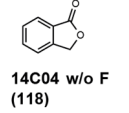
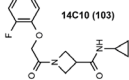
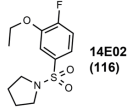
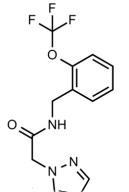
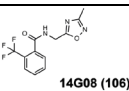
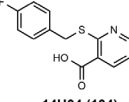
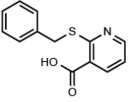
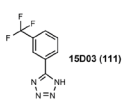
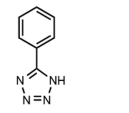
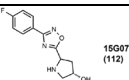
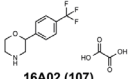
Compound	^{19}F hit	^{19}F competition	CPMG	CPMG competition	FP (inhibitor in %)	TS (dTemp °C)	TS (conc depended)
 3H01 (108)	1	0.5	0	0	0	0.16	n.d.
 04D07 (115)	0	0	1	1	0	<i>0.31</i>	n.d.
 04D12 (113)	0	0	0.5	1	0	-1.19	n.d.
 9F05 (102)	0.5	0	1	1	0	<i>0.26</i>	n.d.
 13H08 (110)	0	0	1	1	n.d.	n.d.	n.d.
 14C04 (114)	0	0	1	1	n.d.	n.d.	n.d.
 14C04 w/o F (118)	n.d.	n.d.	n.d.	n.d.	21.1	<i>0.04</i>	n.d.
 14C10 (103)	0.5	0	1	1	n.d.	n.d.	n.d.

Table 1: Summary of the determined compounds from the screening of a sum of 192 compounds. Results of the screening using ^{19}F (hits marked aubergine) and CPMG (hits marked dark red) sequence. For the ^{19}F screening hits are rated with a 1 if clear effect that includes chemical shift are observed or a 0.5 if unsure effect that is a signal reduction of more than 40% without chemical shift. And for the ^{19}F competition test a 1 if chemical shift after inhibitor addition towards reference chemical shift or 0.5 if a rise in signal intensity of more than 20%. For the CPMG screening a 1 was scored if a clear effect that is a signal reduction of more than 50% or a 0.5 if an unsure effect that is a signal reduction of more than 25% is observed. For the CPMG sequence a 1 is scored if a clear effect that is a rise in signal intensity of more than 50% and a 0.5 if an unsure effect that is a rise in signal intensity of more than 25% is observed. The FP results are listed, and the hits marked in green and bold. The results from the TS assay are shown in orange and the significant this are marked bold, the shifts beyond the threshold of 0.40 °C are marked italic. In summary three compounds (or their flourineless analog) showed binding in a variety of different tests: **14C04**, **14H04**, **15D03**

 14E02 (116)	0	0	1	1	n.d.	n.d.	n.d.
 14E08 (105)	0.5	0.5	0.5	0.5	n.d.	n.d.	n.d.
 14G08 (106)	1	0.5	0	0	n.d.	n.d.	n.d.
 14H04 (104)	0	0	1	1	n.d.	n.d.	n.d.
 119 (14H04 w/o F)	n.d.	n.d.	n.d.	n.d.	16.4	0.97	yes
 15D03 (111)	0	0	1	0.5	20.8	1.53	yes
 15D03 w/o F (117)	n.d.	n.d.	n.d.	n.d.	16.0	0.57	n.d.
 15G07 (112)	0	0	1	1	n.d.	n.d.	n.d.
 16A02 (107)	1	0.5	0	0	n.d.	n.d.	n.d.

In Table 1 all screening hits and their biochemical evaluation are summarized. **105** showed effects in all four NMR sequences, but only scored a 0.5 in each individual sequence. No other compound showed effects in all four NMR measurements. As the score was only 0.5 in all NMR measurements this could be unspecific interaction or rather weak binding affinity. Due to cost limitations and compound availability the compound

Results and Discussion

was not tested in the FP assay or DSF. Thus, it can not be verified if there is specific binding to LecA. **102** did show effects in the ^{19}F measurements (0.5 in the measurement without competitor and 0 with competitor) but scored a 1 in both CPMG sequences. But no effect was seen in the FP or the TS assay. This could be due to very poor affinity or a false positive hit in the NMR measurements. **114** did show clear effects in the CPMG measurements but no effects in the ^{19}F measurement. To evaluate the binding the fluorless derivative **118** was analyzed in the FP and TS assay. In the FP assay no sigmoidal binding curve could be obtained, but in single concentration experiments an inhibition of 21 % was observed. Even though experiments with compound and the reporter ligand alone showed that there is no interaction the fact that no temperature shift (0.04 °C) was determined in the TS assay makes it most likely a false positive hit. **111** showed no effect in the ^{19}F measurement but showed a strong effect in the CPMG sequence (scored a 1) and showed effects upon addition of the competition (scored a 0.5). **111** as well as its fluorless derivative **117** was tested in the FP and TS assay. Both compounds showed no sigmoidal binding curves, but both showed a good inhibition of 21 % for **111** and 16 % for the derivative **117** without fluorine. Also, both compounds showed strong effects on the LecA melting temperature of 1.53 °C for **111** and 0.57 °C **117**. In both biochemical assays the fluorinated derivative showed stronger effects than the one without fluorine suggesting that the fluorine in the structure is either directly involved in the binding or is influencing the distribution of the electron density in the structure in a favorable way. To investigate this, molecular modeling of the compounds in complex with LecA can be done. After this modeling the path forward can be determined, if a fragment growing approach can be used or if chemical derivatization might result in a more potent LecA ligand.

For compound **113** no effect was observed in the ^{19}F experiment, but effects are observed in the CPMG sequence. Astonishingly only weak effects were observed in the sequence without the competitor, but stronger effects were observed with the sugar competitor. Also, no effect was observed in the biochemical TP assay. In the thermal shift assay a destabilization of LecA of -1.19 °C was observed. Negative shifts do not necessarily mean that there is no binding but can be also a hint of unspecific interaction with the protein surface. The absence of binding in the TP assay and the negative shift are most likely the effect of unspecific or unfavorable interaction with the protein resulting in slight changes in the protein structure. These changes cause an effect in the CPMG sequence, and cause destabilization in the TS assay. The reason for the hit in the competitive CPMG sequence cannot be explained by the destabilization theory but might be caused by the stabilization of the protein upon addition of the sugar ligand.

The clearest hit determined in this series was **104** and its derivative **119**. The compound showed no effects in the ^{19}F sequence, it showed clear effects in the CPMG sequence. As for all other compounds, no sigmoidal binding curve could be determined in the TP assay, but final inhibition of 16 % pointed clearly towards a specific binding in the binding pocket. Also, the TS assay showed that **119** stabilized the protein LecA by 0.97°C and moreover in a concentration dependent TS assay it was shown that increasing amounts of **119** showed an increasing stabilization of LecA. This all taken together for compound **119** (and **104**) binding to the carbohydrate binding pocket of LecA is given and thus a fragment growing, or derivatization approach

could be used to develop a new, non carbohydrate structure as a LecA ligand, which might ultimately lead to structures with a higher affinity to LecA.

3.4 A lanthanide-based NMR approach for the determination of new LecA inhibitors

The search for new, more potent LecA inhibitors has been challenging. While there has been a bigger improvement in lectin LecB inhibitors, the galactophilic lectin LecA is more challenging. [6787, 89, 90] In comparison to the natural ligand D-galactose with an affinity of around 80 μM , a dramatic increase in affinity was observed by introduction of an aromatic, hydrophobic moiety in beta position of the anomeric carbon, ending up with ligands of around 10 μM affinity. [68-69] Sebastien Vidal and co-workers further increased the affinity to 5 μM . The replacement of the aglycon with a naphthol moiety did decrease the affinity to 3.2 μM . This is up to date the lowest known affinity for monovalent LecA inhibitors. [272] Since the approach of galactose derivatization did not result in ligand with a strongly decreased binding affinity, another approach to develop ligands with a significantly enhanced affinity is needed. Looking at the crystal structure, a cleft near the carbohydrate binding pocket is observed, bearing aromatic amino acids like Trp42, Tyr36 and Thr38 as well as hydrophobic amino acids like Glu59, Asp47 and Gln40 (Figure 7). It was shown that the π -stack interaction of His50 of a phenyl substituted β -galactosides resulted in an enhanced affinity. So potential ligands should keep the beneficial interaction. In general, fragment growing or fragment linking approaches could potentially be used to develop new, more potent LecA inhibitors. The question remains how to identify fragments binding in the vicinity of the carbohydrate binding pocket to link them together with known D-galactose based ligands to obtain a new and more potent ligand. An NMR approach could be the solution to this fragment identification issue. Since the potential second binding site can be further away from the carbohydrate binding pocket the question arises how to identify ligands binding in the second site. Paramagnetism could be the answer to this, as it has the advantage of long distance influences up to 40Å. In the field of paramagnetic NMR Otting and Bertini are pioneers. They already used the replacement of diamagnetic Ca^{2+} in calcium-binding protein metallo-matrix protease (MMP) and determined ligand binding looking at ligand effects, like paramagnetic relaxation enhancement (PRE) and pseudo-contact shifts (PCS).

LecA also has a Ca^{2+} ion in the binding pocket. To use paramagnetic effects in NMR screening the Ca^{2+} can be replaced by paramagnetic lanthanide ions. Those ions can cause paramagnetic relaxation enhancement (PRE) and pseudo-contact shifts (PCS) on signals. As these effects are distance, and PCS also angle, dependent information on the binding of a potential ligand can be made. This approach is schematically shown in figure 35, where the paramagnetic ion that replaced Ca^{2+} ion is shown in green. It can cause paramagnetic effects on a ligand binding to a potential second binding site. Paramagnetic effects can be distance and angle dependent effects (shown by different sizes of the letters).

3.4.1 Functional replacement of the natural Ca^{2+} with trivalent paramagnetic lanthanide ions in LecA

The screening approach is based on the functional replacement of Ca^{2+} in the binding pocket of LecA. Thus, the potential to functionally substitute the natural salt ligand Ca^{2+} in the binding pocket is examined. For the use of lanthanides ions as tags in NMR screening approach LecA needs to be functional and able to bind to a ligand, in complex with the substituted lanthanide ions. To evaluate which lanthanides can functionally replace Ca^{2+} in the binding pocket the natural binding behavior of LecA was used: LecA can bind to galactose with a good affinity ($K_d = 87.5 \mu\text{M}$) but does not bind to glucose with a reasonable affinity. [67-69, 273] So, to determine if the paramagnetic lanthanides ions Tb^{3+} , Yb^{3+} , Ce^{3+} , Ho^{3+} , Tm^{3+} , Dy^{3+} and Gd^{3+} and the diamagnetic ion La^{3+} are able to functionally replace the natural ligand Ca^{2+} the following modified ELLA experiment was set up:

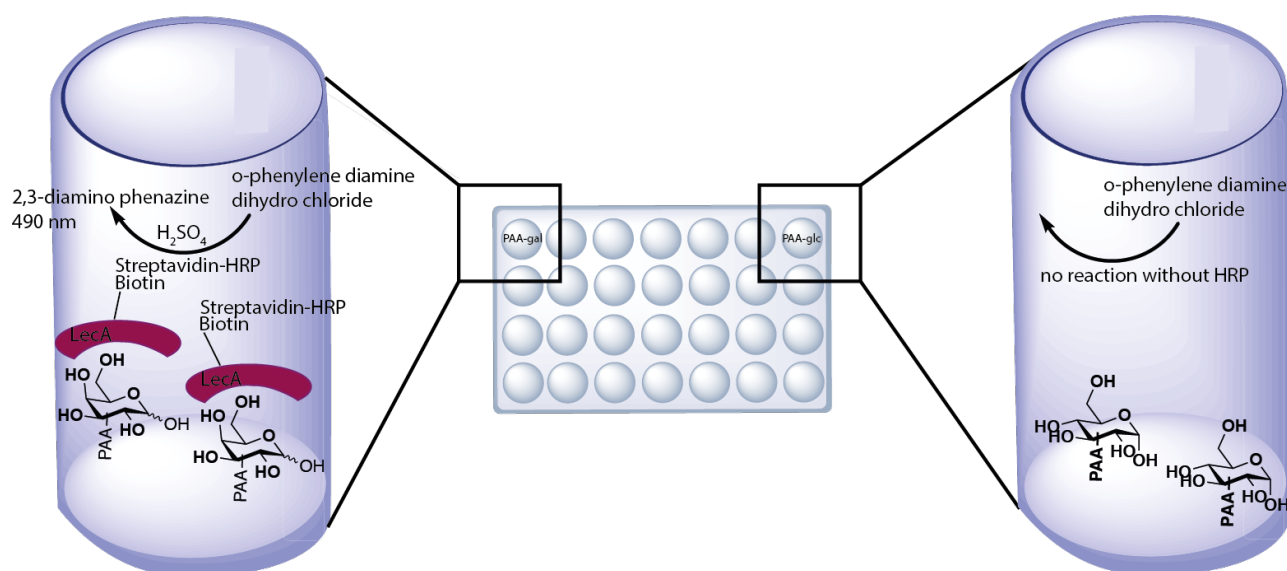


Figure 35: Schematic representation of the ELLA-experiment using a galactosylated and gluosylated surface. LecA has a good affinity to galactose and no significant affinity to glucose. For the ELLA experiments biotinylated LecA is used. After binding of the biotinylated LecA and incubation step with streptavidin coupled with a peroxidase (HRP = horse radish peroxidase) is followed. Binding of LecA to the both surfaces is red out using a chemical reaction catalyzed by HRP of o-phenylene diamine dihydro chloride to 2,3-diamino phenazine. Before the read out of 490 nm the reaction is stopped using H_2SO_4 .

For the determination of the functional replacement of Ca^{2+} in the binding pockets by lanthanide ions, the vials were coated either with galactose (PAA-gal) or glucose (PAA-glc). For the experiment LecA is labeled with biotin to use HRP-Streptavidin to generate a colour reaction of o-phenylene diamine dihydro chloride. To substitute with different lanthanide ions, biotinylated LecA was obtained in its apo form (Ca^{2+} -free) to substitute with different lanthanide ions as well as EDTA as negative control and Ca^{2+} as positive control. To obtain Ca^{2+} free LecA, a dialysis set up using a highly potent Ca^{2+} binding chelator was established. Ethylenediaminetetraacetic acid (EDTA) was chosen as a chelator as it is a highly potent Ca^{2+} ion binder with an affinity of around $0.1 \mu\text{M}$. [200]. To determine if LecA can still functionally bind to D-galactose after

Results and Discussion

replacement with lanthanides, Biotin-labeled LecA was incubated either with the different lanthanides, or the natural ligand Ca^{2+} or with EDTA as control. EDTA is a cheating agent binding Ca^{2+} , thus it was used as a negative control to verify that no binding to the sugar surfaces is possible without salt. Binding is evaluated using a chemical reaction of o-phenylene diamine dihydro chloride. To facilitate this reaction an enzyme, called horse-radish peroxidase (HRP), is used. This enzyme is coupled to Streptavidin, which is binding with a very high affinity to biotin. which is widely used as a tag in combination with horse radish peroxidase.

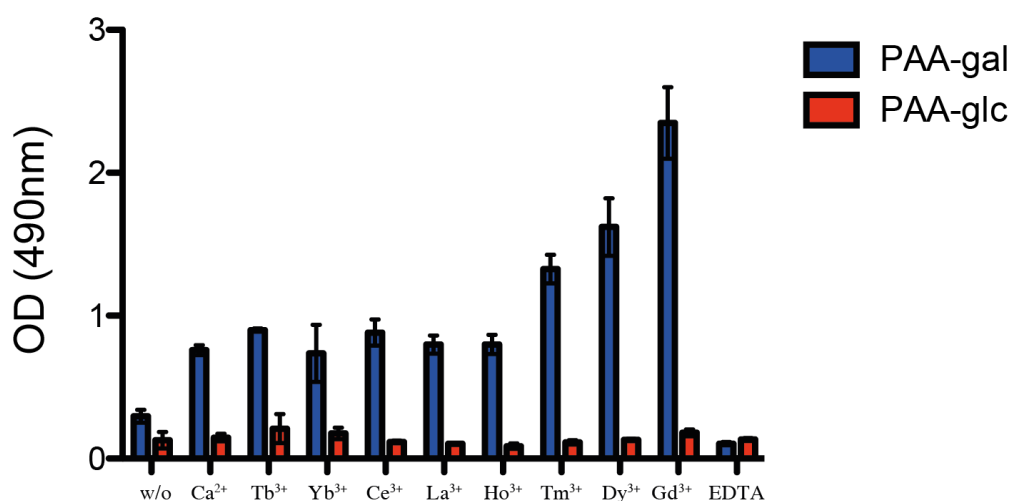


Figure 36: The ELLA assay showed the functional replacement of Ca^{2+} in LecA. The red bars represent the binding to a glucose surface, while the blue bars represent the binding to a galactose surface. In presence of EDTA or without substitution (w/o), no binding was observed. All tested lanthanide ions as well as the natural ligand Ca^{2+} were able to functionally replace Ca^{2+} in the binding pocket of biotinylated LecA.

An ELLA assay was used to get inside in the binding potential of Ca^{2+} free, so-called apo, LecA re-substituted with different lanthanides to D-galactose. For the ELLA experiment LecA was used in its apo-form (Ca^{2+} free). After expression and purification, LecA was dialyzed first against an EDTA solution to remove the naturally bound Ca^{2+} , and subsequent dialysis against a NaCl solution and water was needed to obtain Ca^{2+} -free and EDTA free LecA.

Data from the ELLA experiment shows that there is no binding of LecA with either of the lanthanide salts to the glucosylated surface (Figure 36). In contrast, binding of LecA to the galactosylated surface was observed for all the tested lanthanide ions as well as for the diamagnetic control Ca^{2+} (Figure 36). The presented results suggest an enhanced binding affinity of LecA to galactose in presence of Gd^{3+} . Since ELLA assays are known to have a poor reproducibility between different plates [20], the error of for all tested ions is rather high. Besides the slightly enhanced affinity of Gd^{3+} , a conclusion on the binding affinity of the different lanthanide ions and Ca^{2+} can not be drawn. but the overall conclusion that all tested lanthanides were functionally able to replace

the natural ligand Ca^{2+} in the binding pocket. For comparability reasons all tested lanthanides were used in the same concentration (200 μM). The determination of the binding affinities of the different lanthanide ions can be important, as unbound lanthanide ions in the NMR measurements might cause unspecific side reactions. Protons of ligands might also show enhanced relaxation behavior or signal broadening, if they come close to lanthanide ions that are unbound and thus free in solution.

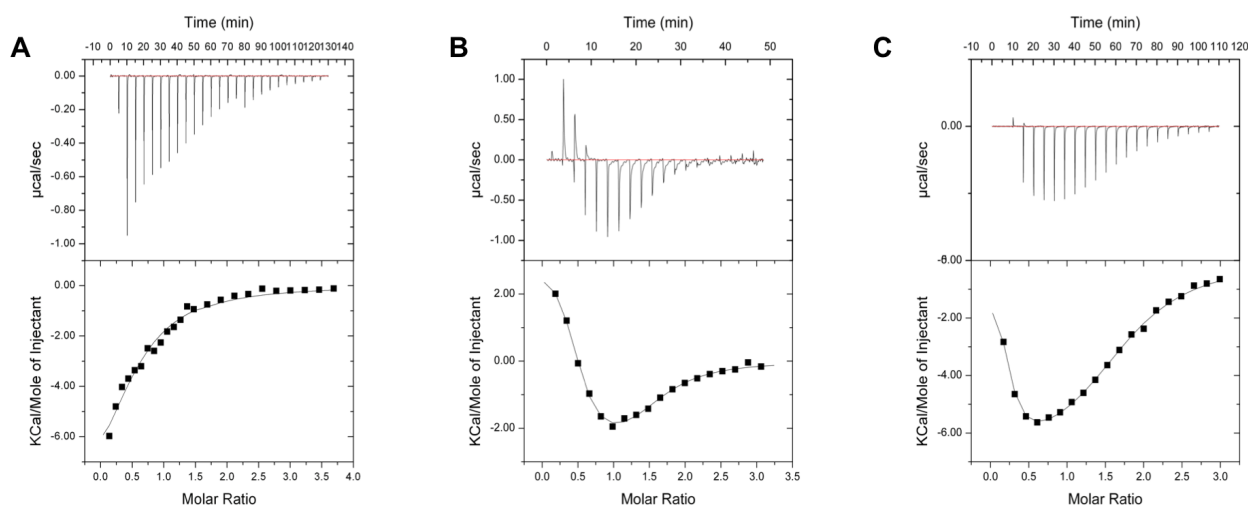


Figure 37: The binding affinity of ITC titrations of Ca^{2+} (A), Tb^{3+} (B) and Dy^{3+} (C) to apo LecA was determined using ITC measurement. For titration of LecA with Ca^{2+} ion one site fit was used and a K_d value of $60 \pm 20 \mu\text{M}$ was determined ($N = 0.6 \pm 0.4$). For the titration with Tb^{3+} a two-site fit was used for calculation and a K_{d1} value of $37 \pm 6 \mu\text{M}$ ($N_1 = 0.9 \pm 0.2$) and K_{d2} value of $13 \pm 16 \mu\text{M}$ ($N_2 = 0.3 \pm 0.1$) was calculated. Also, for the titration with Dy^{3+} a two-site fit was used for calculation and a K_{d1} value of $78 \pm 5 \mu\text{M}$ ($N_1 = 1.1 \pm 0.1$) and K_{d2} value of $27 \pm 2 \mu\text{M}$ ($N_2 = 0.1 \pm 0.1$) was obtained.

Because of the poor reproducibility of absolute absorbance values in ELLA experiments, this method was not suited to determine the binding affinity of the lanthanide ions to LecA. Because lanthanides offer long-life fluorescence, a time-resolved FRET (Förster resonance energy transfer) approach was planned. In this time-resolved FRET the excitation of the Trp42 in the binding pocket of LecA and an energy transfer to the lanthanide ion in the binding pocket of LecA and an emission of long-life fluorescence of LecA was tried. But no fluorescence of the lanthanide ions was detected probably because of quenching of the lanthanide fluorescence due to water molecules in the binding pocket. As the photometric determination of the binding to LecA was not possible the binding of lanthanides to Ca^{2+} free LecA was examined using isothermal titration calorimetry (ITC). For ITC Ca^{2+} free LecA, so called apo-LecA, was used. First apo LecA was measured upon titration with its natural ligand Ca^{2+} . A binding affinity of $60 \pm 20 \mu\text{M}$ was measured for the natural ligand of LecA, and a binding stoichiometry of 0.6 ± 0.4 . In theory a binding stoichiometry of 1 would be expected. One reason why a binding stoichiometry of less than 1 was determined could be that the protein is partially inactivated either during lyophilization or during the resolubilisation process. To exclude damages to the protein the resolubilisation protocol was adapted to mild shaking for two hours at room temperature. More likely, remainders of Ca^{2+} either in the sample cell or the buffer itself might be the reason for the binding stoichiometry. None of the salts are completely Ca^{2+} free, so it is most likely that the poor binding stoichiometry is due to remaining Ca^{2+} or a combination of both reasons presented above. In contrast to the titration with

Results and Discussion

Ca^{2+} a two-site fit had to be used for calculation of Tb^{3+} and Dy^{3+} , which means that the protein has two different binding sites for the lanthanide ions. For Tb^{3+} , the two measured affinities were $K_{d1} = 37 \pm 6 \mu\text{M}$ and $K_{d2} = 13 \pm 16 \mu\text{M}$. For the binding stoichiometry $N_1 = 0.9 \pm 0.2$ and $N_2 = 0.3 \pm 0.1$ were determined. A binding stoichiometry of 1 means, that one ligand, in this case Tb^{3+} , is binding to one protein, in this case LecA. So, for N_1 it can be assumed, that one Tb^{3+} is binding to one LecA. As usually each binding pocket has a Ca^{2+} , this is most likely the values of the Ca^{2+} -binding site. To conclude that would mean that the binding affinity of Tb^{3+} in the Ca^{2+} binding pocket is $37 \pm 6 \mu\text{M}$. But there also is a second binding site for Tb^{3+} but that seems to be an complex interaction of more than one LecA with a Tb^{3+} ion. Also, for Dy^{3+} two binding sites have been determined. Most likely the Ca^{2+} site has an affinity for Dy^{3+} of $78 \pm 5 \mu\text{M}$ and a binding stoichiometry of $N = 1.1 \pm 0.1$. The second binding site has an affinity of $27 \pm 2 \mu\text{M}$ and a binding stoichiometry of $N = 0.1 \pm 0.1$. This binding stoichiometry would mean, that one Dy^{3+} ligand is binding to 10 LecA molecules. As this is rather unlikely this result is most likely an artefact. In summary, both lanthanides are binding to LecA with a comparable affinity as the natural ligand Ca^{2+} .

3.4.3 Determination of paramagnetic effects on protons of the known LecA ligand *p*-nitro phenyl β -D-galactoside using different trivalent lanthanide ions

To establish a screening based on functional replacement of Ca^{2+} in LecA, effects of paramagnetic lanthanides in complex with LecA in NMR set up were examined. To evaluate the effects a ligand known to bind to LecA was used. *p*-nitro phenyl β -D-galactoside (**19**) is a known LecA ligand with a binding affinity of $26.2 \mu\text{M}$. As *p*-NPG (**19**) has not only the sugar protons, but also the phenyl protons which are further away from the paramagnetic center this ligand is ideal to evaluate the ability to obtain distance dependent effects. In the literature, Tb^{3+} , Dy^{3+} , Tm^{3+} and Ho^{3+} are often used for lanthanide-based NMR methods.^[220] Thus, first water suppressed proton spectra and $T_{1\rho}$ measurements were recorded using those four lanthanide ions.^[172, 233, 274-276] All four trivalent lanthanide ions were used in the NMR set up together with apoLecA and the known LecA ligand *p*-nitro phenyl β -D-galactoside (**19**). For all experiments, a para- and diamagnetic control without addition of the protein as well as a diamagnetic reference with Ca^{2+} and LecA were recorded. In literature, different ratios of ligand and protein were used, varying from 2- to 100-fold excess of the ligands.^[154, 192, 213, 277-279] In this experiment a ligand excess of 100-fold was used. LecA was used with $10 \mu\text{M}$. For Tm^{3+} and Ho^{3+} no K_d was determined so equimolar concentration was used. For Dy^{3+} a K_d of $78 \mu\text{M}$ was determined, but due to increasing line broadening with increasing lanthanide concentration only $50 \mu\text{M}$ was used. First, water-suppressed proton spectra were recorded for all samples. The diamagnetic control (Ca^{2+} , Figure 38 blue curve) showed the strongest signal intensity. Ho^{3+} (Figure 38, blue curve) and Tm^{3+} (Figure 38, black curve) both showed a slightly reduced signal intensity compared to the diamagnetic control. Dy^{3+} (Figure 38, purple curve) showed a clear signal reduction in contrast to the diamagnetic control. For all lanthanide samples line broadening in contrast to the diamagnetic control was observed.

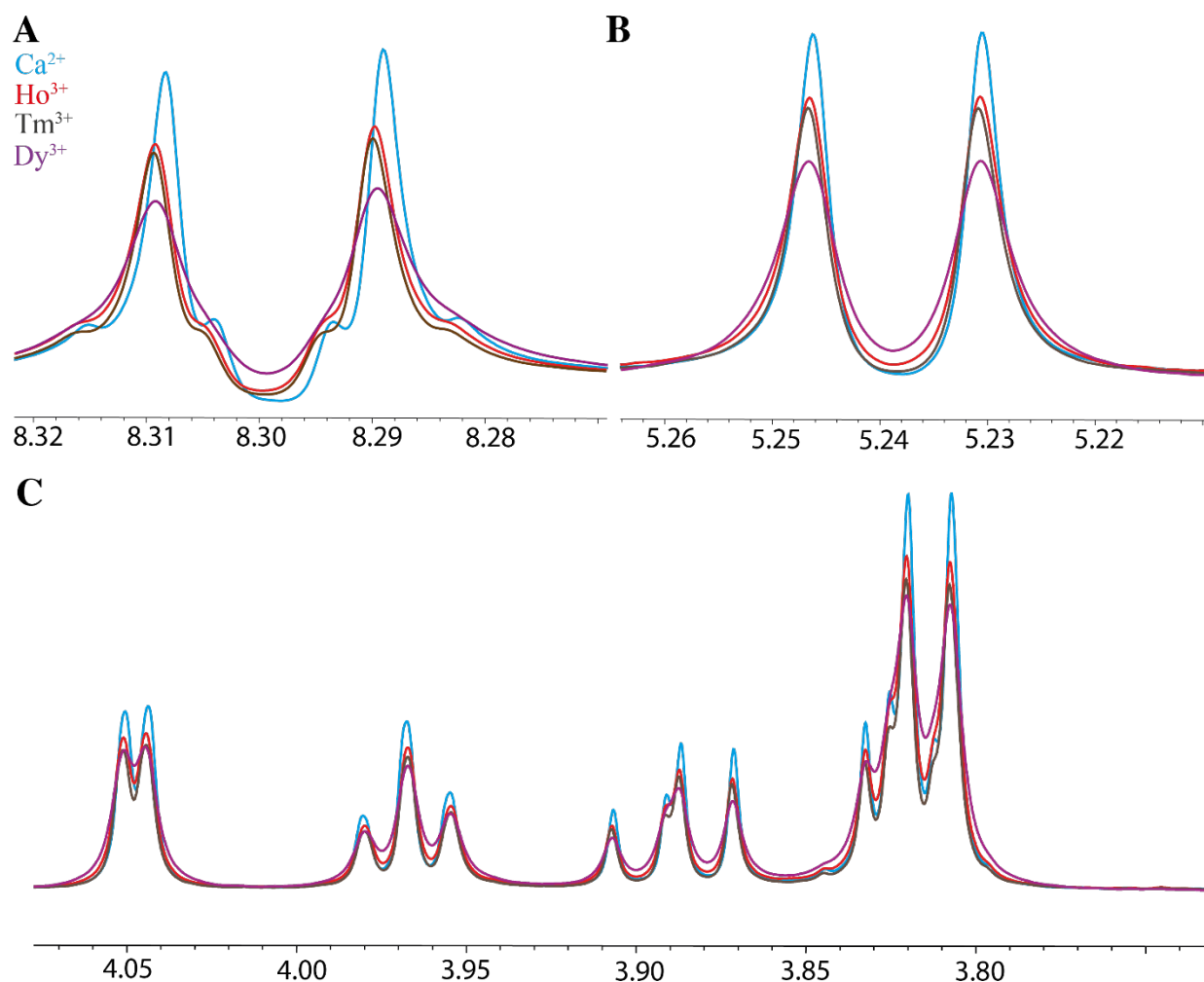


Figure 38: Water suppressed 1D proton spectra of p-nitro phenyl β -galactoside **19** (1 mM) in presence of LecA (10 μ M) and paramagnetic lanthanides Ho³⁺ (10 μ M, red spectra), Tm³⁺ (10 μ M, grey spectra) and Dy³⁺ (50 μ M, purple spectra) or the diamagnetic sample containing Ca²⁺ (blue spectra). Spectra were recorded with a 100-fold ligand excess and 16 scans. All spectra are recorded with 100 μ M TMA and normalized to the internal standard.

To conclude, Ho³⁺ and Tm³⁺ showed only weak effects on the protons of the known LecA ligand p-NPG. Since Tb³⁺ and Dy³⁺ have the strongest PRE and PCS effects, both were tested in more detail. ^[280]

The ligand to protein ratio is important for the determination of distinct PRE effects in T1 ρ experiments using the paramagnetic Tb³⁺ ion

The ligand based T1 ρ NMR technique uses the proton signals of a ligand. Spectra of the same sample with different spin lock times are recorded and used for the determination of paramagnetic relaxation enhancement effects on the ligand protons. Thus, the ligand concentration must fulfill two criteria: first, it must be used in a concentration with a suitable signal to noise ratio, and second it must be an excess to the protein and above the K_d value of the ligand-protein complex to ensure binding and exchange. The examined LecA ligand p-nitro phenyl β -D-galactoside has a binding affinity of 26.2 μ M. ^[272] As first NMR experiments were aimed to have

Results and Discussion

a 100-fold ligand excess with relation to the LecA concentration of 50 μM , a concentration of 5 mM of p-NPG was used. A 200-fold ligand concentration above the K_d of the protein-ligand complex ensures full saturation .

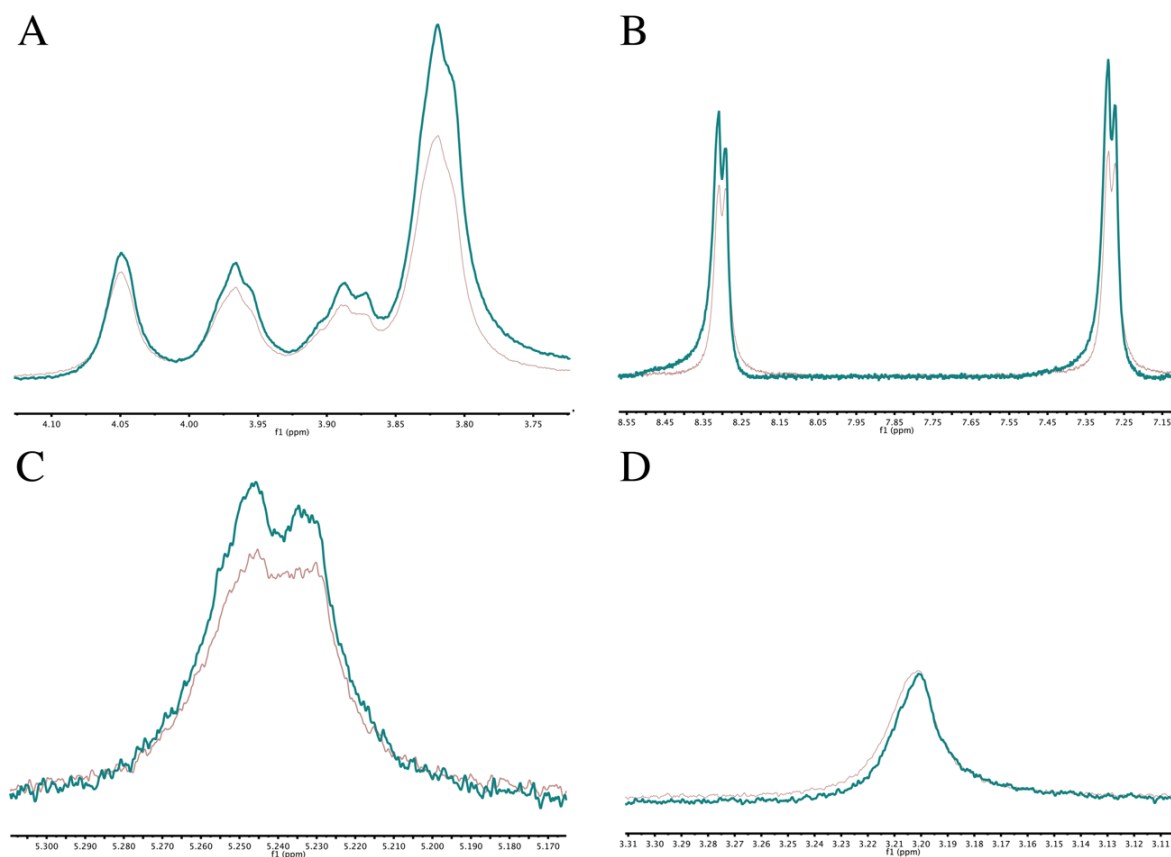


Figure 39: Enhanced signal relaxation in presence of the paramagnetic Tb^{3+} . Proton spectra of p-nitro phenyl β -D-galactoside **19** (5mM, green spectra) together with LecA (50 μM , red spectra) were recorded with paramagnetic TbCl_3 (50 μM) and the internal standard (TMA, 500 μM). **A** shows the sugar signals and **C** the signal of the anomeric proton, while **B** show the aromatic phenyl signals. **D** shows the signal of the internal standard at 3.201 ppm. Spectra were recorded with 16 scans and referenced to the internal standard.

With respect to the determined K_d value of the trivalent Terbium-Ion, a concentration of 50 μM Tb^{3+} was used. Consequently, LecA was used in the same concentration (50 μM) while for a 100-fold ligand excess, 5 mM of p-nitro phenyl β -D-galactoside was used.

Water suppressed proton spectra as well as $T_{1\rho}$ spectra were recorded. Relaxation effects were observed for the sugar protons (Figure 39, A and C) and for the aromatic phenyl protons (Figure 39 B). But no PCS were observed for any of the signals.

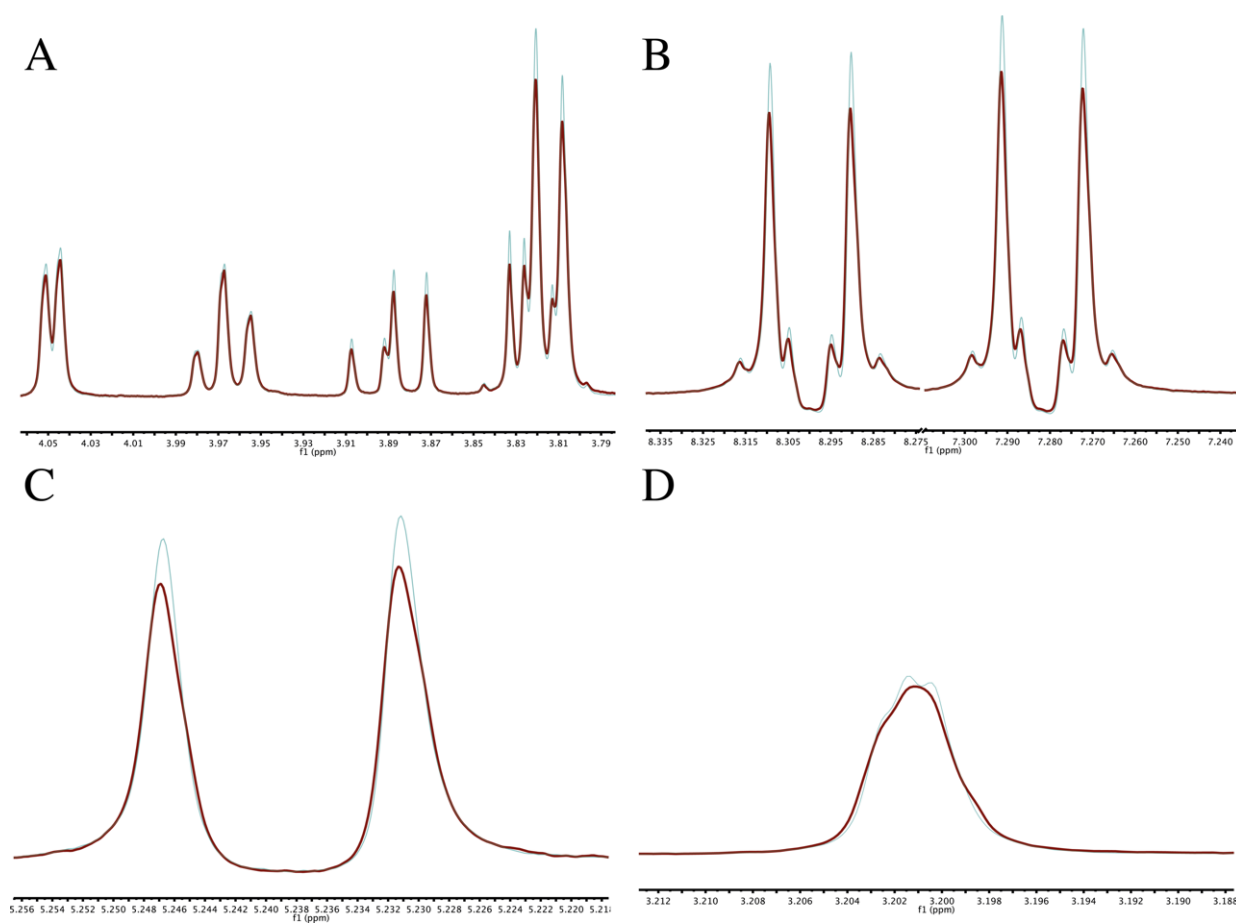


Figure 40: 1D Proton spectra of p-nitro phenyl β -D-galactoside (5mM, alone green) and with LecA (50 μ M, red). All spectra contain CaCl_2 (both 50 μ M) and the internal standard (TMA, 500 μ M). **A** shows the sugar signals and **C** the signal of the anomeric proton, while **B** shows the aromatic phenyl signals. **D** shows the signal of the internal standard at 3.201 ppm. Spectra were recorded with 16 scans.

Results and Discussion

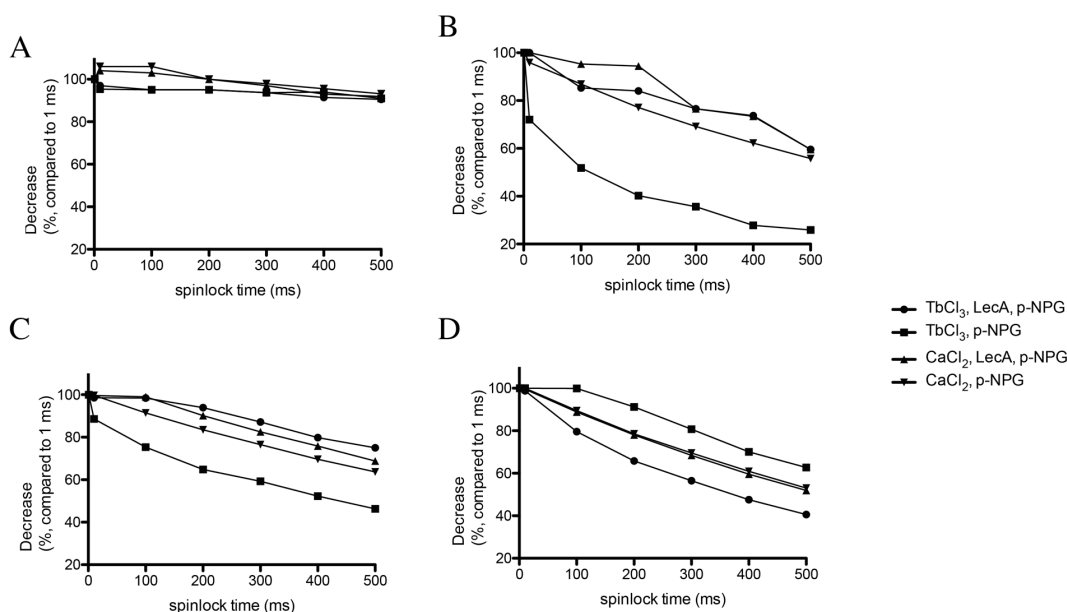


Figure 41: Signal intensity within the series of $T1\rho$ spectra of p-NPG decreased with increasing spin lock times. Concentration of p-nitrophenyl β -D-galactoside 5 mM, LecA 50 μ M and $TbCl_3$ or $CaCl_2$ both with 50 μ M were used. **A** presents the evaluation of relaxation of the phenyl protons, **B** of the anomeric proton Gal-H₁, **C** of Gal-H₄ and **D** of Gal-H₅. Spectra were recorded with 32 scans. The anomeric proton Gal-H₁ showed the strongest relaxation, while the phenyl protons showed no difference in relaxation between the diamagnetic and paramagnetic samples.

For each sample, a water-suppressed proton spectrum and $T1\rho$ spectra with six different spin lock times were recorded and the relaxation was evaluated. In case of the water suppressed proton spectra, a signal decrease of 22.7 % in case of phenyl proton of the paramagnetic sample and 11.2 % in case of the diamagnetic sample was measured. For the Gal-H₅ proton of the sugar a relaxation of 22.2 % was measured in the paramagnetic samples while the diamagnetic samples showed relaxation of 0.4 %. The effects of the paramagnetic Tb^{3+} ion in $T1\rho$ measurements was less pronounced (Figure 41). For the anomeric proton Gal-H₁ a clearly enhanced relaxation of the signal was observed (Figure 41, B). Also, for the other clearly distinguishable sugar signals, Gal-H₄ and Gal-H₅, a slightly enhanced signal relaxation was observed (Figure 41 C and D). In contrast, no enhanced signal relaxation was observed for the phenyl-protons (Figure 41, A). As this method monitors the ligand signals as an average of all protons in the sample, a large excess of ligand might result in minor effects. For this experiment a ligand excess of 100-fold was used, thus a lot of unbound ligands in the sample. To optimize the conditions, a reduced ligand to LecA ratio of 50:1 was also examined with 1D water suppressed proton spectra and $T1\rho$ measurements.

A comparison between paramagnetic- and diamagnetic samples showed no difference in the decrease of the signal upon binding to the protein. In particular, the paramagnetic sample showed a decrease of 15.3 % whereas the diamagnetic samples showed a decrease of 14.1 %. But for the paramagnetic sample (Figure 40) line broadening in presence of LecA was observed, proofing binding of the galactose derivative to the protein. Binding to the protein is expected as LecA was shown to be functional after replacement with a trivalent lanthanide ions and p-NPG is a known LecA ligand. In contrast, no line broadening was observed in presence of the diamagnetic Ca^{2+} ion, but signal decrease as a sign of binding. The relaxation behavior in T1 ρ measurements of the paramagnetic samples was enhanced compared to the paramagnetic control and the diamagnetic samples (Figure 40).

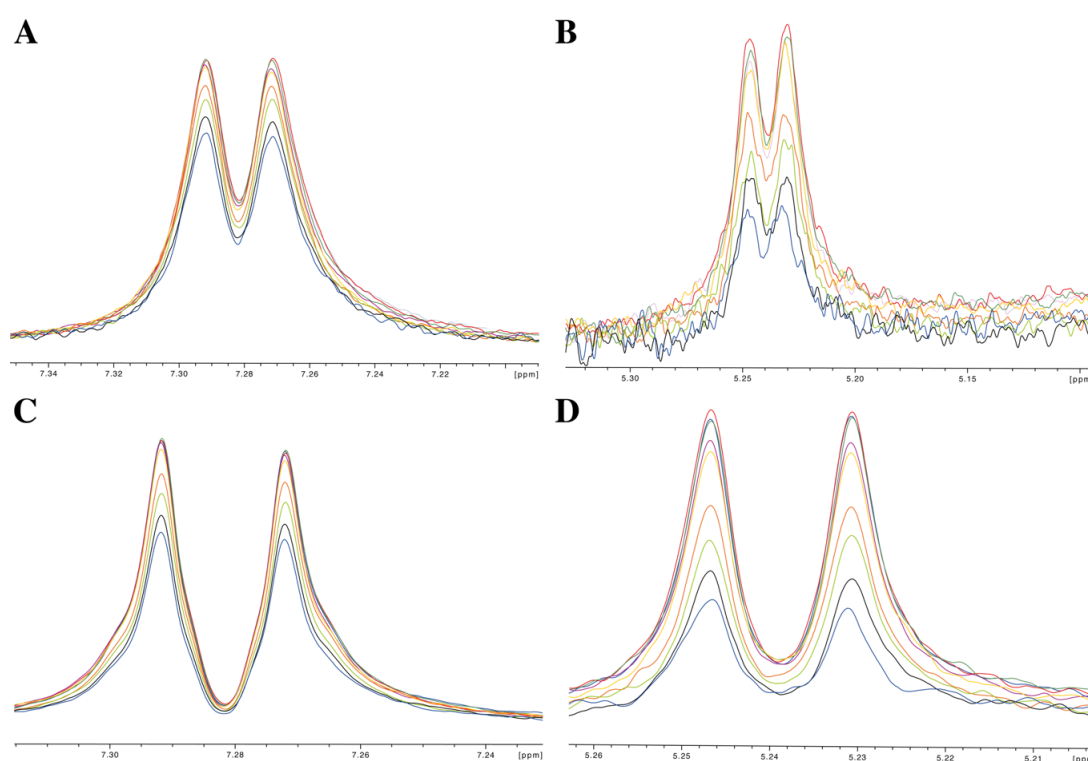


Figure 42: Stacked T1 ρ spectra of p-nitro phenyl β -D-galactoside (2.5 mM) and TbCl₃ (50 μ M) in presence of LecA (50 μ M) (A, B) and absence of LecA (C, D). A and C represent the aromatic phenyl protons at 7.28 ppm while B and D represent the anomeric Gal-H1. All spectra were recorded with 32 scans and spinlock times varying from 0.5 ms (red), 1 ms (blue), 10 ms (green), 50 ms (purple), 100 ms (yellow), 300 ms (orange), 500 ms (light green), 700 ms (black) to 900 ms (dark blue) and in presence of 100 μ M internal standard, to whom the spectra were referenced.

This enhancement was caused by the Tb³⁺ as a paramagnetic spin label in the binding pocket of LecA. Upon binding of the nitro-phenyl D-galactose derivative to LecA with Tb³⁺, the protons showed an enhanced signal relaxation behavior. As previously, no pseudo-contact shifts were observed using a 50-fold excess of ligand compared to LecA. If a great ligand excess is used the problem of ligand that have never been contact with the protein can become more prominent, thus a ligand excess of only 10-fold can be beneficial. [255]

Results and Discussion

To examine this, 1D water suppressed proton spectra and a series of T1ρ spectra were recorded with an excess of 10-fold ligand to protein.

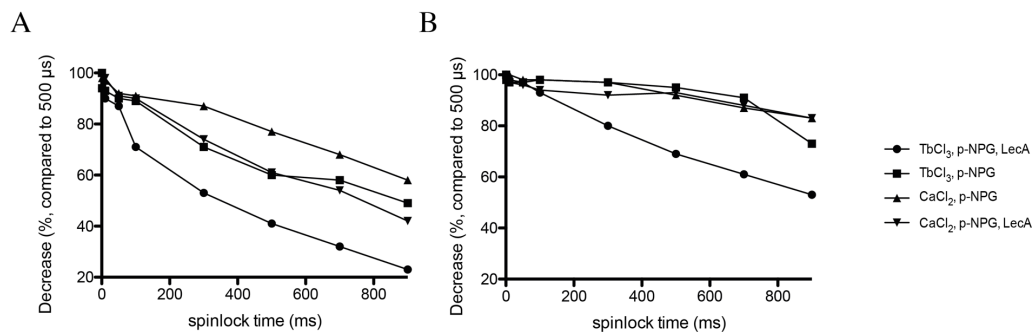


Figure 43: Determined decrease in signal intensity for the proton signals of the LecA ligand p-NPG. Specifically, **A** shows the decrease of the anomeric proton and **B** of the phenyl proton at 8.01 ppm. The spectra were recorded with a ligand concentration of 2.5 mM, a salt concentration of 50 μM. In case of the samples containing LecA (Dots and downward triangle) a LecA concentration of 50 μM was used. Like this, a 50-fold ligand excess was obtained. Only one representative example of the phenyl protons is shown. Because of significant line broadening of the sugar protons, only the anomeric H₁ could be evaluated as a distinct signal. The internal standard TMA was used in 100 μM concentration in all samples and all spectra were recorded with 32 scans.

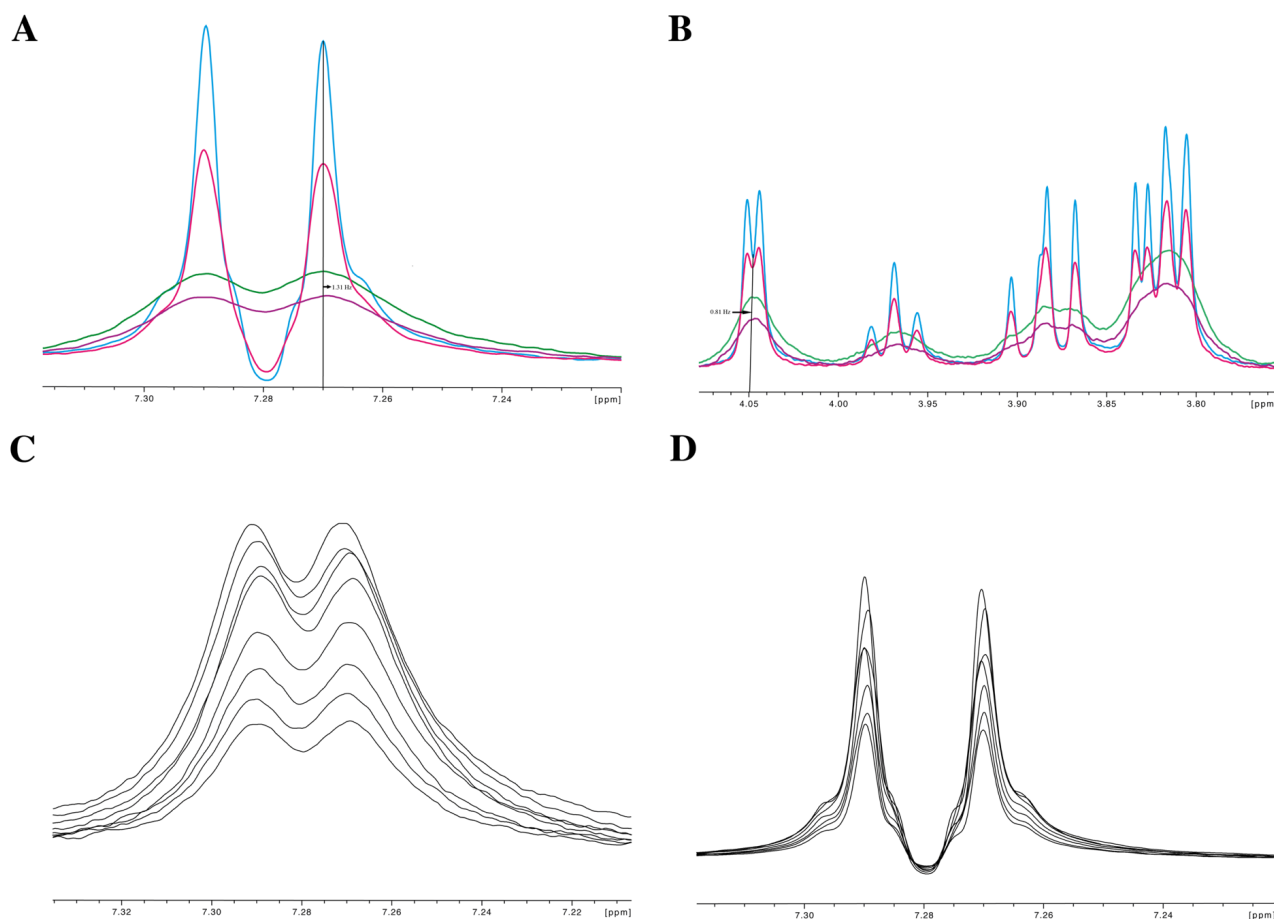


Figure 44: Signal shifts and signal relaxation was observed in NMR measurements of p-NPG, Tb^{3+} and LecA. Water suppressed proton spectra of the aromatic region (A), and the sugar protons (B) showing the diamagnetic control (Ca^{2+}) in blue, the diamagnetic sample in pink (Ca^{2+} , LecA), the paramagnetic control in green (Tb^{3+}) and the paramagnetic sample in purple (Tb^{3+} , LecA). (C) and (D) represent the recorded $T1\rho$ spectra of the paramagnetic sample (C) and the diamagnetic sample (D) of the phenyl protons. $T1\rho$ spectra were recorded with spinlock times of 900 ms, 700 ms, 500 ms, 300ms, 150 ms, 100 ms, 50 ms, 10 ms. LecA concentration in all samples containing LecA was 100 μ M, p-NPG and TMA were used in every sample with 1 mM and 200 μ M, respectively. Ca^{2+} was used in the diamagnetic sample and control with 15 μ M, while Tb^{3+} was used in the paramagnetic sample and control with 30 μ M. Water suppressed proton spectra were recorded with 1000 scans, and the $T1\rho$ spectra with 32 scans.

To increase the ligand to protein ratio a 10-fold ligand excess was used and water-suppressed proton spectra as well as $T1\rho$ spectra with different relaxation times were recorded. The use of a reduced ligand to LecA ratio of 10-fold showed differences in the paramagnetic samples containing Tb^{3+} and the diamagnetic ones with Ca^{2+} (Figure 44). In contrast to the diamagnetic samples (Figure 44, A and B blue and pink curves), the paramagnetic samples (Figure 44, A and B green and purple curves) showed a reduced signal intensity of all signals. For the comparison of all samples, the integral of the internal standard TMA was set to 1 in the spectra containing all samples. The differences in the signal intensity of the diamagnetic control (blue spectra) lacking LecA, and the LecA containing diamagnetic sample (pink spectra) showed binding of p-NPG to LecA. The same effect is observed for the paramagnetic samples were the paramagnetic control (green spectra) has a greater signals intensity than the sample containing LecA (purple spectra). The observed effects are a clear

Results and Discussion

sign for binding of the sugar ligand to LecA. Moreover, there was a very slight change in the peak position between the dia- and paramagnetic sample being potentially so-called pseudo contact shifts (PCS). For the phenyl proton, a shift of 1.35 Hz was observed and for the H₄ proton of the galactose a shift of 0.81 Hz. No shifts were observed for any other sugar proton. While relaxation enhancement caused by paramagnetic metal ions is distance depended, PCS are angle depended. Thus, it can be explained, that there are no PCS for all signals. But as PCS can have very great effects with shifts of more than 50 ppm, and only very slight effects were observed, the specificity of this effect can be questioned. While it makes sense that H₄ proton signal of the galactose experiences shifts, as it is together with H₃ of the galactose the one closest to the paramagnetic center, the phenyl protons are the protons most distant to the paramagnetic center. And while angle depended effects on the sugar protons might explain the absence of shifts in some signals, it cannot be the sole reason the absence of every other sugar proton. It can be concluded that the observed shifts are unspecific effects and cannot be taken as PCS caused by the paramagnetic Tb³⁺ ion.

Influence of the ratio of LecA to paramagnetic lanthanide

While the ligand to protein ratio was determined to be a key parameter, the LecA to dia- or paramagnetic salt was not yet evaluated. The used diamagnetic salt CaCl₂ was used with a concentration of 15 μM, and the TbCl₃ was used with 30 μM, or in earlier studies, the salt and LecA concentration was used in a one-to-one ratio. First experiments using LecA for EPR investigation with Gd³⁺ by Corzilius and co-workers (unpublished data) showed an extraordinarily narrow EPR line with a LecA to Gd³⁺ ratio of 8:1 or 4:1. Thus, a four-fold increased concentration of LecA compared used paramagnetic metal ion Tb³⁺ was evaluated. For the NMR experiment Tb³⁺ instead of Gd³⁺ was chosen, as Gd³⁺ in contrast to Tb³⁺ only causes distance dependent PRE but not distance and angle dependent PCS

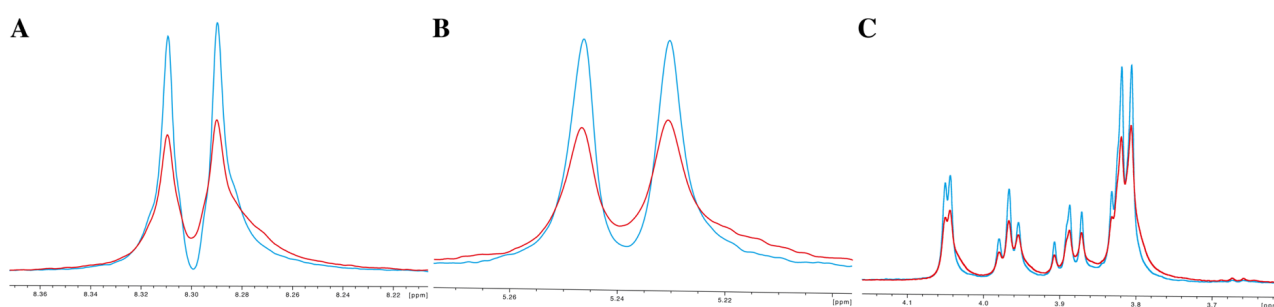


Figure 45: Signal relaxation was observed for proton signals of p-NPG in NMR measurements with Tb³⁺ and LecA. Water suppressed proton spectra of p-NPG and Tb³⁺ are shown, the blue spectra show p-NPG together with Tb³⁺ but in absence of LecA, the red spectra was recorded in presence of LecA. p-NPG was used with 1 mM, LecA with 10 μM, Tb³⁺ was used with 2.5 μM and the internal standard TMA with 100 μM. The water suppressed proton spectra were recorded with 32 scans. **A** and **B** both show the proton signals of the phenyl moiety while **c** shows the sugar signals.

For all determined ligand signals a reduced signal intensity in water suppressed proton spectra were observed (Figure 45, A-C). No differences in the reduced signal intensity were observed between the phenyl protons (Figure 45, A), anomeric H₁ of the galactose derivative (Figure 45, B) or the other sugar signals (Figure 45, C). As the aromatic phenyl signals have a greater distance to the paramagnetic Tb³⁺, relaxation of this protons

should be reduced compared to the galactose protons H₃ and H₄, which are the closest to the paramagnetic center. In contrast to the previously used equimolar ratio of LecA to the used metal ions in this case LecA is in a 4-fold excess. Due to the excess of LecA in this experiment, three portions of the protein in solution have no metal ion bound. This leads to a reduced amount of functional LecA in solution, as it was shown by ELLA experiments that LecA only functionally binds to its sugar ligands when in complex with trivalent metal ions or Ca²⁺. With this calculation a ligand excess of 400- fold is obtained and this method follows the signals of the ligand. With this concentration of p-NPG that is 67-fold above its K_d, there is competitive binding between each ligand in the solution. With a great ligand excess it is more likely that the small portion of ligand that has received the magnetization is in the mean of all the ligand in the solution not strong enough to cause specific effects. It can be concluded, that while an excess of LecA might work well for EPR experiments that are carried out in solid state, but does not lead to specific PRE or PCS using the paramagnetic trivalent Tb³⁺, but is also not expected to work for any other lanthanide using this ligand, protein and salt concentrations. For T1ρ experiments, a receptor saturation with the paramagnetic tag is desirable and thus, equimolar concentrations of lanthanide ions are favored. An excess of lanthanide is not an option, as free lanthanide in solution causes unwanted and unspecific site effects, especially line broadening.

The ligand to protein ratio is important for the determination of distinct PRE effects in T1ρ experiments using the paramagnetic Dy³⁺ ion

As PRE but no PCS were observed with Tb³⁺ other lanthanides were also evaluated as paramagnetic LecA tags, Dy³⁺, Tm³⁺ and Ho³⁺ were tested in NMR measurements using a protein ligand ratio of 1: 100 on their potential to cause PRE and PCS. While Tm³⁺ is classified as a highly paramagnetic lanthanide just as Tb³⁺ and Dy³⁺, Ho³⁺ is only classified as a moderate paramagnetic lanthanide.^[281] But as Ho³⁺ has the same orbital composition for PCS as Dy³⁺ and Tb³⁺ and Tm³⁺ differs in its f-Orbital, all three were tested

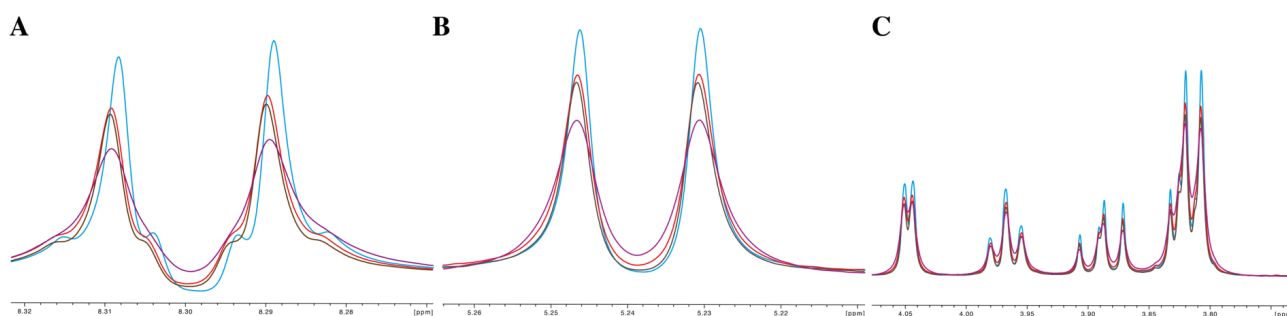


Figure 46: Dy³⁺, Ho³⁺ and Tm³⁺ all show a decrease in signal intensity of p-NPG in complex with LecA. T1ρ spectra of LecA (10 μM) p-NPG (1mM) with Ca²⁺ (10 μM, blue spectra), Tm³⁺ (10 μM, brown spectra), Dy³⁺ (10 μM, purple spectra) and Ho³⁺ (10 μM, red spectra). All spectra were recorded with 0.5 ms spinlock time and 16 scans. The phenyl protons are shown in **A**, **B** shows the anomeric Gal-H₁ of p-NPG, **C** the rest of the sugar protons of p-NPG.

Water suppressed proton spectra and T1ρ measurements of LecA and its known ligand p-NPG as well as the corresponding lanthanide were recorded. For comparability reason, all lanthanides were tested at the same

Results and Discussion

concentration. For Tm^{3+} and Ho^{3+} no K_d was determined using ITC experiments. Compared to the sample containing Ca^{2+} (Figure 46, blue spectra) no line broadening was observed in presence of Ho^{3+} (Figure 56, red spectra), and only weak broadening was observed for Tm^{3+} (Figure 46, brown spectra). In contrast, clear line broadening was observed for Dy^{3+} (Figure 46, purple spectra). For all three tested trivalent lanthanide ions, signal reduction was observed in contrast to the diamagnetic sample containing LecA. Stronger effects were observed for the phenyl protons (Figure 46, A) in contrast to the anomeric Gal-H₁ (Figure 47, B) or the other sugar protons (Figure 46, C). This contrasts with the fact, that the phenyl protons are more distant to the paramagnetic center with distance of 10 Å, compared to 5 Å of the sugar protons. This abnormality can be explained by the general relaxation behavior of the phenyl protons, as also a faster relaxation time was observed in absence of paramagnetic ions or even LecA. So, phenyl protons have a shorter T₁ time and as ligand binding to a macromolecule like LecA and paramagnetic ions enhance this relaxation. No significant effects were obtained using Tm^{3+} and Ho^{3+} . Pseudo-contact shifts are angle depended, so the absence of shifts can be explained using two different theories: one is that the concentration of the used lanthanide ion was too low because the binding affinities of the two lanthanides were not yet determined. Consequently, no effect of the paramagnetic Tm^{3+} or Ho^{3+} ion was observed because the K_d value of Tm^{3+} or Ho^{3+} is significantly higher than the 10 μM used in the experiment. Or second, the effects of the two lanthanides could be too weak to be determined. Either way, none of the two lanthanides were not investigated further. As this method is measuring the free ligand, and all displayed effects are the mean between the ligands that were bound to the protein and the ones that have never been in contact to the protein, it might be, that with a 100-fold excess of the ligands, effects can be missed. This might also be the explanation for the missing pseudo-contact shifts.

Proof of concept for the use of ligand-based NMR measurements in a screening approach for a new LecA ligand using the known LecA inhibitor methyl α-D-galactoside and a small molecule p-nitro phenol

For evaluation of the new NMR screening set up using paramagnetic Tb^{3+} as a spin label as proof of concept the known LecA ligand methyl α-D-galactoside (Me-α-gal) was used together with p-nitro phenol as a fragment. In this set up, the p-nitro phenol represents the screening ligand. As p-NPG is a known ligand it can be assumed that p-nitro phenol is also binding to LecA the same way the phenyl-moieity of p-NPG is binding to LecA. Methyl α-D-galactoside was used to block the first binding site. As specific effects were observed in the presence of Tb^{3+} it was used in the proof-of-concept measurements.

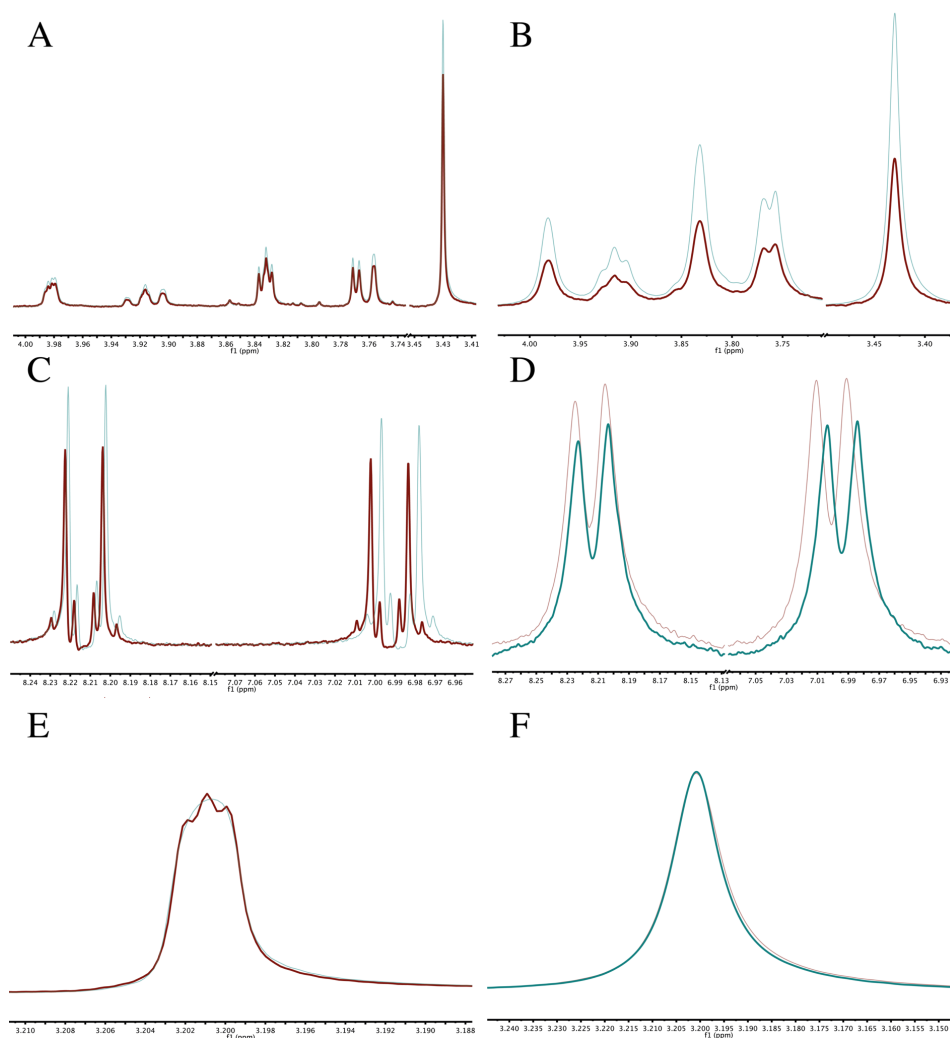


Figure 47: Determined water-suppressed NMR spectra of methyl α -galactoside (1 mM), p-nitro phenol (200 μ M) and LecA (10 μ M) (red) or without LecA (green), containing CaCl_2 (A, C, E) or TbCl_3 (B, D, F). A and B depict the signals of methyl α -galactoside 7 (Me- α -gal) C and D show the phenyl signals.-All spectra were recorded with 0.5 ms spinlock time and 16 scans

Significant decrease in signal intensity have been observed for the sugar signals in presence of Tb^{3+} compared to the control samples either without LecA (Figure 47, B green curve) or for the paramagnetic controls (Figure 47, A). It can be concluded that the decrease in signal intensity proves binding of Me- α -gal 7 to LecA in complex with paramagnetic Tb^{3+} . Also, the signal intensity was decreased for the diamagnetic sample of LecA in complex with Ca^{2+} in contrast to the sample without LecA. For the sample containing the paramagnetic Tb^{3+} the signal is reduced more compared to the diamagnetic sample. It can be concluded, that Tb^{3+} is binding in the carbohydrate binding pocket of LecA and is causing specific paramagnetic relaxation effects on the sugar protons of Me- α -gal 7 binding in the vicinity. In contrast to the sugar protons, only weak decrease in signal intensity was observed for the methyl group on the anomeric center of Me- α -gal 7. For the phenyl protons of p-nitro phenol a decrease in signal intensity was observed for the dia- as well as the paramagnetic samples containing LecA. For both samples the protons signals of the phenyl ring showed a shift. A signal

Results and Discussion

shift of -1.70 Hz for the paramagnetic samples and a shift of -0.74 Hz for the diamagnetic sample. (Figure 47, C and D). Pseudo contact shift were measured for the phenol protons of p-NP-H2 and H4 of 1.05 Hz and 1.28 Hz, and for p-NP-H3 and H5 of 3.85 Hz and 4.12 Hz (Figure 48). Moreover, upon addition of paramagnetic Tb^{3+} the signal intensity was reduced by 62.1 % (Figure 48 A) or 67.4 % (Figure 48 B), respectively.

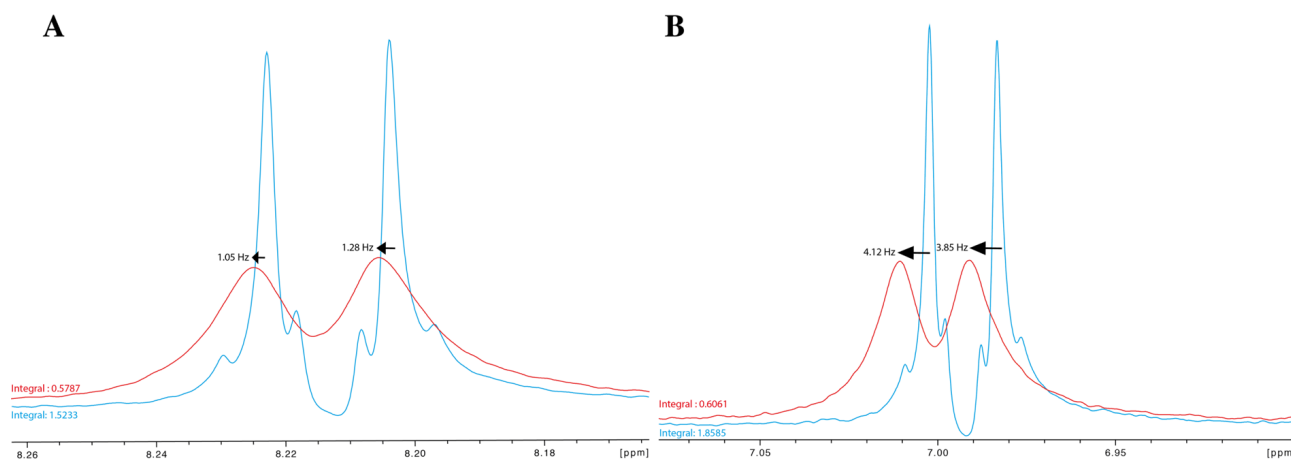


Figure 48: A decrease in signal intensity as well as signal shifts were observed for the phenyl protons of p-nitro phenol in presence of paramagnetic Tb^{3+} . LecA, methyl -galactoside **7** and p-nitro phenol with $CaCl_2$ are shown in blue, and with $TbCl_3$ in red. **A** shows PCSs and PRE for the phenyl protons p-NP-H₂, p-NP-H₄ **B** shows PCS and PRE for p-NP-H₃ and p-NP-H₅. For **A** a decrease in signal intensity of 62.1 % were measured and PCS of 1.05 Hz and 1.28 Hz. For **B** a decrease in signal intensity of 67.4 % and PCS of 4.12 Hz and 3.85 Hz were measured. All spectra were recorded with 32 scans and 0.5 ms spin lock time.

For the determination of relaxation effects caused by the paramagnetic spin label Tb^{3+} the decrease in signal intensity is measured. The signal relaxation behavior in T1ρ NMR spectra was maintained by the presence of Tb^{3+} and LecA (Figure 47) compared to the samples containing the diamagnetic control $CaCl_2$. But a slight increase in the relaxation rate is observed in the samples containing LecA (Figure 47). It can be excluded that LecA was un-functional as no difference between the samples containing LecA and without would have been observed in this case. This result is in accordance with the water suppressed proton spectra (Figure 47). For the phenol signals, no enhanced relaxation was observed.

In this first attempt, a concentration of potential fragment of 200 μM was used. One possibility for lack in relaxation effects might be that the used fragment, p-nitro phenol, has a very low affinity for the LecA and thus the used concentration was too low. As p-nitro phenyl β-D-galactoside is a known ligand and moreover dramatically increases the affinity of D-galactose upon addition, a very weak binding could only be explained by the presence of the hydroxyl-group of the free phenol derivative. Moreover, the co-resident methyl group on the simultaneously used sugar might lead to a steric conflict with the hydroxyl group on the phenol. Additionally, an equimolar concentration of Tb^{3+} compared to LecA was used. As the used concentration was

lower than the determined K_d value for the Tb^{3+} LecA complex, it might also be a reason for observed, weak effect.

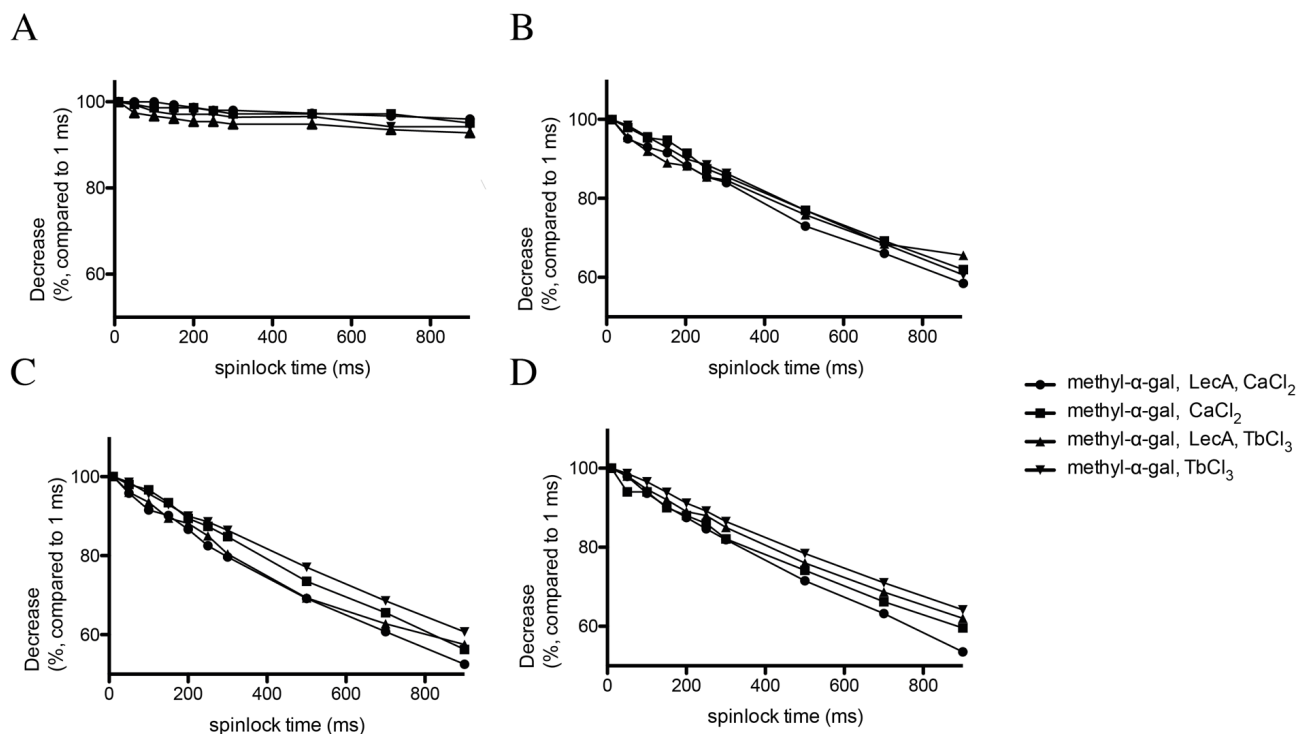


Figure 49: No difference in signal relaxation time was observed between the para- and diamagnetic samples. Evaluated NMR spectra of the T1 measurements of methyl -galactoside and LecA (with $CaCl_2$ presented as dots, and $TbCl_3$ presented as triangles) or without LecA ($CaCl_2$ squares, or $TbCl_3$ triangles) **A** represents the relaxation of the internal standard, and no relaxation is observed **B** represents the anomeric protons H_1 while **C** shows the relaxation behavior of the closest proton to the paramagnetic center H_4 and **D** shows the relaxation of H_2 .

Significant signal relaxation and decrease in signal intensity was observed in the water-suppressed proton spectra while no enhanced signal relaxation were observed in the T1 ρ measurements with spinlock times between 10 and 900 ms. One possible could be that the relaxation is extremely fast and stronger relaxation takes place before 10 ms. In comparison to the sugar signals, the signals of the phenol ring showed only modest decrease in the water suppressed proton spectra, with no difference between the para- and the diamagnetic sample. And no enhanced relaxation in the T1 ρ measurements has been detected. Due to the fact, that lanthanide ions can cause long-distance effects up to 40 Å, effects on the phenol ring were expected as it supposedly binds similar as the phenyl ring of p-nitro phenyl β -D-galactoside having distance of 10 Å. This distance should be short enough to see PRE effects. However, the hydroxyl group of the phenol ring could decrease the binding affinity of the phenol derivative as it could competed with the anomeric position of Me- α -gal 7. 200 μ M of p-nitro phenol might be to less to see strong effects as the binding affinity of the fragment could be rather low. With low binding affinities a concentration of 1 to 5 mM can be used to see distinct effects. But for the first time, pseudo-contact shifts have been observed for the phenol protons, enabling the detection of the angle of binding fragments. For the screening of fragments, the concentration might have to be enhanced to 500 μ M or higher to identify fragments with PRE and PCS.

Results and Discussion

Moreover, Gd^{3+} is a paramagnetic lanthanide that causes only very strong PRE but no PCS, so Gd^{3+} could be tested as a first line screening spin label identifying fragments by strong PRE and using Tb^{3+} or Dy^{3+} in detailed binding studies with fragments derived from the first line screening with Gd^{3+} . However, for modeling and synthesis design of a combined inhibitor based on D-galactose and the identified fragments, detailed structural information is needed and thus angle dependent PCS are a great benefit.

Overcoming weak relaxation effects using Gd^{3+} in a relaxation edited NMR approach for fragment screening

To examine paramagnetic effects of Gadolinium-salt as paramagnetic spin label in LecA ligand screening, effects on known LecA ligands were examined. First, the known LecA ligand p-nitro phenyl β -D-galactoside **8** with an affinity of $K_d 14.1 \pm 0.2 \mu M^{[6]}$ was used. Since no affinity of $GdCl_3$ for LecA was known, $30 \mu M$, the same concentration as for the previously described experiments with $TbCl_3$ and $DyCl_3$ was used. All signal of the LecA ligand p-nitro phenyl β -D-galactoside **8** showed an enhanced relaxation compared to the control without LecA, or the diamagnetic control containing LecA and Ca^{2+} . To evaluate the relaxation effects, the determined intensity was blotted against the measured spinlock times. Significantly faster relaxation of all protons was observed in presence of LecA substituted with $GdCl_3$.

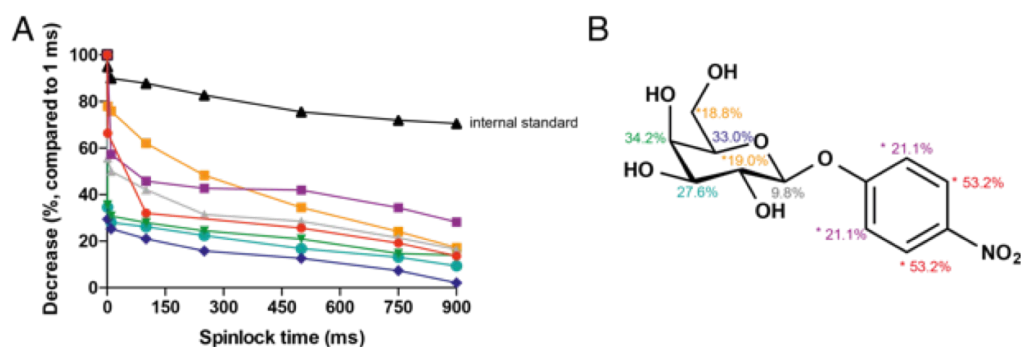


Figure 50: Signal decrease of all protons signals of phenyl β -galactoside **8** was observed upon binding of LecA and Gd^{3+} . **A** Signal decrease of the protons signals as depicted in **B**. NMR spectra were recorded with LecA $10 \mu M$, p-NPG $1 mM$, $CaCl_2$ or $GdCl_3$ $30 \mu M$ and the internal standard with $500 \mu M$. Spectra were recorded with spinlock pulses starting from $1 ms$ to $900 ms$ and 64 scans were used.

The sugar protons H_3 , H_4 and H_5 showed the strongest relaxation. Looking at the crystal structure, H_3 and H_4 are the closest to LecA, and hence the paramagnetic effects of Gd^{3+} are the strongest. Compared to the phenyl-signals, that appeared as two doublets, showing the average of two protons, most sugar signals were better distinguishable. For the determination of the $T_{1\rho}$ spectra, a water suppression prior to excitation sculpting was

used, and for that reason, the signal of the anomeric proton H_1 , appearing at about 5 ppm, was influenced by the water suppression and thus the peak intensity was low.

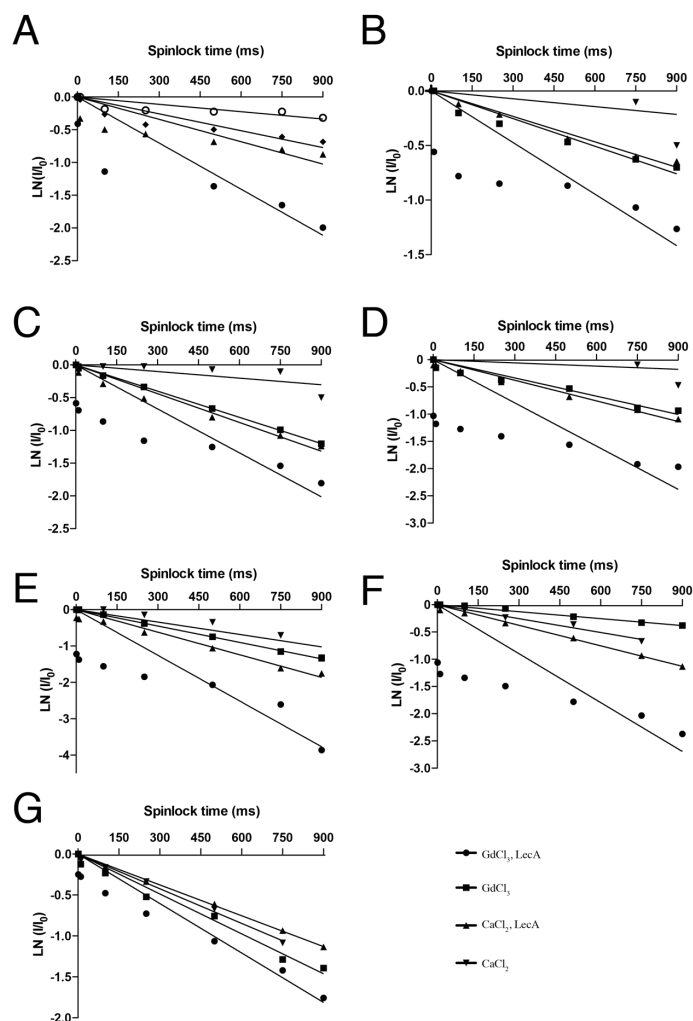


Figure 51: Blotted intensity of the protons signals **A** represent the phenyl protons close to the nitro group **B** represents the phenyl protons close to the sugar moiety **C** shows the relaxation of the anomeric proton H_1 **D** represents the relaxation of proton H_4 **E** the relaxation of H_3 **F** shows the relaxation of H_2 and **G** of proton H_5 . The logarithms of the quotient of the intensity compared to the intensity I_0 was blotted against the spinlock time in ms.

The proton signals of phenyl protons H_3 and H_5 showed the strongest relaxation of 53.2. To start with, the process of relaxation must be examined. To understand this, the determination of the relaxation rates and the factors influencing their values need to be understood. Relaxation involves the transition of energy levels. But it is again important to mention, that there is a difference in the transverse magnetic field. This field is oscillating close to the so-called Larmor frequency. As this effect is global to all spins that experience the same oscillating field and can thus be neglected. In contrast, the local fields effects affecting only a few spins must be examined. These fields are generated inside the sample itself and are based on interactions of spins with neighbors, or environment in some way. [283-284] Besides this quantum mechanics reasons for the enhanced relaxation, it might be also possible that a small portion of unbound Gd^{3+} coordinates to the negatively charges

Results and Discussion

oxygen in the nitro-group, causing some of it to coordinate to the nitro moiety and thus being very close the phenyl protons. [285-286] To examine this, a ligand with more signals having a greater distance than the sugar signals to the paramagnetic center was examined. Moreover, to prevent ionic coordination, only a methoxy substituent in the naphthol aglycon was chosen.

Paramagnetic effects of GdCl₃ on the sterically demanding LecA ligand 6-methoxy naphthalen β-D-galactoside 45

For the examination of Gd³⁺ as potential spin label, a LecA ligand with a greater distance to the paramagnetic label was examined. Since the ligand 6-methoxy naphthalen β-D-galactoside **45** was examined as a potential LecA inhibitor and tested with an IC₅₀ value of 5.3 μM in the FP assay it was then used in NMR experiments.

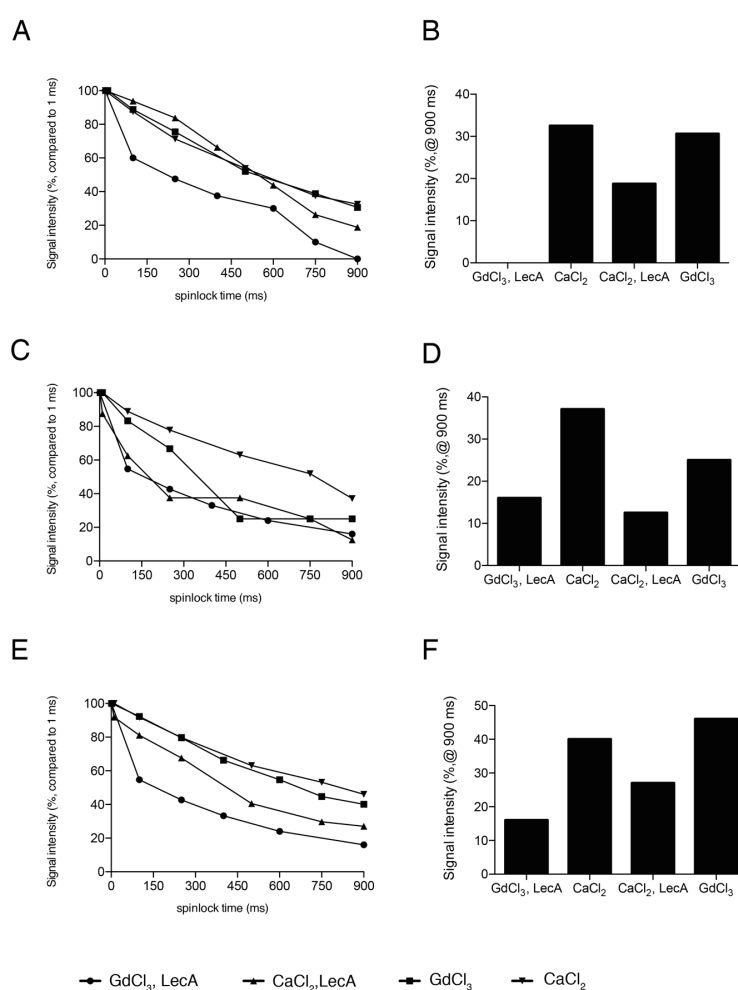


Figure 52: Signal intensity of **45** in complex with LecA and Gd³⁺ is decreased compared to the diamagnetic control. Determined relaxation of the protons signals of the sugar signals **A** shows the relaxation behavior of the H4 protons close to the paramagnetic center, **B** represents the signal intensity of H4 at 900 ms of spinlock time **C** represents the relaxation of the sugar protons of H₂ and H₃ (due to signal overlap), **D** shows the relaxation of those to sugar protons (H₂, H₃) at a spinlock time of 900 ms and **E** shows the relaxation of the signals obtained for H₆ and H₅ (due to signal overlap), **F** shows the signal intensity of H₅ and H₆ at 900 ms of spinlock time. For the T1 experiments, LecA was used with 10 μM, the sugar **45** with 1 mM and CaCl₂ with or GdCl₃ with. All samples contain 500 μM internal standard and were recorded with 64 scans.

Compared to the known LecA ligand p-NPG **8**, signal overlap of sugar as well as aromatic signals made the

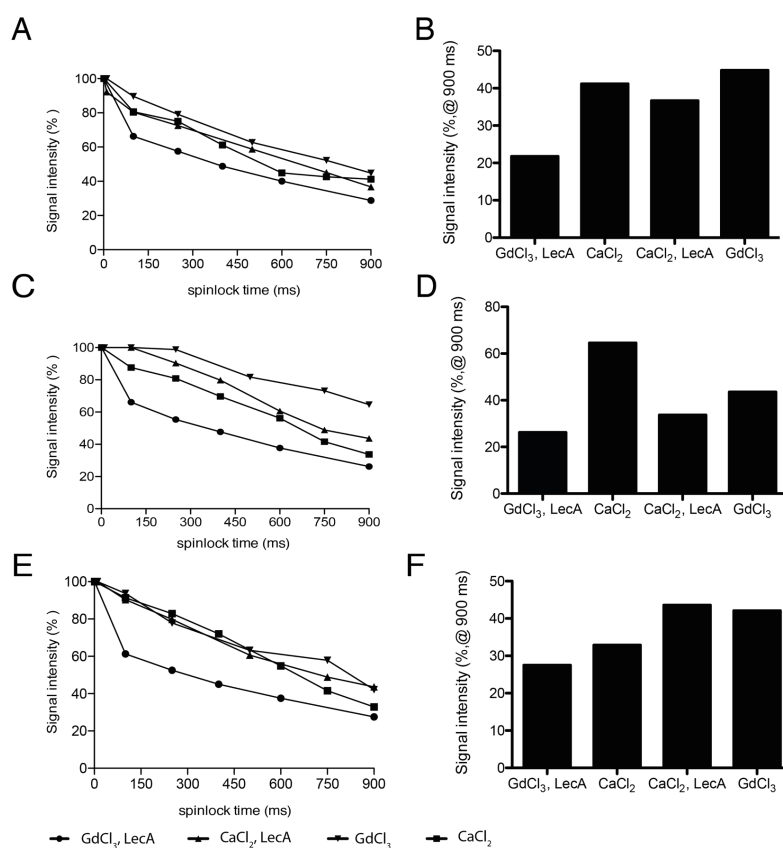


Figure 53: Determined relaxation of the protons signals of **A** shows the relaxation of the anomeric protons of the triplet at 7.8 ppm, **B** shows the signal intensity at 900 ms spinlock time while **C** shows the signal relaxation of the doublet at 7.4 ppm and **D** the signal intensity at 900 ms. **E** shows the relaxation of the aromatic protons of the naphthol aglycon at 7.2 ppm **F** shows the signal intensity of the latter quartet. LecA was used with 10 μ M, the sugar **45** with 1 mM and CaCl₂ or GdCl₃ with 30 μ M. All samples contain 500 μ M internal standard and were recorded with 64 scans.

evaluation difficult. For the sugar signals, as well as for the aromatic proton signals, only three distinct signals could be isolated. For the examined signals, a stronger relaxation of the sugar signals was observed compared to the determined aromatic signals. This finding agrees with the crystal structure, where all sugar signals are closer to the paramagnetic center compared to the aromatic signals. But for all signals from the distant naphthol moiety relaxation enhancement in the presence of Gd³⁺ and LecA was observed. As the methoxy signal overlaps with the sugar signals, no evaluation on the relaxation was possible. Moreover, signal overlap of the signals in the aromatic region makes it difficult to distinguish between the different aromatic protons signal and determine the percentage of relaxation enhancement per proton.

Within the determined relaxation of the protons the strongest relaxation was observed for the proton H₄ with an increase in the relaxation of 51.3 %. For the clearly determinable proton H₃ a relaxation of 12.0 % was observed and for the aromatic protons, 27.8 %, 46.6 % and 25.2 %, respectively. For the proton H₄ the increase in signal relaxation can be explained by the close distance to the paramagnetic center. For all determined T₂

Results and Discussion

relaxation times, a decrease was observed. Compared to the clearly explainable effect of the sugar protons H₃ and H₄, the effects observed for the aromatic protons cannot be explained as easily. All aromatic protons are more distant to the paramagnetic center than the sugar protons. In general, relaxation of protons describes how NMR signals change with time. [39] Stronger relaxation was observed with Gd³⁺ compared to the use of Tb³⁺, Dy³⁺ or Yb³⁺. In contrast, no PCS can be obtained with Gd³⁺. To summarize the best screening set up would be a first line screening using Gd³⁺ to obtain more clear effects on the potential ligands and a second screening with Tb³⁺ to examine pseudo contact shifts and to calculate the anisotropy tensor. In addition, the ¹⁵N LecA can be used to examine the binding of potential ligands.

All in all, this method enables the rapid identification of fragments binding near the paramagnetic spin label with additional structural information on the binding mode by distance dependent PRE and angle dependent PCS. Combining all the obtained data, a new LecA inhibitor based on D-galactose can be developed.

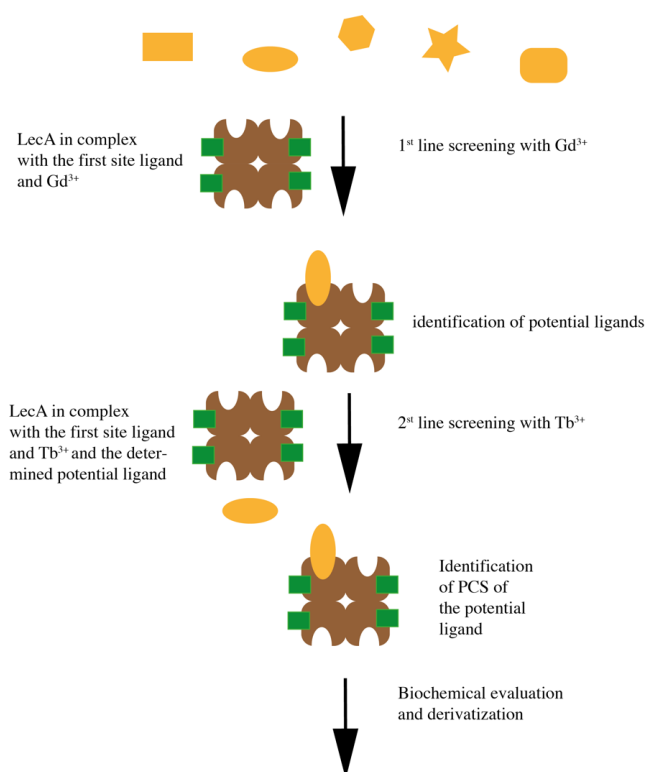


Figure 54: Schematic representation of the screening set up using paramagnetic lanthanide ions Gd³⁺ and Tb³⁺. For the screening set up, a library of potential ligands can be screened with LecA in presence of Gd³⁺ and the first site ligand D-galactose. After identification of a potential ligand, the latter can be evaluated using LecA and Tb³⁺ to potentially obtain more detailed information on the ligand.

3.5 Determination of the carbohydrate binding site by mapping of TROSY-NMR shifts of *P. aeruginosa* lectin LecA

3.5.1 Introduction to TROSY spectroscopy

Within the search for new, more potent LecA inhibitors, verification of potential hits can be challenging. For LecA no NMR signal assignment is known yet. As LecA is a known Ca^{2+} binding protein and is also a known D-galactose binder this knowledge can be used to determine specific signal shifts of the carbohydrate binding pocket. To assign specific shifts to those amino acids in the carbohydrate binding pocket the signal shifts upon Ca^{2+} addition will be used. In addition, the formerly tested trivalent paramagnetic ions Tb^{3+} and Gd^{3+} , which can functionally replace the calcium-ion in the binding pocket as shown previously by ELLA experiments, will be used. In contrast to the diamagnetic Ca^{2+} -ion, both paramagnetic ions Tb^{3+} and Gd^{3+} should cause stronger effects due to paramagnetic relaxation enhancement (PRE) effects. Besides the known LecA salt ligands Ca^{2+} , Tb^{3+} and Gd^{3+} , known D-galactose based LecA ligands will be used to assign all shifts caused by the binding of a carbohydrate ligand. For this methyl α -galactoside **7** and p-nitro phenyl β -galactoside **8** were used to evaluate the influence of two different D-galactose derivatives on LecA signals. Those two ligands mainly differ in the aglycon structure and binding geometry with respect to the D-galactose scaffold: In comparison to the aliphatic methyl in α -position, the aromatic aglycon p-nitro phenyl in β -position of D-galactose should also have effects on His50. Since LecA is a rather small protein consisting only of 122 amino acids, a Transverse Relaxation Optimized Spectroscopy (TROSY) NMR approach was chosen. TROSY is a NMR technique based on transverse relaxation mechanisms, which is used to determine the width and intensity of the acquired NMR signal with enhanced quality resolution. TROSY was developed by Pervushin and co-workers to obtain a magnetization transfer, allowing the seriously reduced magnetization due to a fast decay in T_2 magnetization.^[145] For the NMR experiment a water suppression using a WATERGATE-sequence as described by Piotto and Pervushin was used.^[145,286]

The localization of the carbohydrate-binding site using paramagnetic Tb^{3+} and Gd^{3+} and diamagnetic Ca^{2+}

For the determination of the carbohydrate-binding site a spectrum of the apo-LecA (Ca^{2+} -free) was recorded first. As no assignment of the protein is known up to now, all determined peaks were labeled with numbers unrelated to number of the amino acid residue. For apo-LecA 123 peaks have been determined using ^{15}N labeled lectin in citrate buffer. Citrate buffer was chosen as the solubility of LecA is higher compared to PBS

Results and Discussion

or TBS. LecA has a total number of 122 amino acids, thus 123 signals is in good agreement with the total numbers of amino acids in the protein, as one amino acid can give more than one shift.

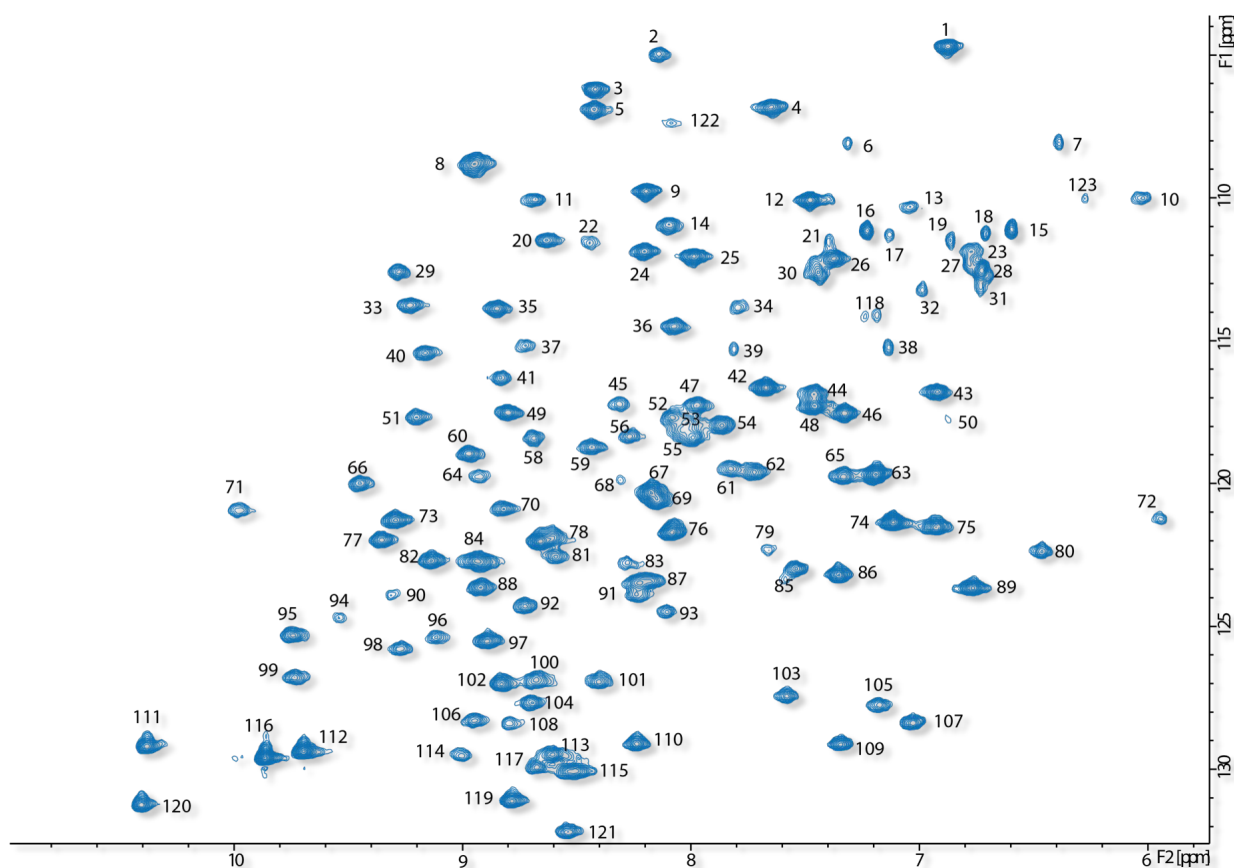


Figure 55: TROSY spectra of ^{15}N apo-LecA (338 μM) in citrate buffer recorded on a 700 MHz NMR spectrometer equipped with a cryo probe. All peak numbers have no relation to the amino acid sequence of LecA. In summary, 123 peaks with different intensities have been detected.

Peaks influenced upon binding of CaCl_2 to LecA

As a spectrum was recorded for apoLecA without its natural Ca^{2+} ligand, the baseline was set to determine shifts that are specifically changed by Ca^{2+} addition. As one LecA monomer has only one known Ca^{2+} binding site it can be assumed that all the shifts that are changing due to addition of Ca^{2+} are caused by either binding of Ca^{2+} or due to structural alteration due to changes after addition of Ca^{2+} . To evaluate shifts the recorded spectra were superimposed. All signals that disappear as well as all signals that showed clearly visible shifts are considered as influenced.

For the determination of specific shifts resulting in Ca^{2+} binding to LecA, apo-LecA was measured with increasing amounts (0.5, 1 and 2 equivalents) of Ca^{2+} . 123 peaks determined for apo-LecA have also been determined for the measurement with Ca^{2+} . Upon addition of a half equivalent of CaCl_2 , seven peaks are influenced (Figure 56; Influenced signals 13, 22, 34, 72, 90, 118, 123). Signal 123 completely vanished upon addition of 0.5 eq of Ca^{2+} and signal number 90 and 118 showed a clear signal reduction. For signal 12, 34 and

72 signal intensities were clearly decreased. Adding one equivalent of the diamagnetic CaCl_2 , in addition to the previously influenced signals seven more peaks were influenced (Figure 56; Influenced signals 13, 22, 34, 45, 56, 64, 68, 71, 72, 79, 90, 111, 118, 122, 123). Upon addition of an equimolare Ca^{2+} concentration seven signal shifts (Figure 56; Signal number 22, 34, 64, 72, 90, 122 and 123) completely disappeared. Also, signal number 13 and 118 showed again reduced signal intensities. In addition, eight more signals showed reduced intensities (Figure 56, signal number 37, 45, 56, 68, 71, 79, 99, 111). With two equivalents of CaCl_2 added, moreover the signal intensities of numbers 17, 32 and 65 were reduced (Figure 56). Increasing the concentration of CaCl_2 , up to 15.4% of 123 signals were influenced.

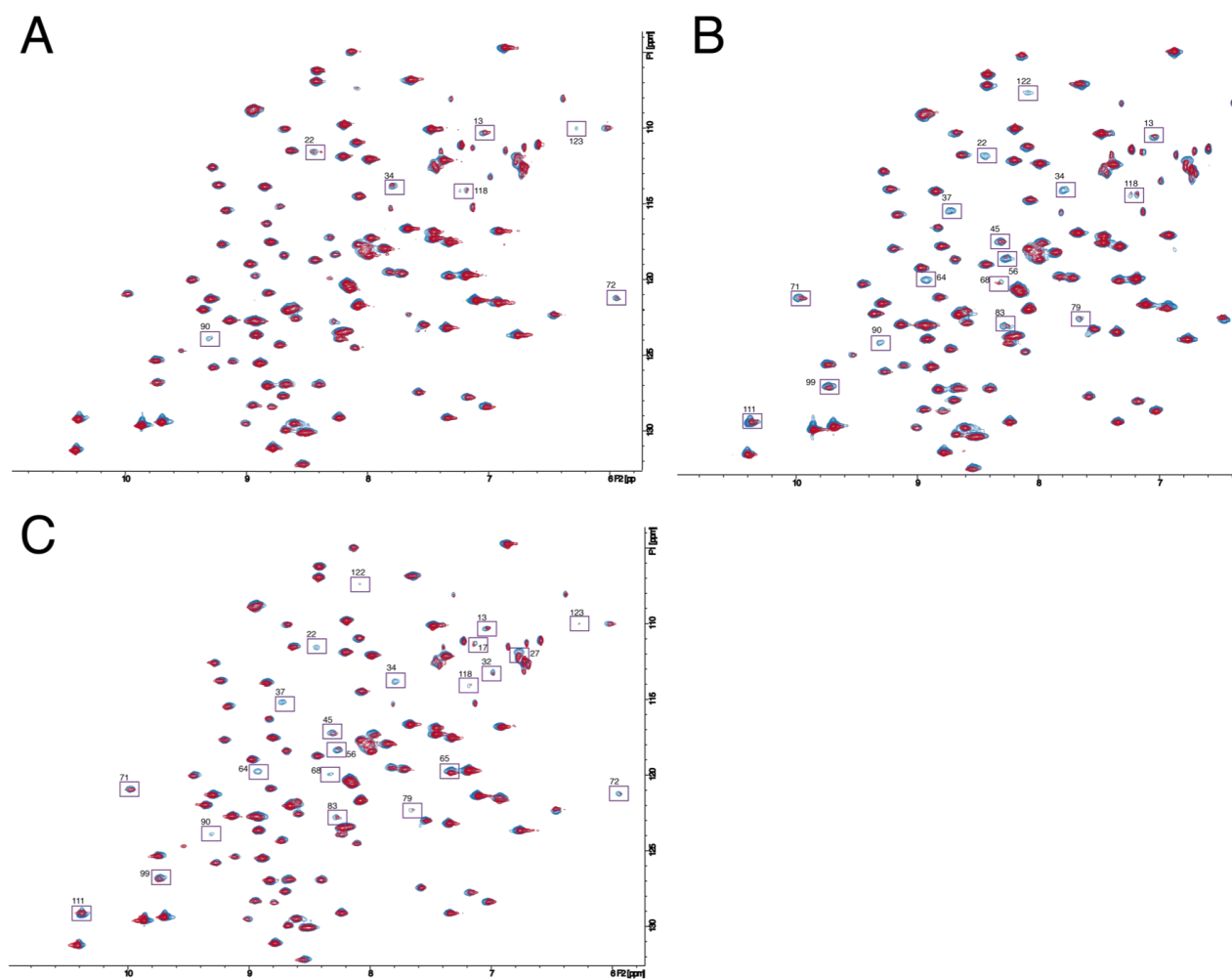


Figure 56: TROSY spectra of the ^{15}N LecA (338 μM) in citrate buffer (apo in blue), with **A** 0.5 eq **B** 1 eq and **C** 2 eq of CaCl_2 . All changes are shown in boxes and are labeled with the according number. For **A** seven signals (number 13, 22, 34, 72, 90, 118, 123) were shifted or reduced. For **B** eight more signals were shifted or reduced (signal number 13, 22, 34, 45, 56, 64, 68, 71, 72, 79, 90, 111, 118, 122, 123). For the addition of 2 equivalents of CaCl_2 (**C**), three more signals were influenced (signal number 13, 17, 22, 32, 34, 45, 56, 64, 65, 68, 71, 72, 79, 90, 111, 118, 122, 123).

Results and Discussion

Peaks influenced upon binding of the paramagnetic $TbCl_3$ to apoLecA

To further determine specific effects of signal shifts of the Ca^{2+} - and carbohydrate binding site apoLecA was titrated with paramagnetic Tb^{3+} . In contrast to the diamagnetic Ca^{2+} , Tb^{3+} is a lanthanide with paramagnetic properties. So, Tb^{3+} causes paramagnetic relaxation enhancement and pseudo contact shifts of signals close to it. Consequently, the addition of Tb^{3+} should cause the same signals to shift as the diamagnetic Ca^{2+} , but in addition signals more distant from the Ca^{2+} binding site should additionally be influenced. For the titration with paramagnetic Tb^{3+} again spectra with an excess of 0.5- 1 and 2 eq Tb^{3+} -ligand compared to LecA were measured.

By addition of 0.5 equivalents of Tb^{3+} a total of 29 peaks (4, 10, 13, 22, 23, 34, 36, 37, 45, 47, 52, 53, 56, 61, 64, 65, 72, 75, 78, 79, 80, 83, 90, 94, 96, 100, 108, 111, 121) were influenced. In contrast, addition of 0.5 equivalents of Ca^{2+} only caused 7 signals to shift.

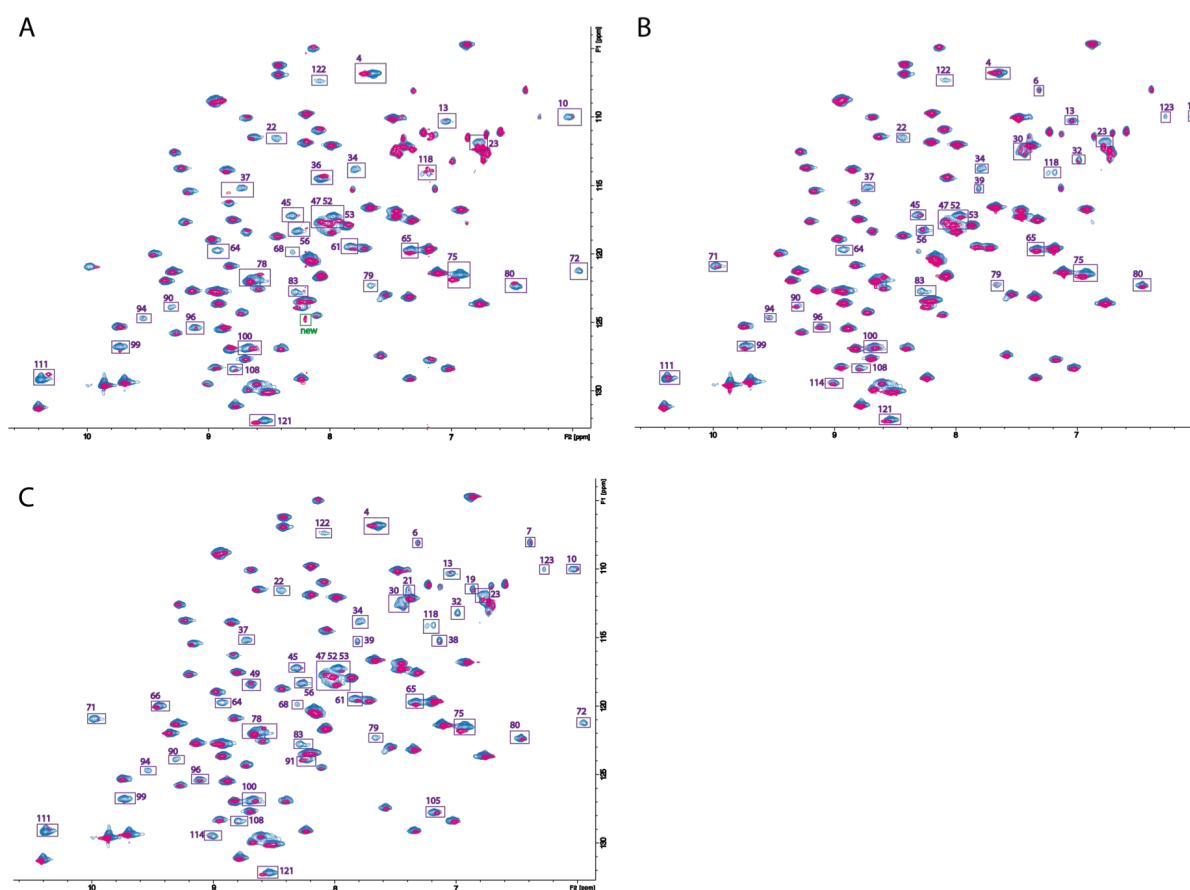


Figure 57: TROSY spectra of the ^{15}N LecA (338 μM) in citrate buffer (apo in blue), with **A** 0.5 eq **B** 1 eq and **C** 2 eq of $TbCl_3$. All changes are shown in boxes and are labeled with the according number. For **A** 29 signals (4, 10, 13, 22, 23, 34, 36, 37, 45, 47, 52, 53, 56, 61, 64, 65, 72, 75, 78, 79, 80, 83, 90, 94, 96, 100, 108, 111, 121) were shifted or reduced. For **B** two more signals were shifted or reduced (4, 10, 13, 22, 23, 34, 37, 39, 45, 47, 52, 53, 56, 61, 64, 65, 71, 72, 75, 79, 80, 83, 90, 94, 96, 100, 108, 111, 114, 121). For the addition of 2 equivalents of $TbCl_3$ (**C**), five more signals were influenced (signal number 4, 6, 10, 13, 22, 23, 34, 37, 39, 45, 47, 52, 53, 56, 61, 64, 65, 66, 71, 72, 75, 79, 80, 83, 90, 94, 96, 100, 105, 108, 111, 114, 121)

All seven peaks (13, 22, 34, 72, 90, 118, 123) which were influenced by the addition of 0.5 equivalents of Ca^{2+} were also influenced by the addition of 0.5 equivalents of Tb^{3+} . Six signals, (34, 64, 68, 79, 90 and 122) completely vanished upon addition of 0.5 equivalents of TbCl_3 . As the protein signals number 34 and 90 were also affected by the addition of Ca^{2+} it those signals are very close to the Ca^{2+} binding site. They are very close because lanthanides can cause blind spots very close to their site of binding, resulting in signals to completely disappear. In addition, six more signals (10, 12, 72, 94, 96, 108 and 118) are reduced in their intensity. Since signal number 72 was also affected by the addition of 0.5 equivalents of Ca^{2+} it is highly likely that signal number 72 is very close to the Ca^{2+} binding site of LecA. In contrast to the titration with CaCl_2 , 11 more peaks showed signal shifts (23, 37, 47, 52, 53, 65, 75, 78, 100, 111 and 121). Interestingly, a new signal at a f_1 frequency of around 125 ppm and f_2 frequency of nearly 8 ppm was observed. This signal could be the result of a very strong signal shift of either of the signals formerly called 122 which supposedly vanished. Increasing the addition of Tb^{3+} to an equimolar concentration a total of 31 peaks (4, 10, 13, 22, 23, 32, 34, 39, 37, 45, 47, 52, 53, 56, 61, 64, 65, 71, 72, 75, 79, 80, 83, 90, 94, 96, 100, 108, 111, 114, 121) were influenced.

In contrast to deficient Tb^{3+} concentration, two more signals completely disappeared (signal number 118 and 123). In addition, three more signals (6, 39, 114) were reduced in intensity upon addition of an equimolar amount of Tb^{3+} and two signals (71, 99) were shifted upon addition of equimolar Tb^{3+} concentration. Adding of an excess of two equivalents of the paramagnetic TbCl_3 , eight more signals were influenced. Six signals (7, 19, 38, 61, 78 and 91) were reduced in intensity but did not completely disappear. Two more signals (66 and 105) were shifted but were not strongly reduced in intensity. In comparison to the titrations with the diamagnetic CaCl_2 , 11 similar signals were reduced in intensity (13, 22, 34, 37, 45, 53, 71, 72, 90, 111 and 122). Signal number 111 is most likely one of the tryptophan signals.^[287] For none of the other signals and signal shifts a conclusion on the corresponding amino acids can be made.

Peaks influenced upon binding of the paramagnetic GdCl_3 to apoLecA

In contrast to the previously used lanthanide Tb^{3+} , Gd^{3+} has the strongest paramagnetic properties among all lanthanide ions and cause very strong relaxation enhancement but in contrast to other lanthanides does not cause pseudo contact shifts. To complete the analysis of specific effects on signals in the region of the carbohydrate binding pocket measurements with LecA in complex with Gd^{3+} were performed. Using a deficient concentration of Gd^{3+} in contrast to LecA five signal shifts have been clearly moved. For all of those for those five signals (22, 37, 56, 64, 78) completely new peaks were observed (Figure 58, green shifts). Ten signal shifts completely disappeared (15, 19, 32, 34, 38, 65, 90, 118, 122 and 123, Figure 58A). The signals intensity of 22 signals was reduced but they did not completely disappear (4, 10, 17, 20, 27, 36, 46, 65, 66, 67, 68, 71, 72, 79, 80, 83, 91, 99, 111, 114, 121, Figure 58A). Using an equimolar amount of Gd^{3+} , two more peaks have been moved completely (75, 80; Figure 58B). In addition, four new peaks not associated with a previously observed hits were observed. New shifts have been observed at a f_1 frequency of around 105 ppm and f_2 frequency of nearly 6.8 ppm, a f_1 frequency of around 109 ppm and f_2 frequency of nearly 9.0 ppm, a f_1 frequency of around 115 ppm and f_2 frequency of nearly 8.2 ppm, a f_1 frequency of around 122 ppm and f_2

Results and Discussion

frequency of nearly 8.4 ppm. For the titration with GdCl_3 evaluable spectra were only obtained for the addition of 0.5 eq and 1 eq of GdCl_3 . By the addition of a half equivalent of GdCl_3 a total number 44 peaks are influenced. By addition of an equimolar concentration of GdCl_3 in total 10 more peaks were influenced. As the addition of two equivalents of the paramagnetic GdCl_3 did cause most of the peaks to disappear, this could be explained by the fact, that the homo tetramer of LecA has four Ca-binding pockets, and thus the same number of Gd^{3+} could be bound to the protein. As the carbohydrate binding pockets are 32 Å and 55 Å apart and the paramagnetic radius of Gadolinium is about 40 Å, it might well be, that the increased amount of Gadolinium-ion in the sample caused a saturation of the Ca-binding pocket with Gd^{3+} resulting in a multitude of signals to disappear. However, it cannot be excluded that the increased free GdCl_3 in solution caused the weak signal intensity of the measured TROSY spectra. Either way, the spectra cannot be used for the determination of the binding pocket.

There are four peaks which were influenced by a deficient concentration of either of the added lanthanide salts. (Peaks 22, 34, 72 and 90) were already influenced by half an equivalent of all three tested salts. Thus, it is most probable that these peaks are close to the carbohydrate-binding pocket, or the binding of the ion influenced the corresponding amino acids. There are several signals which were already influenced with CaCl_2 in contrast to the apoLecA form (Figure 56). So, it can be concluded that the apo-form of the protein is much more flexible. Moreover, five more peaks (37, 45, 71, 83, 111) were influenced in all spectra with the addition of equimolar concentration of all the lanthanide ions. As peaks 111 was identified as a tryptophan signal, it is most likely to be Trp42. As no assignment of the LecA sequence is known up to now, no more amino acids can be assigned.

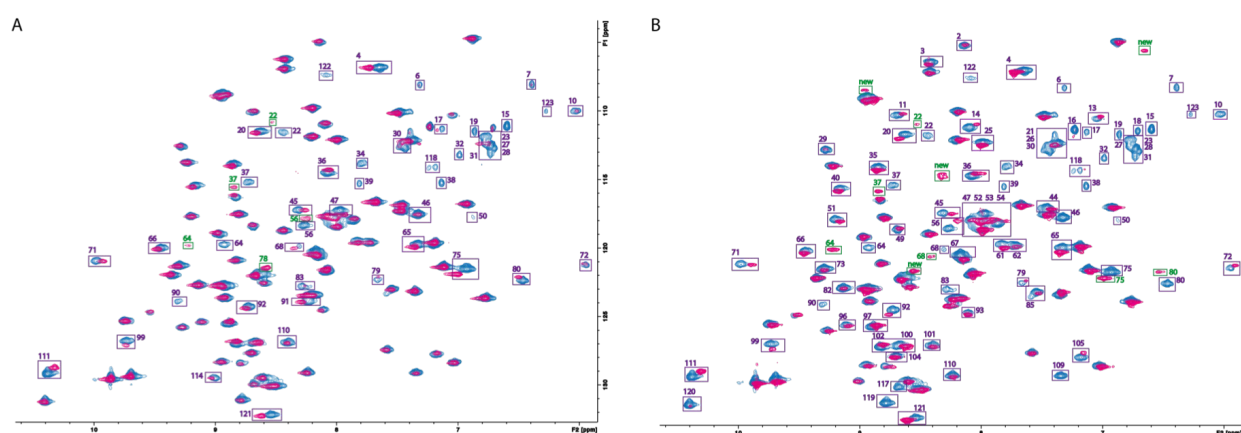


Figure 58: TROSY spectra of the ^{15}N LecA (338 μM) in citrate buffer (apo in blue), with **A** 0.5 eq **B** 1 eq of GdCl_3 . All changes are shown in boxes and are labeled with the according number. All spectra were recorded with a scan number of 16 scans.

In comparison to the diamagnetic CaCl_2 , there are 5 peaks only influenced by the paramagnetic Tb^{3+} and Gd^{3+} , namely peak number 4, 10, 23, 36, and 47. These peaks were only influenced by the paramagnetic ions, suggesting it to be either amino acids more distant from the carbohydrate binding pocket, or amino acids that are close to a potential second binding site for the lanthanide ions. To examine this, a co-titration of CaCl_2 with either of the two lanthanides could be made, targeting the potential second site while occupying the first binding site. As these experiments were aiming at identifying the carbohydrate binding site, to examine potential binders, the examination of a potential second site for the lanthanides ions was neglected and a titration with the known LecA D-galactose based ligands p-nitro phenyl β -D-galactoside and methyl α -D-galactoside were examined.

*The localization of a sugar binding site using the known LecA ligand p-nitro phenyl β -galactoside **19** and methyl α -galactoside **7***

To localize the signals related to the binding of known, sugar-based ligands, LecA was measured either in complex with p-NPG **19** and me- α -gal **7**, which both are known LecA carbohydrate ligands. For both carbohydrate ligands increasing amounts of carbohydrate in complex with LecA was measured to determine specific effects. In addition, Ca^{2+} is crucial for the binding of a carbohydrate ligand to LecA so all measurements with ligands were done using one equivalent of Ca^{2+} .

First the stronger LecA ligand p-NPG **19** with a binding affinity of 26 μM was measured. In contrast to the titration with the diamagnetic Ca^{2+} or the paramagnetic Tb^{3+} the addition of the known LecA carbohydrate ligand p-NPG **19** influenced a huge number of signals. Besides five newly emerged signals, 36 peaks were already affected by the addition of a half equivalent of the carbohydrate ligand. Peak 37 was significantly shifted upon addition of p-NPG **19**. Six signals did completely disappear upon addition of half an equivalent of p-NPG (Figure 67A; peak 22, 23, 34, 64, 90, 122). 17 signals were significantly reduced in their intensity (figure 67 A; peak 10, 13, 14, 20, 36, 47, 52, 58, 66, 72, 79, 83, 85, 92, 93, 102 and 118) and 15 were shifted (Figure 67 A; peak 4, 35, 45, 51, 56, 64, 67, 71, 75, 80, 83, 99, 100, 111, 121). To sum it up, in total 39 peaks were affected by the addition of a deficient concentration of p-NPG **19**. Upon addition of an equimolar concentration of the carbohydrate ligand **19**, 12 new signals were observed (figure 67 B). In addition to 37, which was completely shifted already by the addition of half an equivalent of p-NPG **19**, signal 104 was also completely shifted upon addition of an equimolar concentration of the sugar ligand.

Adding one equivalent of methyl α -galactoside **7**, 11 new signals were observed, and 40 peaks were affected either with shifts or signal decrease. The signals 4, 10, 13, 14, 20, 22, 34, 35, 36, 37, 45, 47, 51, 64, 71, 72, 75, 99, 100, 102, 111, 121 showed a decreased signal intensity most likely caused by the reduced protein rigidity.

To determine between the effects caused by the sugar moiety and the phenyl moiety, TROSY NMR spectra of LecA with methyl α -galactoside (K_d 50 μM) [71, 83, 288] were recorded. With sub-molar amounts of the carbohydrate, only eight protein signals were influenced. Peak 10, 22, 34, 37, 64, 72, 90, 122 were influenced

Results and Discussion

upon addition. Adding one equivalent of sugar to the Ca^{2+} -containing protein, 28 more LecA signals were influenced by the addition of methyl α -galactoside. In detail, Peak 4, 14, 20, 23, 35, 36, 40, 41, 45, 47, 52, 56, 58, 61, 65, 66, 75, 79, 83, 86, 92, 97, 99, 105, 109, 111, 119, 121 were influenced.

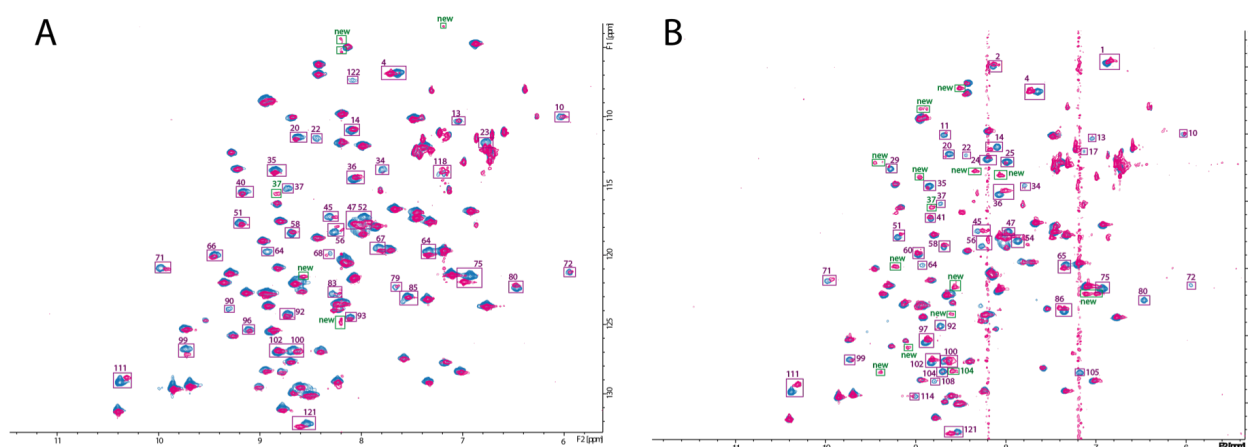


Figure 59: TROSY spectra of the ^{15}N labeled LecA (338 μM). The blue spectra represent the apo form of the lectin, the pink spectra the ones with phenyl-galactoside **A** 169 μM **B** 338 μM

For both tested galactose-derivatives, the aliphatic methyl α -galactoside and the β -hydrophobic phenyl β -galactoside, modest effects were observed for the sub-stoichiometric amount of sugar. While a lot, and global effects. Any magnetic nucleus, sugar or protein origin creates a magnetic field proportional to the magnetic moment in strength. As the molecule tumbles in solution the field fluctuates causing relaxation of nearby spins, either ^{15}N nuclei, $^1\text{H}^{\text{N}}$ or ligand ^1H . Dipolar relaxation strongly depends on the distance of two nuclei, as it changes with the inverse sixth power ($1/r^6$) of its distances.^[7] For protons in the ^{15}N LecA, the main sources of dipolar relaxations are protons of the amino acids nearby. However, it might be that the addition of methyl-galactoside changes the geometries of the LecA tetramer, allowing more DD interactions to take place, resulting in a reduced number of shifts being determined in the TROSY experiment. Even if it highly unlikely, a second reason for the reduced visible proton shifts compared to p-nitro phenyl β -galactoside could be a potential second sugar binding site as reported earlier by Imberty for glucose.^[226]

Determination of the carbohydrate binding site in the Ca^{2+} -binding protein lectin LecA using changes in specific signal shifts

Using the ^{15}N and 1D TROSY shifts of the galactophilic LecA in complex with its natural salt ligand Ca^{2+} or the paramagnetic substitutes Tb^{3+} or Gd^{3+} 11 were influenced by all three salt ligands. Besides the semi-assigned Trp42 (Signal number 111) the signal numbers 22, 34, 37, 56, 64, 65, 79, 90, 122 and 123 were influenced. Looking at the paramagnetic ions alone, 14 more peaks were influenced, suggesting them to be more distant to the Ca^{2+} -binding pocket. For GdCl_3 , only spectra containing half- and one equivalent of salt were evaluated, as the use of two equivalents of the strongly paramagnetic Gd^{3+} did cause most of the signals

to disappear. With a paramagnetic radius of 40 Å, and the tetrameric LecA structure with four known binding pockets for Gd^{3+} , it might be possible that a fully saturated protein might cause most of the signals to disappear because the binding pockets are only about 20- and 35 Å apart.^[226]

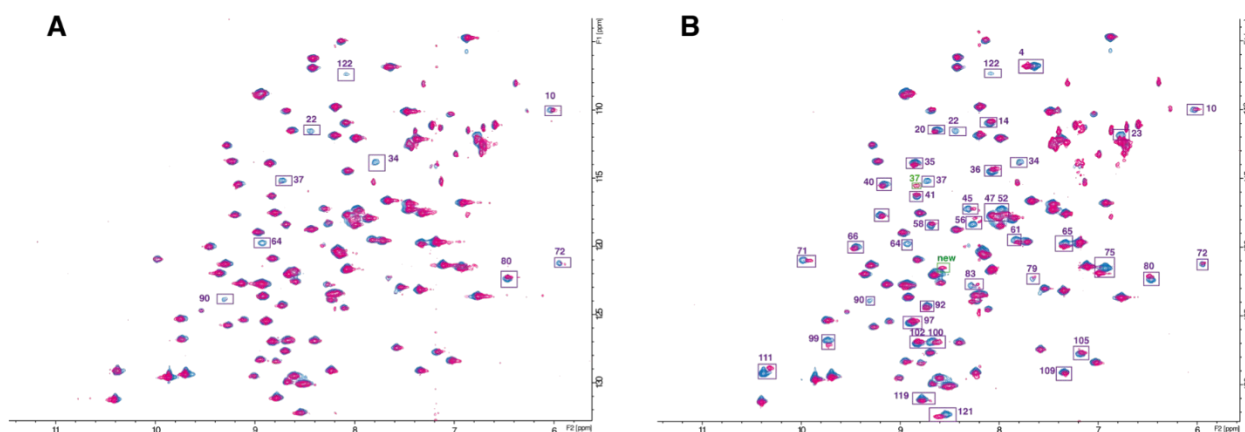


Figure 60: ^{15}N LecA TROSY spectra of **A:** LecA (291 μ M, both with 1 eq $CaCl_2$) with and with 0.5 eq of methyl α -galactoside (red, 145 μ M) or **B:** LecA (338 μ M, both with 1 eq $CaCl_2$, blue) and 1 eq of methyl α -galactoside (338 μ M). The shifts of the carbohydrate containing spectra are depicted in purple. Every new shift is shown in green.

This makes it very likely, that most of the protein signals are quenched by the strong Gadolinium effect. However, it cannot fully be excluded that the weak signal intensity or complete disappearance of most of the signals is caused by an excess of Gadolinium in solution and thus, no interpretation was based on 2 equivalents of $GdCl_3$. Surprisingly, peak 118 showed only a signal reduction in the presence of $CaCl_2$ but was uninfluenced by the addition of $TbCl_3$ or $GdCl_3$. This effect can be explained by small changes in the binding orientation or mode of di- or trivalent salts, in this case influencing peak 118 only with the addition of the divalent Ca^{2+} . A total number of 29 peaks were influenced by both, methyl α -galactoside and p-nitro phenyl β -galactoside. Starting with peak no 4, 10, 13, 20, 22, 34, 36, 37, 40, 45, 47, 51, 52, 56, 58, 64, 65, 66, 71, 72, 75, 83, 90, 92, 97, 100, 102, 111, and 122. In contrast to the hydrophilic ligand p-nitro phenyl β -galactoside, which was shown to interact in a π -stack interaction with the His50, the aliphatic methyl substituent of the methyl α -galactoside should not influence this amino-acid residue. Thus, differences between the two sugars will most likely give a hint on the signals of the corresponding histidine residue. Within all detected protein signals, a total number of 123, the peak with the number 109 was only influenced by the addition of p-nitro phenyl β -galactoside but did not show changes upon addition of either of the salts or the aliphatic D-galactose derivative methyl α -galactoside, making it a promising candidate for the histidine His50. As no assignment is known up to now, the corresponding residue can be only hypothesized for the tryptophan Trp42 129.13/10.344 and the histidine His50 129.16/7.343.

In comparison to the titration of salts alone, the titration of the two known LecA ligands methyl α -galactoside (me- α -gal) and p-nitro phenyl β -galactoside (p-NPG) did influence a sum of ten signals. As the peaks 13, 22,

Results and Discussion

34, 45, 56, 67, 90, 111 and 122 were all influenced by the addition of Ca^{2+} , Tb^{3+} , Gd^{3+} , methyl α -galactoside, and p-nitro phenyl β -galactoside these signals are most likely localized in the carbohydrate binding pocket or influenced by the binding of ligands in its vicinity.

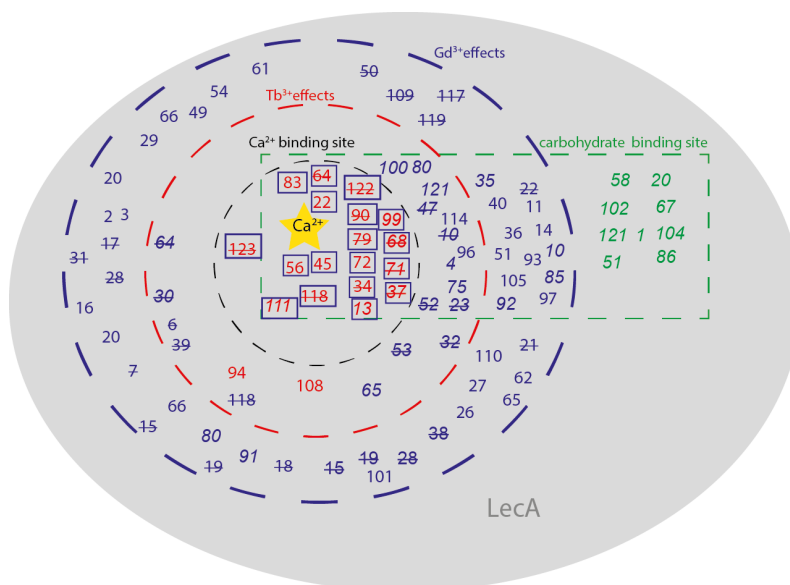


Figure 61: Schematic representation of the TROSY experiments: The colors represent the different experiments. The back circle represents all peaks influenced by Ca^{2+} , the red circle represents all peaks influenced by the Tb^{3+} effects and Gd^{3+} is represented by the blue circle. The effects of the carbohydrate binding site are shown in green, so all signals in the green box are influenced by the addition of the carbohydrate. When a number is marked in another color as the ring, they are in the effects was shown by multiple experiments. The italic numbers represent shifts, the crossed-out numbers are signals reduced in intensity. There are no signals only influenced by Ca^{2+} , but some which are influenced by Ca^{2+} and Tb^{3+} (red numbers). Only peak 94 and 108 are only influenced by Tb^{3+} but not by Ca^{2+} , Gd^{3+} or the carbohydrate. All purple numbers are influenced by Gd^{3+} , but when they are in the red circle, they are also affected by Tb^{3+} . All numbers in the Ca^{2+} binding site ring are also affected by Gd^{3+} , thus they have a blue ring.

To summarize 17 signals are influenced by Ca^{2+} , Tb^{3+} , Gd^{3+} and carbohydrate. This most likely means that the signals are the closest to the paramagnetic center. There are two signals which are only influenced upon addition of Tb^{3+} . This might be caused by the fact, that only Tb^{3+} is causing pseudo contact shifts, Gd^{3+} is not causing shifts, but only paramagnetic relaxation enhancement. There are eight signals which are only influenced by Tb^{3+} and Gd^{3+} but are not influenced by the carbohydrate. This can be explained by the fact that the signals are outside the carbohydrate binding pocket. Many peaks are influenced by the addition of Gd^{3+} . This can be explained by the fact Gd^{3+} has the strongest paramagnetic effects within the paramagnetic lanthanide ions.

4. Conclusion

4.1 Optimization of D-galactose based lectin LecA inhibitors

P. aeruginosa is a multi-drug resistant bacterium causing nosocomial and respiratory tract infections in immune compromised patients, like patients suffering from cystic fibrosis. The bacterium uses its two soluble carbohydrate binding lectins, LecA and LecB, to mediate adhesion to a carbohydrate surface. Inhibition of these lectins with ligands was shown to reduce biofilm formation and thus might be the needed help in therapy and treating infections. As the *P.aeruginosa* lectin LecA can be inhibited by D-galactose 44 inhibitors based on D-galactose have been synthesized. Within the set of synthesized D-galactose derivatives it was shown that most changes on the phenyl ring did not influence the affinity significantly. The most potent ligand was determined to be m-methoxy phenyl β -D-galactoside, but also the sterically more demanding ligands based on a naphthol moiety at the anomeric center showed quite good affinities in the range of 10 μ M. It can be concluded, that without applying a bivalent approach or with a fragment growing approach the affinity of D-galactose based ligands cannot be enhanced significantly.

Within the first detected LecA inhibitors, besides several galactosides, *N*-Acetyl β -galactosamine was discovered to bind to LecA as well.^[58] Consequently, the binding potential of galactosamine derivatives was evaluated but only the tested p-nitro phenyl *N*-acetyl β -galactosamine **76** showed an affinity of 136.3 μ M, which is in the same range as D-galactose. This result agrees with previously reported results which showed a 50 % inhibition of galactosamine after equilibrium dialysis of 400 μ M sugar derivative with 100 μ M sugar.^[58] To conclude there is little room for improvement, the only possibility to improve might be substitution at the nitro moiety using different substituents.

In addition, the screening of a set of Galactonoamidines or Galactolactams showed that only the lactam structure based on galactose showed binding to LecA. All the presented amidines did not show binding, this might be explained by the differences in electronic differences between the nitro- or oxygen in C1 position. In contrast, the lactam structure based on glucose showed no binding, which can be explained by the different hydroxy orientation in the C4 position. Since hydroxy groups in position 3 and position 4 are involved in the binding to LecA, more specifically the coordination to the Ca^{2+} ion. Moreover, there is a difference in the electronic effects between the amidine and lactam ring structure. Within the amidines, the ring opposes and reverse anomeric effect, an effect that is termed after the preference of the positively charged nitrogen. In summary, new potential ligands can only be synthesized based on lactam structures but can not be based on amidine structures.

Conclusion

4.2 Non-carbohydrate glyco mimetic as ligand of the *P. aeruginosa* lectin LecA

One possibility to obtain new inhibitors can be the virtual screening of a huge number of ligands using the crystal structure of LecA. For this purpose, the virtual screening of 1597 different molecules from the National Cancer Institute (NCI) diversity set IV were docked into the binding site of LecA. From these 60 potential ligands were obtained and reduced to 40 by a rational approach. Those 40 have then been tested using the fluorescence polarization assay. The biochemical evaluation using the fluorescence polarization of the obtained screening hits failed to give a clear result on the binding of the potential hits. Since there has been a sign of binding for ligands NSC 27389 (**92**) and NSC 73735 (**93**) they have been examined in ITC experiments, but for both ligands no binding in direct titration experiments have been observed. Both potential hits were expected to have a binding affinity in the milli molar range, and because of the poor solubility of LecA and the ligands, determination of low affinity ligands with ITC is rather difficult but also a replacement titration failed to give a clear result, as well as no binding affinity could have reliably been determined from these experiments. One more method for the determination of binding of the ligands was the use of NMR to obtain more information. Compared to NMR spectrometry, the biochemical fluorescence polarization assay, as well as the thermal shift assay based on the read out of a fluorescent dye have several drawbacks, which can interfere with the obtained results. For both, the assay could have been disturbed by the colored screening hits or their potential of fluorescence enhancement or quenching. With these interferences, it is impossible to determine a clear binding curve and it makes the discrimination between real binders and false positives very difficult. Moreover, for one ligand oxidation was suspected within the incubation time and which caused the fluorescence of the ligand to disappear. It can be hypothesized, that catechol structures are not very suitable starting points for the determination of new, non-carbohydrate lectin LecA ligands. Since NMR is not influenced by fluorescence, this technique can be used to give a more reliable result on the binding in this case.

To conclude, one can say that there is a line broadening of the signal with decreasing amounts of ligand and that there is a shift in the peak signals with changing ligand concentrations. As a binding of a small molecule to a bigger target molecule, LecA in this case, does result in a signal broadening; this can be concluded to be a general hint for binding of NSC 27389 (**92**) to LecA. Moreover, the observed changes in peak signals can be taken as a sign for binding. For the first evaluation method, the blotting of the proton shifts, a K_d value of 16.5 ± 9.6 mM using all four peaks, and 22.5 ± 4.6 mM neglecting the isopropyl proton due to poor fit quality were obtained. In contrast, using the measurement of the full width at half maximum, a K_d of 8.1 ± 2.4 mM was calculated. Comparing both obtained values, the discrepancy of the two obtained values is obvious. Since both values are determined from the same spectra, this discrepancy can only be explained by either the obtained small changes in signal shifts or full width at half maximum due to weak binding or by the fact, that the binding is unspecific. For either of the evaluation methods, the determined K_d in the 10 mM range explained the observed problems in obtaining binding curves using the FP assay. Finally, one problem is the fact, that the binding per se is not clear. All calculations assume that the observed small effects are indeed due to specific

binding. To verify this binding, the method should be applied to a known weak binding LecA ligand with a K_d in the same range, for example D-galactosamine.

4.3 Using a ^{19}F NMR screening for the identification of potential new carbohydrate binding site ligands for *P. aeruginosa* lectin LecA

The group of Christoph Rademacher developed a fragment screening approach based on ^{19}F NMR technique.^[268] In this approach, a fragment library containing only ^{19}F labeled fragments is used. With this screening approach six bins with a sum of 192 compounds were screened and in summary 67 compounds showed binding to LecA. Upon which 14 were competitive, thus 15% of all determined binders might be specific LecA binding site ligands. Within the 14 determined hits **09F05 (102)** and **14C10 (103)** were determined the strongest hit with a score of 1.5 with LecA and a score of 1 in the competition assay. All other 12 hits did not meet the threshold of the hits but have not been as clear as the two above mentioned.

In detail **15D03 (111)**, **04D07 (115)**, **13H08 (110)**, **14C04 (114)**, **14E02 (116)**, **14H04 (104)** and **15G07 (112)** were all clear hits in the CPMG measurement but did not show effects in the ^{19}F screening. This could be due to the enhanced sensitivity of the relaxation based CPMG method in contrast to the ^{19}F measurement.^[228] And in contrast **14E08 (105)**, **14C10 (103)**, **03H01 (108)**, **14G08 (106)** and **16A02 (107)** all showed a clear effect in the ^{19}F measurement (rated with a 1) and for all three compounds the effect in the competition assay was not as pronounced (rated with a 0.5). Only compound showed effects in both, the ^{19}F and the CPMG measurement. **04D12 (113)** was the weakest determined hit with only a score of 0.5 in the CPMG sequence, but due to the fact that the threshold for a score of 1 was 50% reduction and the compound showed 48% signal reduction and a full recovery after addition of the inhibitor the compound was also considered a hit. A set of the determined hits have been ordered and tested using the fluorescence polarization assay. In the FP assay no sigmoidal binding curves were obtained for either of the compounds. But compound **15D03 (111)**, as well as its fluorless analog **15D03 w/o F (117)**, the fluorless derivative **14C04 w/o F (118)**, the fluorless derivative **14H04 w/o F (119)** and **03H01 (108)** showed effects. In Summary, **03H01 (108)**, **04D12 (113)**, **09F05 (102)** and **04D07 (115)** did not show inhibition in the FP assay while **15D03 (111)** (as well as its fluorless analog **15D03 w/o F (117)**) **14C04 w/o F (118)** and **14H04 w/o F (119)** did show inhibition of up to 20% at the highest tested concentration. Since NMR is a highly sensitive method compared to the fluorescence polarization assay it might be possible that hits from the NMR measurement cannot be determined in the FP assay due to limitations in the solubility, the fluorescence intensity or unwanted interactions with the dye or the carbohydrate. In addition, the fluorless derivative of **14H04 (104)** was tested in a TROSY experiment. The examined compound **14H04 w/o F (119)** did show a huge number of shifts, 42 in detail. Within these shifts, 31 concurred with previously observed shifts for methyl -galactoside and p-nitro phenyl β -galactoside. With 74 % all determined shifts been also shifts in case of known LecA ligands, and this shifts within the carbohydrate binding pocket, it can be concluded, that the determined non-carbohydrate inhibitor **14H04 w/o F (119)** is indeed binding within the CRD of LecA. 11 new shifts were observed in contrast to titration with the sugar, but three of them have been observed by titration with GdCl_3 . However, the huge number of shifts

observed also leaves room for speculation on an additional binding site or other side effects caused by this compound.

To put all the above mentioned in a nutshell it can be concluded that the screening approach using the ^{19}F library and the combination of ^{19}F screening as well as CPMG can lead to new LecA inhibitors. As the NMR screening is a highly sensitive method it might be difficult verifying ligand with a poor solubly. Thus, numerous biochemical assays might have to be used to verify binding. As well as the TROSY experiment is a second NMR approach this might be the best verification as specific shift upon addition of a known carbohydrate ligand have been determined and thus can be tested if potential ligands also have and influence those peaks. Using a TROSY approach for screening is however not feasible since the amount of labeled LecA would be too much and screening time would be not reasonable since no libraries can be tested. In case of well soluble ligands without own fluorescence the fluorescence polarization assay is still the best verification method as it specifically verifies binding in the carbohydrate binding pocket.

In addition to NMR experiments biochemical evaluation of 8 ligands, which were selected based on availability of enough material for biochemical evaluation were further analyzed with FP and thermal shift assay. Out of the eight tested compounds only five showed effects. Potentially as a result or combination of poor binding affinities as well as a poor solubility of the ligands it was not possible to obtain a sigmoidal binding curve or any of the tested compounds. In Summary, **4D12**, **9F05** and **4D07** did not show inhibition in the FP assay while **15D03** (as well as its fluorless analog **117**) **118** and **119** did show inhibition of up to 20% at the highest tested concentration. **03H01** only two of three of the experiments showed significant inhibition making its standard deviation unreliably high. Since NMR is a highly sensitive method compared to the fluorescence polarization assay it might be possible that hits from the NMR measurement can not be determined in the FP assay due to limitations in the solubility, the fluorescence intensity or unwanted interactions with the dye or the carbohydrate. The latter can be excluded for the compounds were all tested against the carbohydrate reporter ligand alone and did not show any interactions. For verification of the first biochemical results a second biochemical evaluation using differential scanning fluorometry (DSF, thermal shift assay) based on the melting behavior of LecA was carried out. Of all 8 tested screening hits, **15D03 (111)** had the largest impact on the LecA melting temperature by increasing it up to 1.5 °C. The derivative lacking the fluorine **15D03 w/o F (117)** only increased the LecA complex stability 0.6 °C, suggesting the fluorine to be an important feature for its binding capacities to LecA. Moreover, **14H04 w/o F (104)** also enhanced LecA stability with 1 °C. **14C04 w/o F (118)**, **09F05 (102)**, **04D07 (115)** did not change the melting temperature of LecA. Only **04D12 (113)** decreased the LecA melting temperature about 1 °C, compared to LecA alone having a temperature of 83.6 °C.

For the determined ligand **14H04 (104)** derivatization must be made to enhance the binding affinity. Furthermore, a crystal structure of the ligand in complex with LecA would be the best starting point for a rational ligand design.

4.4 Determination of the carbohydrate binding site by mapping of TROSY-NMR shifts of the *P.aeruginosa* lectin LecA

NMR has emerged during the last better half of a decade and has become one of the most powerful tools in structural biology. Although there is no full assignment of the LecA protein shifts NMR techniques can still be used to get insight in the binding characteristics of this protein. For the determination of the carbohydrate-binding site a spectrum of the apo-LecA (Ca^{2+} -free) was recorded to have a baseline of protein shifts. After addition of increasing amounts of Ca^{2+} known LecA ligand up to 15.4 % of the signals showed shifts or a reduction in their intensity. Due to the availability of the LecA crystal structure in complex with LecA one can know in which structural region the salt ligand is binding. LecA is a C-type lectin, meaning that Ca^{2+} is needed near the carbohydrate binding pocket so bind to the respective ligand. It was shown by ELLA experiments that the salt ligand is needed for binding to a galactosylated surface. Thus, it is very likely that the observed shift is close to the carbohydrate binding pocket.

In comparison to the diamagnetic CaCl_2 , there are 5 peaks only influenced by the paramagnetic Tb^{3+} and Gd^{3+} , namely 4, 10, 23, 36, and 47. Thus, these peaks were highly likely to be close to the carbohydrate-binding pocket or the binding of the ion influenced the corresponding amino acids. In generally, it can be concluded that the apo-form of the protein is much more flexible, as more signals were appearing without the ion. Moreover, the peaks number 37, 445, 71, 83, 111 were influenced in all spectra with the addition of equimolar concentration of the ions. As peaks 111 was identified as a tryptophan signal, it is most likely to be Trp42. As no assignment of the LecA sequence is known up to now, no more amino acids can be assigned. To examine this, a co-titration of CaCl_2 with either of the two lanthanides could be made, targeting the potential second site while occupying the first binding site. As these experiments were aiming at identifying the carbohydrate binding site, to examine potential binders, the examination of a potential second site for the lanthanides ions was neglected and a titration with the known

4.5 A lanthanide-based NMR approach for the determination of new LecA inhibitors

Otting and Bertini, both pioneers in paramagnetic nuclear magnetic resonance with ligand-based methods, already used the replacement of diamagnetic Ca^{2+} in calcium-binding protein MMP and determined ligand binding looking at ligand effects, like paramagnetic relaxation enhancement (PRE) and pseudo-contact shifts (PCS).

It was shown with ELLA experiments that the lanthanide ions Tb^{3+} , Yb^{3+} , Ce^{3+} , Ho^{3+} , Tm^{3+} , Gd^{3+} , Dy^{3+} as well as the diamagnetic La^{3+} can functionally replace Ca^{2+} in the carbohydrate binding pocket as LecA substituted with this ion was still able to specifically bind to a galactosylated surface. Moreover, it was shown, that a specific sequence of dialysis steps, including dialysis against EDTA, a NaCl solution as well as distilled water, needs to be followed to obtain fully Ca^{2+} free protein. p-nitro phenyl β -D-galactoside (p-NPG, **19**) is a known LecA ligand which has not only the sugar protons, but also the phenyl protons which are further away from the paramagnetic center this ligand is ideal to determine specific effects. In addition it is known that the ligand has a good affinity with a K_d of 26.2 μM to the protein LecA. In the literature, Tb^{3+} , Dy^{3+} , Tm^{3+} and Ho^{3+} are often used for lanthanide-based NMR methods.^[220] All four trivalent lanthanide ions were tested with Ca^{2+} free LecA and the known LecA ligand p-nitro phenyl β -D-galactoside (**19**). No effect of Ho^{3+} and Tm^{3+} were observed neither in 1D water suppressed proton spectra nor $T1\rho$ spectra with spinlock times up to 500 ms. In contrast, effects on the ligand protons in presence of Tb^{3+} and Dy^{3+} . In addition it was concluded, that The ligand to protein ratio is important for the determination of distinct PRE effects in T1 experiments using the paramagnetic Tb^{3+} and Dy^{3+} ions.

For evaluation of the screening system using the paramagnetic lanthanide ions as a spin label in fragment screening, methyl α -D-galactoside (Me- α -gal) was investigated together with p-nitro phenol in water suppressed proton spectra and $T1\rho$ measurements. In this set up, the p-nitro phenol represents the second site ligand. Methyl α -D-galactoside was used to block the first binding site. In this experiment it was shown that there is a difficulty in ligand concentration and specific effects, which make the approach difficult so scale to a library of potential second site ligand. To overcome this problem, only fragments without a hydroxyl group were used. Moreover, Gd^{3+} is a paramagnetic lanthanide that causes only very strong PRE but no PCS, so Gd^{3+} could be tested as a first line screening spin label identifying fragments by strong PRE and using Tb^{3+} or Dy^{3+} in detailed binding studies with fragments derived from the first line screening with Gd^{3+} . In model experiments with Gd^{3+} it was shown that bigger effects were seen. However, for modeling and synthesis design of a combined inhibitor based on D-galactose and the identified fragments, detailed structural information is needed and thus angle dependent PCS are a great benefit. All in all, this method enables the rapid identification of fragments binding near the paramagnetic spin label with additional structural information on the binding mode by distance dependent PRE and angle dependent PCS. Combining all the obtained data, a new LecA inhibitor based on D-galactose can be developed.

Conclusion

In conclusion, all the above-mentioned synthesis and screening approaches have not yet led to the identification of significantly more potent LecA inhibitors. But they present the groundwork for further research and development targeting LecA. Optimized D-galactose frameworks as synthesized and evaluated in section 3.1 can occupy the sugar binding site, while ligands screened for using ^{19}F approach (section 3.3) or the approach based on pseudo-contact shift (section 3.4) can be used to target a further binding site. Combining first and second site binders can ultimately result in significantly more potent LecA inhibitors. In general, NMR techniques present a powerful addition to toolbox of biochemical methods like thermal-shift or fluorescence polarization assay. Using the NMR screening approach based on paramagnetic effects can be used to screen fragment or ligand libraries to identify potential new ligands. Like presented in this thesis, hits need to be further verified or evaluated to exclude false positive hits.

Results based on the presented work together with further research and results have been published. [303, 305-307]

5. Experimental section

5.1. Protein expression

LecA expression and purification

The protein LecA was expressed and purified as described previously.^[73] Briefly, *E. coli* BL21(DE3) carrying the plasmid pET25pa11 were grown in 1 L LB supplemented with ampicillin (100 $\mu\text{g mL}^{-1}$) to an OD₆₀₀ = 0.5–0.6 at 37 °C and 180 rpm. Expression was induced with IPTG (0.25 mM final concentration) and bacteria were cultured for 4 h at 30 °C and 180 rpm. The cells were then harvested by centrifugation (3000g, 10 min) and the pellet was washed with PBS. The cells were resuspended in 25 mL TBS/Ca (20 mM Tris, 137 mM NaCl, 2.6 mM KCl at pH 7.4 supplemented with 100 μM CaCl₂) with PMSF (1 mM) and lysozyme (0.4 mg mL) and subsequently disrupted using a homogenizer (5 cycles, microfluidics). Cell debris was removed by centrifugation (60 min, 10 000 g) and the supernatant was loaded on galactosylated sepharose CL-6B.^[67] The column was washed with TBS/Ca and LecA was eluted by addition of 100 mM D-galactose to the buffer. The eluted fractions were extensively dialyzed against distilled water and then, the protein was lyophilized. Between 20 and 35 mg LecA per liter bacterial culture were obtained. The protein was dissolved in TBS/Ca before use and after centrifugation the concentration was determined by UV spectroscopy at 280 nm using a molar extinction coefficient of 27 385 M⁻¹ cm⁻¹.^[293]

¹⁵N labeled lectin LecA expression

The labeled protein was expressed according to Marley et al. using *E. coli* BL21(DE3) carrying the plasmid pET25pa11. ^[289-290] The bacterial culture was grown in 1 L LB supplemented with ampicillin (100 $\mu\text{g/mL}$) to an OD₆₀₀ \approx 0.8 at 37 °C and 180 rpm, and subsequently pelleted and washed twice with a sterile M9-salt solution. Afterwards, the pellet was dissolved in 250 mL of minimal medium containing ¹⁵NH₄Cl. (For 1 L: KH₂PO₄ 3g, Na₂HPO₄*7H₂O 12.8 g, NaCl 500 mg, ¹⁵NH₄Cl 1 g, D-glucose 4 g, 10 mL Vitamin solution (Thiamine-HCl 10 mg/L, Pyridoxine-HCl 50 mg/L, Nicotinic acid 50 mg/L, L-glycine 200 mg/L), 1 M MgSO₄ 2 mL, 1 M CaCl₂ 100 μL). The bacterial were incubated for 1 h at 30 °C and the expression was induced with IPTG (0.5 mM final concentration) and bacteria were cultured for 12 h at 30 °C and 180 rpm. The cells were then harvested by centrifugation (3000 g, 10 min) and the pellet was washed with PBS. The cells were resuspended in 25 mL TBS/Ca (20 mM Tris, 137 mM NaCl, 2.6 mM KCl at pH 7.4 supplemented with 100 μM CaCl₂), PMSF (1 mM) and lysozyme (0.4 mg/mL) were added and subsequently disrupted using a sonicator on ice (5 cycles of 10 s). Cell debris was removed by centrifugation (10 min, 10000 g) and the supernatant was loaded on galactosylated sepharose CL-6B.^[291] The column was washed with TBS/Ca and LecA was eluted by addition of 100 mM D-galactose to the buffer. The eluted fractions were extensively dialyzed against distilled water and then, the protein was lyophilized. Between 10 and 20 mg LecA per liter bacterial culture were obtained.

5.2. Experimental information on NMR measurements

General information on NMR

The experiments were carried out on a 700 MHz NMR by Bruker BioSpin GmbH equipped with a 5 mm cry probe, at 298 K using 5 mm NMR tubes from ABCR (Karlsruhe, Germany) or D₂O Shigemi tubes (Euriso-top, Saarbrücken). The spectra were processed with Bruker Topspin 3.5p15. All deuterated solvents as well ¹³C-Glucose, ¹⁵NH₄Cl were obtained from Euriso-top, Saarbrücken. Methyl α -galactoside was obtained from Sigma Aldrich, p-nitro phenyl β -galactoside from Carbosyn, UK.

Information on used NMR pulse sequences

1D-proton spectra with water suppression

Water suppressed protons spectra were recorded using p3919gp (watergate) pulse sequence with gradients, 8 scans, a spectral width of 14 ppm and 2 sec acquisition time. The transmitter frequency offset was calibrated to 2351.23 Hz and the receiver gain to 2050.

T1 ρ measurements

For the NMR measurement a T1 ρ -sequence provided by Marcel Blommers based on Bruker-T1ir-pulseprogram was used and modified: A spectral width of 10 ppm was recorded using 8 scans. Again, a p3919gp (watergate) was applied. Spinlock times between 0.1 and 900 ms (p8-pulse) were used resulting in acquisition times up to 7 sec.

TROSY measurements

Spectra (using TROSYF3GPPH19 pulse sequence) were recorded with a transmitter frequency offset (F2=¹H, F1=¹⁵N) of 4.650 ppm and 117 ppm. Time domain (F2=¹H, F1=¹⁵N) was set to 2048 and 256, while the spectral width (F2=¹H, F1=¹⁵N) was set to 18 and 35 ppm. Spectra were recorded with 64 scans and an acquisition time of 2 sec including a water suppression using a 3-9-19 pulse sequence with gradient (watergate).

¹⁹F and CPMG measurements

Fluorine spectra were recorded with a spectral width of 140 ppm and a transmitter offset at 120 ppm, acquiring 128 scans, with an acquisition time of 0.8 and 2 s relaxation time. T₂-filtered spectra were recorded using a CPMG pulse sequence with a 180 ° pulse repetition rate of 50 Hz and duration of 1.0 s using same acquisition and relaxation times. [281,282] Two CPMG spectra were recorded per mixture to cover the full spectral width. A spectrum ranging from 50 to 100 ppm and from 100 to 150 ppm was recorded with 96 and 256 scans, respectively

The fragment library

The fragment library developed by Rademacher and co-workers was used as described previously.^[280] In this, the commercially available compounds from different manufacturers (Sigma-Aldrich, St. Louis, MO, USA; Key Organics, Camelford, UK; ACB Blocks, Toronto, ON, Canada; Santa Cruz Biotechnology, Santa Cruz, CA, USA; Vistas-MLab, Moscow, Russia; LifeChemicals, Kyiv, Ukraine; Alfa Aesar, Ward Hill, MA, USA; TCI, Tokyo, Japan; Apollo Scientific, Stockport, UK) are contained, each compound with at least one fluorine atom.^[267] The different fragments mixtures (called bins) used were prepared as described by Aretz et al.^[280] All NMR studies were measured at 298 K in Norell SP5000-7 5 mm tubes (Norell, Landisville, NJ, USA) on a Varian PremiumCOMPACT 600 MHz spectrometer equipped with an oneNMR probe (Agilent, Santa Clara, CA, USA) with TSP and TFA as internal references. All spectra were analyzed in MestReNova 10.0.1 (Mestrelab Research, Santiago de Compostela, Spain). 6 screening mixtures (called bins) consisting of 36 compounds each were tested. The mixtures of 100 μ M compound each, 100 μ M TFA, 150 mM sodium chloride in 20 mM Tris-HCl, pH 7.8, in 20 % D₂O (Euriso-Top) that were stored at 20°C as aliquots until used.

Sample preparation for ¹⁹F and a CPMG sequence

All protein samples were prepared at 20 μ M of final LecA concentration in TBS/Ca (20 mM Tris, 137 mM NaCl, 2.6 mM KCl at pH 7.4 supplemented with 150 μ M CaCl₂) and mixed 1:1 with the screening mixture aliquots resulting in a final protein and compound concentration of 10 and 50 μ M, respectively, in 500 μ L final volume. Screening was performed first in the presence and absence of protein, and in presence and absence of p-nitro phenyl β -D-galactoside (stock 50 mM in D₂O) using a final concentration of 100 μ M. All spectra were analyzed for changes in peak intensity and chemical shift. As an additional quality control, frequent hitters identified during unrelated screening campaigns were removed. All NMR spectra were processed and evaluated using MestReNova 10.0.1 (Mestrelab Research, Santiago de Compostela, Spain)

TROSY experiments with uniformly labeled ¹⁵N LecA

For the TROSY experiments, uniformly labeled ¹⁵N LecA was dissolved in citrate buffer according to Gomori (for pH 6.2 100 mL: 7.2 mL citric acid (0.1 M), 42.8 mL sodium citrate (0.1 M))^[292] by gently shaking for 2 h at r.t.. Afterwards, the protein solution was centrifuged for 30 min at 15 000 g and 25 °C. The concentration was determined by measuring the absorbance at 280 nm (Genesys 10S UV-Vis, Thermo Scientific) and the concentration was calculated using the extinctions coefficient of 27385 M⁻¹ cm⁻¹. To 500 μ L of protein solution 50 μ L of D₂O or the respective salt- or sugar solution in D₂O were added prior to measurement.

T1 ρ measurements with apoLecA substituted with trivalent lanthanide ions and sugar ligands

For T1 ρ measurements, LecA was dissolved in deuterated PBS (1 L in D₂O: 8 g NaCl, 0.2 g KCl, 1.42 g Na₂HPO₄, 0.27 g KH₂PO₄) and incubated for 2 h at r.t. The solution was subsequently centrifuged at 15000 g

Experimental section

for 30 min and at 25 °C and the concentration was determined using UV measurement at 280 nm, and calculation of the amount of dissolved LecA with its extinction factor of $27600 \text{ M}^{-1} \text{ cm}^{-1}$.^[41]

LecA and ligand ratio of 1:10: To a solution of LecA (100 μM) and TbCl_3 (30 μM) or CaCl_2 (15 μM), ligand (1mM) was added, trimethyl ammonium chloride (200 μM) was added as internal standard. The NMR samples were transferred to 5 mm NMR tubes (500 μL final volume), and water suppressed proton spectra with 500 scans were recorded, as well as T1 ρ relaxation edited spectra with different spin lock time (p8-pulse) between 1 and 900 ms.

LecA and ligand ratio of 1:50: To a solution of LecA (50 μM) and TbCl_3 or CaCl_2 (both 50 μM), ligand (2.5 mM) was added, tri-methyl ammonium chloride (1 mM) was added as internal standard. The NMR samples were transferred to 5 mm NMR tubes (500 μL final volume), and water suppressed proton spectra with 500 scans were recorded, as well as T1 ρ relaxation edited spectra with different spin lock time (p8-pulse) between 1 and 900 ms.

LecA and ligand ratio of 1:100: To a solution of LecA (100 μM) and TbCl_3 or CaCl_2 (15 μM), ligand (1 mM) was added, tri-methyl ammonium chloride (500 μM) was added as internal standard. The NMR samples were transferred to 5 mm NMR tubes (500 μL final volume), and water suppressed proton spectra with 500 scans were recorded, as well as T1 ρ relaxation edited spectra with different spin lock time (p8-pulse) between 1 and 900 ms. All spectra were evaluated using the Bruker Topspin 3.5p15. For evaluation the spectra were overlaid and the intensity was adjusted to the internal reference tetra methyl ammonium chloride (500 μM , 3.201 ppm) peak. The signal intensity of each peak was measured and was calculated with respect to the determined value at 1 ms (1 ms = 100 %) and then the calculated signal intensity (in %) was blotted against the spinlock time (in ms). Data analysis was performed with Prism 5.0c

5.3. Experimental information on biochemical methods

Fluorescence Polarization assay^[93]

The FP assay was carried out in Tris buffered saline (TBS): prepared with 8 g NaCl, 200 mg KCl and 2.43 g Tris base dissolved in 900 mL of water and the pH adjusted to 7.4 with 2 M HCl. Finally, the volume was adjusted to 1000 mL. The buffer was supplemented with 100 μM CaCl_2 before use. The measured compounds were dissolved in DMSO p.a. quality. Fluorescence polarization measurement occurred in black non-binding 384 well plates (Greiner bio-one, article: 781900) on a BMGLabtech PheraStar micro plate reader. Concentration of LecA was determined at 280 nm and a theoretical extinction coefficient of $27\,385 \text{ M}^{-1} \text{ cm}^{-1}$ using an Agilent Carry60 UV-Vis Spectrometer. Data were analyzed using BMG Labtech MARS Data Analysis Software (Version 2.40) and Graph pad Prism6. All measurements were performed as triplicates and

an excitation filter of 485 nm and an emission filter of 535 nm were used. The measured intensities were reduced by the values of buffer and LecA.

Thermal Shift assay

All ligands were stored in 5 mM stocks in TBS. A Mastermix containing Sypro Orange (8-fold, Sigma-Aldrich) and LecA (2 μ M) was prepared and vigorously mixed by pipetting. The ligand stock was diluted to 500 μ M final concentration using the mastermix and 20 μ L were shared into white opaque 96-well PCR plate FrameStar (GeneOne) using triplicates. The loaded plate was sealed using PCR sealing foil and centrifuged at 1000 rpm for 1 min. Each plate contained a protein-only control and phenyl -galactoside (500 μ M) as a positive control. The plate was heated in a StepOnePlus real-time PCR system (Applied Biosystems) with 1 K/ min starting from 298 to 368 K. The first derivations of obtained melting curves were analyzed using the StepOne software and referenced against the protein only control.

Enzym linked lectin assay

For the enzyme linked lectin assay, purified LecA was biotinylated following the procedure published by G. Elia.^[293] Determination of the lectin concentration was performed according to Cecioni et al.^[272]: 96-well micro titer plates (Greiner bio-one) were coated with PAA-gal or PAA-glc (Lectinity Holding, Inc.): 100 μ L/ mL in carbonate buffer (pH 9.6) for 1 h at 37 °C. Afterwards, the wells were blocked using 3% BSA in PBS for 1h at 37 °C. The lectin solution (100 μ L) starting from 50 μ g/mL were added in 0.6-fold serial dilutions in triplicates and the solution was incubated for 1h at 37 °C. After incubation, the wells were washed three-times with 120 μ L T-PBS (PBS containing 0.05 % Tween). Horseradish peroxidase with a streptavidin tag (HRP, 1: 5000 dilution, 100 μ L) was added and incubated for 1 h at 37 °C. After incubation, the wells were washed three-times with 120 μ L T-PBS. For the coloration reaction, 0.05 M phosphate/citrate buffer containing o-phenylene diamin dihydro chloride (0.4 mg/ mL) and hydrogen peroxide (0.4 mg/ mL) for 15 minutes. The reaction was stopped by addition of 50 μ L of 30 % sulfuric acid. The absorbance was determined at 490 nm using a micro titer reader (PheraStar FS, BMG Labtech). The determined absorbance was corrected with the values buffer containing o-phenylene diamin dihydro chloride (0.4 mg/ mL) and hydrogen peroxide (0.4 mg/ mL) with sulfuric acid. For the determination of the optimal lectin concentration, the lectin concentration was blotted against the measured absorbance. The value of highest linear response, 5 μ g/ mL, was used in further experiments. Determination of the functional replacement of Ca²⁺ with trivalent lanthanide ions was performed in analogy to Cecioni et al.^[272]: ELLA experiments were carried out in 96-well micro titer plates (Greiner bio-one) coated with PAA-gal or PAA-glc (100 μ L, both 5 μ g/mL) in carbonate buffer for 1 h at 37 °C. Afterwards, 100 μ L of 3 % BSA in PBS solution per well was incubated for 1 h at 37 °C. The Ca²⁺- free LecA-biotin (5 μ g/ mL) was re-substituted with 100 μ M of the respective trivalent lanthanide ion. After BSA blocking, 100 μ L of the reconstituted LecA-biotin solution was incubated for 1 h at 37 °C. Three-times washing with 120 μ L of T-PBS were followed by incubation of Horseradish peroxidase with a streptavidin tag (HRP, 1: 5000 dilution, 100 μ L) for 1 h at 37 °C. After incubation with HRP, the wells were washed with 120 μ L of PBS.

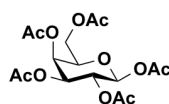
Experimental section

For the coloration reaction, o-phenylene diamin dihydro chloride (0.4 mg/ mL) and hydrogen peroxide (0.4 mg/ mL) was incubated for 30minutes. The reaction was stopped by addition of 50 μ L of 30 % sulfuric acid. The absorbance was determined at 490 nm using a micro titer reader (PheraStar FS, BMG Labtech). The determined absorbance was corrected with the values buffer containing o-phenylene diamin dihydro chloride (0.4 mg/ mL) and hydrogen peroxide (0.4 mg/ mL) with sulfuric acid.

5.4. Experimental information on synthesis

Synthesis of the D-galactose derivatives

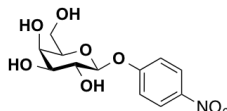
Penta acetylated D-galactose



Chemical Formula: $C_{16}H_{22}O_{11}$
Exact Mass: 390,12

1,2,3,4,6-Penta-O-acetyl- β -D-galactopyranoside was synthesized according to Cohen et al.^[295]

p-nitro phenyl β -D-galactoside



Chemical Formula: $C_{12}H_{15}NO_8$
Exact Mass: 301,08

Molecular sieves (5 g, 3 Å) were dried under vacuum at 350 °C in a two-necked flask for 30 min. After cooling to r.t., the flask was flushed with argon and dry CH_2Cl_2 (25 mL) was added. Galactosyl donor **16** (5.0 g, 12.8 mmol) and p-nitro phenol (2.2 g, 15.9 mmol) were added, the reaction mixture was cooled (0 °C) and BF_3OEt_2 (8.2 mL, 65.3 mmol) was added drop wise. Afterwards, the mixture was allowed to warm to r.t. and stirred for 1 d. The reaction was poured onto ice water (200 mL) and the aqueous phase was extracted with aqueous saturated $NaHCO_3$ (5 \times 50 mL). The combined organic layers were washed with brine (25 mL) and dried over anhydrous Na_2SO_4 . After filtration, the solvent was removed in vacuo. The crude product was dissolved in warm EtOH and left at 4 °C. overnight. Precipitated pure product (3.1 g, 6.6 mmol, 52%) was obtained as light yellow amorphous solid.

1H -NMR (400 MHz, $CDCl_3$) δ 8.25–8.17 (m, 2H, ArH), 7.10–7.05 (m, 2H, ArH), 5.51 (dd, J = 10.4, 7.9 Hz, 1H, H-2), 5.47 (d, J = 3.3 Hz, 1H, H-4), 5.17 (d, J = 7.9 Hz, 1H, H-1), 5.13 (dd, J = 10.4 3.4 Hz, 1H, H-3),

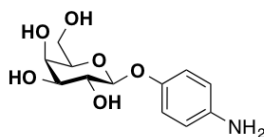
Experimental section

4.25–4.10 (m, 3H, H-5, H-6a,b), 2.18 (s, 3H, CH₃) 2.06 (s, 6H, CH₃) 2.01 (s, 3H, CH₃). ¹³C-NMR (101 MHz, CDCl₃): δ 170.41 (C=O), 170.23 (C=O), 170.15 (C=O), 169.38 (C=O), 161.30 (ArC), 143.31 (ArC), 125.91 (2C, ArCH), 116.68 (2C, ArCH), 98.69 (C-1), 71.57 (C-5), 70.68 (C-3), 68.37 (C-2), 66.79 (C-4), 61.46 (C-6), 20.82 (CH₃), 20.79 (CH₃), 20.76 (CH₃), 20.68 (CH₃); R_f = 0.27 (CH₂Cl₂/MeOH 12 : 1); ESI-MS: [C₂₀H₂₃NO₁₂ + Na]⁺ calcd 492.1 found 492.1. p-Nitro phenyl 2,3,4,6-tetra-O-acetyl-β-D-galactopyranoside was first described by Goebel and Avery,^[296] NMR data obtained are in agreement with the literature ¹H-NMR data by Apparū et al.^[297]

Deprotection was done according to Zemplen conditions.^[298] To deprotect the acetylated derivative sodium (~0.1 eq) was dissolved in dry MeOH (100 eq) and the acetylated starting material (2.6 g, 5.6 mmol, 1 eq) was added. The solution was stirred for 2 h at r.t. Afterwards the solution was neutralized using an acidic Amberlite+ IR 120 (Merck) ion exchanger. The resin was filtered, and the solvent was removed *in vacuo* to give 96.4 % of pure de-acetylated product.

¹H-NMR: (400 MHz, MeOD-d₄) δ 8.23-8.18 (m, 2H, ArH) 7.27-7.21 (m, 2H, ArH) 5.01 (d, J= 7.7 Hz, 1H, H-1) 3.91 (d, J= 3.4 Hz, 1H, H-2) 3.87- 3.68 (m, 3H, H-3& H-5& H-6) 3.60 (dd, J= 9.70 3.4 Hz, 1H, H-4) ¹³C-NMR: (101 MHz, MeOD-d₄) δ 163.97 (C-1') 143.71 (C-4') 126.57 (C-3' & C-5') 117.73 (C-2' & C-6') 102.27 (C-1) 77.27 (C-4) 74.69 (C-5) 71.98 (C-3) 70.14 (C-2) 62.39 (C-6) R_f(CH₂Cl₂: MeOH 10:1) 0.16

p-Amino phenyl β -D-galactoside



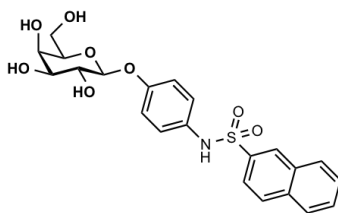
Chemical Formula: C₁₂H₁₇NO₆
Exact Mass: 271.11

For reduction of the nitro-group the nitro phenyl derivative 900 mg (3 mmol, 1 eq) was dissolved in dry MeOH (10 mL) and Pd-C (7 wt%) was added. After three cycles of H₂/ vacuum the mixture was stirred under H₂-atmosphere (1 bar) at r.t. over night. The solution was filtered through a plug of celite and the filtrate was washed with MeOH. The solvent was removed in vacuo to yield 98 % (797 mg, 2.94 mmol) of p-amino phenyl-β-D- galactopyranoside.

The obtained NMR data are in accordance to Masato et al.^[299]

p-Amino phenyl- 2-naphthosulfonamide β –D-galactoside

Experimental section

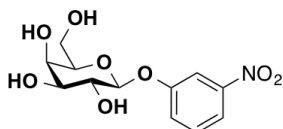


Chemical Formula: C₂₂H₂₃NO₈S
Exact Mass: 461,11

For the sulfonamide synthesis, the p-amino phenyl β-D-galactoside (40 mg, 0.14 mmol, 1 eq) was dissolved in 1 mL of dry DMF and NEt₃ (24.5 μL, 0.15 mmol, 1.2 eq) was added. The mixture was cooled to 0°C and 2-Naphthalen sulfonyl chloride (33 μL, 0.15 mmol, 1.2 eq) were added and the reaction was stirred for 1 h at 0°C and 1 h at r.t.. Afterwards, the reaction was quenched with water and extracted with EtOAc (10x, 5 mL). The solvent was removed in vacuo and the crude product was purified by column chromatography (CH₂Cl₂/MeOH: 0 to 10 % EtOH). 23.2 % (15 mg, 0.03 mmol) of product was obtained.

¹H NMR (500 MHz, CDCl₃) δ 8.31 – 8.21 (m, 1H, ArH), 8.05 – 7.90 (m, 4H, ArH), 7.78 – 7.71 (m, 1H, ArH), 7.62 (dddd, J = 23.7, 8.4, 7.0, 1.3 Hz, 2H, ArH), 7.05 – 7.00 (m, 3H, ArH), 6.98 – 6.93 (m, 2H, ArH), 4.74 (d, J = 7.8 Hz, 1H, H-1), 3.96 – 3.85 (m, 1H, H-4), 3.78 – 3.70 (m, 3H, H2, H-6), 3.63 (qt, J = 7.0, 3.1 Hz, 1H, H-3), 3.54 (dt, J = 9.8, 3.8 Hz, 1H, H-5).

m-nitro phenyl β-D-galactoside



Chemical Formula: C₁₂H₁₅NO₈
Exact Mass: 301,08

3 Å (5 g) molecular sieve was dried under reduced pressure at 350 °C in a two-necked flask for 30 min. After cooling to r.t. the flask was flushed with argon. 25 mL of dry CH₂Cl₂ were added under counter current flow of argon. 5 g (12.8 mmol; 1 eq) of acetylated D-galactose and 2.2 g (15.9 mmol; 1.2 eq) p-nitro phenol were added. The reaction mixture was cooled to 0 °C and 8.2 mL BF₃·OEt₂ (65.3 mmol; 5.1 eq) was added drop wise. Afterwards, the mixture was allowed to warm to r.t. and was stirred for 1 d. The reaction was poured onto ice water and extracted five times with 50 mL saturated NaHCO₃. The organic layers were washed with 25 mL of saturated NaCl and dried with Na₂SO₄. The solvent was removed, and the residue was dissolved in warm ethanol and afterwards put at 4 °C overnight. A light yellow amorphous solid was filtered to give 3.3 g (7.1 mmol; 55.4 %) of pure m-nitro phenyl 2,3,4,6-tetra-O-acetyl β-D-galactopyranoside. The mother liquor was concentrated and dried to give a yellow oil. The oil was heated in EtOH to reflux and put at 4 °C for

crystallization. The white product was filtered and washed with 10 mL of cool EtOH to give 1.0 g (4 mmol; 16.4 %) of m-nitro phenyl-tetra-O-acetyl α -D-galactopyranoside.

α -anomer:

$^1\text{H-NMR}$ (400 MHz, CDCl_3) δ 8.24- 8.19 (m, 2H, ArH) 7.20-7.12 (m, 2H, ArH) 5.88 (d, $J= 3.6$ Hz, 1H, H-1) 5.58-5.49 (m, 2H, H-3 & H-4) 5.31 (dd, $J= 10.7$ 3.6 Hz, 1H, H-2) 4.24 (ddd, $J= 7.2$ 6.2 1.5 Hz, 1H, H-5) 4.07 (qd, $J= 11.3$ 6.5 Hz, 2H, H-6) 2.17 (s, 3H, CH_3) 2.07 (s, 3H, CH_3) 2.03 (s, 3H, CH_3) 1.92 (s, 3H, CH_3) $^{13}\text{C-NMR}$ (101 MHz, CDCl_3) δ 170.36 (C=O) 170.24 (C=O) 170.09 (C=O) 170.04 (C=O) 160.86 (ArC) 143.06 (ArC) 125.83 (ArC) 116.57 (ArC) 94.73 (C-1) 67.81 (C-3) 67.54 (C-2) 67.38 (C-4) 67.19 (C-5) 61.32 (C-6) 20.71 (CH_3) 20.66 (CH_3) 20.62 (CH_3) 20.57 (CH_3)

β -anomer:

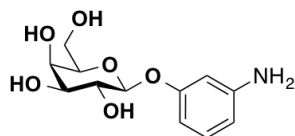
$^1\text{H-NMR}$ (400 MHz, CDCl_3) δ 8.25-8.17 (m, 2H, ArH) 7.10-7.05 (m, 2H, Arh) 5.55-5.46 (m, 2H, H-3 & H-5) 5.17 (d, $J= 7.9$ Hz, 1H, H-1) 5.13 (dd, $J= 10.4$ 3.4 Hz, 1H, H-2) 4.25-4.10 (m, 3H, H-4 & H-6) 2.18 (s, 3H, CH_3) 2.06 (s, 6H, CH_3) 2.01 (s, 3H, CH_3) $^{13}\text{C-NMR}$ (101 MHz, CDCl_3) δ 170.41 (C=O) 170.23 (C=O) 170.15 (C=O) 169.38 (C=O) 161.30 (ArC) 143.31 (ArC) 125.91 (ArC) 116.68 (ArC) 98.69 (C-1) 71.57 (C-4) 70.68 (C-2) 68.37 (C-3) 66.79 (C-5) 61.46 (C-6) 20.82 (CH_3) 20.79 (CH_3) 20.76 (CH_3) 20.68 (CH_3) ESI-MS: $[\text{C}_{20}\text{H}_{23}\text{NO}_{12}+\text{Na}]^+$ calc. 429.4 found 492.6 $[\text{C}_{20}\text{H}_{23}\text{NO}_{12}+\text{K}]^+$ calc. 508.5 found 508.6 R_f: (CH_2Cl_2 12:1) 0.27. The NMR data corresponds to Matta et al. [300]

Deprotection was done according to Zemplen conditions.^[298] To deprotect the acetylated derivatives sodium (~0.1 eq) was dissolved in dry MeOH (100 eq) and the acetylated starting material (3.3g, 7.1 mmol, 1 eq) was added. The solution was stirred for 2 h at r.t. Afterwards the solution was neutralized using an acidic Amberlite+ IR 120 (Merck) ion exchanger. The resin was filtered, and the solvent was removed in vacuo to give the de-acetylated products. Following this method 2.1 g (7.0 mmol; 98.2%) of the white solid product was obtained.

$^1\text{H-NMR}$: (400 MHz, MeOD-d₄) δ 7.97-7.94 (m, 1H, ArH) 7.90 (dt, $J= 7.3$ 2.1 Hz, 1H, ArH) 7.57-7.48 (m, 2H, ArH) 4.97 (d, $J= 7.7$ Hz, 1H, H-1) 3.92 (d, $J= 3.4$ Hz, 1H, H-2) 3.87-3.73 (m, 4H, H-3 & H-5 & H-6) 3.62 (dd, $J= 9.7$, 3.4 Hz, 1H, H-4) $^{13}\text{C-NMR}$: (101 MHz, MeOD-d₄) δ 159.9 (C-1') 150.44 (C-3') 131.34 (C-6') 124.20 (C-5') 117.96 (C-2') 112.71 (C-4') 102.71 (C-1) 77.23 (C-5) 74.71 (C-4) 72.07 (C-3) 70.07 (C-2) 62.36 (C-1) ESI-MS: $[\text{C}_{12}\text{H}_{15}\text{NO}_8+\text{Na}]^+$ calc. 324.2 found 324.4 $[\text{C}_{12}\text{H}_{15}\text{NO}_8+\text{K}]^+$ calc. 340.3 found 340.4 $[\text{C}_{24}\text{H}_{30}\text{N}_2\text{O}_{16}+\text{H}+\text{Na}]^{+2}$ calcd. 626.2 found 626.0 R_f: (CH_2Cl_2 : MeOH 1:10) 0.17

m-Amino phenyl β -D-galactoside

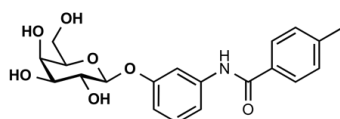
Experimental section



Chemical Formula: $C_{12}H_{17}NO_6$
Exact Mass: 271,11

The amide was synthesized by Maike Lehner and reported in her Bachelor thesis.^[269]

m-Phenyl-1-tolylamide β -D-galactosamide

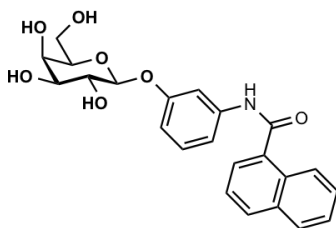


Chemical Formula: $C_{20}H_{23}NO_7$
Exact Mass: 389,15

For the amide coupling, the m-amino phenyl β -D-galactoside (40 mg, 0.147 mmol, 1 eq) was dissolved in 1 mL of dry DMF and NEt_3 (24.5 μ L, 0.177 mmol, 1.2 eq) was added. The mixture was cooled to 0°C and tolyl chloride (23.4 μ L, 0.177 mmol, 1.2 eq) were added and the reaction was stirred for 1 h at 0°C and 1 h at r.t.. Afterwards, the reaction was quenched with NaOH (1 M) and extracted with EtOAc (20x, 5 mL). The solvent was removed in vacuo and the crude product was purified by column chromatography (CH_2Cl_2 /EtOH: 0 to 20 % EtOH). 34.9 % (20 mg, 0.051 mmol) of product was obtained.

1H NMR (400 MHz, MeOD- d_4) δ 7.91 - 7.81 (m, 2H, ArH), 7.58 (t, J = 2.2 Hz, 1H, ArH), 7.43 - 7.33 (m, 3H, ArH), 7.29 (t, J = 8.1 Hz, 1H, ArH), 6.94 (ddd, J = 8.3, 2.4, 1.0 Hz, 1H, ArH), 4.93 (d, J = 7.7 Hz, 1H, H1), 3.96 (dd, J = 3.4, 1.0 Hz, 1H, H4), 3.91 - 3.78 (m, 3H, H2, H3, H6b), 3.74 (ddd, J = 6.7, 5.2, 1.1 Hz, 1H, H6b), 3.68 - 3.60 (m, 1H, H5), 2.45 (s, 3H, CH_3) ^{13}C NMR (101 MHz, MeOD- d_4) δ 168.8 (CO), 159.5 (ArC), 143.7 (ArC), 141.0 (ArC), 133.4 (ArC), 130.4 (ArC), 130.2 (ArC), 128.7 (ArC), 116.0 (ArC), 113.9 (ArC), 110.7 (ArC), 102.9 (C1), 74.9 (C2), 72.3 (C3), 70.2 (C4), 62.5, (C6) 21.5 (CH_3) HRMS: ($C_{20}H_{23}NO_7+Na$)⁺ calc. 412.14 found. 412.135, ($C_{40}H_{46}NO_{14}+Na$)⁺ calc. 801.29 found 801.281

m-Phenyl-1-naphtamide β -D-galactosamide

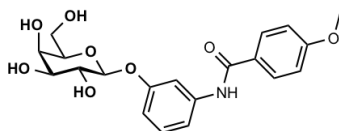


Chemical Formula: $C_{23}H_{23}NO_7$
Exact Mass: 425,15

For the amide coupling, the m-amino phenyl β -D-galactoside (40 mg, 0.147 mmol, 1 eq) was dissolved in 1 mL of dry DMF and NEt_3 (24.5 μ L, 0.177 mmol, 1.2 eq) was added. The mixture was cooled to 0°C and Naphthyl chloride (26.7 μ L, 0.177 mmol, 1.2 eq) were added and the reaction was stirred for 1 h at 0°C and 1 h at r.t.. Afterwards, the reaction was quenched with NaOH (1 M) and extracted with EtOAc (20x, 5 mL). The solvent was removed in vacuo and the crude product was purified by column chromatography (CH_2Cl_2 /EtOH: 0 to 20 % EtOH). 19.1 % (12 mg, 0.028 mmol) of product was obtained.

1H NMR (400 MHz, MeOD- d_4) δ 8.34 - 8.20 (m, 1H, ArH), 8.05 (d, J = 8.3 Hz, 1H, ArH), 8.03 - 7.95 (m, 1H, ArH), 7.76 (dd, J = 7.3, 1.3 Hz, 1H, ArH), 7.69 - 7.55 (m, 4H, ArH), 7.50 - 7.41 (m, 1H, ArH), 7.33 (t, J = 8.1 Hz, 1H, ArH), 6.97 (ddd, J = 7.9, 2.2, 1.1 Hz, 1H, ArH), 4.94 (d, J = 7.7 Hz, 1H, H1), 3.94 (d, J = 3.4 Hz, 1H, H4), 3.90 - 3.70 (m, 4H, H2, H3, H6), 3.69 - 3.59 (m, 3H, H5, $\underline{CH_2}$) ^{13}C NMR (101 MHz, MeOD- d_4) δ 170.7 (C=O), 159.6 (ArC), 141.1 (ArC), 136.0 (ArC), 135.2 (ArC), 131.7 (ArC), 131.4 (ArC), 130.6 (ArC), 129.5 (ArC), 128.1 (ArC), 127.5 (ArC), 126.4 (ArC), 126.1 (ArC), 126.0 (ArC), 115.4 (ArC), 114.0 (ArC), 110.1 (ArC), 102.9 (C1), 77.0 (C2), 74.9 (C5), 72.3 (C4), 70.2 (C2), 62.5 (C6), 58.3 ($\underline{CH_2}$) HRMS: ($C_{23}H_{23}NO_7+Na$) $^+$ calc. 448.44 found. 448.89

m-Phenyl-4-methoxyphenyl β -D-galactosamide



Chemical Formula: $C_{20}H_{23}NO_8$
Exact Mass: 405,14

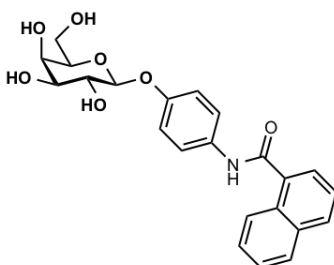
For the amide coupling, the m-amino phenyl β -D-galactoside (40 mg, 0.147 mmol, 1 eq) was dissolved in 1 mL of dry DMF and NEt_3 (24.5 μ L, 0.177 mmol, 1.2 eq) was added. The mixture was cooled to 0°C and 4-Methoxy benzoyl chloride (23.9 μ L, 0.177 mmol, 1.2 eq) were added and the reaction was stirred for 1 h at 0°C and 1 h at r.t.. Afterwards, the reaction was quenched with NaOH (1 M) and extracted with EtOAc (20x,

Experimental section

5 mL). The solvent was removed in vacuo and the crude product was purified by column chromatography (CH₂Cl₂/EtOH: 0 to 20 % EtOH). 28.5 % (17 mg, 0.042 mmol) of product was obtained.

¹H NMR (400 MHz, MeOD-d₄) δ 7.94 (d, J = 8.9 Hz, 1H, ArH), 7.56 (t, J = 2.2 Hz, 1H, ArH), 7.37 (ddd, J = 8.1, 2.1, 1.0 Hz, 1H, ArH), 7.28 (t, J = 8.1 Hz, 1H, ArH), 7.09 - 7.02 (m, 2H, ArH), 6.93 (ddd, J = 8.3, 2.5, 1.0 Hz, 1H, ArH), 4.93 (d, J = 7.7 Hz, 1H, H-1), 3.95 (dd, J = 3.4, 1.0 Hz, 1H, H-4), 3.90 (s, 3H, CH₃), 3.89 - 3.71 (m, 3H, H-2 & H-6), 3.68 - 3.60 (m, 2H, H-3 & H-5) ¹³C NMR (101 MHz, MeOD-d₄) δ 168.4 (C=O), 164.2 (ArC), 159.5 (ArC), 141.1 (ArC), 130.6 (ArC), 130.4 (ArC), 128.2 (ArC), 116.0 (ArC), 114.8 (ArC), 113.8 (ArC), 110.7 (ArC), 102.9 (C-1), 77.0 (C-3), 74.9 (C-5), 72.3 (C-2), 70.3 (C-4), 62.5 (C-6), 56.0 (CH₃)

p-Phenyl-1-naphtamide β-D-galactosamide



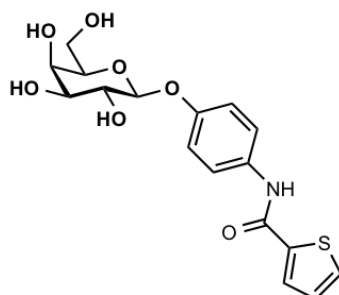
Chemical Formula: C₂₃H₂₃NO₇
Exact Mass: 425,15

For the three-step synthesis to obtain p-phenyl-1-naphtamide β-D-galactosamide, tetra-o-acetyl-p-nitro phenyl β-D-galactoside (50 mg, 0.107 mmol, 1 eq), was dissolved in dry CH₂Cl₂ and Pd-C (5 g, 10 wt-%) were added and after three cycles of H₂ /vacuum, the reaction was stirred at r.t. over night. Afterwards, the reaction was cooled to 0°C and NEt₃ (17 μL, 0.128 mmol, 1.2 eq) and 1-Naphtoyl chloride (19 μL, 0.128 mmol, 1.2 eq) were added and the reaction was stirred at 0°C for one hour and then allowed to warm up to room temperature for an additional hour. The crude product was purified by column, using a mixture a gradient of hexan and ethyl acetate 100 to 50 % of hexane. 78.8 % (50 mg, 0.084 mmol) of acetylated-product were obtained. Subsequently, sodium (≈1 mg) was dissolved in 3.5 mL of dry MeOH. Afterwards, the acetylated-product (50 mg, 0.084 mmol, 1 eq) were added and the solution was stirred at r.t. o/n. The reaction mixture was then neutralized with Amberlite H⁺ ion-exchanger and purified by column using a gradient of CH₂Cl₂ to EtOH 99:1 to 80:20. 81.2 % (29 mg, 0.068 mmol) product was obtained

¹H NMR (400 MHz, MeOD-d₄) δ 8.26 (dd, J = 8.0, 1.8 Hz, 1H, ArH), 8.04 (dd, J = 8.2, 1.2 Hz, 1H, ArH), 8.01 - 7.95 (m, 1H, ArH), 7.76 (dd, J = 7.0, 1.2 Hz, 1H, ArH), 7.73 - 7.67 (m, 2H, ArH), 7.64 - 7.54 (m, 3H, ArH), 7.24 - 7.15 (m, 2H, ArH), 4.89 (d, J = 7.8 Hz, 1H), 3.95 (dd, J = 3.5, 1.1 Hz, 1H, H-4), 3.90 - 3.77 (m, 3H, H-2, H-3, H-6a), 3.75 - 3.70 (m, 1H, H-6b), 3.68 - 3.55 (m, 1H, H-5) ¹³C NMR (101 MHz, MeOD-d₄) δ 170.5 (C=O), 156.2 (ArC), 136.0 (ArC), 135.2 (ArC), 134.5 (ArC), 131.6 (ArC), 131.5 (ArC), 129.5 (ArC),

128.1 (ArC), 127.5 (ArC), 126.4 (ArC), 126.2 (ArC), 126.0 (ArC), 123.1 (ArC), 118.2 (ArC), 103.3 (C-1), 77.0 (C-3), 74.9 (C-5), 72.3 (C-2), 70.2 (C-4), 62.5 (C-6)

p-Amino phenyl 1-thiophen β -D-galactoside

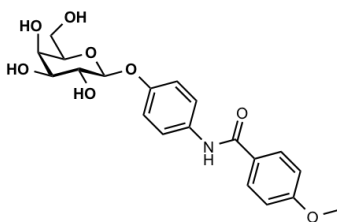


Chemical Formula: $C_{17}H_{19}NO_7S$
Exact Mass: 381,09

For the amide coupling, the amine p-amino phenyl β -D-galactoside (40 mg, 0.15 mmol, 1 eq) was dissolved in 1 mL of dry DMF and NEt_3 (24.5 μ L, 0.18 mmol, 1.2 eq) was added. The mixture was cooled to 0°C and 2-thiophene chloride (24.5 μ L, 0.18 mmol, 1.2 eq) were added and the reaction was stirred for 1 h at 0°C and 1 h at r.t.. Afterwards, the reaction was quenched with water and extracted with EtOAc (10x, 5 mL). The solvent was removed in vacuo and the crude product was purified by column chromatography (CH_2Cl_2 /EtOH: 0 to 20 % EtOH). 98.2 % (55 mg, 0.14 mmol) of product was obtained.

1H NMR (500 MHz, MeOD- d_4) δ 7.88 (dd, $J = 3.8, 1.1$ Hz, 1H, ArH), 7.73 – 7.68 (m, 1H, ArH), 7.59 – 7.54 (m, 2H, ArH), 7.20 – 7.08 (m, 3H, ArH), 4.86 (app. s, 1H, H-1), 3.93 (dd, $J = 3.5, 1.0$ Hz, 1H, H-4), 3.83 – 3.75 (m, 3H, H-2, H-6), 3.73 – 3.67 (m, 1H, H-3), 3.65 – 3.57 (m, 1H, H5). ^{13}C NMR (126 MHz, MeOD- d_4) δ 162.65 (C=O), 156.13 (ArC), 140.79 (ArC), 133.98 (ArC), 132.25 (ArC), 129.98 (ArC), 128.91 (ArC), 123.73 (ArC), 118.09 (ArC), 103.23 (C-1), 76.83 (C-3), 74.84 (C-5), 72.29 (C-2), 70.32 (C-4), 62.48 (C-6)

p-Aminophenyl p-methoxyphenyl β -D-galactoside



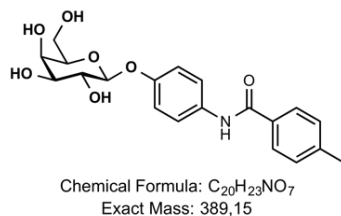
Chemical Formula: $C_{20}H_{23}NO_8$
Exact Mass: 405,14

Experimental section

For the amide coupling, the p-amino phenyl β -D-galactoside (50 mg, 0.18 mmol, 1 eq) was dissolved in 1 mL of dry DMF and NEt_3 (30 μL , 0.22 mmol, 1.2 eq) was added. The mixture was cooled to 0°C and 4-Methoxy benzoyl chloride (30 μL , 0.22 mmol, 1.2 eq) were added and the reaction was stirred for 1 h at 0°C and 1 h at r.t.. Afterwards, the reaction was quenched with water and extracted with EtOAc (10x, 5 mL). The solvent was removed in vacuo and the crude product was purified by column chromatography ($\text{CH}_2\text{Cl}_2/\text{MeOH}$: 0 to 10 % EtOH). 20.6 % (15 mg, 0.04 mmol) of product was obtained.

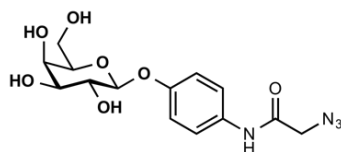
^1H NMR (500 MHz, MeOD- d_4) δ 7.97 – 7.90 (m, 2H, ArH), 7.62 – 7.57 (m, 2H, ArH), 7.15 (d, $J = 9.0$ Hz, 1H, ArH), 7.05 (d, $J = 8.9$ Hz, 2H, ArH), 3.94 (dd, $J = 3.4, 1.0$ Hz, 1H, H-4), 3.90 (s, 3H, CH_3), 3.85 – 3.78 (m, 3H, H-2, H-6), 3.75 – 3.68 (m, 1H, H-3), 3.61 (dd, $J = 9.7, 3.4$ Hz, 1H, H-5). ^{13}C NMR (126 MHz, MeOD- d_4) δ 168.29 (C=O), 164.10 (ArC), 156.07 (ArC), 130.48 (ArC), 123.80 (ArC), 118.09 (ArC), 114.80 (ArC), 103.34 (C-1), 76.96 (C-3), 74.89 (C-5), 72.32 (C-4), 70.26 (C-2), 62.45 (C-6), 55.98 (CH_3)

p-Amino phenyl p-tolyl β -D-galactoside



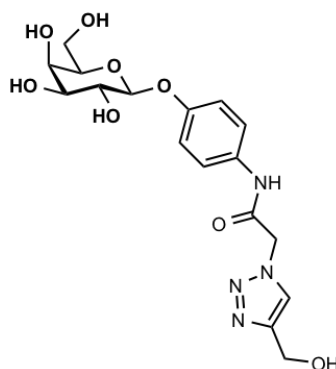
p-Nitro phenyl 2,3,4,6-tetra-O-acetyl- β -D-galactopyranoside (50 mg; 0.107 mmol, 1 eq) was dissolved in dry CH_2Cl_2 (2 mL) and Pd-C (10 wt-%, 5 mg) was added. After three cycles of vacuum and H_2 the solution was stirred under H_2 atmosphere over night. Subsequent, the solution was cooled to 0°C and afterwards NEt_3 (17 μL , 0.125 mmol, 1.2 eq) and p-Tolyl chloride (18 μL , 0.128 mmol, 1.2 eq) were added and the solution was stirred for 1 h at 0°C , and 2 h at r.t.. Then the solution was filtered through celite and purified by column chromatography using hexane and ethyl acetate from 99:1 to 60:40. 67.1 % (40 mg, 0.07 mmol) of product was obtained. For the removal of the acetyl groups, Na (1 mg) was added to dry MeOH (3 mL), and after full dissolution, the acetylated intermediate (40 mg; 0.07 mmol, 1 eq) was added and the solution was stirred o/n. After neutralization of with Amberlite H^+ and the solvent was removed *in vacuo*. After column chromatography using CH_2Cl_2 and EtOH 99:1 to 70:30, 35.7 % (10 mg; 0.026 mmol) of pure product was obtained.

^1H NMR (400 MHz, MeOD- d_4) δ 7.89 – 7.83 (m, 2H, ArH), 7.65 – 7.59 (m, 2H, ArH), 7.39 – 7.33 (m, 2H, ArH), 7.21 – 7.13 (m, 2H, ArH), 4.90 – 4.87 (app s, 1H, H-1), 3.94 (dd, $J = 3.4, 1.0$ Hz, 1H, H-4), 3.86 – 3.79 (m, 3H, H-2 H-3 H-6a), 3.72 (ddd, $J = 7.0, 5.1, 1.1$ Hz, 1H, H-6b), 3.62 (dd, $J = 9.7, 3.4$ Hz, 1H, H-5), 2.45 (s, 3H, CH_3). ^{13}C NMR (101 MHz, MeOD- d_4) δ 167.98 (ArC), 154.74 (ArC), 128.79 (ArC), 127.20 (ArC), 122.36 (ArC), 116.70 (ArC), 101.95 (ArC), 100.00 (C-1), 75.59 (C-3), 73.49 (C-2), 70.92 (C-5), 68.84 (C-4), 63.96 (C-6), 20.04 (CH_3).

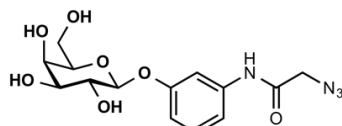
p-(α -Azidoacetamido)-phenyl β -D-galactopyranoside

Chemical Formula: $C_{14}H_{18}N_4O_7$
Exact Mass: 354,12

p-(α -Azidoacetamido)-phenyl β -D-galactopyranoside was synthesized from acetyl-protected p-nitro phenyl β -D-galactopyranoside in 4 chemical steps in as reported in Org. Bioorg. Chem 2016.^[93]

4-(4-Hydroxymethyl-1,2,3-triazol-1-yl) acetamidophenyl β -D-galactopyranoside

4-(4-Hydroxymethyl-1,2,3-triazol-1-yl) acetamidophenyl β -D-galactopyranoside was synthesized in 48 % yield from acetyl-protected p-nitro phenyl β -D-galactopyranoside in 4 chemical steps as reported by Cecioni et al.^[68]

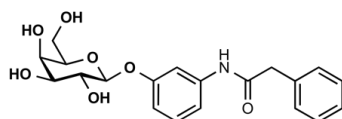
m-(α -Azidoacetamido)-phenyl β -D-galactopyranoside

Chemical Formula: $C_{14}H_{18}N_4O_7$
Exact Mass: 354,12

m-(α -Azidoacetamido)-phenyl β -D-galactopyranoside was synthesized from acetyl-protected m-nitro phenyl β -D-galactopyranoside in 4 chemical steps in as reported in Org. Bioorg. Chem 2016.^[93]

Experimental section

m-Aminophenyl-benzyl β -D-galactoside

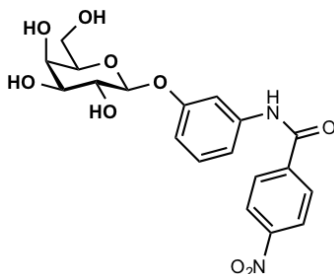


Chemical Formula: $C_{20}H_{23}NO_7$
Exact Mass: 389,15

For the amide coupling, the m-amino phenyl β -D-galactoside (46 mg, 0.17 mmol, 1 eq) was dissolved in 1 mL of dry DMF and NEt_3 (28.2 μ L, 0.20 mmol, 1.2 eq) was added. The mixture was cooled to 0°C and Benzoyl chloride (26.8 μ L, 0.20 mmol, 1.2 eq) were added and the reaction was stirred for 1 h at 0°C and 1 h at r.t.. Afterwards, the reaction was quenched with NaOH (1 M) and extracted with EtOAc (10x, 5 mL). The solvent was removed in vacuo and the crude product was purified by column chromatography (CH_2Cl_2 /EtOH: 0 to 15 % EtOH). 9.1 % (6 mg, 0.015 mmol) of product was obtained.

1H NMR (400 MHz, MeOD- d_4) δ 7.47 (q, $J = 1.5$ Hz, 1H, ArH), 7.37 (d, $J = 1.6$ Hz, 2H, ArH), 7.32 – 7.26 (m, 1H, ArH), 7.23 (dd, $J = 5.0, 2.3$ Hz, 2H, ArH), 6.89 (d, $J = 6.6$ Hz, 1H, ArH), 4.89 (s, 1H, H-1), 3.94 (dd, $J = 3.4, 1.0$ Hz, 1H, H-4), 3.85 – 3.79 (m, 3H, H-2 & H-6), 3.73 – 3.68 (m, 3H, H-3 & CH_2), 3.60 (dd, $J = 9.7, 3.4$ Hz, 1H, H-5). ^{13}C NMR (101 MHz, MeOD- d_4) δ 172.27 (C=O), 159.51 (ArC), 136.78 (ArC), 130.45 (ArC), 130.11 (ArC), 129.58 (ArC), 127.93 (ArC), 114.97 (ArC), 113.54 (ArC), 109.82 (ArC), 102.88 (C1), 76.93 (C3), 74.87 (C5), 72.23 (C2), 70.19 (C4), 62.39 (C6), 44.74(CH_2).

m-Aminophenyl p-nitrophenyl β -D-galactoside



Chemical Formula: $C_{19}H_{20}N_2O_9$
Exact Mass: 420,12

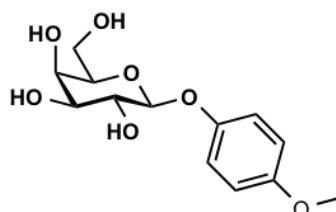
For the amide coupling, the m-amino phenyl β -D-galactoside (40 mg, 0.15 mmol, 1 eq) was dissolved in 1 mL of dry DMF and NEt_3 (24.5 μ L, 0.18 mmol, 1.2 eq) was added. The mixture was cooled to 0°C and 4-

Experimental section

Nitrobenzoyl chloride (32.8 mg, 0.18 mmol, 1.2 eq) were added and the reaction was stirred for 1 h at 0°C and 1 h at r.t.. Afterwards, the reaction was quenched with NaOH (1 M) and extracted with EtOAc (10x, 5 mL). The solvent was removed in vacuo and the crude product was purified by column chromatography (CH₂Cl₂/EtOH: 0 to 20 % EtOH). 76.1 % (47 mg, 0.11 mmol) of product was obtained.

¹H NMR (400 MHz, MeOD) δ 8.44 - 8.37 (m, 2H, ArH), 8.36 - 8.30 (m, 1H, ArH), 8.30 - 8.21 (m, 1H, ArH), 8.19 - 8.11 (m, 2H, ArH), 7.61 (t, J = 2.1 Hz, 1H, ArH), 7.47 - 7.37 (m, 1H, ArH), 7.32 (t, J = 8.1 Hz, 1H, ArH), 6.97 (ddd, J = 8.2, 2.5, 1.0 Hz, 1H, ArH), 4.93 (d, J = 7.7 Hz, 1H, H-1), 3.95 (dd, J = 3.3, 1.0 Hz, 1H, H-4), 3.91 - 3.72 (m, 4H, H-2 H-3 H-6), 3.63 (dd, J = 9.7, 3.4 Hz, 1H, H-5) ¹³C NMR (101 MHz, MeOD) δ 159.5 (CO), 151.1 (ArC), 142.1 (ArC), 140.6 (ArC), 131.8 (ArC), 130.6 (ArC), 130.0 (ArC), 124.6 (ArC), 115.9 (ArC), 114.3 (ArC), 110.7 (ArC), 102.9 (C1), 77.0 (C5), 74.9 (C3), 72.3 (C2), 70.2 (C4), 62.5 (C6)

p-Methoxyphenyl β-D-galactoside



Chemical Formula: C₁₃H₁₈O₇
Exact Mass: 286,11

3 Å Molsieve (150 mg) was dried for 30 min under heating and vacuum. After cool down, CH₂Cl₂ (5 mL, dry) was added. Under stirring, the penta-acetylated sugar (200 mg, 0.51 mmol, 1 eq) and the p-methoxy phenol (78.9 mg, 0.64 mmol, 1.24 eq) were added. The reaction mixture was cooled to 0°C and BF₃OEt₂ (363.8 mg, 325 μL, 2.6 mmol, 5 eq) were added drop wise over a few minutes. The reaction was stirred at r.t. o/n. The reaction was diluted with CH₂Cl₂ (70 mL) then poured onto ice and then extracted three times with a saturated NaHCO₃ (50 mL) solution, and once with NaCl (50 mL). The organic layer was dried over NaSO₄ and the crude product was purified by column using hexane to ethyl acetate 99:1 to 50:50. 65.6 % (152 mg, 0.33 mmol) of acetylated product was obtained.

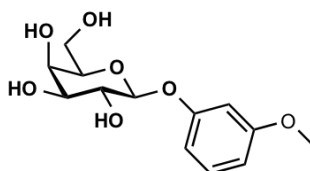
¹H NMR (500 MHz, CDCl₃) δ 6.98 - 6.87 (m, 2H, ArH), 6.84 - 6.71 (m, 2H, ArH), 5.48 - 5.35 (m, 2H, ArH), 5.06 (dd, J = 10.5, 3.4 Hz, 1H, H-3), 4.89 (d, J = 8.0 Hz, 1H, H-1), 4.23 - 4.09 (m, 2H, H-6), 3.99 (td, J = 6.7, 1.2 Hz, 1H, H-5), 3.73 (s, 3H, OCH₃), 2.14 (s, 3H, CH₃), 2.04 (s, 3H, CH₃), 2.01 (s, 3H, CH₃), 1.97 (s, 3H, CH₃). ¹³C NMR (126 MHz, CDCl₃) δ 170.3 (C=O), 170.2 (C=O), 170.1 (C=O), 169.4 (C=O), 155.7 (ArC), 151.0 (ArC), 118.6 (ArC), 114.5 (ArC), 100.8 (C-1), 77.2 (C-3), 70.9 (C-5), 68.8 (C-2), 66.9 (C-4), 61.3 (C-6), 55.6 (OCH₃), 20.7 (CH₃), 20.6 (CH₃), 20.6 (CH₃).

Experimental section

The acetylated sugar (153 mg, 0.33 mmol, 1 eq) was dissolved in dry MeOH (5 mL). After addition of NaOMe (5.3 M, 63 μ L, 0.03 mmol, 0.1 eq) the solution was stirred at r.t. over night. The reaction mixture was then neutralized with Amberlite H⁺ ion-exchanger and purified by column using a gradient of CH₂Cl₂ to MeOH 99:1 to 90:10. 57.2 % (54 mg, 0.19 mmol) product was obtained

¹H NMR (500 MHz, MeOD-d₄) δ 7.04 (dd, J = 8.9, 1.2 Hz, 2H, ArH), 6.86 - 6.77 (m, 2H, ArH), 4.71 (d, J = 7.7 Hz, 1H, H-1), 3.87 (d, J = 3.2 Hz, 1H, H-4), 3.80 - 3.69 (m, 6H, CH₃ & H-6 & H-2), 3.61 (dd, J = 6.8, 5.4 Hz, 1H, H-5), 3.54 (ddd, J = 9.9, 3.4, 1.1 Hz, 1H, H-3). ¹³C NMR (126 MHz, MeOD-d₄) δ 156.6 (ArC), 153.3 (ArC), 119.2 (ArC), 115.4 (ArC), 104.1 (C-1), 76.9 (C-5), 74.8 (C-3), 72.3 (C-2), 70.2 (C-4), 62.4 (C-6), 56.0 (CH₃)

m-Methoxyphenyl β -D-galactoside



Chemical Formula: C₁₃H₁₈O₇
Exact Mass: 286,11

150 mg pre-dried 3 Å Molsieve was dried for 30 min under heating and vacuum. After cool down, CH₂Cl₂ (5 mL, dry) was added. Under stirring, the sugar (200 mg, 0.51 mmol, 1 eq) and the m-methoxy phenol (78.9 mg, 0.64 mmol, 1.24 eq) were added. The reaction mixture was cooled to 0°C and BF₃OEt₂ (363.8 mg, 325 μ L, 2.6 mmol, 5 eq) were added drop wise over a few minutes. The reaction was stirred at r.t. o/n. The reaction was diluted with CH₂Cl₂ (70 mL) then poured onto ice and then extracted three times with a saturated NaHCO₃ (50 mL) solution, and once with NaCl (50 mL). The organic layer was dried over NaSO₄ and the crude product was purified by column using PE: EtOAc 99:1 to 50:50. 66.5 % (154 mg; 0.34 mmol) of pure product was obtained.

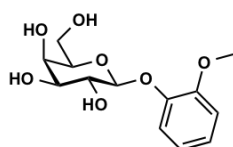
¹H NMR (500 MHz, CDCl₃) δ 7.16 (t, J = 8.2 Hz, 1H, ArH), 6.63 - 6.52 (m, 3H, ArH), 5.48 - 5.44 (m, 1H, H-4), 5.44 - 5.40 (m, 1H, H-2), 5.09 (dd, J = 10.5, 3.4 Hz, 1H, H-3), 5.03 (d, J = 8.0 Hz, 1H, H-1), 4.23 - 4.11 (m, 2H, H-6), 4.04 (ddd, J = 7.2, 6.1, 1.1 Hz, 1H, H-5), 3.75 (s, 3H, CH₃), 2.15 (s, 3H, CH₃), 2.03 (d, J = 4.2 Hz, 6H, CH₃), 1.98 (s, 3H, CH₃). ¹³C NMR (126 MHz, CDCl₃) δ 170.4 (C=O), 170.3 (C=O), 170.1 (C=O), 169.4 (C=O), 160.8 (ArC), 158.1 (ArC), 130.0 (ArC), 108.9 (ArC), 108.5 (ArC), 103.5 (ArC), 99.5 (C-1), 71.1 (C-3), 70.9 (C-5), 68.6 (C-4), 66.9 (C-2), 61.5 (C-6), 55.4 (CH₃), 20.8 (CH₃), 20.7 (CH₃), 20.6 (CH₃), 20.6 (CH₃).

Experimental section

The acetylated sugar (154 mg, 0.33 mmol, 1 eq) was dissolved in dry MeOH (5 mL). After addition of NaOMe (5.3 M, 50 μ L, 0.03 mmol, 0.1 eq) the solution was stirred at r.t. over night. The reaction mixture was then neutralized with Amberlite H⁺ ion-exchanger and purified by column using a gradient of CH₂Cl₂ to MeOH 99:1 to 90:10. 60.6 % (52 mg, 0.18 mmol) product was obtained

¹H NMR (500 MHz, MeOH-d₄) δ 7.19 - 7.12 (m, 1H, ArH), 6.73 - 6.66 (m, 2H, ArH), 6.61 - 6.55 (m, 1H, ArH), 4.84 (d, J = 7.7 Hz, 1H, H-1), 3.90 (dd, J = 3.5, 1.1 Hz, 1H, H-4), 3.81 - 3.72 (m, 6H, H-2, H-6, CH₃), 3.68 (ddd, J = 7.1, 5.1, 1.1 Hz, 1H, H-5), 3.58 (dd, J = 9.7, 3.4 Hz, 1H, H-3). ¹³C NMR (126 MHz, MeOH-d₄) δ 162.2 (ArC), 160.4 (ArC), 130.8 (ArCH), 109.9 (ArCH), 109.0 (ArCH), 103.9 (ArCH), 103.0 (C-1), 77.0 (C-3), 74.8 (C-5), 72.3 (C-2), 70.2 (C-4), 62.4 (C-6), 55.7 (CH₃)

o-Methoxyphenyl β -D-galactoside



Chemical Formula: C₁₃H₁₈O₇
Exact Mass: 286,11

3 Å Molsieve (500 mg) was dried for 30 min under heating and vacuum. After cool down, CH₂Cl₂ (6 mL, dry) was added. Under stirring, the penta-acetylated sugar (500 mg, 1.28 mmol, 1 eq) and the o-methoxy-phenol (200 mg, 1.59 mmol, 1.24 eq) were added. The reaction mixture was cooled to 0°C and BF₃OEt₂ (900 mg, 830 μ L, 6.53 mmol, 5 eq) were added drop-wise over a few minutes. The reaction was stirred at r.t. over night. The reaction was diluted with CH₂Cl₂ (100 mL) then poured onto ice and then extracted three times with a saturated NaHCO₃ (50 mL) solution, and once with NaCl (50 mL). The organic layer was dried over NaSO₄ and the crude product was purified by column using hexane and ethyl acetate 1:99 to 50:50. 11.2 % (65mg, 0.14 mmol) of a alpha beta (0.3: 1) mixture were obtained.

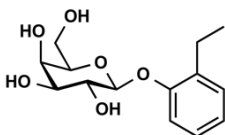
¹H NMR (500 MHz, CDCl₃) δ 7.14 (dd, J = 7.9, 1.6 Hz, 1H, ArH), 7.10 - 6.99 (m, 2H, ArH), 6.95 - 6.83 (m, 3H, ArH), 5.71 (d, J = 3.7 Hz, 0H, H1- α), 5.64 - 5.55 (m, 1H, H-2), 5.54 - 5.48 (m, 1H, H-6 α), 5.43 (dd, J = 3.5, 1.1 Hz, 1H, H-4), 5.35 - 5.32 (m, 0H, H-5 α), 5.24 (dd, J = 10.8, 3.7 Hz, 0H, H-2 α), 5.09 (dd, J = 10.5, 3.4 Hz, 1H, H-3), 4.91 (d, J = 7.9 Hz, 1H, H-1), 4.65 (t, J = 6.6 Hz, 0H, H-4 α), 4.23 (dd, J = 11.3, 6.7 Hz, 1H, H-6 α), 4.20 - 4.05 (m, 2H, H-6 β H-6 α), 3.97 (td, J = 6.8, 1.1 Hz, 1H, H-5), 3.82 (d, J = 3.4 Hz, 4H, OCH₃ α/β), 2.18 (s, 3H, CH₃), 2.16 (d, J = 1.0 Hz, 2H, CH₃), 2.14 (s, 1H, CH₃), 2.09 (s, 3H, CH₃), 2.04 (s, 1H, CH₃), 2.02 (d, J = 2.3 Hz, 1H, CH₃), 2.01 (d, J = 3.6 Hz, 3H, CH₃), 1.99 (s, 1H, CH₃). ¹³C NMR (126 MHz, CDCl₃) δ 170.7 (C=O), 170.5 (C=O), 170.4 (C=O), 170.3 (C=O), 170.1 (C=O), 169.7 (ArC), 150.8 (ArC), 146.5 (ArC), 124.8 (ArC), 121.0 (ArC), 121.0 (ArC), 120.9 (ArC), 120.3 (ArC), 112.9 (ArC), 101.6 (C-1 β), 96.9 (C-1 α), 71.1 (C-5 β), 70.9 (C-3 β), 68.9 (C-2 β), 68.3 (C-2 α), 68.2 (C-3 α), 67.7 (C-4 α), 67.3 (C-4 β), 67.1 (C-5 α), 61.9 (C-6 β), 61.4 (C-6 α), 56.2 (CH₃ β), 55.9 (CH₃ α), 21.0 (CH₃), 20.9 (CH₃), 20.9 (CH₃), 20.8 (CH₃), 20.8 (CH₃).

Experimental section

The acetylated sugar (65 mg, 0.43 mmol, 1 eq) was dissolved in dry MeOH (5 mL). After addition of NaOMe (5.3 M, 81 μ L, 0.04 mmol, 0.1 eq) the solution was stirred at r.t. over night. The reaction mixture was then neutralized with Amberlite H⁺ ion-exchanger and purified by column using a gradient of CH₂Cl₂ to MeOH 99:1 to 90:10. 12.1 % (15 mg, 0.05 mmol) product was obtained.

¹H NMR (500 MHz, MeOD-d₄) δ 7.19 (dt, J = 7.8, 1.0 Hz, 1H, ArH), 7.04 - 6.98 (m, 2H, ArH), 6.90 (ddd, J = 8.0, 5.5, 3.5 Hz, 1H, ArH), 4.85 (d, J = 7.8 Hz, 1H, H-1), 3.92 (dd, J = 3.5, 1.1 Hz, 1H, H-4), 3.87 (s, 3H, CH₃), 3.85 (d, J = 2.0 Hz, 1H, H-2), 3.78 (d, J = 1.8 Hz, 1H, H-6a), 3.76 (d, J = 0.7 Hz, 1H, H-6b), 3.66 (ddd, J = 6.6, 5.4, 1.1 Hz, 1H, H-3), 3.60 (dd, J = 9.7, 3.4 Hz, 1H, H-5). ¹³C NMR (126 MHz, MeOD-d₄) δ 180.6 (ArC), 150.9 (ArC), 148.1 (ArC), 124.1 (ArC), 122.3 (ArC), 118.3 (ArC), 113.8 (ArC), 103.5 (C-1), 76.9 (C-5), 74.7 (C-3), 72.3 (C-2), 70.2 (C-4), 62.4 (C-6), 56.7 (CH₃)

o-Ethylphenyl β -D-galactoside



Chemical Formula: C₁₄H₂₀O₆
Exact Mass: 284,13

3 Å Molsieve (200 mg) was dried for 30 min under heating and vacuum. After cool down, CH₂Cl₂ (5 mL, dry) was added. Under stirring, the penta-acetylated sugar (200 mg, 0.51 mmol, 1 eq) and the 2-ethyl phenol (37.7 μ L, 39.1 mg, 0.64 mmol, 1.24 eq) were added. The reaction mixture was cooled to 0°C and BF₃OEt₂ (330 μ L, 370 mg, 2.6 mmol, 5 eq) were added drop wise over a few minutes. The reaction was stirred at r.t. o/n. The reaction was diluted with EtOAc (150 mL) then poured onto ice and then extracted three times with a saturated NaHCO₃ (100 mL) solution, and three times with NaCl (100 mL). The organic layer was dried over NaSO₄ and the crude product was purified by column using hexane to ethyl acetate 99:1 to 50:50. 37.0 % (87 mg, 0.19 mmol) of pure product was obtained.

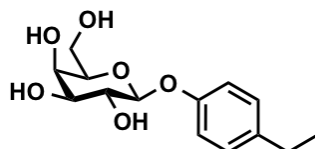
¹H NMR (500 MHz, CDCl₃) δ 7.20 - 7.11 (m, 2H, ArH), 7.07 - 6.94 (m, 1H, ArH), 5.55 (dd, J = 10.4, 8.0 Hz, 1H, H-2), 5.46 (dd, J = 3.5, 1.1 Hz, 1H, H-4), 5.11 (dd, J = 10.5, 3.5 Hz, 1H, H-3), 5.02 (d, J = 8.0 Hz, 1H, H-1), 4.24 (dd, J = 11.3, 7.1 Hz, 1H, H-6a), 4.16 (dd, J = 11.3, 6.1 Hz, 1H, H-6b), 4.07 (ddd, J = 7.2, 6.2, 1.1 Hz, 1H, H-5), 2.58 (qd, J = 7.4, 2.4 Hz, 2H, CH₂CH₃), 2.18 (s, 3H, CH₃), 2.06 (s, 6H, 2 x CH₃), 2.01 (s, 3H, CH₃), 1.15 (t, J = 7.5 Hz, 3H, CH₂CH₃). ¹³C NMR (126 MHz, CDCl₃) δ 170.4 (C=O), 170.4 (C=O), 170.2 (C=O), 169.3 (C=O), 154.8 (ArC), 133.9 (ArC), 129.5 (ArC), 126.9 (ArC), 123.3 (ArC), 115.0 (ArC), 99.7 (C-1), 71.0 (C-2), 71.0 (C-5), 68.6 (C-2), 67.0 (C-4), 61.5 (C-6), 23.0 (CH₂CH₃), 20.9 (CH₃), 20.8 (CH₃), 20.7 (CH₃), 20.7 (CH₃), 14.5 (CH₂CH₃). HRMS: (C₂₂H₂₈O₁₀+Na⁺) calc. 475.17 found 475.16

Experimental section

The acetylated sugar (87 mg, 0.19 mmol, 1 eq) was dissolved in dry MeOH (5 mL). After addition of NaOMe (5.3 M, 70 μ L, 0.3 mmol, 1 eq) the solution was stirred at r.t. over night. The reaction mixture was then neutralized with Amberlite H⁺ ion-exchanger and purified by column using a gradient of CH₂Cl₂ to MeOH 99:1 to 90:10. 52.1 % (29.6 mg, 0.10 mmol) pure product was obtained.

¹H NMR (500 MHz, MeOD-d₄) δ 7.17 - 7.08 (m, 3H, ArC), 6.92 (td, J = 7.2, 1.4 Hz, 1H, ArC), 4.85 (d, J = 7.8 Hz, 1H, H-1), 3.91 (dd, J = 3.5, 1.0 Hz, 1H, H-4), 3.83 (dd, J = 9.7, 7.8 Hz, 1H, H-2), 3.76 (dd, J = 6.1, 2.7 Hz, 2H, H-6), 3.66 (ddd, J = 6.7, 5.4, 1.1 Hz, 1H, H-5), 3.57 (dd, J = 9.7, 3.4 Hz, 1H, H-3), 2.80 - 2.63 (m, 2H, CH₂CH₃), 1.19 (t, J = 7.5 Hz, 3H, CH₂CH₃). ¹³C NMR (126 MHz, MeOD-d₄) δ 156.9 (ArC), 134.9 (ArC), 130.0 (ArC), 127.8 (ArC), 123.3 (ArC), 116.2 (ArC), 103.2 (C-1), 76.9 (C-5), 75.2 (C-3), 72.4 (C-2), 70.2 (C-4), 62.4 (C-6), 24.2 (CH₂CH₃), 15.1 (CH₂CH₃). HRMS: (C₁₄H₂₀O₆ + Na⁺) calc. 307.10 found 307.30

p-Ethylphenyl β -D-galactoside



Chemical Formula: C₁₄H₂₀O₆
Exact Mass: 284,13

3 Å Molsieve (100 mg) was dried for 30 min under heating and vacuum. After cool down, CH₂Cl₂ (5 mL, dry) was added. Under stirring, the penta-acetylated sugar (100 mg, 0.26 mmol, 1 eq) and the p-ethyl-phenol (39.1 mg, 0.32 mmol, 1.24 eq) were added. The reaction mixture was cooled to 0°C and BF₃OEt₂ (101.7 mg, 162 μ L, 1.3 mmol, 5 eq) were added drop wise over a few minutes. The reaction was stirred at r.t. over night. The reaction was diluted with CH₂Cl₂ (70 mL) then poured onto ice and then extracted three times with a saturated NaHCO₃ (50 mL) solution, and once with NaCl (50 mL). The organic layer was dried over NaSO₄ and the crude product was purified by column using toluene and ethyl acetate 1:99 to 30:70. 26.4 % of pure product was obtained.

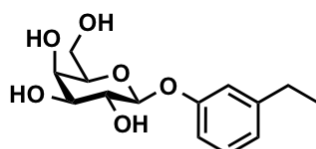
¹H NMR (500 MHz, CDCl₃): 7.05 ppm (2H, d, J = 8.5546 Hz, ArC), 6.85 ppm (2H, d, J = 8.6046 Hz, ArC) 5.41 (1H, dd, J = 6.1366, H-5) 5.38 (1H, d, J = 3.4018, H-3), 5.03 (1H, dd, J = 4.6358, H-2) 4.94 (1H, d, J = 8.0043, H-1), 4.16 (1H, dd, J = 6.0866, H-6a), 4.09 (1H, dd, J = 5.9032, H-6b) 3.98 (t, J = 6.6536 Hz, H-4) 2.53 (2H, q, J = 7.6041, CH₂), 1.14 (t, J = 7.6291, CH₃) ¹³C NMR (500 MHz, CDCl₃): 170.44 (C=O), 170.36 (C=O), 170.23 (C=O), 169.49 (C=O), 155.12 (ArC), 139.34 (ArC), 128.90 (ArC), 116.99 (ArC), 100.05 (C-1), 70.96 (C-4), 70.93 (C-2), 68.74 (C-5), 66.96 (C-3), 61.42 (C-6), 28.14 (CH₂), 20.82 (COCH₃), 20.75 (COCH₃), 20.67 (COCH₃), 15.87 (CH₃)

Experimental section

The acetylated sugar (153 mg, 0.33 mmol, 1 eq) was dissolved in dry MeOH (5 mL). After addition of NaOMe (5.3 M, 63 μ L, 0.03 mmol, 0.1 eq) the solution was stirred at r.t. over night. The reaction mixture was then neutralized with Amberlite H⁺ ion-exchanger and purified by column using a gradient of CH₂Cl₂ to MeOH 99:1 to 90:10. 57.2 % (54 mg, 0.19 mmol) product was obtained

¹H NMR (500 MHz, MeOD-d₄) δ 7.14 (2H, d, J = 8.7547 Hz, ArH), 7.05 (2H, d, J = 8.7047 Hz, ArH), 4.85 (1H, d, J = 7.7542 Hz, H-1), 3.94 (dd, J = 1.4174 Hz, H-4) 3.84- 3.76 (m, 3H, H2 & H-6) 3.71-3.65 (m, 1H, H-3), 3.61 (q, 1H, J = 4.3857 Hz, H-5) 2.61 (dd, J = 7.6041 Hz, 2H, CH₂) 1.23 (t, J = 7.6041 Hz, 3H, CH₃) ¹³C NMR (500 MHz, MeOD-d₄) δ 157.29 (ArC), 139.41 (ArC), 129.57 (ArC), 117.85 (ArC), 103.23 (C-1), 76.87 (C-3), 74.88 (C-5), 72.34 (C-2), 70.21 (C-4), 62.40 (C-6), 29.04 (CH₂), 16.40 (CH₃)

m-Ethylphenyl β -D-galactoside



Chemical Formula: C₁₄H₂₀O₆
Exact Mass: 284,13

3 Å Molsieve (100 mg) was dried for 30 min under heating and vacuum. After cool down, CH₂Cl₂ (5 mL, dry) was added. Under stirring, the penta-acetylated sugar (100 mg, 0.26 mmol, 1 eq) and the p-ethyl-phenol (39.1 mg, 0.32 mmol, 1.24 eq) were added. The reaction mixture was cooled to 0°C and BF₃OEt₂ (101.7 mg, 162 μ L, 1.3 mmol, 5 eq) were added drop-wise over a few minutes. The reaction was stirred at r.t. over night. The reaction was diluted with CH₂Cl₂ (70 mL) then poured onto ice and then extracted three times with a saturated NaHCO₃ (50 mL) solution, and once with NaCl (50 mL). The organic layer was dried over NaSO₄ and the crude product was purified by column using toluene and ethyl acetate 1:99 to 30:70. 26.4 % (32 mg, 0.07 mmol) of pure acetylated product was obtained.

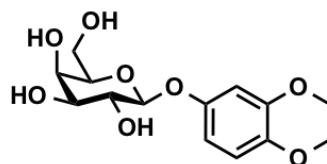
¹H NMR (500 MHz, CDCl₃) δ 7.15 (1H, t, J = 7.9, ArH), 6.86 (1H, d, J = 7.6, ArH), 6.79 (1H, app.s, ArH), 6.76 (1H, dd, J = 8.1, 2.4, ArH), 5.43 (1H, d, J = 10.4, 7.9 Hz, H-4), 5.40 (1H; d, J = 3.6 Hz, H-2), 5.1 (1H, dd, J = 4.6 Hz, H-3), 5.00 (1H, d, J = 8.0 Hz, H-1) 4.18-4.10 (2H, m, H-6), 4.01 (1H, t, J = 6.6 Hz, H-5), 2.60 (2H, q, J = 7.6, CH₂), 2.18 (s, 3H, CH₃), 2.06 (d, J = 5.5 Hz, 6H, CH₃), 2.01 (s, 3H, CH₃), 1.17 (t, J = 7.6 Hz, CH₃) ¹³C NMR (500 MHz, CDCl₃) δ 170.51 (C=O), 170.40 (C=O), 170.28 (C=O), 169.56 (C=O), 157.10 (ArC), 146.27 (ArC), 129.27 (ArCH), 122.97 (ArCH), 116.97 (ArCH), 113.92 (ArCH), 99.68 (C-1), 71.08 (C-5), 70.96 (C-2), 68.77 (C-4), 61.63 (C-6), 28.91 (CH₂), 20.88 (COCH₃), 20.80 (COCH₃), 20.77 (COCH₃), 20.72 (COCH₃), 15.55 (CH₂CH₃)

Experimental section

The acetylated sugar (32 mg, 0.07 mmol, 1 eq) was dissolved in dry MeOH (3 mL). After addition of NaOMe (5.3 M, 2 μ L, 0.01 mmol, 0.1 eq) the solution was stirred at r.t. over night. The reaction mixture was then neutralized with Amberlite H⁺ ion-exchanger and purified by column using a gradient of CH₂Cl₂ to MeOH 99:1 to 90:10. 65.4 % (13 mg, 0.05 mmol) product was obtained.

¹H NMR (500 MHz, MeOD-d₄) δ 7.24 - 7.17 (m, 1H, ArH), 7.00 (td, J = 1.9, 0.6 Hz, 1H, ArH), 6.95 (ddd, J = 8.2, 2.5, 1.0 Hz, 1H, ArH), 6.91 - 6.85 (m, 1H, ArH), 4.88 (d, J = 7.9 Hz, 1H, H-1), 3.94 (dd, J = 3.5, 1.1 Hz, 1H, H-4), 3.85 - 3.76 (m, 3H, H-2 H-6), 3.71 (ddd, J = 7.0, 5.2, 1.1 Hz, 1H, H-5), 3.61 (dd, J = 9.7, 3.4 Hz, 1H, H-3), 2.65 (q, J = 7.6 Hz, 2H, CH₂), 1.30 - 1.18 (m, 3H, CH₃). ¹³C NMR (126 MHz, MeOD-d₄) δ 159.3 (ArC), 147.1 (ArC), 130.2 (ArCH), 122.9 (ArCH), 117.4 (ArCH), 115.0 (ArCH), 103.0 (C-1), 77.0 (C-5), 74.9 (C-3), 72.4 (C-2), 70.2 (C-4), 62.4 (C-6), 29.8 (CH₂), 16.0(CH₃).

3,4-Dimethoxyphenyl β -D-galactoside



Chemical Formula: C₁₄H₂₀O₈
Exact Mass: 316,12

3 Å Molsieve (100 mg) was dried for 30 min under heating and vacuum. After cool down, CH₂Cl₂ (5 mL, dry) was added. Under stirring, the penta-acetylated sugar (100 mg, 0.26 mmol, 1 eq) and the 3,4-dimethoxy phenol (39.1 mg, 0.32 mmol, 1.24 eq) were added. The reaction mixture was cooled to 0°C and BF₃OEt₂ (101.7 mg, 162 μ L, 1.3 mmol, 5 eq) were added drop-wise over a few minutes. The reaction was stirred at r.t. over night. The reaction was diluted with CH₂Cl₂ (70 mL) then poured onto ice and then extracted three times with a saturated NaHCO₃ (50 mL) solution, and once with NaCl (50 mL). The organic layer was dried over NaSO₄ and the crude product was purified by column using hexane and ethyl acetate 1:99 to 50:50. 80.8 % (95 mg, 0.21 mmol) of product were obtained.

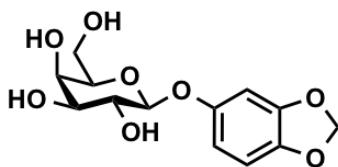
¹H NMR (500 MHz, CDCl₃) δ 6.75 (d, J = 8.8 Hz, 1H, ArH), 6.59 (d, J = 2.7 Hz, 1H, ArH), 6.53 (dd, J = 8.7, 2.7 Hz, 1H, ArH), 5.44 - 5.40 (m, 2H, H-2 H-4), 5.08 (dd, J = 10.5, 3.4 Hz, 1H, H-3), 4.95 (d, J = 8.0 Hz, 1H, H-1), 4.24 - 4.12 (m, 2H, H-6), 4.01 (td, J = 6.6, 1.2 Hz, 1H, H-5), 3.82 (t, J = 0.9 Hz, 7H, 2 x CH₃), 2.16 (d, J = 0.7 Hz, 3H, CH₃), 2.07 (d, J = 0.6 Hz, 3H, CH₃), 2.02 (d, J = 0.7 Hz, 3H, CH₃), 1.99 (d, J = 0.7 Hz, 3H, CH₃) ¹³C NMR (126 MHz, CDCl₃) δ 170.4 (C=O), 170.3 (C=O), 170.2 (C=O), 169.5 (C=O), 151.4 (ArC), 149.8 (ArC), 145.5 (ArC), 111.7 (ArC), 107.8 (ArC), 103.3 (ArC), 100.6 (C-1), 71.1 (C-5, C-3), 68.9 (C-4), 67.0 (C-2), 61.5 (C-6), 56.4 (CH₃), 56.1 (CH₃), 20.9 (CH₃), 20.7 (CH₃), 20.7 (CH₃), 20.6 (CH₃).

Experimental section

The acetylated sugar (95 mg, 0.20 mmol, 1 eq) was dissolved in dry MeOH (10 mL). After addition of NaOMe (5.3 M, 4 μ L, 0.02 mmol, 0.1 eq) the solution was stirred at r.t. over night. The reaction mixture was then neutralized with Amberlite H⁺ ion-exchanger and purified by column using a gradient of EtOAc to EtOH 99:1 to 70:30. 94.9 % (60 mg, 0.19 mmol) product was obtained.

¹H NMR (500 MHz, MeOD -d₄) δ 6.89 - 6.85 (m, 2H, ArH), 6.70 (dd, J = 8.7, 2.8 Hz, 1H, ArH), 4.77 (d, J = 7.8 Hz, 1H, H-1), 3.91 (dd, J = 3.5, 1.0 Hz, 1H, H-4), 3.84 (s, 3H, OCH₃), 3.80 (s, 4H, H-6a OCH₃), 3.81 - 3.73 (m, 2H, H-2 H-6b), 3.70 - 3.66 (m, 1H, H-5), 3.61 - 3.57 (m, 1H, H-3). ¹³C NMR (126 MHz, MeOD -d₄) δ 154.1 (ArC), 151.1 (ArC), 146.0 (ArC), 114.0 (ArCH), 109.4 (ArCH), 104.1 (C-1), 77.1 (C-5), 74.9 (C-3), 72.4 (C-2), 70.3 (C-4), 62.5 (C-6), 57.2 (OCH₃), 56.4 (OCH₃).

Benzo 1,3 dioxole β -D-galactoside



Chemical Formula: C₁₃H₁₆O₈
Exact Mass: 300,08

3 Å Molsieve (100 mg) was dried for 30 min under heating and vacuum. After cool down, CH₂Cl₂ (5 mL, dry) was added. Under stirring, the penta-acetylated sugar (100 mg, 0.26 mmol, 1 eq) and the Benzodix-5-ol (44.2 mg, 0.32 mmol, 1.24 eq) were added. The reaction mixture was cooled to 0°C and BF₃OEt₂ (101.7 mg, 162 μ L, 1.3 mmol, 5 eq) were added drop-wise over a few minutes. The reaction was stirred at r.t. over night. The reaction was diluted with CH₂Cl₂ (70 mL) then poured onto ice and then extracted three times with a saturated NaHCO₃ (50 mL) solution, and once with NaCl (50 mL). The organic layer was dried over NaSO₄ and the crude product was purified by column using hexane and ethyl acetate 1:99 to 50:50. 85.1 % (100 mg, 0.22 mmol) of product was obtained.

¹H NMR (500 MHz, CDCl₃) δ 6.67 (d, J = 8.4 Hz, 1H, ArH), 6.57 (d, J = 2.4 Hz, 1H, ArH), 6.45 (dd, J = 8.4, 2.4 Hz, 1H, ArH), 5.91 (s, 2H, CH₂), 5.46 - 5.36 (m, 2H, H-2 H-4), 5.07 (dd, J = 10.4, 3.4 Hz, 1H, H-3), 4.87 (d, J = 8.0 Hz, 1H, H-4), 4.21 (dd, J = 11.3, 7.0 Hz, 1H, H-6a), 4.16 - 4.06 (m, 1H, H-6b), 3.99 (ddd, J = 7.2, 6.3, 1.2 Hz, 1H, H-5), 2.16 (s, 3H, CH₃), 2.06 (s, 3H, CH₃), 2.04 (s, 3H, CH₃), 1.98 (s, 3H, CH₃). ¹³C NMR (126 MHz, CDCl₃) δ 170.4 (C=O), 170.3 (C=O), 170.2 (C=O), 169.4 (C=O), 152.3 (ArC), 148.2 (ArC), 143.7

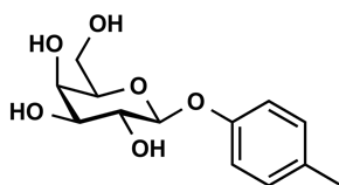
Experimental section

(ArC), 109.7 (ArC), 108.0 (ArC), 101.6 (ArC), 101.1 ($\underline{\text{CH}_2}$), 100.6 (C-1), 71.1 (C-5), 70.9 (C-3), 68.8 (C-2), 67.0 (C-4), 61.5 (C-6), 20.8 ($\underline{\text{CH}_3}$), 20.7 (CH_3), 20.7 ($\underline{\text{CH}_3}$), 20.6 ($\underline{\text{CH}_3}$).

The acetylated sugar (100 mg, 0.22 mmol, 1 eq) was dissolved in dry MeOH (10 mL). After addition of NaOMe (5.3 M, 10 μL , 0.05 mmol, 0.4 eq) the solution was stirred at r.t. over night. The reaction mixture was then neutralized with Amberlite H^+ ion-exchanger and purified by column using a gradient of CH_2Cl_2 to MeOH 99:1 to 90:10. 86.4 % (57 mg, 0.19 mmol) product was obtained.

^1H NMR (500 MHz, MeOD- d_4) δ 6.75 - 6.72 (m, 1H, ArH), 6.71 (s, 1H, ArH), 6.62 (dd, $J = 8.5, 2.4$ Hz, 1H, ArH), 5.92 (s, 2H, $\underline{\text{CH}_2}$), 4.72 (d, $J = 7.8$ Hz, 1H, H-1), 3.90 (dd, $J = 3.5, 1.0$ Hz, 1H, H-4), 3.84 - 3.73 (m, 3H, H-2 H-6), 3.65 (ddd, $J = 6.7, 5.3, 1.1$ Hz, 1H, H-5), 3.57 (dd, $J = 9.7, 3.4$ Hz, 1H, H-3) ^{13}C NMR (126 MHz, MeOD- d_4) δ 154.6 (ArC), 149.4 (ArC), 144.3 (ArC), 110.4 (ArCH), 108.8 (ArCH), 104.3 (ArCH), 102.5 (C-1), 101.2 ($\underline{\text{CH}_2}$), 76.9 (C-5), 74.8 (C-3), 72.3 (C-2), 70.2 (C-4), 62.4 (C-6)

p-Tolyl β -D-galactoside



Chemical Formula: $\text{C}_{13}\text{H}_{18}\text{O}_6$

Exact Mass: 270,11

3 \AA Molsieve (170 mg) was dried for 60 min under heating and vacuum. After cool down, CH_2Cl_2 (7 mL, dry) was added. Under stirring, the penta-acetylated sugar (150 mg, 0.38 mmol, 1 eq) and the p-cresol (51.7 mg, 50 μL , 0.48 mmol, 1.24 eq) were added. The reaction mixture was cooled to 0°C and BF_3OEt_2 (270 mg, 240 μL , 1.9 mmol, 5 eq) were added drop-wise over a few minutes. The reaction was stirred at r.t. over night. The reaction was diluted with CH_2Cl_2 (70 mL) then poured onto ice and then extracted three times with a saturated NaHCO_3 (3 times, 20 mL) solution, and once with NaCl (20 mL). The organic layer was dried over NaSO_4 and the crude product was purified by column using hexane and ethyl acetate 1:99 to 50:50. 64.2 % (107 mg, 0.24 mmol) of product were obtained.

^1H NMR (500 MHz, CDCl_3) δ 7.13 - 7.04 (m, 2H, ArH), 6.92 - 6.87 (m, 2H, ArH), 5.49 - 5.41 (m, 2H, H-2, H-4), 5.09 (dd, $J = 10.5, 3.5$ Hz, 1H, H-3), 4.98 (d, $J = 8.0$ Hz, 1H, H-1), 4.23 (dd, $J = 11.3, 6.9$ Hz, 1H, H-6a), 4.15 (dd, $J = 11.3, 6.4$ Hz, 1H, H-6b), 4.03 (td, $J = 6.7, 1.2$ Hz, 1H, H-5), 2.30 (s, 3H, Phenyl- $\underline{\text{CH}_3}$), 2.18 (s, 3H, $\underline{\text{CH}_3}$), 2.06 (d, $J = 4.2$ Hz, 6H, $\underline{\text{CH}_3}$), 2.01 (s, 3H, $\underline{\text{CH}_3}$). ^{13}C NMR (126 MHz, CDCl_3) δ 170.49 (C=O),

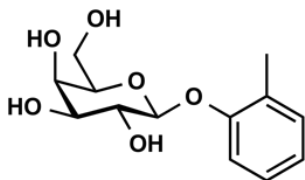
Experimental section

170.40 (C=O), 170.27 (C=O), 169.53 (C=O), 155.07 (ArC), 132.98 (ArC), 130.12 (ArC), 117.09 (ArC), 100.24 (C-1), 71.07 (C-3), 71.02 (C-5), 68.85 (C-4), 67.04 (C-2), 61.49 (C-6), 20.88 ($\underline{\text{C}}\text{H}_3$), 20.81 ($\underline{\text{C}}\text{H}_3$), 20.80 ($\underline{\text{C}}\text{H}_3$), 20.74 ($\underline{\text{C}}\text{H}_3$).

The acetylated sugar (70 mg, 0.16 mmol, 1 eq) was dissolved in dry MeOH (5 mL). After addition of NaOMe (5.3 M, 15 μL , 0.08 mmol, 0.5 eq) the solution was stirred at r.t. over night. The reaction mixture was then neutralized with Amberlite H^+ ion-exchanger and purified by column using a gradient of CH_2Cl_2 to MeOH 99:1 to 90:10. 83.3 % (36 mg, 0.13 mmol) product was obtained.

^1H NMR (500 MHz, MeOD- d_4) δ 7.08 – 7.02 (m, 2H, ArH), 6.99 – 6.94 (m, 2H, ArH), 4.78 (d, $J = 7.8$ Hz, 1H, H-1), 3.87 (dd, $J = 3.4, 1.0$ Hz, 1H, H-4), 3.78 – 3.70 (m, 3H, H-2; H-3, H-6b), 3.66 – 3.60 (m, 1H, H-6a), 3.54 (dd, $J = 9.7, 3.4$ Hz, 1H, H-5), 2.24 (s, 3H, $\underline{\text{C}}\text{H}_3$). ^{13}C NMR (126 MHz, MeOD- d_4) δ 157.14 (ArC), 132.72 (ArC), 130.72 (ArC), 117.74 (ArC), 103.24 (C-1), 76.86 (C-2), 74.86 (C-5), 72.32 (C-3), 70.19 (C-4), 62.38 (C-6), 20.60 ($\underline{\text{C}}\text{H}_3$).

m-Tolyl β -D-galactoside



Chemical Formula: $\text{C}_{13}\text{H}_{18}\text{O}_6$
Exact Mass: 270,11

3 Å Molsieve (150 mg) was dried for 60 min under heating and vacuum. After cool down, CH_2Cl_2 (7 mL, dry) was added. Under stirring, the penta-acetylated sugar (150 mg, 0.38 mmol, 1 eq) and the p-cresol (51.7 mg, 50 μL , 0.48 mmol, 1.24 eq) were added. The reaction mixture was cooled to 0°C and BF_3OEt_2 (270 mg, 240 μL , 1.9 mmol, 5 eq) were added dropwise over a few minutes. The reaction was stirred at r.t. over night. The reaction was diluted with CH_2Cl_2 (70 mL) then poured onto ice and then extracted three times with a saturated NaHCO_3 (3 times, 20 mL) solution, and once with NaCl (20 mL). The organic layer was dried over Na_2SO_4 and the crude product was purified by column using hexane and ethyl acetate 1:99 to 50:50. 51.7 % (92.9 mg, 0.21 mmol) of product were obtained.

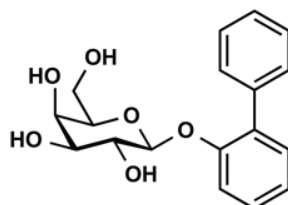
Experimental section

^1H NMR (500 MHz, CD_2Cl_2) δ 7.60 (t, $J = 7.8$ Hz, 1H, ArH), 7.32 (ddt, $J = 7.6, 1.7, 0.9$ Hz, 1H, ArH), 7.23 (ddt, $J = 8.2, 2.5, 0.8$ Hz, 1H, ArH), 5.88 (dd, $J = 3.6, 1.1$ Hz, 1H, H-4), 5.83 (dd, $J = 10.5, 8.0$ Hz, 1H, H-2), 5.54 (dd, $J = 10.5, 3.5$ Hz, 1H, H-3), 5.49 (d, $J = 7.9$ Hz, 1H, H-1), 4.66 – 4.56 (m, 2H, H-6), 4.55 – 4.48 (m, 1H, H-5), 2.75 (d, $J = 0.7$ Hz, 3H, Ar- CH_3), 2.60 (s, 3H, CH_3), 2.47 (d, $J = 2.8$ Hz, 6H, CH_3), 2.42 (s, 3H, CH_3). ^{13}C NMR (126 MHz, CD_2Cl_2) δ 165.72 (C=O), 165.50 (C=O), 164.84 (C=O), 152.53 (ArC), 135.38 (ArC), 124.78 (ArC), 119.50 (ArC), 113.11 (ArC), 109.25 (ArC), 95.11 (C-1), 66.70 (C-3), 66.37 (C-5), 64.12 (C-2), 62.61 (C-4), 57.16 (C-6), 16.70 (Ar CH_3), 16.05 (CH_3), 15.99 (CH_3), 15.97 (CH_3), 15.92 (CH_3).

The acetylated sugar (91 mg, 0.21 mmol, 1 eq) was dissolved in dry MeOH (5 mL). After addition of NaOMe (5.3 M, 2 μL , 0.01 mmol, 0.5 eq) the solution was stirred at r.t. over night. The reaction mixture was then neutralized with Amberlite H^+ ion-exchanger and purified by column using a gradient of CH_2Cl_2 to MeOH 99:1 to 90:10. 23.8 % (15 mg, 0.05 mmol) product was obtained.

^1H NMR (500 MHz, MeOD- d_4) δ 7.15 – 7.08 (m, 1H, ArH), 6.91 (ddd, $J = 2.3, 1.5, 0.7$ Hz, 1H, ArH), 6.87 (ddt, $J = 8.2, 2.5, 0.8$ Hz, 1H, ArH), 6.79 (ddt, $J = 7.5, 1.6, 0.8$ Hz, 1H, ArH), 4.81 (d, $J = 7.7$ Hz, 1H, H-1), 3.87 (dd, $J = 3.5, 1.0$ Hz, 1H, H-4), 3.80 – 3.70 (m, 3H, H-2, H-3, H-6a), 3.64 (ddd, $J = 6.9, 5.2, 1.1$ Hz, 1H, H-6b), 3.55 (dd, $J = 9.7, 3.4$ Hz, 1H, H-5), 2.28 (d, $J = 0.7$ Hz, 3H, CH_3). ^{13}C NMR (126 MHz, MeOD- d_4) δ 159.22 (ArC), 140.48 (ArC), 130.09 (ArC), 124.02 (ArC), 118.48 (ArC), 114.74 (ArC), 102.93 (C-1), 76.91 (C-3), 74.86 (C-5), 72.31 (C-2), 70.21 (C-4), 62.41 (C-6), 21.50 (CH_3).

1-Phenyl-phenol β -D-galactoside



Chemical Formula: $\text{C}_{18}\text{H}_{20}\text{O}_6$
Exact Mass: 332,13

3 Å Molsieve (150 mg) was dried for 30 min under heating and vacuum. After cool down, dry CH_2Cl_2 (5 mL) was added. Under stirring, the acetylated sugar (150 mg, 0.30 mmol, 1 eq) and the 1-phenyl phenol (81.7 mg, 0.48 mmol, 1.24 eq) were added. The reaction mixture was cooled to 0°C and BF_3OEt_2 (269.7 mg, 240 μL , 1.90 mmol, 5 eq) were added dropwise over a few minutes. The reaction was stirred at r.t. o/n. The reaction was diluted with CH_2Cl_2 (50 mL) then poured onto ice and then extracted three times with a saturated NaHCO_3 (30 mL) solution, and once with NaCl (30 mL). The organic layer was dried over NaSO_4 and the crude product was purified by column using $\text{CH}_2\text{Cl}_2/\text{EtOAc}$ 99:1 to 80:20. 38.7 % (58 mg, 0.116 mmol) of pure product were obtained.

^1H NMR (500 MHz, CDCl_3) δ 7.58 - 7.49 (m, 2H, ArH), 7.46 - 7.40 (m, 2H, ArH), 7.39 - 7.27 (m, 2H, ArH), 7.24 - 7.21 (m, 1H, ArH), 7.07 (d, $J = 8.7$ Hz, 1H, ArH), 6.98 (ddd, $J = 8.1, 2.5, 1.1$ Hz, 1H, ArH), 5.52 (dd, J

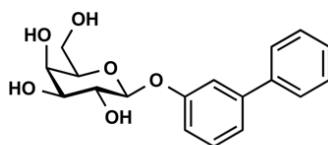
Experimental section

= 10.5, 7.9 Hz, 1H, H-3), 5.46 (dd, $J = 3.4, 1.1$ Hz, 1H, H-4), 5.12 (d, $J = 7.8$ Hz, 1H, H-1), 4.26 - 4.06 (m, 3H, H-5 & H-6), 2.18 (s, 2H, $\underline{\text{CH}}_3$), 2.07 (s, 2H, $\underline{\text{CH}}_3$), 2.03 (s, 2H, $\underline{\text{CH}}_3$), 2.01 (s, 2H, $\underline{\text{CH}}_3$), 1.95 (s, 2H, $\underline{\text{CH}}_3$). ^{13}C NMR (126 MHz, CDCl_3) δ 171.2 (C=O), 170.5 (C=O), 170.3 (C=O), 170.2 (C=O), 169.5 (C=O), 157.4 (ArC), 143.1 (ArC), 140.7 (ArC), 130.0 (ArC), 128.9 (ArC), 128.4 (ArC), 127.7 (ArC), 127.2 (ArC), 127.0 (ArC), 122.2 (ArC), 117.3 (ArC), 115.9 (ArC), 99.7 (C-1), 71.0 (C-5), 68.8 (C-2), 67.1 (C-3), 61.8 (C-4), 60.5 (C-6), 21.1 ($\underline{\text{CH}}_3$), 20.9 ($\underline{\text{CH}}_3$), 20.8 ($\underline{\text{CH}}_3$), 20.7 ($\underline{\text{CH}}_3$).

The acetylated sugar (39 mg, 0.078 mmol, 1 eq) was dissolved in dry MeOH (2 mL). After addition of NaOMe (5.3 M, 10 μL , 0.053 mmol, 0.7 eq) the solution was stirred at r.t. o/n. The reaction mixture was then neutralized with Amberlite H⁺ ion-exchanger and purified by column using a gradient of CH_2Cl_2 to MeOH 99:1 to 90:10. 50.1 % (13 mg, 0.039 mmol) product was obtained.

^1H NMR (500 MHz, MeOD- d_4) δ 7.62 – 7.57 (m, 2H, ArH), 7.43 – 7.28 (m, 5H, ArH), 7.27 – 7.24 (m, 1H, ArH), 7.08 (ddd, $J = 8.2, 2.5, 1.0$ Hz, 1H, ArH), 4.91 (d, $J = 7.8$ Hz, 1H, H-1), 3.88 (dd, $J = 3.5, 1.0$ Hz, 1H, H-4), 3.83 – 3.71 (m, 3H, H-2, H-6), 3.69 (ddd, $J = 7.1, 4.9, 1.1$ Hz, 1H, H-3), 3.58 (dd, $J = 9.7, 3.4$ Hz, 1H, H-5). ^{13}C NMR (126 MHz, MeOD- d_4) δ 159.67 (ArC), 143.90 (ArC), 142.12 (ArC), 130.77 (ArC), 129.82 (ArC), 128.47 (ArC), 128.01 (ArC), 121.97 (ArC), 116.71 (ArC), 116.45 (ArC), 103.02 (C-1), 77.10 (C-3), 74.87 (C-5), 72.32 (C-2), 70.27 (C-4), 62.49 (C-6).

2-Phenyl-phenol β -D-galactoside



Chemical Formula: $\text{C}_{18}\text{H}_{20}\text{O}_6$
Exact Mass: 332,13

3 Å Molsieve (250 mg) was dried for 30 min under heating and vacuum. After cool down, CH_2Cl_2 (5 mL, dry) was added. Under stirring, the penta-acetylated sugar (250 mg, 0.64 mmol, 1 eq) and the 3-phenyl phenol (134 mg, 0.79 mmol, 1.24 eq) were added. The reaction mixture was cooled to 0°C and BF_3OEt_2 (455 mg, 406 μL , 3.20 mmol, 5 eq) were added drop wise over a few minutes. The reaction was stirred at r.t. o/n. The reaction was diluted with EtOAc (70 mL) then poured onto ice and then extracted three times with a saturated NaHCO_3 (50 mL) solution, and once with NaCl (50 mL). The organic layer was dried over NaSO_4 and the crude product was purified by column using hexane to ethyl acetate 99:1 to 50:50. 51.5 % (65 mg, 0.33 mmol) of product was obtained.

^1H NMR (500 MHz, CDCl_3) δ 7.57 – 7.54 (m, 2H, ArH), 7.46 – 7.41 (m, 2H, ArH), 7.39 – 7.33 (m, 2H, ArH), 7.30 (ddd, $J = 7.7, 1.7, 1.1$ Hz, 1H, ArH), 7.24 – 7.22 (m, 1H, ArH), 6.99 (ddd, $J = 8.1, 2.5, 1.0$ Hz, 1H, ArH), 5.53 (dd, $J = 10.5, 8.0$ Hz, 1H, H-2), 5.47 (dd, $J = 3.4, 1.1$ Hz, 1H, H-4), 5.15 – 5.11 (m, 2H, H-1 & H-3), 4.26 – 4.14 (m, 2H, H-6), 4.13 – 4.06 (m, 1H, H-5), 2.19 (s, 3H, $\underline{\text{CH}}_3$), 2.08 (s, 3H, $\underline{\text{CH}}_3$), 2.02 (s, 3H, $\underline{\text{CH}}_3$), 1.96

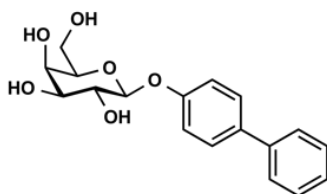
Experimental section

(s, 3H, $\underline{\text{C}}\text{H}_3$). ^{13}C NMR (126 MHz, CDCl_3) δ 170.6 (C=O), 170.4 (C=O), 170.3 (C=O), 169.6 (C=O), 157.4 (ArC), 143.2 (ArC), 140.7 (ArC), 130.0 (ArC), 129.0 (ArC), 127.8 (ArC), 127.3 (ArC), 122.3 (ArC), 115.9 (ArC), 115.7 (ArC), 110.1 (ArC), 99.8 (C-1), 71.3 (C-5), 71.0 (C-3), 68.8 (C-2), 67.1 (C-4), 61.8 (-C6), 20.9 ($\underline{\text{C}}\text{H}_3$), 20.8 ($\underline{\text{C}}\text{H}_3$), 20.8 ($\underline{\text{C}}\text{H}_3$), 20.7 ($\underline{\text{C}}\text{H}_3$).

The acetylated sugar (160 mg, 0.32 mmol, 1 eq) was dissolved in dry MeOH (10 mL). After addition of NaOMe (5.3 M, 60 μL , 0.03 mmol, 0.1 eq) the solution was stirred at r.t. o/n. The reaction mixture was then neutralized with Amberlite H⁺ ion-exchanger and purified by column using a gradient of CH_2Cl_2 to MeOH 99:1 to 90:10. 53.6 % (57 mg, 0.17 mmol) product was obtained.

^1H NMR (500 MHz, MeOD- d_4) δ 7.63 – 7.59 (m, 2H, ArH), 7.44 – 7.37 (m, 3H, ArH), 7.35 – 7.29 (m, 2H, ArH), 7.26 (ddd, $J = 7.7, 1.7, 1.0$ Hz, 1H, ArH), 7.09 (ddd, $J = 8.1, 2.5, 1.0$ Hz, 1H, ArH), 4.93 (d, $J = 7.8$ Hz, 1H, H-1), 3.91 (dd, $J = 3.5, 1.0$ Hz, 1H, H-4), 3.86 – 3.73 (m, 3H, H-2, H3, H-6a), 3.71 (ddd, $J = 7.2, 4.9, 1.1$ Hz, 1H, H-6b), 3.60 (dd, $J = 9.7, 3.4$ Hz, 1H, H-5). ^{13}C NMR (126 MHz, MeOD- d_4) δ 159.64 (ArC), 143.88 (ArC), 142.10 (ArC), 130.77 (ArC), 129.81 (ArC), 128.45 (ArC), 128.00 (ArC), 121.97 (ArC), 116.71 (ArC), 116.46 (ArC), 103.02 (C-1), 77.07 (C-3), 74.86 (C-5), 72.32 (C-2), 70.26 (C-4), 62.48 (C-6). HRMS: ($\text{C}_{18}\text{H}_{20}\text{O}_6 + \text{Na}^+$)⁺ calc. 355.12 found 355.13

3-Phenyl-phenol β -D-galactoside



Chemical Formula: $\text{C}_{18}\text{H}_{20}\text{O}_6$
Exact Mass: 332,13

3 Å Molsieve (150 mg) was dried for 30 min under heating and vacuum. After cool down, dry CH_2Cl_2 (5 mL) was added. Under stirring, the acetylated sugar (150 mg, 0.30 mmol, 1 eq) and the 4-phenyl phenol (81.7 mg, 0.48 mmol, 1.24 eq) were added. The reaction mixture was cooled to 0°C and BF_3OEt_2 (269.7 mg, 240 μL , 1.90 mmol, 5 eq) were added drop wise over a few minutes. The reaction was stirred at r.t. o/n. The reaction was diluted with CH_2Cl_2 (50 mL) then poured onto ice and then extracted three times with a saturated NaHCO_3 (30 mL) solution, and once with NaCl (30 mL). The organic layer was dried over NaSO_4 and the crude product was purified by column using CH_2Cl_2 / EtOAc 99:1 to 80:20. 50.7 % (76 mg, 0.152 mmol) of pure product were obtained.

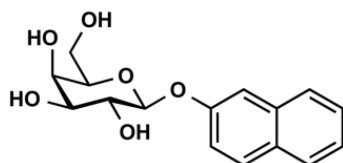
Experimental section

^1H NMR (500 MHz, CDCl_3) δ 7.56 - 7.49 (m, 3H, ArH), 7.46 - 7.38 (m, 2H, ArH), 7.33 (d, $J = 7.4$ Hz, 1H, ArH), 7.11 - 7.03 (m, 2H, ArH), 5.52 (dd, $J = 10.5, 7.9$ Hz, 1H, H-2), 5.47 (dd, $J = 3.5, 1.1$ Hz, 1H, H-4), 5.13 (dd, $J = 10.4, 3.4$ Hz, 1H, H-5), 5.09 (d, $J = 7.9$ Hz, 1H, H-1), 4.25 (dd, $J = 11.3, 7.0$ Hz, 1H, H-6b), 4.18 (dd, $J = 11.3, 6.3$ Hz, 1H, H-6a), 4.15 - 4.04 (m, 1H, H-3), 2.19 (s, 3H, CH_3), 2.08 (s, 3H, CH_3), 2.06 (s, 3H, CH_3), 2.02 (s, 3H, CH_3). ^{13}C NMR (126 MHz, CDCl_3) δ 170.4 (C=O) 170.3 (C=O) 170.2 (C=O) 169.5 (C=O) 156.5 (ArC) 140.5 (ArC) 136.6 (ArC) 128.9 (ArC) 128.4 (ArC) 127.2 (ArC) 127.0 (ArC) 117.3 (ArC) 99.8, (C-1) 71.2 (C-5) 71.0 (C-3) 68.8 (C-2) 67.0 (C-4) 61.5 (C-6) 20.8 (CH_3) 20.8 (CH_3) 20.7 (CH_3) HRMS: ($\text{C}_{26}\text{H}_{28}\text{O}_{10}+\text{Na}$) $^+$ calc. 523.16 found. 523.15

The acetylated sugar (76 mg, 0.152 mmol, 1 eq) was dissolved in dry MeOH (3 mL). After addition of NaOMe (5.3 M, 30 μL , 0.016 mmol, 0.1 eq) the solution was stirred at r.t. o/n. The reaction mixture was then neutralized with Amberlite H $^+$ ion-exchanger and purified by column using a gradient of CH_2Cl_2 to MeOH 99:1 to 90:10. 61.4 % (31 mg, 0.093 mmol) product was obtained.

^1H NMR (500 MHz, DMSO- d_6) δ 7.60 (ddd, $J = 12.3, 7.6, 1.9$ Hz, 4H, ArH), 7.43 (t, $J = 7.7$ Hz, 2H, ArH), 7.35 - 7.28 (m, 1H, ArH), 7.14 - 7.07 (m, 2H, ArH), 5.20 (d, $J = 4.9$ Hz, 1H, OH), 4.89 (d, $J = 5.5$ Hz, 1H, OH), 4.86 (d, $J = 7.7$ Hz, 1H, H-1), 4.69 (t, $J = 5.3$ Hz, 1H, OH), 4.53 (d, $J = 4.5$ Hz, 1H, OH), 4.07 (s, 1H, OH), 3.71 (t, $J = 3.7$ Hz, 1H, H-4), 3.64 - 3.47 (m, 5H, H-2, H-3, H-5, H-6). ^{13}C NMR (126 MHz, DMSO- d_6) δ 157.2 (ArC), 139.8 (ArC), 133.7 (ArC), 128.9 (ArC), 127.7 (ArC), 126.9 (ArC), 126.3 (ArC), 116.7 (ArC), 101.1 (C-1), 75.6 (C-2), 73.3 (C-3), 70.3 (C-5), 68.2 (C-4), 60.4 (C-6). HRMS: ($\text{C}_{18}\text{H}_{20}\text{O}_6+\text{H}$) $^+$ calc. 332.10 found. 332.13

2-naphthyl β -D-galactoside



Chemical Formula: $\text{C}_{16}\text{H}_{18}\text{O}_6$
Exact Mass: 306,11

3 Å Molsieve (150 mg) was dried for 30 min under heating and vacuum. After cool down, CH_2Cl_2 (5 mL, dry) was added. Under stirring, the acetylated sugar (50 mg, 0.38 mmol, 1 eq) and the 2-naphthol (69.2 mg, 0.48 mmol, 1.24 eq) were added. The reaction mixture was cooled to 0 $^\circ\text{C}$ and BF_3OEt_2 (269.8 mg, 240 μL , 1.90 mmol, 5 eq) were added drop wise over a few minutes. The reaction was stirred at r.t. o/n. The reaction was diluted with CH_2Cl_2 (50 mL) then poured onto ice and then extracted three times with a saturated NaHCO_3 (30 mL) solution, and once with NaCl (30 mL). The organic layer was dried over NaSO_4 and the crude product was purified by column using hexane and ethyl acetate 99:1 to 60:40. 57.7 % (104 mg; 0.22 mmol) of acetylated product were obtained.

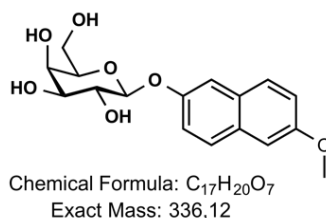
Experimental section

^1H NMR (500 MHz, CDCl_3) δ 7.84 - 7.70 (m, 3H, ArH), 7.50 - 7.43 (m, 1H, ArH), 7.43 - 7.37 (m, 1H, ArH), 7.35 (d, $J = 2.4$ Hz, 1H, ArH), 7.19 (dd, $J = 8.9, 2.5$ Hz, 1H, ArH), 5.56 (dd, $J = 10.5, 7.9$ Hz, 1H, H-2), 5.49 (dd, $J = 3.5, 1.1$ Hz, 1H, H-4), 5.19 (d, $J = 8.0$ Hz, 1H, H-1), 5.15 (dd, $J = 10.4, 3.4$ Hz, 1H, H-3), 4.26 (dd, $J = 11.2, 7.1$ Hz, 1H, H-6a), 4.23 - 4.09 (m, 2H, H-5, H-6b), 2.20 (s, 3H, CH_3), 2.08 (d, $J = 3.4$ Hz, 6H, CH_3), 2.03 (s, 3H, CH_3) ^{13}C NMR (126 MHz, CDCl_3) δ 170.5 (C=O), 170.4 (C=O), 170.3 (C=O), 169.6 (C=O), 154.8 (ArC), 134.2 (ArC), 130.3 (ArC), 129.8 (ArC), 127.9 (ArC), 127.2 (ArC), 126.8 (ArC), 124.8 (ArC), 118.9 (ArC), 111.5 (ArC), 99.8 (C-1), 71.3 (C-5), 71.0 (C-3), 68.8 (C-2), 67.1 (C-4), 61.7 (C-6), 20.9 (CH_3), 20.8 (CH_3), 20.8 (CH_3), 20.7 (CH_3). HRMS: ($\text{C}_{24}\text{H}_{26}\text{O}_{10}+\text{Na}$) $^+$ calc. 497.14 found. 497.17

The acetylated sugar (80 mg, 0.17 mmol, 1 eq) was dissolved in dry MeOH (4 mL). After addition of NaOMe (5.3 M, 4 μL , 0.02 mmol, 0.1 eq) the solution was stirred at r.t. o/n. The reaction mixture was then neutralized with Amberlite H $^+$ ion-exchanger and purified by column using a gradient of CH_2Cl_2 to MeOH 99:1 to 90:10. 65.3 % (34 mg, 0.111 mmol) product was obtained.

^1H NMR (500 MHz, MeOD- d_4) δ 7.82 (td, $J = 8.4, 1.0$ Hz, 3H, ArH), 7.58 - 7.53 (m, 1H, ArH), 7.47 (ddd, $J = 8.1, 6.8, 1.3$ Hz, 1H, ArH), 7.42 - 7.31 (m, 2H, ArH), 5.07 (d, $J = 7.7$ Hz, 1H, H-1), 3.98 (d, $J = 3.2$ Hz, 1H, H-4), 3.86 - 3.81 (m, 2H, H-2 H-6a), 3.71 (dd, $J = 5.5, 4.1$ Hz, 2H, H-3, H-6b), 3.63 - 3.59 (m, 1H, H-5). ^{13}C NMR (126 MHz, MeOD- d_4) δ 156.93 (ArC), 135.86 (ArC), 131.21 (ArC), 130.26 (ArC), 128.58 (ArC), 128.17 (ArC), 127.31 (ArC), 125.18 (ArC), 120.05 (ArC), 112.04 (ArC), 103.03 (C-1), 77.08 (C-3), 74.90 (C-5), 73.64 (C-2), 70.27 (C-4), 62.49 (C-6).

6-Methoxy-2-naphthyl β -D-galactoside



3 Å Molsieve (150 mg) was dried for 30 min under heating and vacuum. After cool down, CH_2Cl_2 (5 mL, dry) was added. Under stirring, the acetylated sugar (150 mg, 0.30 mmol, 1 eq) and the 6-Methoxy-2-naphthol (83.6 mg, 0.48 mmol, 1.24 eq) were added. The reaction mixture was cooled to 0°C and BF_3OEt_2 (269.7 mg, 240 μL , 1.90 mmol, 5 eq) were added drop wise over a few minutes. The reaction was stirred at r.t. o/n. The reaction was diluted with CH_2Cl_2 (50 mL) then poured onto ice and then extracted three times with a saturated NaHCO_3 (30 mL) solution, and once with NaCl (30 mL). The organic layer was dried over NaSO_4 and the crude product was first purified by column using hexane and ethyl acetate 99:1 to 50:50. 62.5 % (114 mg, 0.3 mmol) of pure product were obtained.

^1H NMR (500 MHz, CDCl_3) δ 7.64 (dd, $J = 16.7, 8.9$ Hz, 2H, ArH), 7.30 (d, $J = 2.5$ Hz, 1H, ArH), 7.20 - 7.06 (m, 3H, ArH), 5.53 (dd, $J = 10.4, 7.9$ Hz, 1H, H-2), 5.47 (dd, $J = 3.5, 1.1$ Hz, 1H, H-4), 5.15 - 5.12 (m, 1H,

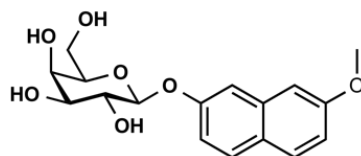
Experimental section

H-3), 5.11 (d, $J = 8.0$ Hz, 1H, H-1), 4.25 (dd, $J = 11.3, 7.1$ Hz, 1H, H-6a), 4.18 (dd, $J = 11.3, 6.1$ Hz, 1H, H-6b), 4.14 – 4.04 (m, 1H, H-5), 3.89 (s, 3H, OCH₃), 2.19 (s, 3H, CH₃), 2.08 (s, 3H, CH₃), 2.06 (s, 3H, CH₃), 2.02 (s, 3H, CH₃) ¹³C NMR (126 MHz, CDCl₃) δ 170.46 (C=O), 170.37 (C=O), 170.24 (C=O), 169.54 (C=O), 156.97 (ArC), 153.34 (ArC), 131.24 (ArC), 129.39 (ArC), 128.58 (ArC), 128.39 (ArC), 119.56 (ArC), 119.34 (ArC), 112.04 (ArC), 105.95 (ArC), 100.12 (C-1), 77.16 (C-3), 71.16 (C-5), 70.98 (C-2), 68.83 (C-4), 61.61 (C-6), 55.40 (OCH₃), 20.88 (CH₃), 20.80 (CH₃), 20.78 (CH₃), 20.71 (CH₃).

The acetylated sugar (114 mg, 0.3 mmol, 1 eq) was dissolved in dry MeOH (5 mL). After addition of NaOMe (5.3 M, 70 μ L, 0.03 mmol, 0.1 eq) the solution was stirred at r.t. o/n. The reaction mixture was then neutralized with Amberlite H⁺ ion-exchanger and first purified by column using a gradient of CH₂Cl₂ to MeOH 99:1 to 90:10 and second by HPLC using a gradient of water and acetonitrile. After lyophilization, 27.8 % (28 mg, 0.083 mmol) product was obtained.

¹H NMR (500 MHz, MeOD-d₄) δ 7.65 (t, $J = 9.1$ Hz, 2H, ArH), 7.40 (d, $J = 2.4$ Hz, 1H, ArH), 7.17 – 7.09 (m, 2H, ArH), 6.97 (dd, $J = 8.9, 2.5$ Hz, 1H, ArH), 4.98 (d, $J = 7.7$ Hz, 1H, H-1), 3.91 (d, $J = 3.3$ Hz, 1H, H-4), 3.87 (s, 3H, OCH₃), 3.86 – 3.73 (m, 4H, H-2, H-3, H-6), 3.60 (dd, $J = 9.7, 3.4$ Hz, 1H, H-5). ¹³C NMR (126 MHz, MeOD-d₄) δ 159.61 (ArC), 157.58 (ArC), 137.30 (ArC), 130.00 (ArC), 129.94 (ArC), 126.61 (ArC), 117.83 (ArC), 117.39 (ArC), 111.39 (ArC), 106.36 (ArC), 102.99 (C-1), 77.10 (C-2), 74.90 (C-5), 72.33 (C-3), 70.29 (C-5), 62.51 (C-6), 55.67 (OCH₃). HRMS: (C₁₇H₂₀O₇+Na)⁺ calc. 359.11 found. 359.10

7-Methoxy-2-naphtyl β -D-galactoside



Chemical Formula: C₁₇H₂₀O₇
Exact Mass: 336,12

3 Å Molsieve (150 mg) was dried for 30 min under heating and vacuum. After cool down, CH₂Cl₂ (5 mL, dry) was added. Under stirring, the acetylated sugar (150 mg, 0.30 mmol, 1 eq) and 7-Methoxy-2-naphtol (83.6 mg, 0.48 mmol, 1.24 eq) were added. The reaction mixture was cooled to 0°C and BF₃OEt₂ (269.7 mg, 240 μ L, 1.90 mmol, 5 eq) were added drop wise over a few minutes. The reaction was stirred at r.t. o/n. The reaction was diluted with CH₂Cl₂ (50 mL) then poured onto ice and then extracted three times with a saturated NaHCO₃ (30 mL) solution, and once with NaCl (30 mL). The organic layer was dried over NaSO₄ and the crude product was purified first by column using hexane and ethyl acetate in a 99:1 to 50:50 ratio and second with a gradient of CH₂Cl₂ and ethyl acetate 99: 1 to 90:10. 45.5 % (111 mg, 0.22 mmol) of pure product was obtained.

¹H NMR (500 MHz, CDCl₃) δ 7.88 (dd, $J = 8.7, 4.4$ Hz, 2H, ArH), 7.49 – 7.44 (m, 1H, ArH), 7.29 – 7.21 (m, 3H, ArH), 5.74 (dd, $J = 10.5, 7.9$ Hz, 1H, H-4), 5.68 (dd, $J = 3.5, 1.1$ Hz, 1H, H-2), 5.36 (d, $J = 7.9$ Hz, 1H, H-1), 5.35 – 5.31 (m, 1H, H-3), 4.48 (dd, $J = 11.2, 6.9$ Hz, 1H, H-6a), 4.38 (dd, $J = 11.2, 6.3$ Hz, 1H, H-6b), 4.35

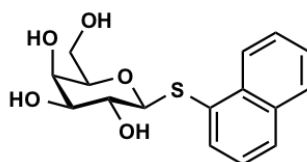
Experimental section

– 4.29 (m, 1H, H-5), 4.10 (s, 3H, OCH₃), 2.39 (s, 3H, CH₃), 2.28 (d, J = 2.6 Hz, 6H, CH₃), 2.23 (s, 3H, CH₃).
¹³C NMR (126 MHz, CDCl₃) δ 170.46 (C=O), 170.38 (CO), 170.27 (C=O), 169.55 (C=O), 158.41 (ArC), 155.46 (ArC), 135.57 (ArC), 129.50 (ArC), 129.32 (ArC), 125.62 (ArC), 117.54 (ArC), 116.22 (ArC), 110.78 (ArC), 105.34 (ArC), 99.79 (C-1), 71.12 (C-5), 70.95 (C-3), 68.77 (C-4), 66.98 (C-2), 61.54 (C-6), 55.37 (OCH₃), 20.89 (CH₃), 20.80 (CH₃), 20.73 (CH₃).

The acetylated sugar (111 mg, 0.22 mmol, 1 eq) was dissolved in dry MeOH (5 mL). After addition of NaOMe (5.3 M, 70 μL, 0.02 mmol, 0.1 eq) the solution was stirred at r.t. o/n. The reaction mixture was then neutralized with Amberlite H⁺ ion-exchanger and first purified by column using a gradient of CH₂Cl₂ to MeOH 99:1 to 90:10. 47.3 % (38 mg, 0.104 mmol) product was obtained.

¹H NMR (500 MHz, MeOD-d₄) δ 7.66 (dd, J = 15.8, 9.0 Hz, 2H, ArH), 7.44 (d, J = 2.4 Hz, 1H, ArH), 7.26 (dd, J = 8.9, 2.5 Hz, 1H, ArH), 7.17 (d, J = 2.5 Hz, 1H, ArH), 7.08 (dd, J = 8.9, 2.5 Hz, 1H, ArH), 4.95 (d, J = 7.7 Hz, 1H, H-1), 3.91 (dd, J = 3.4, 1.0 Hz, 1H, H-4), 3.87 (s, 3H, OCH₃), 3.85 – 3.71 (m, 4H, H-2, H-3, H-6), 3.60 (dd, J = 9.7, 3.4 Hz, 1H, H-5). ¹³C NMR (126 MHz, MeOD-d₄) δ 158.04 (ArC), 155.49 (ArC), 132.25 (ArC), 131.06 (ArC), 129.54 (ArC), 129.03 (ArC), 120.39 (ArC), 120.02 (ArC), 112.52 (ArC), 106.76 (ArC), 103.38 (C-1), 77.06 (C-2), 74.91 (C-5), 72.37 (C-3), 70.28 (C-4), 62.50 (C-6), 55.69 (OCH₃). HRMS: (C₁₇H₂₀O₇+Na)⁺ calc. 359.11 found. 359.10

1-Naphtol β-D-thiogalactoside



Chemical Formula: C₁₆H₁₈O₅S
Exact Mass: 322,09

3 Å Molsieve (500 mg) was dried for 45 min under heating and vacuum. After cool down, CH₂Cl₂ (6 mL, dry) was added. Under stirring, the penta-acetylated sugar (500 mg, 1.28 mmol, 1 eq) and the 2-thio naphthol (250 mg, 1.59 mmol, 1.24 eq) were added. The reaction mixture was cooled to 0°C and BF₃OEt₂ (900 mg, 830 μL, 1.3 mmol, 5.1 eq) were added drop-wise over a few minutes. The reaction was stirred at r.t. over night. The reaction was diluted with CH₂Cl₂ (70 mL) then poured onto ice and then extracted three times with a saturated NaHCO₃ (50 mL) solution, and once with NaCl (50 mL). The organic layer was dried over NaSO₄ and the crude product was purified by column using toluene and ethyl acetate 1:99 to 30:70. 58.9 % (370 mg, 0.75 mmol) acetylated product were obtained.

¹H NMR (500 MHz, CDCl₃) δ 8.02 (d, J = 1.8 Hz, 1H, ArH), 7.99 – 7.95 (m, 1H, ArH), 7.86 – 7.76 (m, 4H, ArH), 7.76 – 7.71 (m, 1H, ArH), 7.62 (dd, J = 8.7, 2.0 Hz, 1H, ArH), 7.58 (dd, J = 8.5, 1.9 Hz, 1H, ArH), 7.53 – 7.41 (m, 4H, ArH), 5.42 (dd, J = 3.3, 1.1 Hz, 1H, H-4), 5.28 (t, J = 9.9 Hz, 1H, H-2), 5.07 (dd, J = 9.9, 3.3

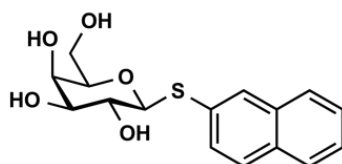
Experimental section

Hz, 1H, H-3), 4.81 (d, $J = 10.0$ Hz, 1H; H-1), 4.21 (dd, $J = 11.4, 7.0$ Hz, 1H; H-6b), 4.13 (dd, $J = 11.4, 6.1$ Hz, 1H, H-6a), 3.96 (ddd, $J = 7.1, 6.1, 1.1$ Hz, 1H, H-5), 2.12 (s, 3H, $\underline{\text{CH}}_3$), 2.07 (s, 3H, $\underline{\text{CH}}_3$), 2.01 (s, 3H, $\underline{\text{CH}}_3$), 1.97 (s, 3H, $\underline{\text{CH}}_3$). ^{13}C NMR (126 MHz, CDCl_3) δ 170.53 (C=O), 170.34 (C=O), 169.59 (C=O), 169.49 (C=O), 133.61 (ArC), 132.92 (ArC), 132.15 (ArC), 129.94 (ArC), 129.72 (ArC), 129.12 (ArC), 128.58 (ArC), 127.86 (ArC), 127.78 (ArC), 126.80 (ArC), 86.81 (C-1), 74.68 (C-5), 72.17 (C-3), 67.49 (C-4), 67.41 (C-2), 61.86 (C-6), 21.03 ($\underline{\text{CH}}_3$), 20.81 ($\underline{\text{CH}}_3$), 20.73 ($\underline{\text{CH}}_3$).

The acetylated sugar (102 mg, 0.21 mmol, 1 eq) was dissolved in dry MeOH (10 mL). After addition of NaOMe (5.3 M, 20 μL , 0.10 mmol, 0.5 eq) the solution was stirred at r.t. over night. The reaction mixture was then neutralized with Amberlite H^+ ion-exchanger and purified by column using a gradient of PE to EtOAc 99:1 to 70:30. 75.5 % (66.8 mg, 0.16 mmol) product was obtained.

^1H NMR (500 MHz, MeOD- d_4) δ 8.61 – 8.51 (m, 1H, ArH), 7.92 (dd, $J = 7.3, 1.1$ Hz, 1H, ArH), 7.89 – 7.85 (m, 1H, ArH), 7.81 (dt, $J = 8.5, 1.1$ Hz, 1H, ArH), 7.60 – 7.47 (m, 2H, ArH), 7.43 (dd, $J = 8.2, 7.2$ Hz, 1H, ArH), 4.63 (d, $J = 9.8$ Hz, 1H, H-1), 3.91 (dd, $J = 3.4, 1.1$ Hz, 1H, H-4), 3.79 – 3.67 (m, 3H, H-2, H-6), 3.55 – 3.47 (m, 2H, H-3, H-5). ^{13}C NMR (126 MHz, MeOD- d_4) δ 135.39 (ArC), 134.76 (ArC), 132.99 (ArC), 131.94 (ArC), 129.44 (ArC), 129.22 (ArC), 127.36 (ArC), 127.17 (ArC), 126.71 (ArC), 126.61 (ArC), 90.60 (C-1), 80.46 (C-5), 76.32 (C-3), 71.50 (C-2), 70.31 (C-4), 62.45 (C-6).

2-Naphthol β -D-thiogalactoside



Chemical Formula: $\text{C}_{16}\text{H}_{18}\text{O}_5\text{S}$
Exact Mass: 322,09

3 Å Molsieve (150 mg) was dried for 30 min under heating and vacuum. After cool down, CH_2Cl_2 (5 mL, dry) was added. Under stirring, the acetylated sugar (200 mg, 0.531 mmol, 1 eq) and the 1-thio naphthol (76.9 mg, 65.5 μL , 0.658 mmol, 1.24 eq) were added. The reaction mixture was cooled to 0°C and BF_3OEt_2 (363.8 mg, 375 μL , 12.5 mmol, 5 eq) were added drop wise over a few minutes. The reaction was stirred at r.t. o/n. The reaction was diluted with CH_2Cl_2 (50 mL) then poured onto ice and then extracted three times with a saturated NaHCO_3 (30 mL) solution, and once with NaCl (30 mL). The organic layer was dried over NaSO_4 and the crude product was purified by column. 66.4 % (156.7 mg, 0.32 mmol) of pure product was obtained.

^1H NMR (500 MHz, CDCl_3) δ 8.53 - 8.39 (m, 1H, ArH), 7.91 - 7.79 (m, 3H, ArH), 7.63 - 7.50 (m, 1H, ArH), 7.42 (dd, $J = 8.2, 7.2$ Hz, 1H, ArH), 5.35 (s, 1H, H-2), 5.02 (dd, $J = 10.0, 3.4$ Hz, 1H, H-4), 4.70 (d, $J = 10.1$

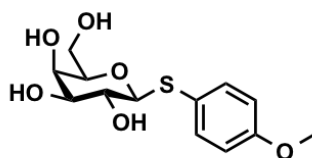
Experimental section

Hz, 1H, H-1), 4.19 - 4.01 (m, 2H, H-6), 3.86 - 3.77 (m, 1H, H-5), 2.15 (t, $J = 3.6$ Hz, 7H, CH_3), 2.03 (d, $J = 1.6$ Hz, 1H, CH_3), 1.97 (d, $J = 5.5$ Hz, 6H, CH_3). ^{13}C NMR (126 MHz, CDCl_3) δ 170.4 (C=O) 170.3 (C=O) 170.1 (C=O) 169.6 (C=O) 134.2 (ArC) 133.1 (ArC) 130.0 (ArC) 129.8 (ArC) 128.7 (ArC) 126.9 (ArC) 126.5 (ArC) 125.6 (ArC) 87.6 (C-1) 74.5 (C-5) 72.1 (C-4) 67.8 (C-2) 67.4 (C-3) 61.7 (C-6) 21.0 (CH_3) 20.8 (CH_3) 20.7 (CH_3) 20.7(CH_3)

The acetylated sugar (101.7 mg, 0.316 mmol, 1 eq) was dissolved in dry MeOH (10 mL). NaOMe (20 μL , 106 μmol , 0.3 eq) and stirred for 2 h at r.t. and afterwards neutralized using Amberlite H+. The solvent was removed in vacuo and the crude product was purified by flash chromatography to yield 75.5 % (50.6 mg, 0.157 mmol) of pure product.

^1H NMR (500 MHz, MeOD- d_4) δ 8.61 - 8.50 (m, 1H, ArH), 7.92 (dd, $J = 7.3, 1.2$ Hz, 1H, ArH), 7.88 - 7.83 (m, 1H, ArH), 7.81 (d, $J = 8.3$ Hz, 1H, ArH), 7.60 - 7.48 (m, 2H, ArH), 7.43 (dd, $J = 8.2, 7.2$ Hz, 1H, ArH), 4.63 (d, $J = 9.8$ Hz, 1H, H-1), 3.91 (dd, $J = 3.4, 1.0$ Hz, 1H, H-4), 3.77 - 3.69 (m, 3H, H3, H-6), 3.54 - 3.48 (m, 2H, H2, H-5). ^{13}C NMR (126 MHz, MeOD- d_4) δ 135.4 (ArC) 134.8 (ArC) 133.0 (ArC) 131.9(ArC) 129.4(ArC) 129.2 (ArC) 127.4 (ArC) 127.2 (ArC) 126.7 (ArC) 126.6 (ArC) 90.6 (C-1) 80.5 (C-5) 76.3 (C-3) 71.5 (C-2) 70.3 (C-4) 62.4 (C-6)

p-Methoxyphenyl β -D-thiogalactoside



Chemical Formula: $\text{C}_{13}\text{H}_{18}\text{O}_6\text{S}$
Exact Mass: 302,08

3 Å Molsieve (500 mg) was dried for 30 min under heating and vacuum. After cool down, CH_2Cl_2 (6 mL, dry) was added. Under stirring, the penta-acetylated sugar (500 mg, 1.28 mmol, 1 eq) and the 4-methoxy phenol (200 μL , 1.59 mmol, 1.24 eq) were added. The reaction mixture was cooled to 0°C and BF_3OEt_2 (830 μL , 1.3 mmol, 5.1 eq) were added drop-wise over a few minutes. The reaction was stirred at r.t. over night. The reaction was diluted with CH_2Cl_2 (70 mL) then poured onto ice and then extracted three times with a saturated NaHCO_3 (50 mL) solution, and once with NaCl (50 mL). The organic layer was dried over NaSO_4 and the crude product was purified by column using toluene and ethyl acetate 1:99 to 30:70. 58.9 % (370 mg, 0.75 mmol) acetylated product were obtained.

^1H NMR (500 MHz, CDCl_3 - d) δ 7.50 - 7.44 (m, 2H, ArH), 7.42 - 7.36 (m, 1H, ArH), 6.89 - 6.79 (m, 4H, ArH), 5.38 (dd, $J = 3.3, 1.1$ Hz, 1H, H-4), 5.17 (t, $J = 9.9$ Hz, 1H, H-2), 5.02 (dd, $J = 9.9, 3.3$ Hz, 1H, H-3), 4.56 (d, $J = 9.9$ Hz, 1H, H-1), 4.17 (dd, $J = 11.3, 6.8$ Hz, 1H, H-6a), 4.09 (dd, $J = 11.3, 6.5$ Hz, 1H, H-6b), 3.88

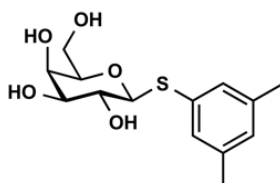
Experimental section

(td, $J = 6.6, 1.2$ Hz, 1H, H-5), 3.80 (d, $J = 5.6$ Hz, 3H, OCH₃), 2.11 (s, 3H, CH₃), 2.09 (s, 3H, CH₃), 2.03 (s, 3H, CH₃), 1.96 (s, 3H, CH₃). ¹³C NMR (126 MHz, CDCl₃) δ 170.50 (C=O), 170.31 (C=O), 170.21 (C=O), 169.55 (C=O), 160.39 (ArC), 160.04 (ArC), 136.04 (ArC), 132.79 (ArC), 128.57 (ArC), 122.17 (ArC), 114.75 (ArC), 114.48 (ArC), 87.11 (C-1), 74.44 (C-5), 72.21 (C-3), 67.46 (C-2), 67.36 (C-4), 61.66 (C-6), 55.50 (OCH₃), 21.03 (CH₃), 20.81 (CH₃), 20.75 (CH₃), 20.73 (CH₃).

The acetylated sugar (220 mg, 0.46 mmol, 1 eq) was dissolved in dry MeOH (12 mL). After addition of NaOMe (5.3 M, 4 μ L, 0.01 mmol, 0.2 eq) the solution was stirred at r.t. over night. The reaction mixture was then neutralized with Amberlite H⁺ ion-exchanger and purified by column using a gradient of EtOAc to EtOH 99:1 to 50:50. 83.5 % (116 mg, 0.38 mmol) product was obtained.

¹H NMR (500 MHz, MeOD-d₄) δ 7.24 – 7.19 (m, 2H, ArH), 7.12 (ddd, $J = 7.7, 1.7, 1.0$ Hz, 1H, ArH), 6.82 (ddd, $J = 8.3, 2.6, 1.0$ Hz, 1H, ArH), 4.65 (d, $J = 9.7$ Hz, 1H, H-1), 3.95 (dd, $J = 3.3, 1.1$ Hz, 1H, H-4), 3.82 (s, 4H, CH₃, H-2), 3.76 (dd, $J = 11.5, 5.2$ Hz, 1H, H-3), 3.68 (t, $J = 9.5$ Hz, 1H, H-6a), 3.63 (ddd, $J = 6.9, 5.1, 1.1$ Hz, 1H, H-6b), 3.56 (dd, $J = 9.2, 3.3$ Hz, 1H, H-5). ¹³C NMR (126 MHz, MeOD-d₄) δ 161.19 (ArC), 137.19 (ArC), 130.54 (ArC), 123.80 (ArC), 116.57 (ArC), 114.14 (ArC), 89.97 (C-1), 80.54 (C-3), 76.19 (C-5), 70.80 (C-2), 70.35 (C-4), 62.63 (C-6), 55.78 (OCH₃).

3,5-Dimethylphenyl β -D-thiogalactoside



Chemical Formula: C₁₄H₂₀O₅S
Exact Mass: 300,10

3 Å Molsieve (150 mg) was dried for 30 min under heating and vacuum. After cool down, CH₂Cl₂ (5 mL, dry) was added. Under stirring, the acetylated sugar (150 mg, 0.38 mmol, 1 eq) and the 3,5 diethyl-benzene-1-thiol (66.4 mg, 65.5 μ L, 0.48 mmol, 1.24 eq) were added. The reaction mixture was cooled to 0°C and BF₃OEt₂ (269.7mg, 240 μ L, 11.9 mmol, 5 eq) were added drop wise over a few minutes. The reaction was stirred at r.t. o/n. The reaction was diluted with CH₂Cl₂ (50 mL) then poured onto ice and then extracted three times with a saturated NaHCO₃ (30 mL) solution, and once with NaCl (30 mL). The organic layer was dried over NaSO₄ and the crude product was purified by column. 79.8 % (142.9 mg, 0.30 mmol) of pure product was obtained.

¹H NMR (500 MHz, CDCl₃) δ 7.41 (s, 1H, ArH), 7.26 (s, 2H, ArH), 5.57 (dd, $J = 3.4, 1.1$ Hz, 1H, H-4), 5.39 (t, $J = 10.0$ Hz, 1H, H-2), 5.20 (dd, $J = 10.0, 3.4$ Hz, 1H, H-3), 4.87 (d, $J = 10.0$ Hz, 1H, H-1), 4.39 - 4.20 (m, 2H, H-6), 4.09 (ddd, $J = 7.1, 6.1, 1.2$ Hz, 1H, H-5), 2.45 (t, $J = 0.7$ Hz, 6H, CH₃), 2.29 (s, 3H, CH₃), 2.24 (s,

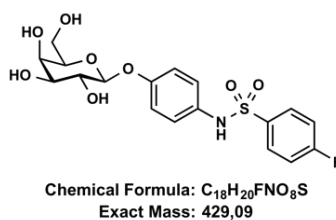
Experimental section

3H, $\underline{\text{CH}_3}$), 2.19 (s, 3H, $\underline{\text{CH}_3}$), 2.13 (s, 3H, $\underline{\text{CH}_3}$). ^{13}C NMR (126 MHz, CDCl_3) δ 170.5 (C=O), 170.4 (C=O), 170.2 (C=O), 169.6 (C=O), 138.7 (ArC), 132.4 (ArC), 130.0 (ArC), 129.9 (ArC), 87.3 (C-1), 74.5 (C-5), 72.1 (C-3), 67.4 (C-2), 61.9 (C-6), 21.4 ($\underline{\text{CH}_3}$), 21.0 ($\underline{\text{CH}_3}$), 20.8 ($\underline{\text{CH}_3}$), 20.8 ($\underline{\text{CH}_3}$), 20.7 ($\underline{\text{CH}_3}$).

The acetylated sugar (137.2 mg, 0.293 mmol, 1 eq) was dissolved in MeOH (10 mL, dry). NaOMe (20 μL , 146 μmol , 0.5 eq) and stirred o/n at r.t. and afterwards neutralized using Amberlite H+. The solvent was removed *in vacuo* and the crude product was purified by flash chromatography with EtOAc to EtOH 99:1 to 50:50 to yield 96.7 % (50.6 mg, 0.157 mmol) of pure product.

^1H NMR (500 MHz, MeOD- d_4) δ 7.20 - 7.13 (m, 2H, ArH), 6.85 (s, 1H, ArH), 4.55 (d, $J = 9.7$ Hz, 1H, H-1), 3.89 (dd, $J = 3.4, 1.1$ Hz, 1H, H-4), 3.79 - 3.67 (m, 3H, H-6 & H-2), 3.63 - 3.47 (m, 2H, H-3 & H-5), 2.25 (s, 6H, CH_3). ^{13}C NMR (126 MHz, MeOD- d_4) δ 139.6 (ArC), 135.5 (ArC), 129.6 (ArC), 129.5 (ArC), 90.3 (C-1), 80.6 (C-5), 76.3 (C-3), 71.0 (C-2), 70.4 (C-4), 62.6 (C-6), 21.3 ($\underline{\text{CH}_3}$).

p-phenyl-4-fluorophenyl-sulfonamide β -D-thiogalactoside

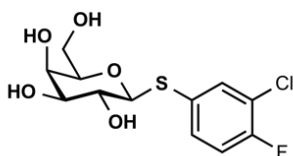


p-Amino phenyl β -D-galactoside (204 mg, 0.75 mmol, 1 eq) were dissolved in DMF (5 mL, dry). NEt_3 (89.6 mg, 0.89 mmol, 1.2 eq) and 4-Fluoro benzene sulfonyl chloride (90.9 mg, 0.47 mmol, 0.6 eq) were added and the reaction was stirred at r.t. o/n. The solvent was removed *in vacuo* and the remaining solid was dissolved in EtOAc. The mixture was extracted with extracted three times with a saturated NaHCO_3 (30 mL) solution, and once with NaCl (30 mL). The crude product was purified using CH_2Cl_2 / MeOH 99:1 to 90:10 to yield 10.6 % (34 mg, 0.08 mmol) of pure product.

^1H NMR (500 MHz, MeOD- d_4) δ 7.72 (dd, $J = 8.9, 5.1$ Hz, 1H), 7.18 (t, $J = 8.7$ Hz, 2H, ArH), 6.97 (s, 4H, ArH), 4.76 (d, $J = 7.7$ Hz, 1H, H-1), 3.87 (dd, $J = 3.5, 1.0$ Hz, 1H, H-4), 3.79 - 3.69 (m, 3H, H-2, H-6), 3.64 (ddd, $J = 7.0, 5.0, 1.1$ Hz, 1H, H-3), 3.54 (dd, $J = 9.7, 3.4$ Hz, 1H, H-5) ^{13}C NMR (126 MHz, MeOD- d_4) δ 167.4 (ArC), 165.4 (ArC), 157.0 (ArC), 137.1 (ArC), 132.7 (ArC), 131.2 (ArC), 131.1 (ArC), 125.2 (ArC), 118.3 (ArC), 117.1 (ArC), 116.9 (ArC), 103.0 (C-1), 76.9 (C-3), 74.8 (C-3), 72.2 (C-2), 70.2 (C-4), 62.4 (C-6). HRMS: $(\text{C}_{18}\text{H}_{20}\text{FNO}_8\text{S}+\text{Na})^+$ calc. 452.08 found. 452.05

3-Chloro-4-Fluoro-phenyl β -D-thiogalactoside

Experimental section



Chemical Formula: C₁₂H₁₄ClFO₅S
Exact Mass: 324,02

3 Å Molsieve (150 mg) was dried for 30 min under heating and vacuum. After cool down, CH₂Cl₂ (5 mL, dry) was added. Under stirring, the acetylated sugar (150 mg, 0.30 mmol, 1 eq) and the 3-chloro-4-fluoro-thio phenol (77.9 mg, 0.49 mmol, 1.24 eq) were added. The reaction mixture was cooled to 0°C and BF₃OEt₂ (269.7 mg, 240 μL, 1.90 mmol, 5 eq) were added drop wise over a few minutes. The reaction was stirred at r.t. o/n. The reaction was diluted with CH₂Cl₂ (50 mL) then poured onto ice and then extracted three times with a saturated NaHCO₃ (30 mL) solution, and once with NaCl (30 mL). The organic layer was dried over NaSO₄ and the crude product was purified by column using CH₂Cl₂/ EtOAc 99:1 to 65:35. 56.2% (83.6 mg, 0.169 mmol) of pure product were obtained.

¹H NMR (500 MHz, CDCl₃) δ 7.64 (dd, J = 6.9, 2.2 Hz, 1H, ArH), 7.37 (ddd, J = 8.6, 4.5, 2.3 Hz, 1H, ArH), 7.08 (t, J = 8.7 Hz, 1H, ArH), 5.40 (dd, J = 3.3, 1.1 Hz, 1H, H-4), 5.14 (t, J = 9.9 Hz, 1H, H-2), 5.03 (dd, J = 10.0, 3.3 Hz, 1H, H-2), 4.63 (d, J = 9.8 Hz, 1H, H-1), 4.17 (dd, J = 11.4, 7.1 Hz, 1H, H-6a), 4.14 – 4.05 (m, 1H, H-6b), 3.93 (ddd, J = 7.0, 5.8, 1.1 Hz, 1H, H-5), 2.09 (d, J = 7.8 Hz, 6H, CH₃), 2.05 (s, 3H, CH₃), 1.95 (s, 3H, CH₃). ¹³C NMR (126 MHz, CDCl₃) δ 170.50 (C=O), 170.18 (C=O), 170.08 (C=O), 169.42 (C=O), 159.45 (ArC), 157.45 (ArC), 135.45 (ArC), 133.59 (ArC), 128.22 (ArC), 121.44 (ArC), 116.98 (ArC), 86.00 (C-1), 74.71 (C-3), 71.96 (C-4), 67.28 (C-2), 67.01 (C-5), 61.86 (C-6), 20.91 (CH₃), 20.80 (CH₃), 20.69 (CH₃), 20.66 (CH₃). HRMS: (C₂₀H₂₂ClFO₉S+Na)⁺ calc. 515.05 found. 515.03

The acetylated sugar (83 mg, 0.256 mmol, 1 eq) was dissolved in MeOH (3 mL, dry). NaOMe (96 μL, 26 μmol, 0.1 eq) and stirred o/n at r.t. and afterwards neutralized using pre-washed Amberlite H⁺. The solvent was removed *in vacuo* and the crude product was purified by flash chromatography with CH₂Cl₂ to MeOH 99:1 to 90:10 to yield 22.9 % (19 mg, 0.06 mmol) of pure product.

¹H NMR (500 MHz, MeOD-d₄) δ 7.74 - 7.68 (m, 1H, ArH), 7.51 (ddd, J = 8.6, 4.5, 2.3 Hz, 1H, ArH), 7.20 - 7.11 (m, 1H, ArH), 4.50 (d, J = 9.6 Hz, 1H, H-1), 3.86 (dd, J = 3.3, 1.1 Hz, 1H, H-4), 3.80 - 3.65 (m, 2H, H-6), 3.59 - 3.52 (m, 2H, H-2 & H-5), 3.47 (dd, J = 9.2, 3.3 Hz, 1H, H-3) ¹³C NMR (126 MHz, MeOD-d₄) δ 159.8 (ArC), 157.9 (ArC), 134.9 (ArC), 133.5 (ArC), 132.4 (ArC), 122.0 (ArC), 117.9 (ArC), 111.4 (ArC), 90.0 (C-1), 80.7 (C-5), 76.3 (C-3), 70.8 (C-2), 70.4 (C-4), 62.7 (C-6)

6. References

- [1] '<http://www.who.int/mediacentre/news/releases/2017/bacteria-antibiotics-needed/en/>', **2017-11-03**, **15:32**
- [2] N. Mesaros, P. Nordmann, P. Plésiat, M. Roussel-Delvallez, J. Van Eldere, Y. Glupczynski, Y. Van Laethem, F. Jacobs, P. Lebecque, A. Malfroot, et al., *Clin. Microbiol. Infect.* **2007**, *13*, 560–78.
- [3] D. Monroe, *PLoS Biol* **2007**, *5*, 1–4.
- [4] T. R. Garrett, M. Bhakoo, Z. Zhang, *Prog. Nat. Sci.* **2008**, *18*, 1049–1056.
- [5] P. Klemm, M. A. Schembri, *Int. J. Med. Microbiol.* **2000**, *290*, 27–35.
- [6] J. W. Costerton, *Int. J. Antimicrob. Agents* **1999**, *11*, 217–221.
- [7] H.-C. Flemming, J. Wingender, U. Szewzyk, P. Steinberg, S. A. Rice, S. Kjelleberg, *Nat Rev Micro* **2016**, *14*, 563–575.
- [8] R. M. Donlan, *Emerg. Infect. Dis.* **2002**, *8*, 881–890.
- [9] T. Rasamiravaka, Q. Labtani, P. Duez, M. El Jaziri, *Biomed Res. Int.* **2015**, *2015*, 1–17.
- [10] S. Wagner, R. Sommer, S. Hinsberger, C. Lu, R. W. Hartmann, M. Empting, A. Titz, *J. Med. Chem.* **2016**, *59*, 13, 5929–5969 .
- [11] L. Passador, J. M. Cook, M. J. Gambello, L. Rust, B. H. Iglewski, *Science.* **1993**, *260*, 1127 LP-1130.
- [12] U. A. Ochsner, J. Reiser, *Proc. Natl. Acad. Sci. U. S. A.* **1995**, *92*, 6424–6428.
- [13] U. A. Ochsner, A. K. Koch, A. Fiechter, J. Reiser, *J. Bacteriol.* **1994**, *176*, 2044–2054.
- [14] E. C. Pesci, J. B. J. Milbank, J. P. Pearson, S. McKnight, A. S. Kende, E. P. Greenberg, B. H. Iglewski, *Proc. Natl. Acad. Sci.* **1999**, *96*, 11229–11234.
- [15] E. Déziel, F. Lépine, S. Milot, J. He, M. N. Mindrinos, R. G. Tompkins, L. G. Rahme, *Proc. Natl. Acad. Sci. U. S. A.* **2004**, *101*, 1339–1344.
- [16] G. Xiao, E. Déziel, J. He, F. Lépine, B. Lesic, M.-H. Castonguay, S. Milot, A. P. Tampakaki, S. E. Stachel, L. G. Rahme, *Mol. Microbiol.* **2006**, *62*, 1689–1699.
- [17] H. Cao, G. Krishnan, B. Goumnerov, J. Tsongalis, R. Tompkins, L. G. Rahme, *Proc. Natl. Acad. Sci.* **2001**, *98*, 14613–14618.
- [18] L. D. Christensen, M. van Gennip, M. T. Rybtke, H. Wu, W.-C. Chiang, M. Alhede, N. Høiby, T. E. Nielsen, M. Givskov, T. Tolker-Nielsen, *Infect. Immun.* **2013**, *81*, 2705–2713.
- [19] A. Yamazaki, J. Li, Q. Zeng, D. Khokhani, W. C. Hutchins, A. C. Yost, E. Biddle, E. J. Toone, X. Chen, C.-H. Yang, *Antimicrob. Agents Chemother.* **2012**, *56*, 36–43.
- [20] P. Gilbert, T. Maira-Litran, A. J. McBain, A. H. Rickard, F. W. Whyte, in (Ed.: B.T.-A. in M. Physiology), Academic Press, **2002**, pp. 203–256.
- [21] K. Sauer, M. C. Cullen, A. H. Rickard, L. A. H. Zeef, D. G. Davies, P. Gilbert, *J. Bacteriol.* **2004**, *186*, 7312–7326.
- [22] P. S. Stewart, *J. Bacteriol.* **2003**, *185*, 1485–1491.
- [23] N. Q. Balaban, J. Merrin, R. Chait, L. Kowalik, S. Leibler, *Science* **2004**, *305*, 1622 LP-1625.

References

- [24] J. J. Harrison, R. J. Turner, H. Ceri, *Environ. Microbiol.* **2005**, *7*, 981–94.
- [25] N. Høiby, *J. Cyst. Fibros.* **2002**, *1*, 249–254.
- [26] R. M. Donlan, *Emerg. Infect. Dis.* **2001**, *7*, 277–281.
- [27] L. Ganderton, J. Chawla, C. Winters, J. Wimpenny, D. Stickler, *Eur. J. Clin. Microbiol. Infect. Dis.* **1992**, *11*, 789–796.
- [28] K. Hori, S. Matsumoto, *Biochem. Eng. J.* **2010**, *48*, 424–434.
- [29] K. C. Marshall, R. Stout, R. Mitchell, *J. Gen. Microbiol.* **1971**, *68*, 337–348.
- [30] S. K. Arora, B. W. Ritchings, E. C. Almira, S. Lory, R. Ramphal, *Infect. Immun.* **1998**, *66*, 1000–1007.
- [31] G. P. Bodey, R. Bolivar, V. Fainstein, L. Jadeja, *Rev. Infect. Dis.* **1983**, *5*, 279–313.
- [32] H. P. Hahn, *Gene* **1997**, *192*, 99–108.
- [33] B. R. Borlee, A. D. Goldman, K. Murakami, R. Samudrala, D. J. Wozniak, M. R. Parsek, *Mol. Microbiol.* **2010**, *75*, 827–842.
- [34] M. T. Rybtke, B. R. Borlee, K. Murakami, Y. Irie, M. Hentzer, T. E. Nielsen, M. Givskov, M. R. Parsek, T. Tolker-Nielsen, *Appl. Environ. Microbiol.* **2012**, *78*, 5060–5069.
- [35] N. Gilboa-Garber, *Biochim. Biophys. Acta - Gen. Subj.* **1972**, *273*, 165–173.
- [36] S. Kirkeby, A. K. Hansen, A. d’Apice, D. Moe, *Microb. Pathog.* **2006**, *40*, 191–197.
- [37] N. Gilboa-Garber, L. Mizrahi, N. Garber, *Can. J. Biochem.* **1977**, *55*, 975–981.
- [38] D. Tielker, S. Hacker, R. Loris, M. Strathmann, J. Wingender, S. Wilhelm, F. Rosenau, K.-E. Jaeger, *Microbiology* **2005**, *151*, 1313–23.
- [39] E. Mitchell, C. Houles, D. Sudakevitz, M. Wimmerova, C. Gautier, S. Pérez, A. M. Wu, N. Gilboa-Garber, A. Imberty, *Nat. Struct. Biol.* **2002**, *9*, 918–21.
- [40] E. P. Mitchell, C. Sabin, L. Šnajdrová, M. Pokorná, S. Perret, C. Gautier, C. Hofr, N. Gilboa-Garber, J. Koča, M. Wimmerová, et al., *Proteins Struct. Funct. Genet.* **2005**, *58*, 735–746.
- [41] R. S. Laughlin, M. W. Musch, C. J. Hollbrook, F. M. Rocha, E. B. Chang, J. C. Alverdy, *Ann. Surg.* **2000**, *232*, 133–142.
- [42] S. P. Diggle, R. E. Stacey, C. Dodd, M. Cámara, P. Williams, K. Winzer, *Environ. Microbiol.* **2006**, *8*, 1095–104.
- [43] P. von Bismarck, R. Schneppenheim, U. Schumacher, *Klin Padiatr* **2001**, *213*, 285–287.
- [44] H.-P. Hauber, M. Schulz, A. Pforte, D. Mack, P. Zabel, U. Schumacher, *Int. J. Med. Sci.* **2008**, *5*, 371–376.
- [45] J. Wingender, T. R. Neu, H.-C. Flemming, in *Microb. Extracell. Polym. Subst. Charact. Struct. Funct.* (Eds.: J. Wingender, T.R. Neu, H.-C. Flemming), Springer Berlin Heidelberg, Berlin, Heidelberg, **1999**, pp. 1–19.
- [46] H. Rüdiger, *Chemie unserer Zeit* **1981**, *15*, 155–162.
- [47] E. C. Adam, D. U. Schumacher, U. Schumacher, *J. Laryngol. Otol.* **1997**, *111*, 760–762.
- [48] E. C. Adam, B. S. Mitchell, D. U. Schumacher, G. Grant, U. Schumacher, *Am. J. Respir. Crit. Care Med.* **1997**, *155*, 2102–2104.

- [49] R. A Dwek, *Chem. Rev.* **1996**, *96*, 683–720.
- [50] T. B. H. Geijtenbeek, S. I. Gringhuis, *Nat Rev Immunol* **2009**, *9*, 465–479.
- [51] T. B. . Geijtenbeek, D. S. Kwon, R. Torensma, S. J. van Vliet, G. C. . van Duijnhoven, J. Middel, I. L. M. H. . Cornelissen, H. S. L. . Nottet, V. N. KewalRamani, D. R. Littman, et al., *Cell* **2000**, *100*, 587–597.
- [52] A. J. Noll, Y. Yu, Y. Lasanajak, G. Duska-McEwen, R. H. Buck, D. F. Smith, R. D. Cummings, *Biochem. J.* **2016**, *473*, 1343–1353.
- [53] S. Akira, S. Uematsu, O. Takeuchi, *Cell* **2006**, *124*, 783–801.
- [54] S. I. Gringhuis, J. den Dunnen, M. Litjens, B. van het Hof, Y. van Kooyk, T. B. H. Geijtenbeek, *Immunity* **2007**, *26*, 605–616.
- [55] J. Hirabayashi, Ed. , in *Methods Mol. Biol.*, **2014**.
- [56] N. Gilboa-Garber, *Methods Enzymol.* **1982**, *83*, 378–385.
- [57] N. Gilboa-Garber, *FEBS Lett.* **1972**, *20*, 242–244.
- [58] A. Titz, in *Carbohydrates as Drugs* (Eds.: H.P. Seeberger, C. Rademacher), Springer International Publishing, Cham, **2014**, pp. 169–186.
- [59] J. Glick, N. Garber, *J. Gen. Microbiol.* **1983**, *129*, 3085–3090.
- [60] V. E. Wagner, B. H. Iglewski, *Clin. Rev. Allergy & Immunol.* **2008**, *35*, 124–134.
- [61] K. Winzer, C. Falconer, N. C. Garber, S. P. Diggle, M. Camara, P. Williams, *J. Bacteriol.* **2000**, *182*, 6401–6411.
- [62] A. N. Zelensky, J. E. Gready, *FEBS J.* **2005**, *272*, 6179–217.
- [63] M. Vijayan, N. Chandra, *Curr. Opin. Struct. Biol.* **1999**, *9*, 707–714.
- [64] N. Garber, U. Guempel, N. Gilboa-Garber, R. J. Royle, *FEMS Microbiol. Lett.* **1987**, *48*, 331–334.
- [65] G. Cioci, E. P. Mitchell, C. Gautier, M. Wimmerová, D. Sudakevitz, S. Pérez, N. Gilboa-Garber, A. Imberty, *FEBS Lett.* **2003**, *555*, 297–301.
- [66] C.-P. Chen, S.-C. Song, N. Gilboa-Garber, K. S. S. Chang, A. M. Wu, *Glycobiology* **1998**, *8*, 7–16.
- [67] N. Garber, U. Guempel, A. Belz, N. Gilboa-Garber, R. J. Doyle, *Biochim. Biophys. Acta - Gen. Subj.* **1992**, *1116*, 331–333.
- [68] S. Cecioni, J.-P. Praly, S. E. Matthews, M. Wimmerová, A. Imberty, S. Vidal, *Chemistry* **2012**, *18*, 6250–63.
- [69] R. U. Kadam, D. Garg, J. Schwartz, R. Visini, M. Sattler, A. Stocker, T. Darbre, J. L. Reymond, *ACS Chem. Biol.* **2013**, *8*, 1925–1930.
- [70] R. U. Kadam, M. Bergmann, D. Garg, G. Gabrieli, A. Stocker, T. Darbre, J.-L. Reymond, *Chemistry* **2013**, *19*, 17054–63.
- [71] Y. M. Chabre, D. Giguère, B. Blanchard, J. Rodrigue, S. Rocheleau, M. Neault, S. Rauthu, A. Papadopoulos, A. A. Arnold, A. Imberty, et al., *Chemistry* **2011**, *17*, 6545–62.
- [72] R. U. Kadam, M. Bergmann, M. Hurley, D. Garg, M. Cacciarini, M. A. Swiderska, C. Nativi, M. Sattler, A. R. Smyth, P. Williams, et al., *Angew. Chem. Int. Ed. Engl.* **2011**, *50*, 10631–10635.

References

- [73] B. Blanchard, A. Nurisso, E. Hollville, C. Tétaud, J. Wiels, M. Pokorná, M. Wimmerová, A. Varrot, A. Imberty, *J. Mol. Biol.* **2008**, *383*, 837–853.
- [74] C. Fasting, C. A. Schalley, M. Weber, O. Seitz, S. Hecht, B. Kokscho, J. Dervede, C. Graf, E.-W. Knapp, R. Haag, *Angew. Chem. Int. Ed. Engl.* **2012**, *51*, 10472–98.
- [75] R. J. Pieters, *Org. Biomol. Chem.* **2009**, *7*, 2013–2025.
- [76] I. Otsuka, B. Blanchard, R. Borsali, A. Imberty, T. Kakuchi, *Chembiochem* **2010**, *11*, 2399–408.
- [77] S. Cecioni, V. Oerthel, J. Iehl, M. Holler, D. Goyard, J.-P. Praly, A. Imberty, J.-F. Nierengarten, S. Vidal, *Chemistry* **2011**, *17*, 3252–61.
- [78] S. Cecioni, S. Faure, U. Darbost, I. Bonnamour, H. Parrot-Lopez, O. Roy, C. Taillefumier, M. Wimmerová, J.-P. Praly, A. Imberty, et al., *Chemistry* **2011**, *17*, 2146–59.
- [79] S. Cecioni, R. Lalor, B. Blanchard, J.-P. Praly, A. Imberty, S. E. Matthews, S. Vidal, *Chemistry* **2009**, *15*, 13232–40.
- [80] J.-F. Nierengarten, J. Iehl, V. Oerthel, M. Holler, B. M. Illescas, A. Munoz, N. Martin, J. Rojo, M. Sanchez-Navarro, S. Cecioni, et al., *Chem. Commun.* **2010**, *46*, 3860–3862.
- [81] L. Baldini, A. Casnati, F. Sansone, R. Ungaro, *Chem. Soc. Rev.* **2007**, *36*, 254–266.
- [82] M. Reynolds, M. Marradi, A. Imberty, S. Penadés, S. Pérez, *Chemistry* **2012**, *18*, 4264–73.
- [83] R. U. Kadam, M. Bergmann, M. Hurley, D. Garg, M. Cacciarini, M. A. Swiderska, C. Nativi, M. Sattler, A. R. Smyth, P. Williams, et al., *Angew. Chem. Int. Ed. Engl.* **2011**, *50*, 10631–10635.
- [84] A. V. Pukin, A. J. Brouwer, L. Koomen, H. C. van Ufford, J. Kemmink, N. J. de Mol, R. J. Pieters, *Org. Biomol. Chem.* **2015**, *13*, 10923–10928.
- [85] C. Sabin, E. P. Mitchell, M. Pokorná, C. Gautier, J.-P. Utille, M. Wimmerová, A. Imberty, *FEBS Lett.* **2006**, *580*, 982–7.
- [86] S. Perret, C. Sabin, C. Dumon, M. Pokorná, C. Gautier, O. Galanina, S. Ilia, N. Bovin, M. Nicaise, M. Desmadril, et al., *Biochem. J.* **2005**, *389*, 325–332.
- [87] R. Sommer, T. E. Exner, A. Titz, *PLoS One* **2014**, *9*, e112822.
- [88] R. Sommer, S. Wagner, A. Varrot, C. M. Nycholat, A. Khaledi, S. Haussler, J. C. Paulson, A. Imberty, A. Titz, *Chem. Sci.* **2016**, *7*, 4990–5001.
- [89] R. Sommer, D. Hauck, A. Varrot, S. Wagner, A. Audfray, A. Prestel, H. M. Möller, A. Imberty, A. Titz, *ChemistryOpen* **2015**, *4*, 756–767.
- [90] A. Hofmann, R. Sommer, D. Hauck, J. Stifel, I. Göttker-Schnetmann, A. Titz, *Carbohydr. Res.* **2015**, *412*, 34–42.
- [91] J. L. Magnani, J. T. Patton, A. Sarkar, *Glycomimetic Inhibitors of the PA-IL Lectin, PA-III Lectin or Both the Lectins from Pseudomonas*, **2005**, US20070037775A1.
- [92] I. Deguise, D. Lagnoux, R. Roy, *New J. Chem.* **2007**, *31*, 1321–1331.
- [93] I. Joachim, S. Rikker, D. Hauck, D. Ponader, S. Boden, R. Sommer, L. Hartmann, A. Titz, *Org. Biomol. Chem.* **2016**, *14*, 7933–7948.
- [94] P. H. Seeberger, C. Rademacher, *Carbohydrates as Drugs*, Springer Berlin Heidelberg, **n.d.**
- [95] B. A. Manjasetty, A. S. Halavaty, C.-H. Luan, J. Osipiuk, R. Mulligan, K. Kwon, W. F. Anderson, A. Joachimiak, *Data Br.* **2016**, *7*, 537–539.

- [96] R. Perozzo, G. Folkers, L. Scapozza, *J. Recept. Signal Transduct.* **2004**, *24*, 1–52.
- [97] M. W. Freyer, E. A. Lewis, *Methods Cell Biol.* **2008**, *84*, 79–113.
- [98] J. B. Chaires, *Annu. Rev. Biophys.* **2008**, *37*, 135–151.
- [99] G. A. Holdgate, W. H. J. Ward, *Drug Discov. Today* **2005**, *10*, 1543–1550.
- [100] F. E. Torres, M. I. Recht, J. E. Coyle, R. H. Bruce, G. Williams, *Curr. Opin. Struct. Biol.* **2010**, *20*, 598–605.
- [101] S. Núñez, J. Venhorst, C. G. Kruse, *Drug Discov. Today* **2012**, *17*, 10–22.
- [102] S. Leavitt, E. Freire, *Curr. Opin. Struct. Biol.* **2001**, *11*, 560–566.
- [103] J. J. Lavinder, S. B. Hari, B. J. Sullivan, T. J. Magliery, *J. Am. Chem. Soc.* **2009**, *131*, 3794–5.
- [104] J. K. Kranz, C. Schalk-Hihi, in *Methods Enzymol.*, **2011**, pp. 277–298.
- [105] U. B. Ericsson, B. M. Hallberg, G. T. DeTitta, N. Dekker, P. Nordlund, *Anal. Biochem.* **2006**, *357*, 289–298.
- [106] M. Zender, F. Witzgall, S. L. Drees, E. Weidel, C. K. Maurer, S. Fetzner, W. Blankenfeldt, M. Empting, R. W. Hartmann, *ACS Chem. Biol.* **2016**, *11*, 1755–1763.
- [107] A. P. Yeh, A. McMillan, M. H. B. Stowell, *Acta Crystallogr. Sect. D* **2006**, *62*, 451–457.
- [108] F. Perrin, *J. Phys. le Radium* **1926**, *7*, 390–401.
- [109] G. Weber, *Biochem. J.* **1952**, *51*, 145–155.
- [110] G. Weber, *Biochem. J.* **1952**, *51*, 155–167.
- [111] D. M. J. and J. C. Croney, *Comb. Chem. High Throughput Screen.* **2003**, *6*, 167–176.
- [112] C. Chakraborty, C.-H. Hsu, Z.-H. W. and C.-S. Lin, *Curr. Pharm. Des.* **2009**, *15*, 3552–3570.
- [113] T. J. Burke, K. R. Loniello, J. A. B. and K. M. Ervin, *Comb. Chem. High Throughput Screen.* **2003**, *6*, 183–194.
- [114] J. C. Owicki, *J. Biomol. Screen.* **2000**, *5*, 297–306.
- [115] P. Sörme, B. Kahl-Knutsson, M. Huflejt, U. J. Nilsson, H. Leffler, *Anal. Biochem.* **2004**, *334*, 36–47.
- [116] Z. Han, J. S. Pinkner, B. Ford, R. Obermann, W. Nolan, S. A. Wildman, D. Hobbs, T. Ellenberger, C. K. Cusumano, S. J. Hultgren, et al., *J. Med. Chem.* **2010**, *53*, 4779–92.
- [117] M. I. Khan, A. Surolia, N. Surolia, M. K. Mathew, P. Balaram, *Eur. J. Biochem.* **2005**, *115*, 149–152.
- [118] G. S. Jacob, C. Kirmaier, S. Z. Abbas, S. C. Howard, C. N. Steininger, J. K. Welply, P. Scudder, *Biochemistry* **1995**, *34*, 1210–1217.
- [119] D. Hauck, I. Joachim, B. Frommeyer, A. Varrot, B. Philipp, H. M. Möller, A. Imberty, T. E. Exner, A. Titz, *ACS Chem. Biol.* **2013**, *8*, 1775–1784.
- [120] P. Sörme, B. Kahl-Knutson, U. Wellmar, U. J. Nilsson, H. Leffler, *Methods Enzymol.* **2003**, *362*, 504–512.
- [121] S. Kleeb, L. Pang, K. Mayer, D. Eris, A. Sigl, R. C. Preston, P. Zihlmann, T. Sharpe, R. P. Jakob, D. Abgottspon, et al., *J. Med. Chem.* **2015**, *58*, 2221–39.

References

- [122] G. Beshr, R. Sommer, D. Hauck, D. C. B. Siebert, A. Hofmann, A. Imberty, A. Titz, *Med. Chem. Commun.* **2016**, *7*, 519–530.
- [123] W. A. Lea, A. Simeonov, *Expert Opin. Drug Discov.* **2011**, *6*, 17–32.
- [124] S. G. Patching, *Biochim. Biophys. Acta - Biomembr.* **2014**, *1838*, 43–55.
- [125] M. Raghavan, P. J. Bjorkman, *Structure* **1995**, *3*, 331–333.
- [126] J. Homola, S. S. Yee, G. Gauglitz, *Sensors Actuators B Chem.* **1999**, *54*, 3–15.
- [127] T. Neumann, H.-D. Junker, K. S. and R. Sekul, *Curr. Top. Med. Chem.* **2007**, *7*, 1630–1642.
- [128] J. P. McCoy, J. Varani, I. J. Goldstein, *Exp. Cell Res.* **1984**, *151*, 96–103.
- [129] L. Wide, J. Porath, *Biochim. Biophys. Acta - Gen. Subj.* **1966**, *130*, 257–260.
- [130] R. Thompson, A. Creavin, M. O’Connell, B. O’Connor, P. Clarke, *Anal. Biochem.* **2011**, *413*, 114–122.
- [131] R. Rosenfeld, H. Bangio, G. J. Gerwig, R. Rosenberg, R. Aloni, Y. Cohen, Y. Amor, I. Plaschkes, J. P. Kamerling, R. B.-Y. Maya, *J. Biochem. Biophys. Methods* **2007**, *70*, 415–426.
- [132] S. Chen, T. LaRoche, D. Hamelinck, D. Bergsma, D. Brenner, D. Simeone, R. E. Brand, B. B. Haab, *Nat Meth* **2007**, *4*, 437–444.
- [133] K. T. Pilobello, L. Krishnamoorthy, D. Slawek, L. K. Mahal, *Chembiochem* **2005**, *6*, 985–9.
- [134] C. Maierhofer, K. Rohmer, V. Wittmann, *Bioorg. Med. Chem.* **2007**, *15*, 7661–7676.
- [135] M. Pellicchia, I. Bertini, D. Cowburn, C. Dalvit, E. Giralt, W. Jahnke, T. L. James, S. W. Homans, H. Kessler, C. Luchinat, et al., *Nat. Rev. Drug Discov.* **2008**, *7*, 738–745.
- [136] D. M. Dias, A. Ciulli, *Prog. Biophys. Mol. Biol.* **2014**, *116*, 101–112.
- [137] G. Bodenhausen, D. J. Ruben, *Chem. Phys. Lett.* **1980**, *69*, 185–189.
- [138] M. P. Williamson, *Prog. Nucl. Magn. Reson. Spectrosc.* **2013**, *73*, 1–16.
- [139] S. B. Shuker, P. J. Hajduk, R. P. Meadows, S. W. Fesik, *Science (80-.)*. **1996**, *274*, 1531–1534.
- [140] P. J. Hajduk, R. P. Meadows, S. W. Fesik, *Q. Rev. Biophys.* **1999**, *32*, 211–240.
- [141] P. J. Hajduk, S. Boyd, D. Nettlesheim, V. Nienaber, J. Severin, R. Smith, D. Davidson, T. Rockway, S. W. Fesik, *J. Med. Chem.* **2000**, *43*, 3862–3866.
- [142] T. K. Oost, C. Sun, R. C. Armstrong, A.-S. Al-Assaad, S. F. Betz, T. L. Deckwerth, H. Ding, S. W. Elmore, R. P. Meadows, E. T. Olejniczak, et al., *J. Med. Chem.* **2004**, *47*, 4417–4426.
- [143] J. M. Moore, *Curr. Opin. Biotechnol.* **1999**, *10*, 54–58.
- [144] L. Skjærven, L. Codutti, A. Angelini, M. Grimaldi, D. Latek, P. Monecke, M. K. Dreyer, T. Carlomagno, *J. Am. Chem. Soc.* **2013**, *135*, 5819–27.
- [145] K. Pervushin, R. Riek, G. Wider, K. Wüthrich, *Proc. Natl. Acad. Sci.* **1997**, *94*, 12366–12371.
- [146] M. Piotto, V. Saudek, V. Sklenář, *J. Biomol. NMR* **1992**, *2*, 661–665.
- [147] M. Mayer, STD-NMR-Spektroskopie: Eine Neue Methode Zur Identifizierung Und Charakterisierung von Ligand-Rezeptor-Interaktionen, Universität Hamburg, **2001**.

- [148] N. A. Lakomek, C. Farès, S. Becker, T. Carlomagno, J. Meiler, C. Griesinger, *Angew. Chem. Int. Ed. Engl.* **2005**, *44*, 7776–8.
- [149] G. C. K. Roberts, *Drug Discov. Today* **2000**, *5*, 230–240.
- [150] A. Watts, *Curr. Opin. Biotechnol.* **1999**, *10*, 48–53.
- [151] B. Stockman, *Prog. Nucl. Magn. Reson. Spectrosc.* **1998**, *33*, 109–151.
- [152] W. Jahnke, *J. Biomol. NMR* **2007**, *39*, 87–90.
- [153] C. Dalvit, *Drug Discov. Today* **2009**, *14*, 1051–7.
- [154] C. Dalvit, M. Flocco, S. Knapp, M. Mostardini, R. Perego, B. J. Stockman, M. Veronesi, M. Varasi, *J. Am. Chem. Soc.* **2002**, *124*, 7702–7709.
- [155] C. Peng, A. Frommlet, M. Perez, C. Cobas, A. Blechschmidt, S. Dominguez, A. Lingel, *J. Med. Chem.* **2016**, *59*, 3303–3310.
- [156] A. D. Gossert, C. Henry, M. J. J. Blommers, W. Jahnke, C. Fernández, *J. Biomol. NMR* **2009**, *43*, 211–217.
- [157] M. J. Harner, A. O. Frank, S. W. Fesik, *J. Biomol. NMR* **2013**, *56*, 65–75.
- [158] T. Carlomagno, *Annu. Rev. Biophys. Biomol. Struct.* **2005**, *34*, 245–266.
- [159] M. Coles, M. Heller, H. Kessler, *Drug Discov. Today* **2003**, *8*, 803–810.
- [160] M. Vega-Vázquez, J. C. Cobas, F. F. Oliveira de Sousa, M. Martin-Pastor, *Magn. Reson. Chem.* **2011**, *49*, 464–468.
- [161] C. A. Lepre, J. M. Moore, J. W. Peng, *Chem. Rev.* **2004**, *104*, 3641–3676.
- [162] C. Dalvit, *Concepts Magn. Reson. Part A Bridg. Educ. Res.* **2008**, *32*, 341–372.
- [163] D. G. Davis, M. E. Perlman, R. E. London, *J. Magn. Reson. B* **1994**, *104*, 266–275.
- [164] K. Wuethrich, G. Wagner, R. Richarz, S. J. Perkins, *Biochemistry* **1978**, *17*, 2253–2263.
- [165] B. Meyer, T. Peters, *Angew. Chem. Int. Ed. Engl.* **2003**, *42*, 864–90.
- [166] P. Balaram, A. A. Bothner-By, E. Breslow, *J. Am. Chem. Soc.* **1972**, *94*, 4017–4018.
- [167] H. N. Moseley, W. Lee, C. H. Arrowsmith, N. R. Krishna, *Biochemistry* **1997**, *36*, 5293–9.
- [168] D. Li, L. A. Levy, S. A. Gabel, M. S. Lebetkin, E. F. DeRose, M. J. Wall, E. E. Howell, R. E. London, *Biochemistry* **2001**, *40*, 4242–4252.
- [169] S. Forsén, R. A. Hoffman, *J. Chem. Phys.* **1963**, *39*, 2892.
- [170] A. Viegas, J. Manso, F. L. Nobrega, E. J. Cabrita, *J. Chem. Educ.* **2011**, *88*, 990–994.
- [171] G. M. Clore, G. C. K. Roberts, A. Gronenborn, B. Birdsall, J. Feeney, *J. Magn. Reson.* **1981**, *45*, 151–161.
- [172] M. Mayer, B. Meyer, *Angew. Chemie Int. Ed.* **1999**, *38*, 1784–1788.
- [173] L. Poppe, G. S. Brown, J. S. Philo, P. V Nikrad, B. H. Shah, *J. Am. Chem. Soc.* **1997**, *119*, 1727–1736.
- [174] C. Dalvit, P. Pevarello, M. Tatò, M. Veronesi, A. Vulpetti, M. Sundström, *J. Biomol. NMR* **2000**, *18*, 65–68.
- [175] P. J. Hajduk, E. T. Olejniczak, S. W. Fesik, *J. Am. Chem. Soc.* **1997**, *119*, 12257–12261.

References

- [176] M. Betz, K. Saxena, H. Schwalbe, *Curr. Opin. Chem. Biol.* **2006**, *10*, 219–25.
- [177] D. Chandler, J. K. Percus, *Introduction to Modern Statistical Mechanics*, **1988**.
- [178] C. Deverell, R. E. Morgan, J. H. Strange, *Mol. Phys.* **1970**, *18*, 553–559.
- [179] H. Y. Carr, E. M. Purcell, *Phys. Rev.* **1954**, *94*, 630–638.
- [180] S. Meiboom, D. Gill, *Rev. Sci. Instrum.* **1958**, *29*, 688–691.
- [181] W. Jahnke, S. Rüdissler, M. Zurini, *J. Am. Chem. Soc.* **2001**, *123*, 3149–3150.
- [182] W. Jahnke, L. B. Perez, C. G. Paris, A. Strauss, G. Fendrich, C. M. Nalin, *J. Am. Chem. Soc.* **2000**, *122*, 7394–7395.
- [183] N. U. Jain, A. Venot, K. Umamoto, H. Leffler, J. H. Prestegard, *Protein Sci.* **2001**, *10*, 2393–2400.
- [184] C. S. Johnson, *Advances in Magnetic Resonance*, Elsevier, **1965**.
- [185] P. E. Johnson, E. Brun, L. F. MacKenzie, S. G. Withers, L. P. McIntosh, *J. Mol. Biol.* **1999**, *287*, 609–25.
- [186] I. Bertini, C. Luchinat, L. Messori, M. Vasak, *Eur. J. Biochem.* **1993**, *211*, 235–240.
- [187] J. P. Renault, C. Verchère-Béaur, I. Morgenstern-Badarau, M. Piccioli, *FEBS Lett.* **1997**, *401*, 15–19.
- [188] M. Gochin, H. Roder, *Protein Sci.* **1995**, *4*, 296–305.
- [189] C. Dalvit, D. Caronni, N. Mongelli, M. Veronesi, A. Vulpetti, *Curr. Drug Discov. Technol.* **2006**, *3*, 115–124.
- [190] N. Niccolai, R. Spadaccini, M. Scarselli, A. Bernini, O. Crescenzi, O. Spiga, A. Ciutti, D. Di Maro, L. Bracci, C. Dalvit, et al., *Protein Sci.* **2001**, *10*, 1498–1507.
- [191] F. Arnesano, L. Banci, I. Bertini, I. C. Felli, C. Luchinat, A. R. Thompsett, *J. Am. Chem. Soc.* **2003**, *125*, 7200–7208.
- [192] G. Pintacuda, G. Otting, *J. Am. Chem. Soc.* **2002**, *124*, 372–373.
- [193] G. Otting, *J. Biomol. NMR* **2008**, *42*, 1–9.
- [194] H. M. McConnell, R. E. Robertson, *J. Chem. Phys.* **1958**, *29*, 1361.
- [195] D. J. Felitsky, M. A. Lietzow, H. J. Dyson, P. E. Wright, *Proc. Natl. Acad. Sci. U. S. A.* **2008**, *105*, 6278–6283.
- [196] C. Tang, J. Iwahara, G. M. Clore, *Nature* **2006**, *444*, 383–386.
- [197] A. N. Volkov, J. A. R. Worrall, E. Holtzmann, M. Ubbink, *Proc. Natl. Acad. Sci. U. S. A.* **2006**, *103*, 18945–50.
- [198] J. Iwahara, G. M. Clore, *Nature* **2006**, *440*, 1227–1230.
- [199] C. Tang, C. D. Schwieters, G. M. Clore, *Nature* **2007**, *449*, 1078–1082.
- [200] I. Bertini, M. Fragai, Y.-M. Lee, C. Luchinat, B. Terni, *Angew. Chem. Int. Ed. Engl.* **2004**, *43*, 2254–6.
- [201] I. Bertini, C. Luchinat, G. Parigi, *Concepts Magn. Reson. Part A Bridg. Educ. Res.* **2002**, *14*, 259–286.
- [202] I. Bertini, C. Luchinat, G. Parigi, *Prog. Nucl. Magn. Reson. Spectrosc.* **2002**, *40*, 249–273.

- [203] J. R. Tolman, J. M. Flanagan, M. A. Kennedy, J. H. Prestegard, *Proc. Natl. Acad. Sci. U. S. A.* **1995**, *92*, 9279–9283.
- [204] M. Allegrozzi, I. Bertini, M. B. L. Janik, Y.-M. Lee, G. Liu, C. Luchinat, *J. Am. Chem. Soc.* **2000**, *122*, 4154–4161.
- [205] R. R. Biekofsky, F. W. Muskett, J. M. Schmidt, S. R. Martin, J. P. Browne, P. M. Bayley, J. Feeney, *FEBS Lett.* **1999**, *460*, 519–526.
- [206] W. Nils, **2008**, DOI 10.1515/9783110177701.
- [207] *Chem. Int. -- Newsmag. IUPAC* **2004**, *26*, 8.
- [208] B. J. Aylett, *Polyhedron* **1985**, *4*, 1799–1800.
- [209] N. N. Greenwood, A. Earnshaw, *Chemistry of the Elements*, **1997**.
- [210] L. H. Pettit, *Biochem. Educ.* **1979**, *7*, 24.
- [211] B. Bleaney, *J. Magn. Reson.* **1972**, *8*, 91–100.
- [212] I. Bertini, M. B. L. Janik, Y. M. Lee, C. Luchinat, A. Rosato, *J. Am. Chem. Soc.* **2001**, *123*, 4181–4188.
- [213] G. Pintacuda, M. John, X.-C. Su, G. Otting, *Acc. Chem. Res.* **2007**, *40*, 206–212.
- [214] M.-F. Bellin, *Eur. J. Radiol.* **2006**, *60*, 314–23.
- [215] J. Wöhnert, K. J. Franz, M. Nitz, B. Imperiali, H. Schwalbe, *J. Am. Chem. Soc.* **2003**, *125*, 13338–13339.
- [216] C. Ma, S. J. Opella, *J. Magn. Reson.* **2000**, *146*, 381–4.
- [217] A. Dvoretzky, V. Gaponenko, P. R. Rosevear, *FEBS Lett.* **2002**, *528*, 189–192.
- [218] T. Ikegami, L. Verdier, P. Sakhaii, S. Grimme, B. Pescatore, K. Saxena, K. M. Fiebig, C. Griesinger, *J. Biomol. NMR* **2004**, *29*, 339–349.
- [219] A. Leonov, B. Voigt, F. Rodriguez-Castañeda, P. Sakhaii, C. Griesinger, *Chem. - A Eur. J.* **2005**, *11*, 3342–3348.
- [220] X. C. Su, T. Huber, N. E. Dixon, G. Otting, *ChemBioChem* **2006**, *7*, 1599–1604.
- [221] F. Rodriguez-Castañeda, P. Haberz, A. Leonov, C. Griesinger, *Magn. Reson. Chem.* **2006**, *44*, DOI 10.1002/mrc.1811.
- [222] P. Haberz, F. Rodriguez-Castañeda, J. Junker, S. Becker, A. Leonov, C. Griesinger, *Org. Lett.* **2006**, *8*, 1275–1278.
- [223] X.-C. Su, K. McAndrew, T. Huber, G. Otting, *J. Am. Chem. Soc.* **2008**, *130*, 1681–1687.
- [224] P. H. J. Keizers, J. F. Desreux, M. Overhand, M. Ubbink, *J. Am. Chem. Soc.* **2007**, *129*, 9292–9293.
- [225] L. J. Martin, M. J. Hähnke, M. Nitz, J. Wöhnert, N. R. Silvaggi, K. N. Allen, H. Schwalbe, B. Imperiali, *J. Am. Chem. Soc.* **2007**, *129*, 7106–7113.
- [226] M. D. Vlasie, C. Comuzzi, A. M. C. H. Van Den Nieuwendijk, M. Prudêncio, M. Overhand, M. Ubbink, *Chem. - A Eur. J.* **2007**, *13*, 1715–1723.
- [227] I. Bertini, V. Calderone, L. Cerofolini, M. Fragai, C. F. G. C. Geraldès, P. Hermann, C. Luchinat, G. Parigi, J. M. C. Teixeira, *FEBS Lett.* **2012**, *586*, 557–67.

References

- [228] J. W. Peng, C. A. Lepre, J. Fejzo, N. Abdul-Manan, J. M. Moore, *Methods Enzymol.* **2001**, *338*, 202–229.
- [229] J. Reuben, *Paramagnetic Lanthanide Shift Reagents in NMR Spectroscopy*, Pergamon Pr., Oxford [U.a.], **1973**.
- [230] G. N. La Mar, Ed. , *Princ. Appl.* **1973**, XV, 678 S.
- [231] I. Bertini, Ed. , *Proc. NATO Adv. Study Inst. held Acquafredda di Maratea, Italy, June 3-15, 1979* **1980**, XX, 434 S.
- [232] O. Zerbe, Ed., **2003**, BioNMR in drug research, Wiley-VCH, Weinheim S. 484
- [233] S. P. Salowe, A. I. Marcy, G. C. Cuca, C. K. Smith, I. E. Kopka, W. K. Hagmann, J. D. Hermes, *Biochemistry* **1992**, *31*, 4535–4540.
- [234] I. Bertini, C. Luchinat, L. Messori, A. Scozzafava, *Eur. J. Biochem.* **1984**, *141*, 375–378.
- [235] I. Bertini, V. Calderone, M. Fragai, C. Luchinat, S. Mangani, B. Terni, *Angew. Chemie* **2003**, *115*, 2777–2780.
- [236] R. Lang, A. Kocourek, M. Braun, H. Tschesche, R. Huber, W. Bode, K. Maskos, *J. Mol. Biol.* **2001**, *312*, 731–42.
- [237] L. Banci, *J. Mol. Catal. A Chem.* **2003**, *204–205*, 401–408.
- [238] H. Nar, K. Werle, M. M. Bauer, H. Dollinger, B. Jung, *J. Mol. Biol.* **2001**, *312*, 743–51.
- [239] J. H. Prestegard, C. M. Bougault, A. I. Kishore, *Chem. Rev.* **2004**, *104*, 3519–3540.
- [240] J. H. Prestegard, H. M. Al-Hashimi, J. R. Tolman, *Q. Rev. Biophys.* **2000**, *33*, S0033583500003656.
- [241] J. R. Tolman, *Curr. Opin. Struct. Biol.* **2001**, *11*, 532–539.
- [242] A. Bax, G. Kontaxis, N. Tjandra, *Nuclear Magnetic Resonance of Biological Macromolecules - Part B*, Elsevier, **2001**.
- [243] J. H. Prestegard, *Nat. Struct. Biol.* **1998**, *391*, 517–522.
- [244] I. Bertini, C. Del Bianco, I. Gelis, N. Katsaros, C. Luchinat, G. Parigi, M. Peana, A. Provenzani, M. A. Zoroddu, *Proc. Natl. Acad. Sci. U. S. A.* **2004**, *101*, 6841–6846.
- [245] N. A. Lakomek, T. Carlomagno, S. Becker, C. Griesinger, J. Meiler, *J. Biomol. NMR* **2006**, *34*, 101–115.
- [246] G. N. La Mar, W. D. Horrocks, L. C. Allen, *J. Chem. Phys.* **1964**, *41*, 2126.
- [247] W. D. Horrocks, J. P. Sipe, *Science (80-)*. **1972**, *177*, 994–996.
- [248] W. B. Lewis, J. A. Jackson, J. F. Lemons, H. Taube, *J. Chem. Phys.* **1962**, *36*, 694.
- [249] J. Reuben, D. Fiat, *Chem. Commun.* **1967**, 729.
- [250] J. Reuben, *J. Chem. Phys.* **1969**, *51*, 4909.
- [251] N. S. Bhacca, N. Ahmad, J. Selbin, J. D. Wander, *J. Am. Chem. Soc.* **1971**, *93*, 2564–2565.
- [252] V. Gaponenko, S. P. Sarma, A. S. Altieri, D. A. Horita, J. Li, R. A. Byrd, *J. Biomol. NMR* **2004**, *28*, 205–212.
- [253] M. John, A. Y. Park, N. E. Dixon, G. Otting, *J. Am. Chem. Soc.* **2007**, *129*, 462–463.

- [254] Mitchell Jon Stanton-Cook, '<http://comp-bio.anu.edu.au/mscook/>', **2017.03.16, 21:02**
- [255] M. John, G. Pintacuda, A. Y. Park, N. E. Dixon, G. Otting, *J. Am. Chem. Soc.* **2006**, *128*, 12910–12916.
- [256] G. Pintacuda, M. A. Keniry, T. Huber, A. Y. Park, N. E. Dixon, G. Otting, *J. Am. Chem. Soc.* **2004**, *126*, 2963–2970.
- [257] I. Bertini, J. Faraone-Mennella, H. B. Gray, C. Luchinat, G. Parigi, J. R. Winkler, *JBIC J. Biol. Inorg. Chem.* **2004**, *9*, 224–230.
- [258] I. Bertini, M. Fragai, C. Luchinat, M. Melikian, E. Mylonas, N. Sarti, D. I. Svergun, *J. Biol. Chem.* **2009**, *284*, 12821–12828.
- [259] M. Prudêncio, J. Rohovec, J. A. Peters, E. Tocheva, M. J. Boulanger, M. E. P. Murphy, H.-J. Hupkes, W. Kosters, A. Impagliazzo, M. Ubbink, *Chemistry* **2004**, *10*, 3252–60.
- [260] G. Pintacuda, A. Y. Park, M. A. Keniry, N. E. Dixon, G. Otting, *J. Am. Chem. Soc.* **2006**, *128*, 3696–3702.
- [261] J.-L. Reymond, M. Bergmann, T. Darbre, *Chem. Soc. Rev.* **2013**, *42*, 4814–4822.
- [262] K. Marotte, C. Sabin, C. Préville, M. Moumé-Pymbock, M. Wimmerová, E. P. Mitchell, A. Imberty, R. Roy, *ChemMedChem* **2007**, *2*, 1328–38.
- [263] N. Gilboa-Garber, D. J. Katcoff, N. C. Garber, *FEMS Immunol. & Med. Microbiol.* **2000**, *29*, 53 LP-57.
- [264] S. Cecioni, A. Imberty, S. Vidal, *Chem. Rev.* **2015**, *115*, 525–561.
- [265] J. E. Moses, A. D. Moorhouse, *Chem. Soc. Rev.* **2007**, *36*, 1249–1262.
- [266] J. Aretz, E.-C. Wamhoff, J. Hanske, D. Heymann, C. Rademacher, *Front. Immunol.* **2014**, *5*, 323.
- [267] J. Aretz, P. R. Wratil, E.-C. Wamhoff, H. G. Nguyen, W. Reutter, C. Rademacher, *Can. J. Chem.* **2016**, *94*, 920–926.
- [268] E.-C. Wamhoff, J. Hanske, L. Schnirch, J. Aretz, M. Grube, D. Varón Silva, C. Rademacher, *ACS Chem. Biol.* **2016**, *11*, 2407–2413.
- [269] M. Lehner, Derivatives of Phenyl β -D-Galactoside as Inhibitors of *Pseudomonas Aeruginosa* Lectin LecA, University Konstanz, **2013**.
- [270] M. R. Berthold, N. Cebron, F. Dill, T. R. Gabriel, T. Kötter, T. Meinl, P. Ohl, C. Sieb, K. Thiel, B. Wiswedel, in *Data Anal. Mach. Learn. Appl. Proc. 31st Annu. Conf. Gesellschaft für Klassif. e.V., Albert-Ludwigs-Universität Freiburg, March 7--9, 2007* (Eds.: C. Preisach, H. Burkhardt, L. Schmidt-Thieme, R. Decker), Springer Berlin Heidelberg, Berlin, Heidelberg, **2008**, pp. 319–326.
- [271] J. B. Baell, G. A. Holloway, *J. Med. Chem.* **2010**, *53*, 2719–40.
- [272] Y. V. Griko, *Biophys. Chem.* **1999**, *79*, 117–127.
- [273] J. Rodrigue, G. Ganne, B. Blanchard, C. Saucier, D. Giguère, T. C. Shiao, A. Varrot, A. Imberty and R. Roy, *Org. Biomol. Chem.*, **2013**, *11*(40), 6906–6918.

References

- [274] S. J. Franklin, K. N. Raymond, *Inorg. Chem.* **1994**, *33*, 5794–5804.
- [275] J. A. Peters, J. Huskens, D. J. Raber, *Prog. Nucl. Magn. Reson. Spectrosc.* **1996**, *28*, 283–350.
- [276] R. Barbieri, I. Bertini, G. Cavallaro, Y.-M. Lee, C. Luchinat, A. Rosato, *J. Am. Chem. Soc.* **2002**, *124*, 5581–5587.
- [277] J. B. Jordan, D. A. Whittington, M. D. Bartberger, E. A. Sickmier, K. Chen, Y. Cheng, T. Judd, *J. Med. Chem.* **2016**, DOI 10.1021/acs.jmedchem.5b01917.
- [278] R. Campos-Olivas, *Curr Top Med Chem* **2011**, *11*, 43–67.
- [279] M. Fruth, A. Plaza, S. Hinsberger, J. H. Sahner, J. Hauptenthal, M. Bischoff, R. Jansen, R. Müller, R. W. Hartmann, *ACS Chem. Biol.* **2014**, *9*, 2656–63.
- [280] J. Kastl, J. Braun, A. Prestel, H. M. Möller, T. Huhn, T. U. Mayer, *ACS Chem. Biol.* **2015**, *10*, 1661–6.
- [281] K. J. Donovan, A. Lupulescu, L. Frydman, *Chemphyschem* **2014**, *15*, 436–43.
- [283] K. Koyano, H. Suzuki, *Bull. Chem. Soc. Jpn.* **1969**, *42*, 3306–3309.
- [284] L. Frullano, P. Caravan, *Curr. Org. Synth.* **2011**, *8*, 535–565.
- [285] I. Pashkunova-Martic, C. Kremser, M. Galanski, P. Schluga, V. Arion, P. Debbage, W. Jaschke, B. Keppler, *Mol. Imaging Biol.* **2011**, *13*, 432–442.
- [286] T. R. Nelson, S. M. Tung, *Magn. Reson. Imaging* **1987**, *5*, 189–199.
- [287] S. Shimotakahara, K. Furihata, M. Tashiro, *Magn. Reson. Chem.* **2005**, *43*, 69–72.
- [288] M. Rance, J. P. Loria, A. G. Palmer, *J. Magn. Reson.* **1999**, *136*, 92–101.
- [289] J. Marley, M. Lu, C. Bracken, *J. Biomol. NMR* **2001**, *20*, 71–75
- [290] B. Blanchard, A. Imberty, A. Varrot, *Proteins* **2014**, *82*, 1060–5.
- [291] N. Fornstedt, J. Porath, *FEBS Lett.* **1975**, *57*, 187–191.
- [292] G. Gomori, in (Ed.: B.T.-M. in Enzymology), Academic Press, **1955**, pp. 138–146
- [293] M. Wilkins, E. Gasteiger, A. Bairoch, J. Sanchet, K. Williams, R. Appel, D. Hochstrasser, *Methods Mol. Biol.* **1999**, *112*, 531–552.
- [294] V. Sklenar, M. Piotto, R. Leppik, V. Saudek, *J. Magn. Reson. Ser. A* **1993**, *102*, 241–245.
- [295] R. B. Cohen, K.-C. Tsou, S. H. Rutenburg, A. M. Seligman, *J. Biol. Chem.* **1952**, *195*, 239–249.
- [296] W. F. Goebel, O. T. Avery, *J. Exp. Med.* **1929**, *50*, 521 LP-531.
- [297] M. Apparau, M. Blanc-Muesser, J. Defaye, H. Driguez, *Can. J. Chem.* **1981**, *59*, 314–320.
- [298] Z. Wang, in *Compr. Org. Name React. Reagents*, John Wiley & Sons, Inc., **2010**
- [299] M. Amaike, H. Kobayashi, S. Shinkai, *Bull. Chem. Soc. Jpn.* **2000**, *73*, 2553–2558.
- [300] A. Temeriusz, T. Gubica, P. Rogowska, K. Paradowska, M. K. Cyrański, *Carbohydr. Res.* **2005**, *340*, 1175–1184.
- [301] C. Maierhofer, K. Rohmer, V. Wittmann, *Bioorg. Med. Chem.* **2007**, *15*, 7661–7676.
- [302] Young B., Yu W., Rodríguez D., Varney K., MacKerell A., Weber D. *Molecules*, **2021**, *26*, 381.

- [303] Kuhaudomlarp S.S., Siebs E., Shanina, E., Topin J., Joachim I., Gomes P., Varrot A., Rognan D., Rademacher, C., Imberty A., Titz, A. *Angewandte Chemie Int. Ed.* **2020**, 60, 15
- [304] Cimmerman P., Baranauskienė L., Jachimovičiūtė S., Jachno J., Torresan J., Michailovienė V., Matulienė J., Sereikaitė J., Bumelis V., Matulis D. *Biophysical Journal*, **2008**, 95, 7, 3222-3231
- [305] Shanina E., Siebs E., Zhang H., Varon Silva D., Joachim I., Titz A., Rademacher, C. **2020**. *Glycobiology*. 31
- [306] Wagner S., Hauck D., Hoffmann M., Sommer R., Joachim I., Müller R., Imberty A., Varrot A., Titz A., **2017**, *Angew. Chem. Int Ed*, 56, 16559 – 16564
- [307] Joachim I., Rikker S., Hauck D., Ponader D., Boden S., Sommer R. Hartmann L., Titz A. **2016**, *Org. Biomol. Chem.* 14, 7933 – 7948

References

Appendix

Curriculum vitae

Ines Alexandra Bräutigam, geb. Joachim

Birth: 14.10.1987 in Stuttgart Citizenship: German

Scientific Education and professional experience

Jun 2016 – to date	CSL Behring AG Bern, Switzerland and CSL Behring GmbH Marburg, Germany
	Various positions within the Quality Organization
Aug 2013- Mai 2016	Helmholtz-Institute for pharmaceutical research Saarland (HIPS), Saarbrücken, Germany
	PhD student in the group of Prof. Dr. A. Titz Topic: Specific <i>Pseudomonas aeruginosa</i> LecA inhibitors
Oct 2012 - Jul 2013	University of Konstanz, Konstanz, Germany
	PhD student in the group of Prof. Dr. A. Titz Topic: Specific <i>Pseudomonas aeruginosa</i> LecA inhibitors
Sept 2010 – Oct 2012	University of Konstanz, Konstanz, Germany
	Program: Life Science (Master of Science; final grad 1,0) Master thesis in the group of Prof. Dr. A Titz: ‘Lectin-mediated adhesion of <i>Pseudomonas aeruginosa</i> ’
Aug 2011 - Sept 2011	Institute of Medical Microbiology and Hygiene Universitätsklinikum Tübingen, Tübingen
	Internship with PD Dr. Klaus Schröppel on <i>Candida albicans</i> and <i>Pseudomonas aeruginosa</i> biofilms
Oct 2007 - Aug 2010	University of Konstanz, Konstanz, Germany
	Program: Life Science (Bachelor of Science, final grade 2,3) Bachelor thesis in the group of Prof. Dr. V. Wittmann: ‘Metabolisches Oligosaccharid-Engineering mit N-Acetylhexosaminderivaten.’

Appendix

Sept 1998 - June 2007	Carlo-Schmidt-Gymnasium, Tübingen, Germany
	Abitur 2007, final grade 1,8

List of scientific publications

- Kuhadomlarp S., Siebs, E., Shanina E., Topin, J., Joachim I., Gomes P., Varrot A., Rognan D., Rademacher C., Imberty A., Titz A. **2020**. *Angewandte Chemie Int. Ed.* 60, 8104 - 8114
- Shanina E., Siebs E., Zhang H., Varon Silva D., Joachim I., Titz A., Rademacher, C. **2020**. *Glycobiology*. 31.
- Wagner S., Hauck D., Hoffmann M., Sommer R., Joachim I., Müller R., Imberty A., Varrot A., Titz A., **2017**, *Angew. Chem. Int Ed*, 56, 16559 - 16564.
- Joachim I., Rikker S., Hauck D., Ponader D., Boden S., Sommer R. Hartmann L., Titz A. **2016**, *Org. Biomol. Chem.* 14, 7933 - 7948
- Hauck D., Joachim I., Frommeyer B., Varrot A., Philipp B., Möller H., Imberty A., Exner T., Titz A. **2013**, *ACS chemical biology*. 8 (8)
- Sommer R., Joachim I., Wagner S., Titz A., **2013**. *Chimia*, 67, 286-290.